Thesis for doctoral degree (Ph.D.)
2015

Study of the mechanisms behind the additive effect of neoadjuvant castration on radiotherapy for prostate cancer

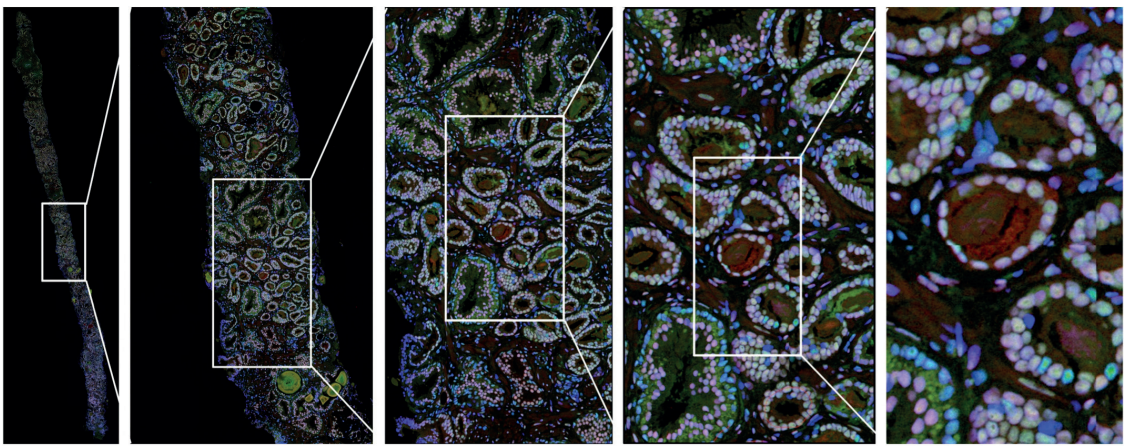

Firas L. Tarish

Karolinska Institutet

From the department of medical biochemistry and biophysics,
Karolinska Institutet, Stockholm, Sweden

STUDY OF THE MECHANISMS BEHIND THE ADDITIVE EFFECT OF NEOADJUVANT CASTRATION ON RADIOTHERAPY FOR PROSTATE CANCER

Firas L.Tarish

Karolinska Institutet

Stockholm 2015

Published by Karolinska Institute.
Printed by *E-PRINT, Karolinska Institute, Box 23109, 10435 Stockholm, Sweden*

ISBN 978-91-7676-113-7

STUDY OF THE MECHANISMS BEHIND THE ADDITIVE EFFECT OF NEOADJUVANT CASTRATION ON RADIOTHERAPY FOR PROSTATE CANCER

THESIS FOR DOCTORAL DEGREE (Ph.D.)

By

Firas L. Tarish

Principal Supervisor:
Thomas Helleday
Karolinska Institutet
Department of medical biochemistry and biophysics
Division of Translational Medicine and Chemical Biology

Co-supervisor:
Niklas Schultz
Karolinska Institutet
Department of medical biochemistry and biophysics
Division of Translational Medicine and Chemical Biology

Opponent:
Sten Nilsson
Karolinska Institutet
Department of Oncology-Pathology (OnkPat), K7

Examination Board:
Monica Nister
Karolinska Institutet
Department of Oncology-Pathology (OnkPat), K7

Peter Wiklund
Karolinska Institutet
Department of Molecular Medicine and Surgery (MMK), K1

Stefan Åström
Stockholm University
Department of Molecular Biosciences

"The life is like a journey, and this is only one of many stations"

ABSTRACT

Castration improves responses to radiotherapy (RT) in prostate cancer with unknown mechanism. An understanding of what happens at the cellular and molecular level in prostate cancer cells, while reducing their access to androgens and then exposing them to ionizing radiation (IR), would give us an opportunity to optimize the treatment and may also inspire novel therapeutic approaches.

Paper I: Growth of solid tumours such as prostate cancer is characterized by neovascularization and increased glycolysis as a result of the hypoxic microenvironment of the tumour. HIF-1α is an important transcription factor that regulates cell adaptation to hypoxia and transcription of genes involved in angiogenesis, cell survival, glucose metabolism, and tumour invasion. To test whether any connection between castration therapy and intra-tumoural hypoxia, measured by HIF-1α expression, prostate biopsy specimens from 14 patients with prostate cancer were investigated. Downregulation of HIF-1α expression after castration was observed in five patients with initial high HIF-1α expression. HIF-1α expression was also reduced in two of three patients with initial low HIF-1α expression. These data suggest that neoadjuvant castration reduces tumour cell hypoxia in prostate cancer, which may contribute to the increased radiosensitivity after castration.

Paper II: We investigated whether castration impairs non-homologous end-joining (NHEJ) repair of DNA double-strand breaks (DSBs) by downregulation of Ku70 expression. The same cohort of patients used in paper I was analysed. After castration, the nuclear Ku70 levels were reduced in 12 patients (levels varied from 43% to 97% after castration, $p < 0.001$). The reduction in Ku70 expression correlated significantly with the decrease of serum PSA level after castration, suggesting that AR activity regulates Ku70 protein levels in prostate cancer tissue. Our conclusion was that castration results in decreased levels of Ku70 protein. Since Ku70 protein is necessary for NHEJ repair of DSBs, a downregulation of DNA repair leads to increased radiosensitivity.

Paper III: Emerging data demonstrate homologous recombination (HR) defects in castration resistant malignant prostate tumours, rendering these sensitive to PARP inhibitor treatments. Here, we demonstrate a direct link between the androgen receptor (AR) being required for maintenance of HR gene expression and activity in prostate cancer cells, as well as in maintenance of DNA damage response signalling. As a consequence, we show PARP-mediated backup repair pathway is upregulated in prostate cancer tissues in patients following androgen-deprivation therapy (ADT). Furthermore, upregulation of PARP activity is essential for prostate cancer survival, and we demonstrate a synthetic lethality between ADT and PARP inhibitors in vivo. These data demonstrate that HR may be functionally impaired earlier in prostate cancer etiology as a consequence of ADT; prior to emerging castration resistance and that this potentially can be exploited therapeutically

using PARP inhibitors in combination with an ADT upfront in advanced or high risk prostate cancer.

Paper IV: Since castration improves responses to radiotherapy (RT) in prostate cancer, we hypothesized that this radiosensitization is caused by castration-mediated down-regulation of non-homologous end joining (NHEJ) repair of DNA double-strand breaks (DSBs). To test this, forty-eight patients with localized prostate cancer were enrolled in two arms, either treating with RT upfront or after receiving neo-adjuvant castration. We biopsied patients at diagnosis, before and after castration and RT treatments to monitor androgen receptor (AR), NHEJ and DSB repair in verified cancer tissue. We show that patients receiving neo-adjuvant castration prior to RT had reduced levels of the NHEJ protein Ku70, impaired RT-induced NHEJ activity and a higher level of unrepaired DSBs, measured by γ-H2AX foci in cancer tissues. This study demonstrates that castration impairs NHEJ activity in prostate cancer tissue, explaining improved RT responses in tumours.

Paper V: Despite the early diagnosis and subsequently effective treatment of intermediate and high-risk prostate cancer, the recurrence rate remains regrettably high. Here, we wanted to investigate how effectively castration suppresses androgen receptor (AR) signalling, thereby affecting DNA damage repair in primary hormone-naïve prostate cancer. From the same cohort of patients as in Paper IV, four patients from arm 1 and one patient from arm 2 were analysed. The levels of AR, Ku70, phosphorylated DNA-PKcs and PAR were measured. A significant correlated reduction in the mean intensity of nuclear AR was observed in four patients whose serum PSA was reduced to the greatest extent, about 90% ($\rho=1$, $p<0.001$). Although complete castration was obtained using serum testosterone levels in these patients, the levels of AR, and consequently of Ku70 and phosphorylated DNA-PKcs remained high and positively co-varied in clusters of cells throughout prostate tumour areas. Meanwhile, a tendency towards an inverse correlation was observed between AR, Ku70 and phosphorylated DNA-PKcs as compared with PARP-1 activity. In conclusion, we are first to demonstrate the heterogeneous landscape of AR and the consequent divergent although co-varied response of DNA damage repair. To date, it remains unclear whether the emergence of these castration-resistant cells in hormone-naïve prostate cancer, is due to the high levels of intra-tumoural residual androgen following castration and consequently suboptimal androgen suppression of otherwise androgen-dependent cells or caused by quiescent castration-resistant cells that promote progression according to clonal selection pressure. The current finding certainly warrants further investigation in the future.

LIST OF SCIENTIFIC PAPERS

This dissertation is based on the following papers, which is referred to by their roman numerals

I. **Castration therapy of prostate cancer results in downregulation of HIF-1α levels. Int J Radiat** Oncol Biol Phys. 2012 Mar 1;82(3):1243-8. doi:10.1016/j.ijrobp.2011.10.038. **Al-Ubaidi FL,** Schultz N, Egevad L, Granfors T, Helleday T.

II. **Castration Therapy Results in Decreased Ku70 Levels in Prostate Cancer.** *Clin Cancer Res*. 19(6);1-10. 2013 Mar 15;19(6):1547-56. doi: 10.1158/1078-0432.CCR-12-2795. Epub 2013 Jan 24. ***Al-Ubaidi FL,*** Schultz N, Loseva O, Egevad L, Granfors T, Helleday T.

III. **Synthetic Lethality between PARP inhibition and Androgen Deprivation Therapy in Prostate Cancer, explained by Androgen Receptor driving Homologous Recombination.** Mohammad Asim, Heather Ireland Zecchini, **Firas L. Tarish,** Charles E. Massie, Ajoeb Baridi, Anne Y. Warren, Wanfeng Zhao, Leigh-Anne McDuffus, Patrice Mascalchi, Harveer Dev, Karan Wadhwa, Paul Wijnhoven, Josep Forment, Scott Lyons, Roslin Russell, Andy G. Lynch, Cormac O'Neill, Vincent R. Zecchini, Paul S. Rennie, Aria Baniahmad, Simon Tavaré, Ian G. Mills, Niklas Schultz, Yaron Galanty,Thomas Helleday and David Neal. *Under preparation.*

IV. **Castration radiosensitizes prostate cancer by impairing DNA-PK-mediated DNA double-strand break repair. Firas L. Tarish,** Niklas Schultz, Anna Tanoglidi, Hans Hamberg, Henry Letocha, Katalin Karaszi, Freddie Hamdy, Torvald Granfors, Thomas Helleday. *Accepted in Science Translational Medicine.*

V. **Androgen Receptor Heterogeneity in hormone-naïve prostate cancer. Firas L. Tarish,** Niklas Schultz, Anna Tanoglidi, Hans Hamberg, Henry Letocha, Katalin Karaszi, Freddie Hamdy, Torvald Granfors, Thomas Helleday. *Under preparation.*

CONTENTS

LIST OF ABBREVIATIONS

ADT	Androgen Deprivation Therapy
AR	Androgen Receptor
AREs	Androgen Response Elements
ATM	Ataxia Telangiectasia Mutated
ATR	ATM-Rad3-related
B-NHEJ	Backup Non-Homologous End Joining
BPH	Benign Prostatic Hyperplasia
BRCA	Breast Cancer Associated Gene
CD	Cluster Differentiation
CRPC	Castration Resistant Prostate Cancer
CSCs	Cancer Stem Cells
3D-CRT	Three-Dimensional Conformal Radiation Therapy
D-NHEJ	Dependent Non-Homologous End Joining
DDR	DNA damage response
DHT	Dihydrotestosterone
DNA	Deoxyribonucleic acid
DNA-PKcs	DNA-dependent protein kinase, catalytic subunit
DRE	Digital Rectal Examination
DSB	Double Strand Break
EBRT	External Beam Radiation Therapy
GnRH	Gonadotropin Releasing Hormone
Gy	Gray
HE	Haematoxylin and Eosin
HIF-1α	Hypoxia-Inducible Factor-1 alpha
HR	Homologous Recombination
IMRT	Intensity Modulated Radiation Therapy
IR	Ionizing Radiation
kDa	kilo Dalton
LBD	Ligand-Binding Domain
MRN complex	MRE11-RAD50-NBS1 complex

PAR	Poly(ADP-ribosyl)
PARP	Poly(ADP-ribose) Polymerases
PCa	Prostate Cancer
PSA	Prostate Specific Antigen
RP	Radical Prostatectomy
RPA	Replication protein A
RT	Radiation Therapy
ssDNA	single stranded DNA
TNM	Tumour, Node, Metastasis
TRAMP	Transgenic Adenocarcinoma Mouse Prostate
VEGF	Vascular Endothelial Growth Factor
XRCC4	X-ray repair cross-complementing protein 4

1 INTRODUCTION

Prostate cancer (PCa) is the second most common diagnosed cancer and a major cause of cancer-related death worldwide [1, 2]. The highest incidence is found in Western Europe, North America, and Australia/New Zeeland, which might be due to the frequent use of prostate specific antigen (PSA) testing and subsequent biopsies of the prostate in these parts of the world. The goal of treatment of non-metastatic PCa is to cure the patient, and extend survival. One treatment modality with curative intention is the combination of radiotherapy (RT) and neoadjuvant castration; a short-term endocrine therapy prior to and during RT, which has shown a significant improvement in local tumour control and disease-specific survival combined with reduced incidence of distant metastases. However, the overall survival is improved only in a subset of patients with locally advanced disease and low graded tumours [3-5].

Several randomised trials demonstrate the synergistic effect between castration and RT. Yet the underlying mechanisms are not fully understood [6]. An understanding of the mechanisms at the cellular and molecular level in PCa cells, how reducing their access to androgens and then exposing them to ionizing radiation (IR) kill cells, would give us an opportunity to optimize the treatment and may also inspire novel therapeutic approaches.

1.1 HISTOPATHOLOGY AND STAGING OF PROSTATE CANCER

The prostate gland is located below the urinary bladder neck. There are three distinct zones, the peripheral zone about 70%, the central zone about 25% and the transitional zone about 5% of the prostatic volume (Figure 1). The prostate gland consists of glandular and non-glandular tissue. Glandular tissue consists of epithelial cells forming glands and their main function is to elaborate and secrete prostate-specific antigen (PSA). Non-glandular tissue consists of fibromuscular stroma. The vast majority of prostatic cancer is acinar adenocarcinoma 90-95 % and the remaining 5-10% are neuroendocrine prostate carcinomas; a non-acinar carcinoma that includes a subset of rare prostate cancer phenotypes, which are characterized by low or negative PSA levels, androgen receptor resistance and aggressive phenotype [3, 7]. About 80% of prostatic acinar adenocarcinomas arise in the peripheral zone. It is multifocal in about 85% of cases. Adenocarcinomas of the prostate are histologically scored according to Gleason; the most widely accepted grading system that is based on the architectural pattern of the prostate tumour.

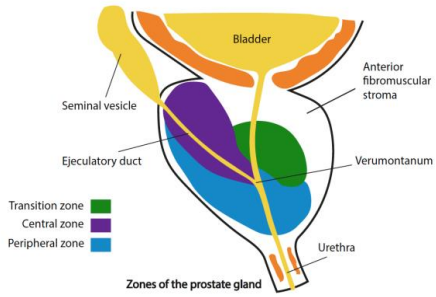

Figure 1. Side view, shows the location and the different zones of the prostate gland.

The Gleason grading system combines the two most common (primary and secondary) architectural patterns of cancer within the sampled specimen. Each of the two most common patterns is assigned a grade from one to five, with the grade 1 being the most well-differentiated and least aggressive and grade 5, the poorly differentiated or most aggressive. Gleason score, which is a number from 2-10, is reported as the sum of the two dominant patterns added together [4, 7, 8] (Figure 2).

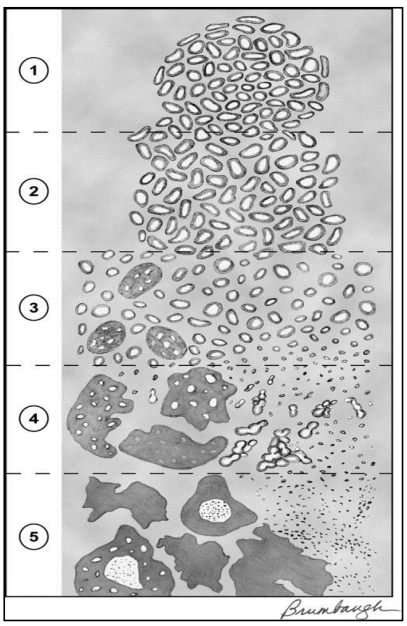

FIGURE 2. Modified Gleason grading system. Pattern 1: Circumscribed nodule of closely packed but separate, uniform, rounded to oval, medium-sized acini (larger glands than pattern 3). Pattern 2: Like pattern 1, fairly circumscribed, yet at the edge of the tumor nodule, there may be minimal infiltration. Glands are more loosely arranged and not quite as uniform as Gleason pattern 1. Pattern 3: Discrete glandular units; typically smaller glands than seen in Gleason pattern 1 or 2; infiltrates in and among nonneoplastic prostate acini; marked variation in size and shape; smoothly circumscribed small cribriform nodules of tumor. Pattern 4: Fused microacinar glands; ill-defined glands with poorly formed glandular lumina; large cribriform glands; cribriform glands with an irregular border; hypernephromatoid. Pattern 5: Essentially no glandular differentiation, composed of solid sheets, cords, or single cells; comedocarcinoma with central necrosis surrounded by papillary, cribriform, or solid masses. *Epstein et al. Adv Anat Pathol. 2006 Jan; 13(1): 57-9*

1.2 TNM CLASSIFICATION

The clinical staging of PCa is according to the TNM system.

- T represents the size of the primary tumour.
- N describes the involvement of regional lymph nodes
- M describes distant metastases in different organs.

T1 - The tumour remains confined to the prostate and is too small to be detected on digital rectal examination (DRE).

T1a - Incidentally diagnosed tumour through transurethral resection of prostatic adenoma in ≤ 5% of resected tissue.

T1b - Incidentally diagnosed tumour through transurethral resection of prostatic adenoma in ≥ 5% of resected tissue.

T1c -The tumour diagnosed through needle core biopsy following elevated PSA value.

T2 - The tumour is still confined to the prostate, but is now large enough to be felt on DRE.

T2a- The tumour invades one-half or less of one lobe of the prostate gland.

T2b- The tumour invades more than one half of only one lobe of the prostate gland.

T2c- The tumour invades both lobs of the prostate gland.

T3 - The tumour has extracapsular extension.

T3a -The tumour spread through the prostatic capsule.

T3b - The tumour invades the seminal vesicles.

T4 - The tumour invades adjacent organs or structures other than the seminal vesicles, i.e. external sphincter, rectum, levator muscles, or pelvic wall.

(TNM Classification of Malignant Tumours, 7th Edition. Oxford, UK: Wiley-Blackwell, 2009)

1.3 RISK STRATIFICATION OF LOCALIZED PROSTATE CANCER ACCORDING TO D´AMICO CRITERIA [9]:

Low risk prostate cancer: PSA<10 and Gleason score < 7 and T1-2a

Intermediate risk prostate cancer: PSA 10-20 or Gleason score =7 or T2b

High risk prostate cancer: PSA >20 or Gleason score = 8-10 or T2c-T3a

1.4 DIAGNOSIS OF PROSTATE CANCER USING THE PSA TEST

Prostate specific antigen (PSA) is a protein produced by normal and malign prostatic cells and its expression is primarily regulated by the androgen receptor (AR). PSA is considered the most effective single biomarker for monitoring the metabolic activity of PCa cells before, during and after treatment [10, 11]. The PSA test measures the serum levels of this protein and is often elevated in men with PCa. However, neuroendocrine differentiated carcinomas of the prostate may appear without initial significant high levels of serum PSA [3].

1.5 TREATMENT FOR LOCALIZED PROSTATE CANCER

Treatment of organ confined PCa may differ according to risk classification of cancer and expected survival of patients [12]. Conventional treatment options for men with intermediate risk and high risk, clinically localized PCa have included radical prostatectomy (RP) and radiotherapy (RT) techniques. However, active surveillance may be recommended for patients with an indolent low risk tumour. Moreover, the combination of RT with neoadjuvant castration has proven beneficial in patients with intermediate and high risk disease [13].

1.6 SURGERY

RP is an established therapeutic option for treatment of patients with localized PCa. RP, which means removal of the entire prostate gland and the seminal vesicles, can be achieved through different techniques like open, laparoscopic or robotic assisted laparoscopic radical prostatectomy. Although neoadjuvant castration using gonadotropin releasing hormone (GnRH) analogues have been demonstrated to produce significant reduction in the positive surgical margin rate, yet they have not shown to affect disease-specific or overall survival and are therefore not recommended prior to surgery [14, 15].

1.7 RADIOTHERAPY

RT is an alternative curable approach widely used to treat localized and locally advanced PCa in patients, in whom surgery is either not suitable or not desired. However, to date, there are still no comparative, randomised studies between radiotherapy and surgery as primary treatment in prostate cancer. Nevertheless, substantial evidence based on pre-treatment prognostic markers such as serum PSA level, Gleason score and T-stage, suggest equivalent outcome of RT to radical prostatectomy in low risk prostate cancer [16, 17]. Different delivery technique of RT, e.g. external beam radiation therapy (EBRT) or brachytherapy as well as different RT-fractionation regimes, e.g. hypofractionation, hyperfractionation, and accelerated fractionation are used as single treatment modalities or in combination. Rather poor historical results of RT as a single modality in patients with intermediate and high risk PCa have led to the use of dose escalation conformal RT methods like three-dimensional conformal radiation therapy (3D-CRT) and intensity modulated radiation therapy (IMRT), which has proven to be highly effective in intermediate risk cancer [18]. Nevertheless, Hanks et al has shown that RT dose escalation does not improve the 5-years biochemical non-evidence of disease rate (bNED) for patients with high risk disease [19].

1.8 ENHANCED RADIOSENSITIVITY

Experimental and randomised clinical trials have shown that PCa patients have longer survival after combined castration and RT of the primary tumour than after RT alone [13, 21]. Thereby one might conclude that the reduction of androgenic stimuli makes PCa cells more sensitive to RT. Animal studies in vivo have shown that castration before radiation decreases the number of clonogenic cancer cells and increases the overall cell kill and diminishes growth velocity of the surviving PCa cells [22, 23]. Another in vitro study using cell line LNCaP (PCa metastatic to lymph nodes) could not demonstrate any increased radiosensitivity after removal of androgens from the culture medium [24].

Today the most accepted rationale underlying the synergistic effect between castration and RT is that the volume reduction and shrinkage of the prostate tumour achieved with neoadjuvant castration facilitates the dose escalation of RT with higher dosage applied to the prostate without increasing the toxicity on the adjacent organs [25]. Furthermore, the neoadjuvant approach is believed to induce apoptosis and reduce tumour hypoxia, which may explain improved radiosensitization [26].

1.9 COMBINATION OF HORMONAL THERAPY AND RADIOTHERAPY

Neoadjuvant castration combined with RT is currently the standard of care treatment for a patient with a localized and unfavourable tumour. It may in addition to its systemic effect on any subclinical distant disease, aim on improving local disease control, disease-specific and overall survival. Using gonadotropin-releasing hormone (GnRH) analogues, castration levels of serum testosterone will be achieved after approximately four weeks [27], while bilateral orchiectomy leads to an almost immediate castration effect. The often-quoted EORTC-study [13] showed an advantageous disease-specific and overall survival after neoadjuvant castration with RT versus. RT alone. However, in that study, the hormonal therapy with a GnRH analogue was started concurrently with RT, which meant that the castration effect was not achieved until the second half of RT. Presumably, the effect of combined castration and RT is more beneficial, if serum testosterone is on castration level from the start of the RT. The optimal duration of androgen deprivation in conjunction with RT is not clear. To date, many studies have tried to relate the time of neoadjuvant hormonal therapy to its effect on prostate volume [28]. However, other studies have tried to find out a cut-off point for the serum prostate specific antigen (PSA) level [29, 30]. A widespread international recommendation points out that two months of neoadjuvant castration will be enough before the start of RT [31, 32]. The changes in the PSA value indicate the overall metabolic activity in PCa cells before, during and after treatment [10].

1.10 ANDROGEN RECEPTOR

The androgen receptor (AR) plays an important role in the initiation, growth and survival of normal prostate tissue. However, AR knockout in ARKO male mice model showed a feminized appearance with prostate growth agenesis [33]. It is believed to play an important role in the development of resistance to hormonal therapy [34]. Animal models show that prostate epithelial cells express AR already in early fetal life, where it has a role in morphogenesis of the prostate [35]. The AR is a protein molecule in the cell cytoplasm, to which steroid molecules bind as ligands. Such complexes then act as transcription factors in the cell nucleus and regulate the genes involved in prostate cell growth and survival. AR is a 110-kDa protein and a member of the nuclear receptor super family [36] and consists of an N-terminal transactivation domain, central DNA binding domain and a C-terminal ligand-binding/transactivation domain [37, 38]. Epidemiological studies have failed to show any relevance between elevated serum levels of testosterone, dihydrotestosterone, or adrenal androgen and the risk for PCa [39]. Reduction of serum DHT after castration results in 70 % loss of secretary epithelial prostate cells by apoptosis in an adult rat model [40]. In cytoplasm, AR is found in an inactive complex bound to heat shock protein HSP 70 and HSP 90 and co-repressor. DHT binds to AR as a ligand, which lead to homo-dimerization and nuclear translocation of AR where it binds to androgen response elements (AREs) of androgen responsive genes as a transcription factor [34] (Figure 3).

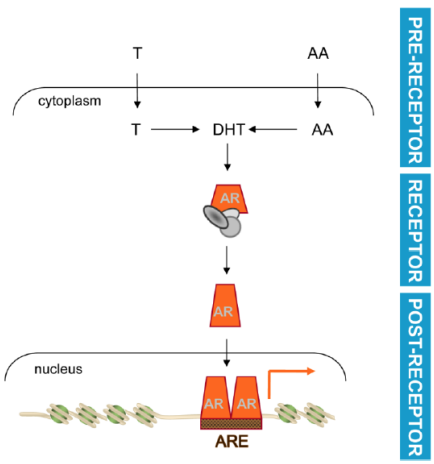

Figure 3. Basic mechanism of androgen receptor (AR). Testosterone (T) or adrenal androgens (AA) are converted to DHT in PCa cells. Ligand activation induces a conformational change and nuclear translocation of AR. Within the nucleus, AR binds AREs in target genes to regulate their transcription and modulate PCa cell behavior. Pre-receptor level ADT interferes with AR ligand production. Receptor level ADT impedes AR-ligand interaction. Post-receptor level ADT exploits AR-dependent action downstream of AR for therapeutic intervention. *Heemers HV. Int J Biol Sci. 2014 Jun 1; 10(6): 576-87. doi: 10.7150/ijbs.8479*

Androgen ablation either by bilateral orchiectomy or by GnRH analogues results in 90-95% reduction of serum testosterone levels with no difference in long term survival between these two methods [41, 42]. As shown in clinical and animal studies, the effect of androgen ablation on prostate tumours leads to decreased proliferation determined by Ki67, but there is no significant effect on the rate of apoptosis [43, 44]. The castration level of serum testosterone (< 1.7 ng/ml) is achieved almost immediately after surgical castration and in

approximately four weeks after the first injection of a GnRH analogue [27]. Randomised clinical trials have shown longer survival of prostates cancer patients after combined castration and RT of primary tumour than after RT alone [13, 21, 45]. This clinically observed increased radiosensitivity of PCa after androgen ablation has failed to be shown in vitro studies using prostate cancer cell lines LNCaP and PC3 [24, 47].

Castration results in 75-80% decrease of intraprostatic androgens; testosterone and DHT, levels in benign prostatic hyperplasia (BPH) patients [48]. However, in castration resistant prostate cancer (CRPC) tissue the intraprostatic testosterone remains at a normal level despite castration, whereas DHT levels are reduced by 75% [49]. In patients with aggressive cancer castration reduces intraprostatic DHT levels less than in patients with more favourable disease [50]. The CRPC is a heterogeneous disease but the cancer cells are still dependent upon androgen signalling for their survival and growth. In fact, many of patients with CRPC remain androgen-dependent and respond to further hormone manipulation such as second-generation antiandrogens [51]. Together these results demonstrate that serum androgen concentration does not directly reflect the high levels of intraprostatic androgens, which probably are sufficient to stimulate the growth of aggressive PCa.

1.11 IONIZING RADIATION AND DNA DAMAGE

The therapeutic effect of ionizing radiation (IR) in cancer relies on its ability to induce lethal DNA damage of tumour cells leading to their death. The tumour responses to IR depend on the magnitude of delivered dose as well as on the DNA damage response (DDR) of the tumour cells. The IR-induced DNA damages trigger a DDR signalling cascade that determines the final fate of each single cell. Successful repair of the DNA lesions will allow the cell to survive and continue its cell cycle (Figure 4). However, an unsuccessful DNA repair results either in tumour cells leaving the cell cycle, entering senescence or apoptosis, or in emerging of DNA mutations, which might lead to drug- or radioresistance.

IR generates different kinds of DNA damage either due to direct effect on the DNA molecule or indirectly by free radicals [52]. It may lead to a variety of DNA lesions including base damage, base release, crosslinking and strand breakage [53]. The most lethal DNA lesion is the double strand break (DSB), which triggers DDR and repair pathways that are mainly dependent non-homologous end joining (D-NHEJ) and homologous recombination (HR) (Figure 4). Nevertheless, when none of these repair pathways are active, an alternative PARP-mediated repair pathway called backup non-homologous end joining (B-NHEJ) will repair DSBs (Figure 6).

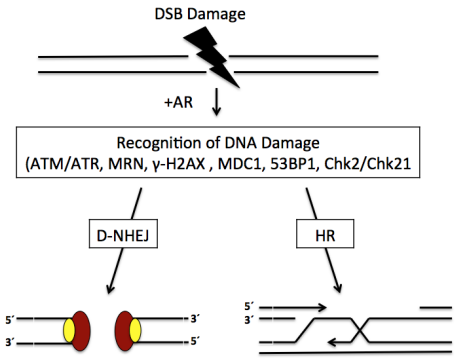

Figure 4. The two major DSB repair pathways. IR-induced DSB leads to activation of DDR signalling cascade that leads to activation of the error-prone pathway of D-NHEJ in G0/G1 of the cell cycle or the error–free pathway of HR in S/G2 phase of the cell cycle and the repair of DSB.

1.12 DNA DAMAGE SIGNALLING

The DNA damage response (DDR) is a complex of protein signalling network that monitors the genome integrity during different phases of the cell cycle. Diverse genotoxic insults induced by replication stress, various kinds of genotoxic drugs or IR activates the DDR machinery, which subsequently activates a plethora of signalling pathways and may lead to cell cycle arrest followed by DNA repair, cellular senescence or apoptosis [54].

Following DNA damage, two master protein kinases, the ataxia telangiectasia mutated (ATM) and the ATM-Rad3-related (ATR) are activated. ATM is mainly activated in response to DSBs through all the cell cycle, meanwhile ATR activity is restricted to S/G2 phases and it is mostly triggered in response to replication stress [55]. The MRN (Mer11-Rad50-Nbs1) complex, which plays a vital role in various DNA repair pathways, including NHEJ and HR, act as a DSBs sensor that initiate DDR. MRN complex recognize DNA damage and activates ATM and ATR [56]. ATM phosphorylates a number of target proteins including the MRN complex, a histone variant H2AX that generates γ-H2AX foci which in turn activates DNA damage checkpoint protein 1 (MDC1). Analogously, 53BP1; a key regulator of DSB repair, rapidly recruited and makes large foci at the DNA damage sites. The MRN complex together with 53BP1 governs whether D-NHEJ or HR repairs a DSB. During the G1 phase of the cell cycle, 53PB1 binds to RAP1-interacting factor1 (Rif1) that block the end-resection of DSB and preventing further accumulation of breast cancer susceptibility gene 1(BRCA1) at the site of DNA damage, hence promoting NHEJ repair. However, during S/G2 phase of the cell cycle and in a cyclin-dependent kinase (CDK)-dependent manner, CtBP-interacting protein (CtIP) recruits by Nbs1; part of MRN complex, at the site of DSB. CtIP binds to BRCA1 and block Rif1 from further binding to 53BP1, allowing extensive end-resection and 3´overhang formation at the site of DSB, thereby promoting HR repair [46, 58, 59] (Figure 5).

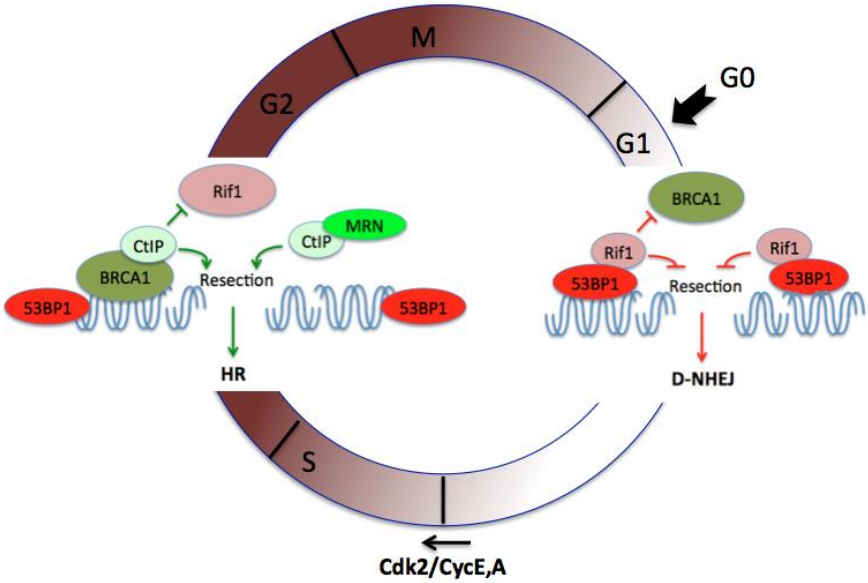

Figure 5. Cell cycle dependent mutual exclusion of BRCA1 and Rif1 from DSBs. In G1, Rif1 prevents the accumulation of BRCA1 at DSBs and acts downstream of 53BP1 to block resection, thereby promoting D-NHEJ. In S/G2, phosphorylated CtIP blocks Rif1 from binding to 53BP1, thereby allowing resection and promoting HDR. CtIP also plays a part in promoting resection but this attribute appears to be independent of its binding to BRCA1. Abbreviations: D-NHEJ, dependent non-homologous end joining; HDR, homology-directed repair; Cdk2, cyclin dependent kinase 2; CycE,A, cyclin E, cyclin A.

Zimmermann M et al. Trends Cell Biol. 2014 Feb;24(2):108-17. doi: 10.1016/j.tcb.2013.09.003.

After DNA damage, activated ATM/ATR lead to activation of cell cycle checkpoints that leads to cell cycle arrest and more time for the cell to repair the damage. ATM/ATR phosphorylate and activates Chk2 and Chk1, respectively. ATM/Chk2 pathway controls mainly G1/S checkpoint and ATR/Chk1 controls G2/M checkpoint [57]. In order to initiate cell cycle arrest, Chk2 and Chk1 phosphorylate Cdc25A to be inactivated and degraded. Lack of active Cdc25A lead to accumulation of inactive cyclin E-CDK2 complex; a vital regulator proteins promoting cell cycle progression from G1 to S phase of the cell cycle, and cell cycle arrest in G1 phase. In addition, inactive Cdc25A leads to inactivation of cyclin B-Cdc2; regulator proteins that promote the cell cycle progression from G2 to M phase, thus the cell will remain in G2 phase until the damage is repaired. Furthermore, to maintain the cell cycle arrest, activated ATM/ATR and subsequent activation of Chk2/Chk1 leads to phosphorylation and thus stabilization of p53; a tumour suppressor gene and transcriptional activator, which activate several target genes including p21. Activated p21; a potent CDK inhibitor that regulate cell cycle proliferation and DNA replication, leads to further inhibition of cyclin E-CDK2 / B-Cdc2 complexes, thereby the cell will continue arrested in G1/S or G2/M phase until the DNA damage is sufficiently repaired and the cell re-enter the cell cycle again. Otherwise it will go to apoptosis if the damage is remained unrepaired.

1.13 NON-HOMOLOGOUS END JOINING

DNA-dependent protein kinase catalytic subunit (DNA-PKcs) dependent non-homologous end joining (D-NHEJ) is the major DNA repair pathway involved in repair of toxic DNA double-strand breaks (DSBs) after IR [58]. D-NHEJ is operating during all phases of the cell cycle however mainly in G0/G1. Since D-NHEJ is directly ligated DSBs without the need for a homologous template, it is an error-prone process, which might contribute to intra-chromosomal deletion and translocation [59]. Misrepaired DSBs lead either to cell death or chromosomal deletion, chromosomal translocation and genomic instability. The cornerstone in D-NHEJ repair pathway is the Ku heterodimer, which consists of two tightly, associated polypeptides of approximately 70 kDa (Ku70) and 80 kDa (Ku80). Ku proteins are the regulatory subunits that detect and bind the two ends of DSB, tethering them together and recruits DNA-PKcs to form the DNA-PK complex [60, 61]. DNA-PKcs then attracts the ligase IV complex (comprised of ligase IV, XRCC4 and XLF), which together seal the DNA ends [59]. AR interacts via its ligand-binding domain (LBD) directly with both Ku70 and Ku80 regulatory subunits of DNA-PKcs in a DNA-independent manner. Ku proteins bind the AR in both the cytoplasm and the nucleus and are recruited to the promoter of AR target genes such as prostate specific antigen (PSA) promoter in an androgen-dependent manner. A Ku-protein defines as a recycle co-activator of AR [62]. Cells deficient in Ku proteins are more sensitive to IR [63].

1.14 HOMOLOGOUS RECOMBINATION

Homology directed repair or homologous recombination (HR) is another pathway involved in repair of IR-induced DSBs. HR accomplished by using a homologous DNA template (often on a sister chromatid or rarely from a homologous chromosome) from which the missing sequence is copied. In contrast to D-NHEJ, HR is generally error-free and mainly operating in the S and G2 phases of the cell cycle. The initiating step of HR is 5′ to 3′ end resection, generating a 3′ ended single-stranded overhang. Resection involves MRN complex activation. Replication protein A (RPA) rapidly binds to the ssDNA overhang, preventing the formation of secondary structures. Subsequently, RPA is displaced by RAD51 via a breast cancer susceptibility gene 2 (BRCA2)–dependent process. RAD51 loading promotes invasion onto the undamaged template and strand displacement, generating D-loop formation, which is necessary to generate a Holliday junction and a heteroduplex molecule with help of Rad54. Repair synthesis uses the undamaged strand as a template, followed by ligation of the DNA ends. It is generally believed that there is a second Holliday junction formed. Finally, resolution of the Holliday junctions completes the process, giving crossover or non–crossover products, depending on the direction of resolution.

Since D-NHEJ does not require homologous template, it is a faster repair process compared to HR and hence predominates repair of IR-induced DSBs [59].

1.15 PARP1 AND DNA DAMAGE RESPONSE

Poly (ADP-ribose) polymerases-1 (PARP1) is the most important member of PARPs protein family that is involved in cellular stress responses such as inflammatory, metabolic or genotoxic stress including DNA repair. PARPs proteins composed of different ADP-ribosyl transferase enzyme that regulate the synthesis of Poly (ADP-ribose) (PAR); a branching polymer chain of several hundred ADP-ribose units, via process called Poly (ADP-ribosyl)ation (PARylation) [64, 65]. PARP1 can be triggered by several forms of DNA damages and consequently catalyses the PARylation of different target proteins, including itself, that involves in a wide range of cellular response, such as chromatin remodelling, transcriptional regulation, DNA repair, cell cycle arrest, cell senescence or cell death [20, 66].

Alternative or backup non-homologous end joining (B-NHEJ) is PARP1-dependent DNA repair of DSBs, activates in D-NHEJ deficient cells [67] (Figure 6). PARP-1 is effectively competing with Ku-heterodimer for DNA end-binding and repair of DSBs, however the higher bindings affinity of Ku70 to damaged DNA ends inhibit its recruitment and subsequent PARylation. B-NHEJ, like D-NHEJ, is an error-prone process and it is active throughout the cell cycle, however mainly during S and G2. PARP-1 is mainly involved in base excision and single strand break (SSB) repair of DNA [68]. Compelling evidence suggest its dual action in HR repair and showed that PARP-1 senses and binds to the stalled replication forks and promoting recruitment of MRN complex in HR-dependent repair process [69]. Failing HR repair caused by defective BRCA1/BRCA2, during S/G2 of the cell cycle, leads to predominance activation of backup DNA repair machinery mediated by PARP-1 [70] (Figure 6). Currently, taking the advantage of synthetic lethality, which is defined as independent loss of function one of two compatible genes will not affect cell survival, whereas simultaneous loss of function of these two genes is lethal [71]. This fact provides PARP inhibitor a key role as a target cancer therapy in patients with BRCA1/BRCA2 defected tumours.

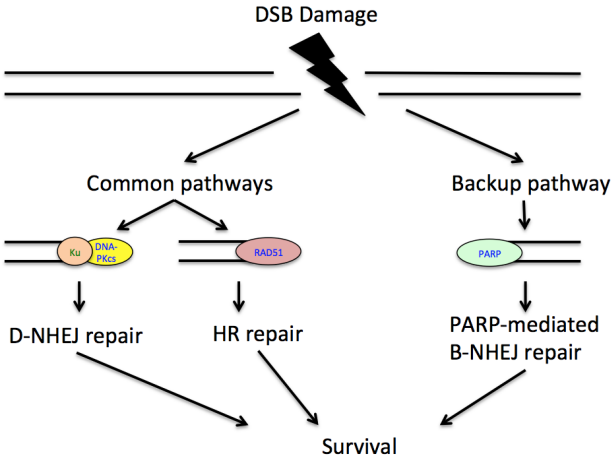

Figure 6. DNA damages are repaired by AR-dependent D-NHEJ and homologous recombination repair pathways. However in the absence of AR, PARP is activated as a backup pathway to mediate survival.

1.16 HYPOXIC MICROENVIRONMENT IN SOLID TUMOURS

It is well established that solid tumours, such as PCa, are characterized by hypoxic microenvironment, which promotes resistance to IR-induced DNA damage.

Hypoxia-inducible factor-1 alpha (HIF-1α) is an essential transcription factor that activates transcription of genes involved in angiogenesis, cell survival, glucose metabolism and tumour invasion. HIF-1α level is affected by several genetic, epigenetic and environmental elements. Microenvironment and intra-tumoural hypoxia generates reactive oxygen species (ROS) by mitochondria, which lead to stabilization and upregulation of HIF-1α and subsequent vascular endothelial growth factor (VEGF) production [72, 73]. Clinical data show high levels of HIF-1α in primary and metastatic PCa as compared to benign prostate tissue [74]. Studies in the Transgenic Adenocarcinoma Mouse Prostate (TRAMP) transgenic model of PCa support the correlative clinical observations and HIF-1α is associated with the angiogenic switch in early PCa progression [75].

In vitro studies on androgen positive LNCaP cells have shown that DHT stimulates HIF-1α transcription activity, leading to a high level of HIF-1α protein and VEGF, while an anti-androgen agent (flutamide) leads to the converse effect [76]. AR regulates expression of HIF-1α and VEGF in androgen sensitive tumours [77], through androgen-regulated autocrine receptor tyrosine kinase receptor signalling [76].

2 AIMS OF THE STUDIES

The overall purpose of this thesis is to explore the mechanism behind the synergistic effect of neoadjuvant castration on radiotherapy. We investigate

1: If castration reduces the expression of HIF-1α levels, as a measure of hypoxia, in prostate tumour cells, thereby enhancing radiosensitivity.

2: If castration downregulates expression of the Ku70 protein in PCa cells leading to defective DNA repair.

3: If androgen deprivation therapy (ADT) reduces the expression of HR repair and activates PARP signalling. If so, ADT is synthetically lethal with PARP inhibitors.

4: If combination of castration and RT provides superior suppression of D-NHEJ mediated DNA repair compared with RT alone.

5: The heterogeneous landscape of AR in hormone-naïve PCa.

3 PATIENTS AND METHODS

3.1 PAPER I & PAPER II

Ethical approval was granted from regional ethics committee at Uppsala University (Dnr 2007/170). We enrolled 20 patients with locally advanced and metastasized PCa. All patients were treated with castration. Surgical castrations with bilateral orchidectomy were performed in eight patients and pharmacological castration with leuprorelin, a GnRH analogue, was performed in twelve patients. Several needle core biopsy specimens were obtained from each patient at diagnosis and after castration, approximately one month after surgical castration or two months after pharmacological castration (see Flowchart 1).

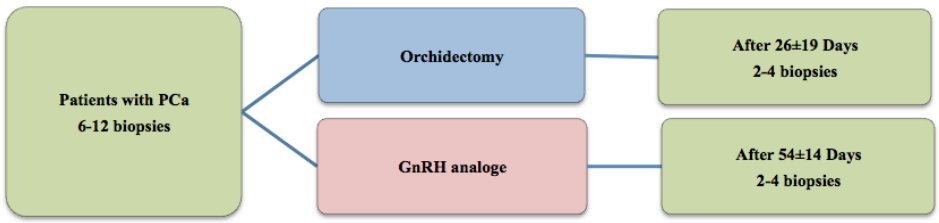

Flowchart 1. Flowchart of patients enrolled in papers I & II. After enrolment, all patients treated with castration. Needle core biopsy specimens were obtained before and after treatment.

All biopsies were paraffin embedded and sectioned. First section from each biopsy was haematoxylin and eosin (HE) stained and examined for identification of cancer areas that has been graded according to the Gleason grading system. Before and after castration two biopsy specimens rich in cancer cells, were analysed with immunofluorescence staining in each patient. Since six patients were excluded from the study because their post-castration biopsy specimens were free from cancer, fourteen patients were included. The base-line characteristics are summarized in Table 1.

Table 1. Base-line characteristics of the patients in Paper I & Paper II

					PSA, ng/mL		Testosterone, nmol/L			
Patient number	Patient age	Prostate volume, ml	cT	GS	Before castration	After castration	Before castration	After castration	Days between castration and biopsies II	Castration method
6	70	71	4	8	1,021	21	12	0.9	47	GnRH agonist
9	83	20	3	7	8	0.3	14	0.8	62	GnRH agonist
10	87	59	3	7	34	1.9	15	0.7	36	GnRH agonist
12	61	26	2	7	17	6.4	ND	1.7	36	GnRH agonist
14	78	90	3	7	326	55	7	0.3	48	GnRH agonist
18	69	50	3	10	380	5.4	11	0.3	83	GnRH agonist
19	77	34	3	7	107	2.6	11	1.0	48	GnRH agonist
2	67	65	3	10	2.9	3.7	23	0.3	4	Orchidectomy
5	86	52	3	9	70	53	7	1.0	6	Orchidectomy
8	63	44	3	8	650	134	13	0.9	8	Orchidectomy
15	59	90	4	9	736	29	8	0.9	46	Orchidectomy
16	82	ND	3	7	16	1.1	16	0.6	49	Orchidectomy
17	84	46	4	8	438	138	9	0.6	29	Orchidectomy
20	83	100	3	9	89	23	10	0.3	40	Orchidectomy

Abbreviations: cT, clinical tumor stadium; GS, Gleason score; ND, not done.

Al-Ubaidi FL et al. Clin Cancer Res. 2013 Mar 15; 19(6): 1547-56. doi: 10.1158/1078-0432.CCR-12-2795.

3.2 PAPER III

For comprehensive details, see supplementary information in Paper III.

3.2.1 Cell culture

LNCaP, PC3, PNT1a, DUCaP are different prostate cell models used for diverse analyses in the study. We generated and cultured C4-2-NT control (expressing non-targeting RNA; siNT) and C4-2-shAR cells achieved by the doxycycline-mediated induction of a short-hairpin RNA targeting the AR. To investigate the role of AR expression on cell growth under genotoxic stress, we employed an isogenic inducible AR mutant (T877A) expressed in the PC3 cell line in which doxycycline treatment triggered AR expression.

3.2.2 Cell viability assay

Cell viability was determined by incubating the culture with MTS reagent based (3-(4,5-dimethylthiazol-2-yl)-5-(3-carboxymethoxyphenyl)-2-(4-sulfophenyl)-2H-tetrazolium) colorimetric assay as per manufacturers protocol (Promega). Using a Vicell instrument, cells were trypsinised and counted. Cell growth assay was carried out in 96 well plates.

3.2.3 Clonogenic assay

The clonogenic potential of PCa cell lines after different treatments were evaluated by colony formation assays using colony analyser from Oxford Optronix.

3.2.4 Live cell imaging/confluence analyses

Using the IncuCyte instrument from Essen Bioscience, confluence analyses were performed. Live cell images were recorded every three hours. However, for ease of understanding only 12 hours time interval data are shown.

3.2.5 Ex vivo prostate explant culture

After informed consent according to the institutional policy, patients with locally advanced, hormone-naïve PCa and median PSA levels of 82 ng/ml were enrolled. Needle core biopsy specimens with fresh PCa tissue were obtained. Collagen mix (rat tail collagen) was solidified on a nylon membrane to make collagen cushions and PCa tissue was fixed in formalin for immunohistochemistry analysis of Ki67 (Rabbit polyclonal from Santa Cruz, sc-816 at 1:750 dilution) and CC3 (cleaved caspase-3; 9664, Cell signalling Technology).

3.2.6 Generation of tumour xenografts

PC3/PC3-AR and C4-2 xenografts experiments were performed in compliance with the Home office directive of Animal (scientific procedures) act, under a project and personal license. Tumour size was measured weekly with callipers. The mice were culled at the completion of the experiment or when the tumours had reached 10% of body weight.

3.2.7 Patients and leuprorelin (GnRH analogue) study design

Ethical approval was granted from regional ethics committee at Uppsala University (Dnr 2011/066). For details information, see patients and methods in Paper IV &V or in supplementary information Paper III.

3.2.8 Degarelix study design

Full ethical approval was obtained (11/H0311/2) for clinical studies NCT01852864 and NCT00967889. 15 patients with high risk organ confined PCa were treated with degarelix, a GnRH antagonist, seven days before surgery. Fresh PCa tissue samples were obtained at radical prostatectomy and were snap frozen. Degarelix treated patients achieved castration levels of serum testosterone. These samples were compared with matched controlled samples from 19 untreated patients. They were spotted on microscopic slides to generate tissue microarray.

3.3 PAPER IV

Ethical approval was granted from regional ethics committee at Uppsala University (Dnr 2011/066). Fifty-two patients with newly diagnosed, localized or locally advanced, non-metastasized PCa were recruited for the study. All patients had high risk cancers and were thereby eligible for combined neoadjuvant castration with RT. The patients were allocated to one of the two study arms following the assignment of a written informed consent by each patient. Three patients in arm 1 and one patient in arm 2 were excluded from the study since they refused further subsequent biopsies during the study. Thus 48 patients were eligible for the final analysis, 25 in arm 1 and 23 patients in arm 2. Their base-line characteristics are summarized in Table 2.

Table 2. Base-line characteristics of the patients in Paper IV

	Arm 1	Arm 2	p value
Number of patients	**25**	**23**	
Median age years (Min – Max)	70 (56-78)	69 (55-78)	0.6
Median Gleason Score (%)	6 (4%) 7 (60%) 8 (12%) 9 (24%)	6 (8%) 7 (65%) 8 (8%) 9 (17%)	ns ns ns ns
Median time to prostate needle biopsy specimen in days (Quartiles)	55 (54-59)	58 (55-57)	ns
Median serum PSA ng/ml (Quartiles) At diagnoses After castration After castration and RT After RT After RT and castration	 11 (7.6-19.5) 0.8 (0.36-1.6) 1.2 (0.34-2.2)	 8.3 (3.9-15) 9.5 (4.7-19.25) 0.69 (0.26-1.5)	 0.16
Median serum Testosterone nmol/L (Quartiles) At diagnosis After castration After castration and RT After RT After RT and castration	 ND 0,7 (0-0.95) 0.5 (0-0.93)	 ND 9,4 (7.8-12.5) 0,7 (0-1.0)	
Median volume prostate cm^3 (Quartiles) At diagnosis After castration After castration and RT After RT After RT and castration	 41 (30-49) 24 (19-36) 24 (19-33)	 35 (26-49) 37 (30-47) 26 (19-34)	 0.4

- ND: not done
- ns: not significant

Patients in arm 1 received neoadjuvant pharmacological castration, leuprorelin followed by external beam RT, 2 Gy fractions daily to a total dose of 78 Gy. Patients in arm 2 started treatment with external beam RT, 2 Gy fractions daily for five consecutive days, followed by neoadjuvant pharmacological castration, and after that an equivalently higher dose RT to a total of 82 Gy. The first prostate needle-core biopsy setting was obtained from all patients at diagnosis. In arm 1, a second biopsy setting was obtained eight weeks after the leuprorelin injection and a third biopsy setting obtained about three hours after the fifth RT fraction. In arm 2, a second biopsy setting were obtained about three hours after the fifth RT fraction and a third biopsy setting was obtained eight weeks after the leuprorelin injection (see Flowchart 2).

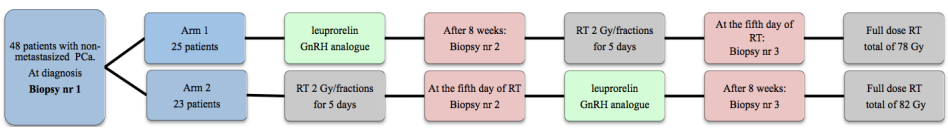

Flowchart 2. Flowchart of patients enrolled in the paper IV & V. Patients received castration treatment by GnRH-agonist for 8 weeks. 2 Gy x5 radiotherapy (RT) treatments were given on consecutive days and biopsies taken 3 hours after the fifth dose RT

3.4 PAPER V:

From the same cohort of patients in paper IV, we investigated 5 patients (4 from arm 1 and one patient from arm 2) (see Flowchart 2). Their base-line characteristics are summarized in Table 3.

Table 3. Patients and tumour characteristics

Patient nu	Patient Age (y)	cT	GG	GS	PSA, ng/ml		Testosterone nmol/L	Nuclear AR mean intensity, AU		Nuclear Ku70 mean intensity, AU	
					Before castration	After castration (decrease %)	After castration	Before castration	After castration (decrease %)	Before castration	After castration (decrease %)
1	60	3	4+3	7	274	2.4 (99)	<0.4	72	23 (67)	44	21 (51)
2	65	3	4+5	9	95	11 (89)	0.78	57	26 (55)	42	25 (40)
3	62	3	3+4	7	19	1.3 (93)	<0.4	42	23 (46)	45	34 (24)
4	71	3	4+5	9	59	18 (70)	0.43	64	66 (-4)	47	45 (4)
5	62	3	3+3	6	4	0.12 (97)	0.87	41	21 (58)	64	46 (27)

Abbreviations: cT, clinical tumour stadium; GG, Gleason grade; GS, Gleason score; AR, androgen receptor; AU, arbitrary unit.

3.4.1 Histological and immunofluorescence evaluation

We embedded all prostatic needle biopsy specimens in paraffin before they were sectioned and stained with haematoxylin and eosin (HE). A pathologist examined all specimens, identified the cancer areas in each specimen and scored those areas according to the Gleason system [78]. From all patients and from every biopsy setting, two cancer-rich biopsy specimens were selected and sectioned for immunofluorescence analysis. These sections were deparaffinised and rehydrated for antigen retrieval with Tris/EDTA (paper I and II) and buffer A (paper III-V), pH 9 in a pressure cooker. After blocking with 2% BSA, the sections were incubated with different primary antibodies at 40C overnight. Extensive rinsing was performed once; the sections were incubated with the secondary antibodies (donkey anti mouse IgG-alexa 488 (1:500), Molecular probe and donkey anti rabbit IgG-alexa 555 (1:500), Molecular probe) for one hour at room temperature. DNA was counterstained with TO-PRO-3 iodide (Molecular probe) and slides mounted with ProLong Gold (Molecular probe).

In Paper I, the chosen biopsy sections where immunofluorescence stained with HIF-1α antibody.

In Paper II, the chosen biopsy sections where immunofluorescence stained with Ku70 and γ-H2AX antibodies.

In Paper III, the chosen biopsy sections where immunofluorescence stained simultaneously with PARP-1 and PAR antibodies.

In Paper IV, the chosen biopsy sections where immunofluorescence stained simultaneously with two antibodies on the same slide; AR together with Ku-70, 53BP1 together with γ-H2AX, while phosphorylated DNA-PKcs and finally Ki67 where stained alone.

In paper V, the chosen biopsy sections where immunofluorescence stained simultaneously with AR together with Ku-70 and phosphorylated DNA-PKcs together with PAR.

Images from a tumour area with a good degree of immunofluorescence signals were selected from each biopsy. The corresponding areas in the HE-stained section were identified for histological verification of the tumour area.

In papers I and II, three images 100 × 100 μm, containing approximately 50 to 150 cells, were chosen for analysis.

In papers III and IV two images from each slide containing 300-600 cells were chosen for analysis.

In paper V the whole slides were analysed. ToPro (Molecular probe) was used as a DNA marker. Slides were mounted with prolong gold (Molecular probe).

All images were analysed, with respect to medium intensity inside the nuclei and in the cytoplasm. The nuclear area was defined by the ToPro signal and the cytoplasmic area as a 5 μm extension outside the nuclear area. For proteins with exclusive nuclear localisation (53BP1 and phosphorylated DNA-PKcs), the cytoplasmic intensity was subtracted as background activity. For other proteins, with both nuclear and cytoplasmic localisation (Ku70, AR and PARP-1), intensity values are presented without background subtraction. The number of Ki67 positive cells was counted with a threshold for Ki67 intensity in the nucleus in order to distinguish positive from negative cells. For markers forming foci the number and area of foci per DNA unit were measured. All measurements were performed using in house-written programme for NIH-imageJ [79].

Fluorescence images were obtained with either a Zeiss LSM 510-inverted confocal microscope or a Zeiss LSM 780-inverted confocal microscope, using a planapochromat 40X/NA 1.2 objective. Through-focus maximum projection images were acquired from optical sections 0.5 μm apart and with a section thickness of 1.0 μm. HE-stained images were obtained with a Leica scan system (Figure 7).

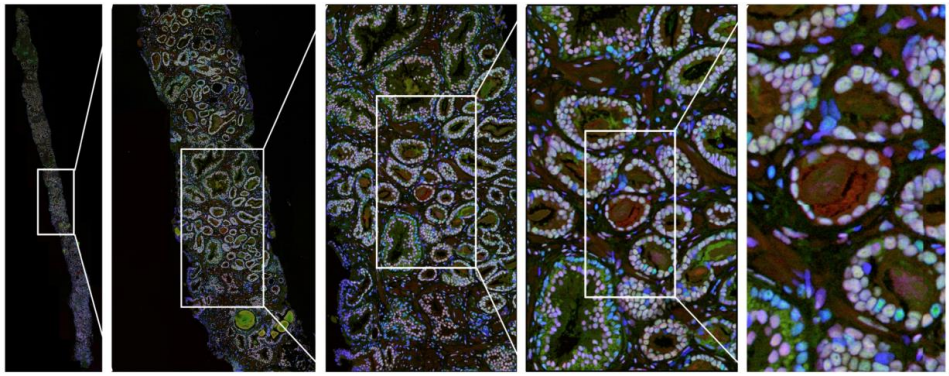

Figure 7. A whole needle biopsy is shown at the left panel. Each of the consecutive panels shows a magnification of the square plotted in the panel on its left. The biopsy is stained for DNA (blue), KU 70 (green) and Androgen receptor (red).

3.4.2 Coimmunoprecipitation of AR with Ku70 (Paper II):

The disintegrated frozen prostate tissue biopsies were incubated with lysis buffer (10 mM HEPES pH 7.5, 300 mM NaCl, 0.2 mM EDTA, 10 mM DTT, 20% glycerol, 0.1% Triton X-100, protease inhibitors) and after centrifugation the supernatant was incubated with anti-Ku70 Ab and Protein A/G-agarose beads. The proteins eluted from beads were separated by SDS-PAGE, blotted onto nitrocellulose membrane and probed with the anti-human AR Ab (Dako, M356201-2), anti-Ku70 Ab (sc-12729) and anti-actin Ab (sc-1616) followed by incubation with HRP-conjugated secondary antibody and protein bands were visualized using SuperSignal West Femto chemiluminescence substrate (Thermo Scientific).

4 STATISTICAL ANALYSIS

Paper I: Data in the bar graphs are shown as the mean ± SEM (standard error of mean). Non-parametric Wilcoxon matched pair's tests and 2-tailed student´s t-test were applied. Statistical significance is expressed as follows: *P < 0.05, **P < 0.01, ***P < 0.001.

Paper II: Data in the bar graphs are shown as the mean ± SEM and 2-tailed student´s t-test was applied. Correlation was measured using Spearman rank correlation coefficient. Statistical significance is expressed as follows: *P < 0.05, **P < 0.01, ***P < 0.001.

Paper III: 2-tailed Student's t-test was used in all statistical analyses. In ex vivo culture and xenograft experiments used Mann-Whitney U test. Data in the bar graphs are shown as the mean ± SEM., and statistical significance is expressed as follows: *P < 0.05, **P < 0.005, ***P < 0.0005.

Paper IV: Non-parametric test methods were applied. Related outcomes after different treatments within each arm were compared using the Wilcoxon Signed Ranks Test. Unrelated outcomes between the two arms were compared using the Mann-Whitney U Test. Correlation analysis was conducted using Spearman´s rho rank correlation test (ρ). All statistical tests were two-tailed with significance established at p <0.05. Statistical analysis was performed using the Statistical Package for the Social Sciences (SPSS), version 21.0. *P < 0.05, **P < 0.01, ***P < 0.001.

Paper V: Correlation analysis was conducted using Spearman´s rho rank correlation test (ρ). All statistical tests were two-tailed with significance established at p <0.05. Statistical analysis was performed using the Statistical Package for the Social Sciences (SPSS), version 21.0. *P < 0.05, **P < 0.01, ***P < 0.001.

5 RESULTS

5.1 PAPER I:

5.1.1 Castration reduces the levels of HIF-1α protein

Divergent levels of HIF-1α were observed among patients enrolled in this study. The HIF-1α levels varied from strong expression (mean intensity > 30) in five patients, week expression (mean intensity 10-30) in three patients, to background expression (mean intensity 0-10) in six patients. Castration reduced HIF-1α levels predominantly in patients who initially had a strong expression. However, in patients with initially background levels the HIF-1α were unaffected. Furthermore, the reduction in the level of the HIF-1α after castration was only correlated to initial levels of HIF-1α before castration. We observed no correlation between reduction in the level of HIF-1α and other parameters investigated like initial serum PSA and testosterone levels before castration or their levels after castration, age, Gleason grade, or days between biopsies (Figure 8).

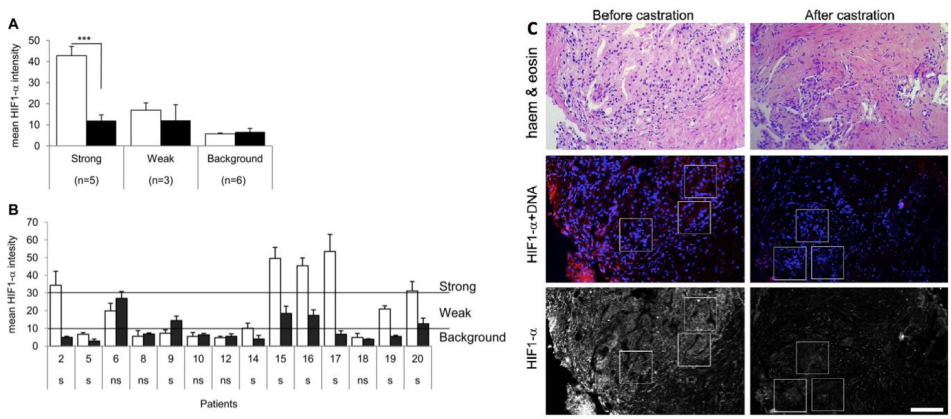

Figure 8. HIF-1α is up-regulated in a fraction of prostate tumors. Quantification of HIF-1α immunofluorescent staining intensity in prostate tumor biopsy specimens before (white bars) and after (black bars) castration. Upregulation of HIF-1α was classified as strong, weak, or at background level. **(A)** Patients pooled after HIF-1α classification. The means and standard errors of indicated number of patients are shown. Values marked with asterisks are statistically significant ($p < 0.001$; *t* test). **(B)** Individual patients are depicted. The means and standard errors of six images from two different biopsy specimens are shown (s = significant, $p < 0.05$; ns = not significant, $p > 0.05$; *t* test). **(C)** HIF-1α levels in prostate tumors decrease after castration. Prostate tumor biopsy specimens from prostate cancer patients before castration (left) and after surgical castration (right). Above, common hematoxylin and eosin staining. Below, immunofluorescent staining with antibodies against HIF-1α. Middle, HIF-1α expression (red) superimposed on ToPro-staining (DNA, blue). Bar = 100 μm. *Al-Ubaidi FL et al. Int J Radiat Biol Phys. 2012 Mar 1;82(3):1243-8. doi: 10.1016/j.ijrobp.2011.10.038.*

5.2 PAPER II:

5.2.1 Ku70 interacts with the androgen receptor and is reduced by castration

We showed that the AR and Ku70 proteins bind and interact with each other directly in prostate tissue both under normal circumstances and after castration and this interaction was not influenced by castration (Figure 1, Paper II). In paired slides, immunofluorescence staining of Ku70 in cancer areas before and after castration demonstrates a higher intensity of Ku70 proteins inside nuclei than in cytoplasm (Figure 9). However, the variation in these two fractions before castration was well correlated for each patient ($R2 = 0.817$, $P < 0.0001$). Despite the observed large individual variations in Ku70 expression both in nucleic and cytoplasmic fractions before castration, a decrease in the Ku70 level was seen in both fractions after castration in almost all patients (p=0,001, p=0,006). Furthermore, the reduction of Ku70 levels after castration was significantly correlated to initial Ku70 levels before castration both in nucleic and cytoplasmic fractions ($R2 = 0.811$ and $R2 = 0.944$ respectively, $P \leq 0.0001$ for both). Despite of castration method, there was a significant correlation between the decrease in Ku70 levels and the decrease in serum PSA levels after castration ((chemical nuclear $R2 = 0.91$, $P = 0.003$, cytoplasmic $R2 = 0.77$, $P = 0.023$ and surgical nuclear $R2 = 0.73$, $P = 0.018$, cytoplasmic $R2 = 0.84$, $P = 0.005$). Nevertheless, there was no such correlation between the decrease in Ku70 and the decrease in serum testosterone levels after castration (chemical nuclear $R2 = 0.014$, $P = 0.96$, cytoplasmic $R2 = 0.002$, $P = 0.70$ and surgical nuclear $R2 = 0.002$, $P = 0.96$, cytoplasmic $R2 = 0.11$, $P = 0.62$). An insight analysis of Ku70 and PSA kinetics revealed significant correlation between the decrease in Ku70 and serum PSA levels and the interval between first and second biopsies only among patients treated with surgical castration ($R2 = 0.77$, $P = 0.02$ and $R2 = 0.84$, $P = 0.019$ respectively). However, despite of castration method, no such correlation was observed between the decreased serum testosterone levels and the interval between first and second biopsies.

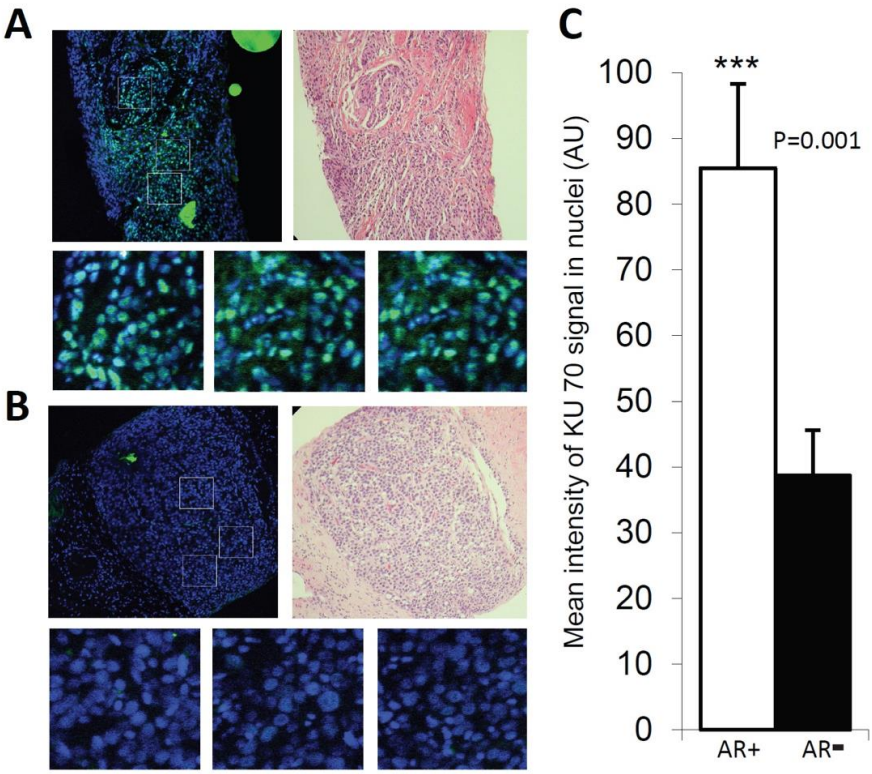

Figure 9. Determination of Ku70 in prostate tumours. **A,** top left, an immunehistofluorescence-stained section of a prostate biopsy before castration. The 3 squares outlined in the middle of the image mark the area chosen for intensity measurement. Ku70 is stained with a mouse-monoclonal antibody (green) and the DNA is costained with TO-PRO-3 (blue). Top right, a corresponding area from an adjacent section stained with hematoxylin and eosin. The 3 panels below are close-ups of the 3 areas depicted for intensity measurements. **B,** as in A, but the biopsy is taken after castration, but from the same patient. **C,** effect of castration on Ku70 in prostate tumours. Mean intensity of Ku70 in nuclei before (white bars) and after (black bars) castration. Error bars show SEM. ***, $P < 0.001$, Student *t* test. *Al-Ubaidi FL et al. Clin Cancer Res. 2013 Mar 15; 19(6): 1547-56. doi: 10.1158/1078-0432.CCR-12-2795.*

5.2.2 Ku70 reduction after castration correlates with an increase of γ-H2AX foci

Furthermore, to assess the repair kinetics, γ-H2AX staining was carried out and found a positive correlation between reduced Ku70 level and the increased expression of γ-H2AX foci after castration (R2 = 0.37, P = 0.022) (Figure 6E, paper II).

There were large individual variations in the initial Ku70 levels in both the nuclei and the cytoplasm. However, neither nuclear nor cytoplasmic fractions of initial Ku70 showed any significant correlation between Ku70 and prostate size, serum PSA, serum testosterone, Gleason score, or patient age.

5.3 PAPER III

5.3.1 Androgen Receptor promotes Homologous Recombination Repair

Since HR has a major role in IR-induced DSB repair in the late S/G2 phase of the cell cycle, we wanted to investigate whether there is a functional link between AR signalling and HR and whether castration downregulates expression of HR signalling in PCa.

We observed that AR signalling mediates the expression of many key mediators of HR in LNCaP prostate cancer cell line (Figures 1A, paper III). To investigate the AR regulatory role of HR, DR-GFP was performed and AR knockdown cells showed 40% reduction of HR activity (Figure 1C, paper III). Furthermore, using CRPC model cell line C4-2 with "high AR" and "low AR" levels, we showed that AR promotes IR-induced Rad51 foci, hence further support the functional link between AR and HR (Figures 1B, paper III).

To test the effect of androgen signalling on the DDR, in vivo study observed that the levels of γ-H2AX foci, a marker involved in early DDR, were reduced in PCa specimens after castration (Supplementary Figure 1E, paper III). Furthermore, in vitro study observed that AR promotes IR-induced γ-H2AX foci in C4-2 "high AR", whereas siRNA depletion of ATM in "high AR" cells bring down the γ-H2AX intensity to "low AR" levels (Supplementary Figure 1F, paper III). Moreover, reduced the expression of AR and ATM synergistically repress the growth kinetics of C4-2 cells following IR. There were no differences in growth kinetics in PC3-EV cells or PC3-AR cells prior to IR irrespective to AR status. IR repressed the growth response in PC3-AR cells, which expressed low AR (AR null) as compared with cells expressing high AR (AR full). However, those differences were abrogated upon ATM inhibition suggesting that AR regulates DDR via ATM signalling (Supplementary Figure 1G, paper III). The expression of MRE11, an integral component of the MRN complex that is involved in early activation ATM signalling, was reduced in AR knockdown cell lines (Supplementary Figure 1I & 1J, paper III). Furthermore, hydroxyurea-induced replication stress leads to increased MRE11 foci expression in C4-2 "high AR" cells compared to "low AR" cells, though this gained difference was lost by MRE11 inhibition (Figure 1E, paper III). Studies on LNCaP cell lines showed that inhibition of AR, ATM or MRE11 reduced activation of ATM downstream targets such as KAP-1 or p53 (unpublished data). Overall these experiments demonstrate that AR regulates HR signalling throughout a direct regulation of MRE11 expression, which consequently stimulates activation of ATM signalling and thereby HR essential protein Rad51.

5.3.2 Castration activates PARP in prostate cancer

Previously it has been shown that PARP1 activity is increased in HR defective cells and that sensitivity to PARP inhibitors is related to PARP activation [80]. Since ADT perturb HR repair, we hypothesized that PARP activity is increased following castration. To test that in vivo, we set up a prospective study with 48 patients. Immunofluorescence signalling levels of PARP-1 and its substrate PAR were quantified in cancer areas in corresponding paired slides (Figure 2A, paper III). To measure the activity of the PARP-1 enzyme, we calculated

the ratio of PAR and PARP-1 intensity in the nuclei. In castrated patients, we found a significant increase in PARP1 activity as reflected in increased PARylation (p=0.003) (Figure 2A and 2B, paper III) suggesting that PARP1 is activated as a result of androgen repression further strengthening our findings that AR regulates HR in Prostate cancer.

5.3.3 Androgen deprivation therapy is synthetically lethal with PARP inhibition in prostate cancer

It is well-established that PARP inhibitor can have a synthetic lethal effect in tumours with defective BRCA1/BRCA2, which are essential for efficient HR repair [81, 82]. Since we previously showed that castration leads to downregulation of HR activity, and since we observed high PARP activity in patients (Figure 2A, paper III) and in different PCa cell lines (Supplementary Figure 2B, paper III), we hypothesized that ADT combined with PARP inhibitor is synthetically lethal.

We showed that the combination of anti-androgens and PARP inhibitor repressed cell viability and growth kinetics in CRPC model cell lines indicating synthetic lethality (Figure 3A, 3C & Supplementary Figure 3B, paper III). Comparable repressions of cell viability and growth kinetics were observed when AR knockdown combined with PARP inhibitor (Figure 3D, Supplementary Figure 3D & 3E, paper III). However, AR expression in PC3-AR cells, a cell model transfected with AR mutant (T877A), abrogate the growth repression induced by PARP inhibitor. To evaluate the long-term effect of combined ADT and PARP inhibitor, the clonogenic potential of cells were assessed. Significant repression of the clonogenic potential of androgen sensitive DuCaP cells were observed not only as expected after anti-androgens or PARP inhibitor when given as a single treatment but even more significantly after combined treatment. Moreover, anti-androgens alone did not change the clonogenic potential of CRPC model LN3 cells, while combined treatment with PARP inhibitors sensitize these cells and repress the clonogenic potential. Using xenograft models of C4-2 and PC3 cells, we showed that the combined treatment of anti-androgens and PARP inhibitors reduces tumour size and weight (Figure 4A, 4B, 4C, paper III) without any adverse effect on the mice weight (Supplementary Figure 4B, paper III). In summary, these experiments support our hypothesis of contextual synthetic lethality between ADT and PARP inhibitors in cell line models and AR expression opposes growth repression by PARP inhibitor.

5.4 PAPER IV

5.4.1 Castration combined with RT increases the level of DNA damage in prostate cancer

Ki67, a proliferative marker, was used to evaluate in what way castration and/or RT would affect cycling PCa cells. Interestingly, the overall Ki67 cell numbers were about 7% in both arms prior to castration and RT (Supplementary Figure 2, paper IV). Castration treatment resulted in a drop to about 1.5% Ki67 positive cells in both Arms and 5 days RT treatment resulted in a dramatic reduction of Ki67 levels in both Arms to about 0.5%. These results suggest that the prostate cancer cells had exited from the cell cycle and entered into cell cycle

arrest, i.e. G_0, following both castration and RT and hence only relying on NHEJ for repair of RT-induced DSBs.

To assess the degree of DNA damage after castration and/or RT, γ-H2AX and 53BP1, DSBs markers, were used. In arm 1, following castration, observed non-significant changes in the number of nuclear γ-H2AX foci or 53BP1 foci ($p=0.8$, $p=0.7$). However, a significant increase in nuclear γ-H2AX foci or 53BP1 foci number following combined castration and RT ($p<0.001$ for both). In arm 2 we observed a significant increase in nuclear γ-H2AX foci or 53BP1 foci number following RT ($p<0.001$). Furthermore, we observed that subsequent RT to neoadjuvant castration induced significantly more γ-H2AX foci than those induced after RT alone. We conclude that combined castration and RT were more genotoxic than RT alone (Figure 10)

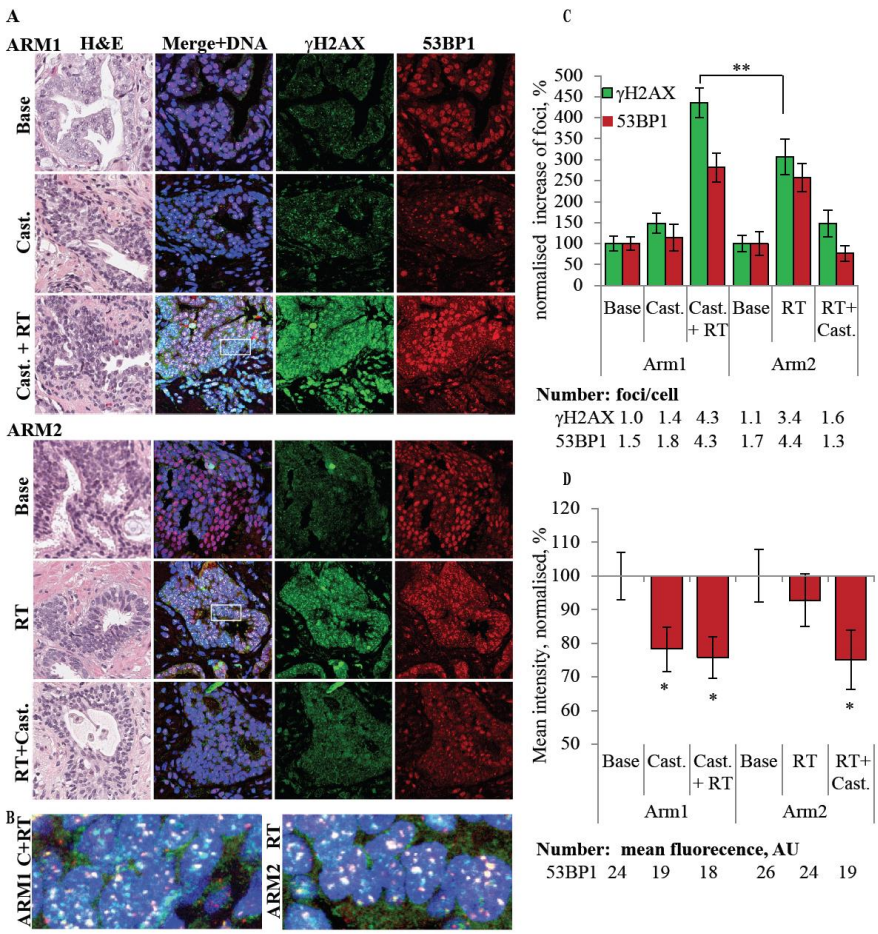

Figure 10. Determination of nuclear γH2AX and 53BP1 levels in prostate cancer tissue before treatment (Base) and after different treatment modalities in Arm 1 and Arm 2. **A)** Different sections of prostate biopsies are shown and each biopsy is sectioned and stained. The first section was stained with haematoxylin and eosin staining for identifying cancer areas. A further corresponding adjacent section obtained from the same biopsy was stained with immunofluorescence staining with γH2AX

mouse-monoclonal antibody (green) and 53BP1 rabbit-polyclonal antibody (red). The DNA was co-stained with TO-PRO-3 (blue). Upper sections were from a patient in Arm 1; the upper panel was before treatment (base), middle panel was after castration and lower panel was after castration and RT. Lower sections were from a patient in Arm 2; the upper panel was before treatment (base), middle panel was after RT and lower panel was after RT and castration.

B) A close up selected section from previous patients in Arm 1 after castration and RT and Arm 2 after RT (merge γH2AX and 53BP1with DNA). **C)** Normalised percentage of number of γH2AX foci (green bars) and 53BP1 foci (red bars) in nuclei before treatment (base) and after different modalities of treatment in Arm 1 and Arm 2 for all patients. Error bars show standard error of mean. **D)** Normalised percentage of mean intensity of 53BP1 levels in nuclei before treatment (base) and after different modalities of treatment in Arm 1 and Arm 2 for all patients. Error bars show standard error of mean.

5.4.2 Castration reduced level of AR, Ku70 and phosphorylated DNA-PKcs proteins

Here we wanted to investigate the effect of castration on expression levels of AR and D-NHEJ essential proteins, ku70 and phosphorylated DNA-PKcs. In arm 1, mean intensity of nuclear AR and Ku70 proteins reduced after castration ($p<0.001$, $p=0.005$) and after combined castration and RT ($p<0.001$, $p=0.001$).

In arm 2 we observed no difference in the mean intensity of nuclear AR after 5 X 2 Gy RT ($p=0.5$). However, a significant increase in mean intensity of nuclear Ku70 was observed after similar dose radiation ($p=0.014$). After subsequent RT and castration the mean intensity of nuclear AR and Ku70 proteins were decreased significantly ($p<0.001$, $p=0001$). A significant correlation was observed between the mean intensity of nuclear AR and Ku70 before treatment ($\rho=0.62$, $p<0.001$) and following castration in Arm 1 ($\rho=0.65$, $p<0.001$). Furthermore we observed a significant correlation between the induced changes in nuclear AR and Ku70 proteins in arm 1 after castration ($\rho=0.52$, $p<0.001$), and, after combined castration and RT ($\rho=0.33$, $p=0.001$) and in arm 2, after RT ($\rho=0.64$, $p<0.001$) and after subsequent castration ($\rho=0.53$, $p<0.001$) (Figure 11).

Phosphorylated DNA-PKcs was examined to reveal the activity of D-NHEJ repair. In Arm 1, the mean area of foci of phosphorylated DNA-PKcs remained unchanged after both castration and combined castration and RT. However in arm 2 we observed a significant increase in the mean area of foci of phosphorylated DNA-PKcs after RT ($p=0.01$) followed by significant reduction after subsequent castration ($p<0.001$) (Figure 12).

We observed no significant correlation between mean intensity of nuclear AR, Ku70 or DNA-PKcs proteins and pre-treatment serum PSA levels, prostate size or Gleason grade.

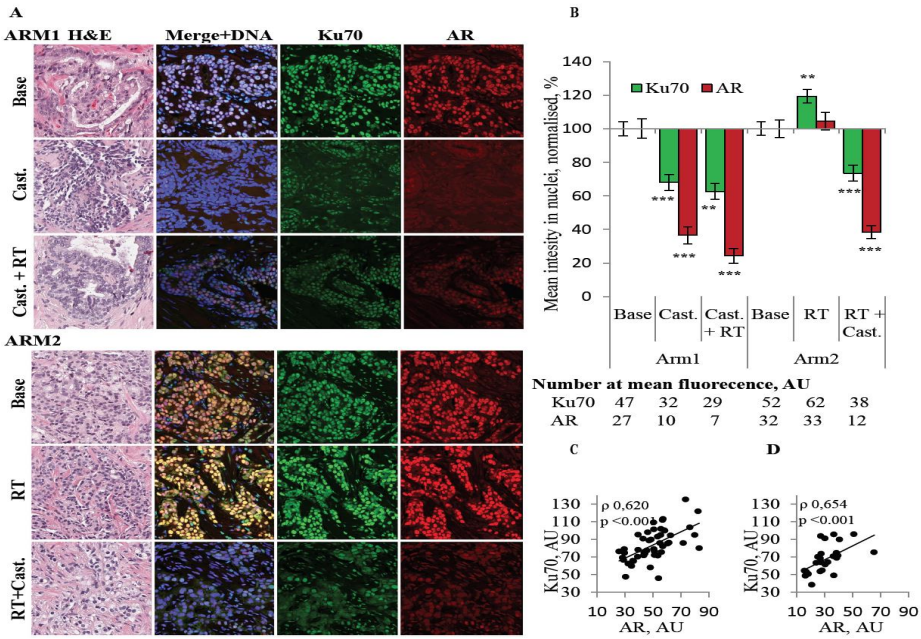

Figure 11. Determination of nuclear androgen receptor (AR) and Ku70 levels in prostate cancer tissue before treatment (Base) and after different treatment modalities in Arm 1 and Arm 2. **A)** Different sections of prostate biopsies are shown and each biopsy is sectioned and stained. The first section was stained with haematoxylin and eosin staining for identifying cancer areas. A further corresponding adjacent section obtained from the same biopsy was stained with immunofluorescence staining with Ku70 mouse-monoclonal antibody (green) and AR rabbit-polyclonal antibody (red). The DNA was co-stained with TO-PRO-3 (blue). Upper sections were from a patient in Arm 1; the upper panel was before treatment (base), middle panel was after castration and lower panel was after castration and RT. Lower sections were from a patient in Arm 2; the upper panel was before treatment (base), middle panel was after RT and lower panel was after RT and castration. **B)** Percentage of normalized mean intensity of AR (red bars) and Ku70 (green bars) in nuclei before treatment (base) and after different modalities of treatment in Arm 1 and Arm 2 for all patients. Error bars show standard error of mean. **C)** Spearman´s rho rank correlation test (ρ) between mean intensity of AR and Ku70 in nuclei for all patients before treatment (base) in Arm 1 and Arm 2. **D)** Spearman´s rho rank correlation test (ρ) between mean intensity of AR and Ku70 in nuclei for patients in Arm 1 after castration.

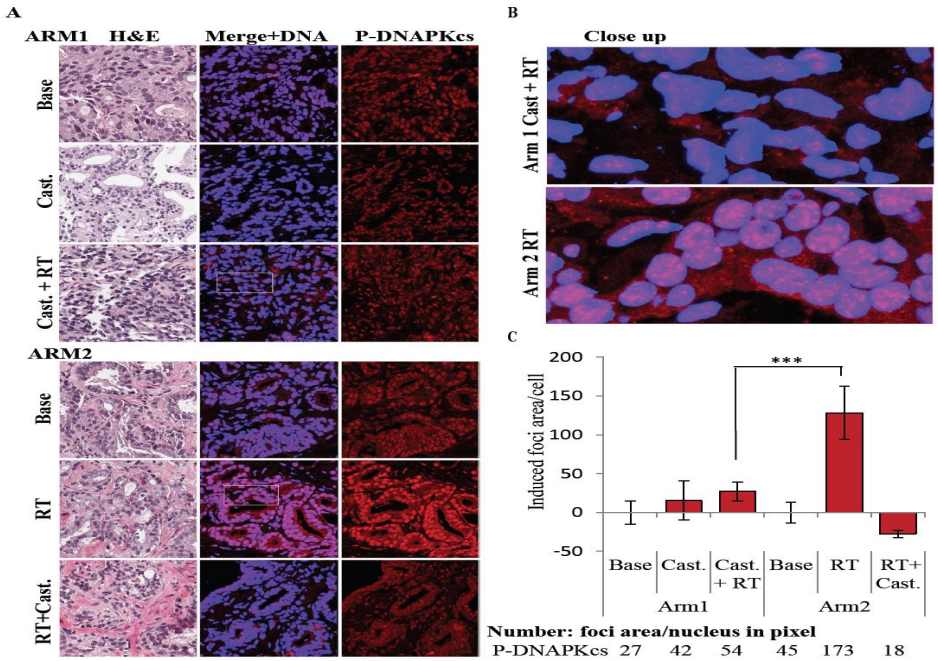

Figure 12. Determination of nuclear phosphorylated DNA-PKcs levels in prostate cancer tissue before treatment (Base) and after different treatment modalities in Arm 1 and Arm 2. **A)** Different sections of prostate biopsies are shown and each biopsy is sectioned and stained. The first section was stained with haematoxylin and eosin staining for identifying cancer areas. A further corresponding adjacent section obtained from the same biopsy was stained with immunofluorescence staining with P-DNA-PKcs rabbit-polyclonal antibody (red). The DNA was co-stained with TO-PRO-3 (blue).). Upper sections were from a patient in Arm 1; the upper panel was before treatment (base), middle panel was after castration and lower panel was after castration and RT. Lower sections were from a patient in Arm 2; the upper panel was before treatment (base), middle panel was after RT and lower panel was after RT and castration. **B)** A close up selected section from previous patients both in Arm 1 after castration and RT and in Arm 2 after RT (merge P-DNA-PKcs with DNA). **C)** Induced P-DNA-PKcs foci/cell (normalised) in nuclei before treatment (base) and after different modalities of treatment in Arm 1 and Arm 2 for all patients. Error bars show standard error of mean.

5.5 PAPER V

5.5.1 Hormone-naïve prostate tumour cells have heterogeneous response to castration with a co-variation between AR and D-NHEJ activity

In this study, we observed a heterogeneous response of prostate tumour cells to castration. Surprisingly, two kinds of prostate tumour cells were identified following castration. The majority of tumour cells had a significant low level of nuclear AR. However, sub-populations of tumour cells that varied from a few cells to a dozens of cells and gathered as subclones were still expressing high levels of AR after castration (Figure 13).

A significant correlation was observed between the mean intensity of nuclear AR and Ku70 levels in each examined patient before and after different treatments. Moreover, the expressions of AR in clusters of cells co-varied with the expression pattern of both Ku70 and P-NA-PKcs foci. This finding is likely to strengthen our conclusion that cells retaining high levels of AR after castration, may retain their ability of a proficient DNA damage repair and vice versa.

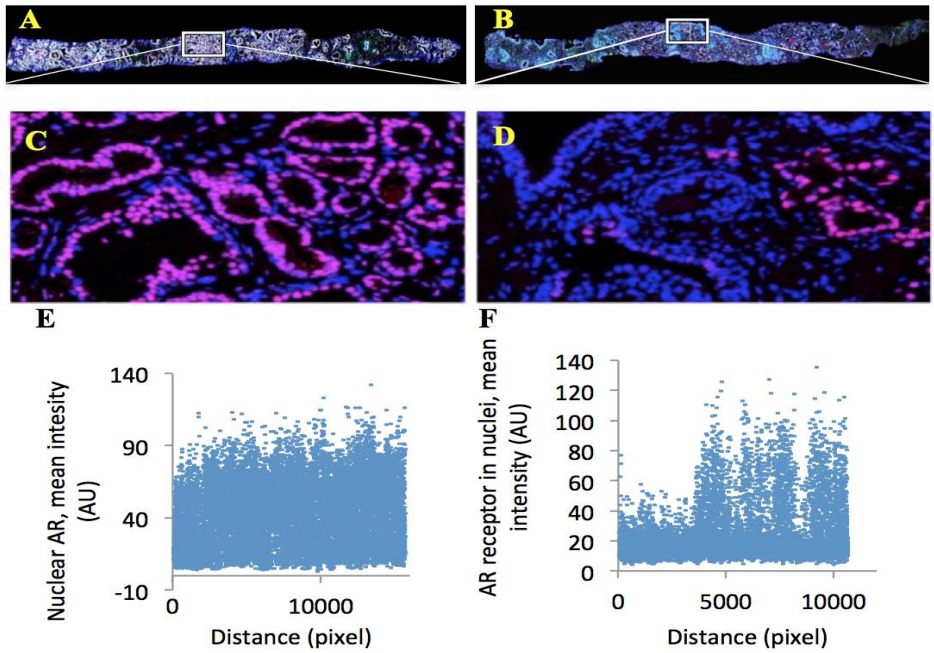

Figure 13. Data from tiled fluorescence images of whole prostate needle biopsies stained for androgen receptor (AR). **A)** Tiled images of prostate needle biopsy stained for AR before castration and **B)** after castration. **C)** Close-up tiled fluorescence images of prostate epithelial cells stained for AR showed the homogeneous staining of AR before castration and **D)** after castration, where we can see an incomplete suppression of AR in clusters of epithelial cells in different areas throughout the prostate needle biopsy. **E)** Signals of nuclear AR from epithelial cells of the same prostate needle biopsy in 4A, plotted against the distance along the length axis of the whole needle biopsies were measured in approximately 16,000 cells before castration. **B)** Signals of nuclear AR from epithelial cells of the same prostate needle biopsy in 4B, plotted against the distance along the length axis of the whole needle biopsies were measured in approximately 12,000 cells after castration.

5.5.2 Neo-adjuvant castration may trigger alternative DNA repair machinery mediated via PARP-1

A significant inverse correlation between the mean intensities of PAR and the mean intensities of AR and Ku70 after castration and combined castration and RT. Furthermore, a tendency to inverse correlation between the PAR level and the levels of AR, Ku70 and phosphorylated DNA-PKcs were observed in different tumour areas. Following castration,

tumour areas that retain high levels of AR, Ku70 and phosphorylated DNA-PKcs express low levels of PAR and vice versa (Figure 14).

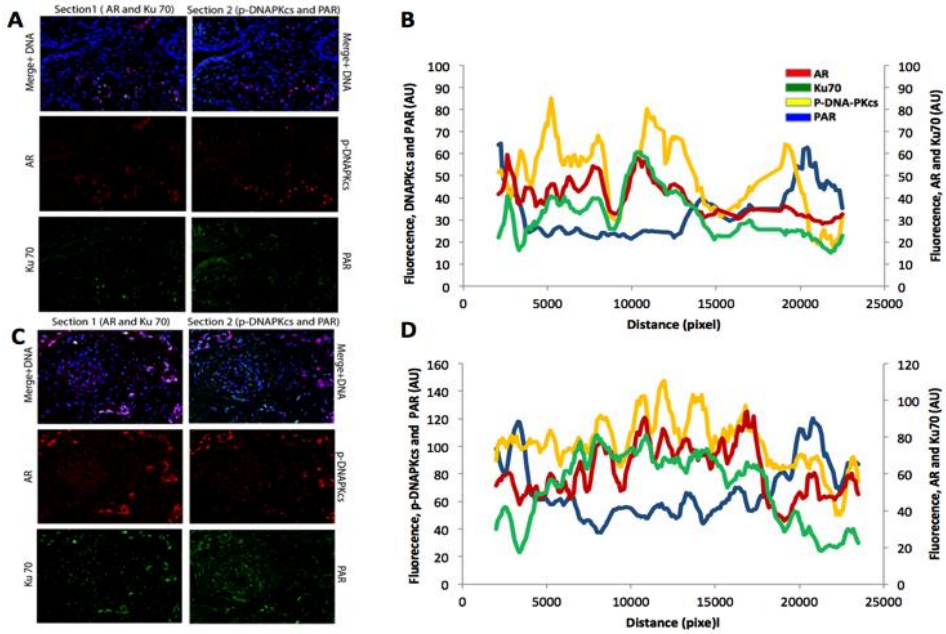

Figure 14. Determination of nuclear AR, Ku70, P-DNA-PKcs and PAR levels from prostate epithelial cells in prostate needle biopsies. **A)** Tiled fluorescence images of two matched adjacent sections in one needle biopsy before castration, where AR and Ku70 signals in section 1 were merged with P-DNA-PKcs and PAR signals from a corresponding area in the adjacent section 2. **B)** Graphs showing signals of AR (red), Ku70 (green), P-DNA-PKcs (yellow) and PAR (blue) plotted against the distance along the length axis of two matched adjacent sections of one whole needle biopsy before castration. The graph shows the positive co-variation between AR (red), Ku70 (green) and P-DNA-PKcs (yellow) and how these three proteins inversely co-vary with PAR (blue). **C)** The same as in fig. 5A, although after castration. **D)** The same as in fig 5B, although after castration.

5.5.3 Divergent responses in AR, Ku70 or PSA despite castration serum testosterone levels

Previously, a significant correlation was demonstrated between the decrease in serum PSA and nuclear Ku70 levels in patients with metastatic PCa following castration, suggesting that the PSA nadir may reflect simultaneously the nadir value of DNA repair activity [83]. A significant reduction in the mean intensities of nuclear AR and Ku70 levels were observed following castration in patients 1-3 and 5, whose serum PSA reduced most, by 89-99%, after castration. However, in patient number 4, whose serum PSA was only reduced by70% despite castrate levels of serum testosterone, no reduction was observed in the mean intensity of nuclear AR or Ku70 after castration.

5.5.4 Nuclear AR and serum PSA levels correlate

A significant correlation between the levels of AR in nuclei and serum PSA levels after castration was observed in all five patients ($\rho=1$, $p<0.001$). Indeed, the finding was expected, since AR controls PSA expression.

6 DISCUSSION

Since androgens and AR signalling are crucial for the initiation and development of most prostate tumours, ADT remains a backbone therapeutic of the disease. Currently, RP and RT are radical treatment methods for localised PCa with excellent long-term results. However, in locally advanced and high risk disease RT is the method of choice. Yet the outcome is frequently poor and combined with high risk of local failure, especially when RT is administered as a single treatment modality. Dose-response studies have shown that dose-escalation over 78 Gy results in non-significant difference in 5 years recurrence rate among patients with high risk PCa [19, 84].

Currently several prospective randomised trials showed that combined ADT, in neoadjuvant setting, with RT are superior to RT alone in high risk disease. However the optimal timing and underlying mechanisms of neoadjuvant castration have remained undetermined [17,25, 28-32].

We hypothesized that castration reduces the level of hypoxia, as measured by HIF-1α level, in PCa and this may be a mechanistic model of how radiosensitivity improves following castration. We observed that castration reduces the HIF-1α levels in PCa cells with an initial high level of this protein. Furthermore, an individual variety of HIF-1α levels, which was in accordance with other previous studies, were observed [85, 86]. The hypoxic characterisation of PCa becomes evident in a prospective clinical study, using needle electrode measurements in patients with a localised disease, and obviously is the hypoxic microenvironment of the tumours that drives tumourigenesis to more aggressive phenotypes with an early biochemical relapse following RT, independent of pre-treatment tumour clinical stage, Gleason score or serum PSA [87]. Another prospective clinical trial [88] measured the levels of HIF-1α in diagnostic prostate needle core biopsies from patients with untreated localised PCa, who then were treated with either RT or RP. Similarly, the pre-treatment hypoxia, measured by the HIF-1α level, was significantly correlated with high biochemical recurrence rate after treatment, independent of local tumour stage, Gleason score or serum PSA. Worthwhile to note the diversity of factors that influence the regulation of HIF-1α including the expressions of tumour oncogenes or tumour suppressor genes, reactive oxygen radicals, different growth factors and androgens [89-91]. In *in vivo* studies, it has been shown that AR is co-expressed with HIF-1α and VEGF in androgen sensitive PCa and that AR stimulates angiogenesis in early PCa via changes of both HIF-1α and VEGF levels [74, 77]. Therefore, the castration-induced reduction of the HIF-1α levels observed in our study is possibly related to altered AR expression.

It is well known that the presence of tumour hypoxia is associated with increased radioresistance. Likewise, the need for oxygen in the target cancer tissue at the time of irradiation is a critical factor that enhances tissue toxicity after RT, hence influences irradiation efficacy [92, 93]. In an *in vivo* study [87], using needle electrode measurements on patients with localised PCa, it has been shown that castration reduces hypoxia and increases intraprostatic oxygen tension, a mechanism that may explain the improved

radiosensitivity and paralleled may suggest that the reduced HIF-1α level observed in our study, could be explained by the reduced hypoxia and subsequently by the improved oxygenation following castration. It is also well-established that hypoxic tumour cells are associated with impaired DNA repair [92] and acquisition of an aggressive phenotype frequently leading to treatment resistance and metastasis [94].

Since RT induces a number of genotoxic events that jeopardise the genomic integrity and survival of tumour cells, the activation of DDR, which comprises several DNA repair pathways, will be essential to maintain the genomic integrity and the survival of these cells. Consequently, we hypothesized that ADT influences DDR in PCa. Since an *in vitro* study using LNCaP cells, has reported an interaction between AR and Ku70 [95], we hypothesized that castration impairs the D-NHEJ-repair system by downregulating expression of its essential proteins Ku70 and DNA-PKcs, thus improving radiosensitivity.

To date, it's well recognised that AR mediates the transcription of a network of DDR genes that facilitates the repair of DSBs [95, 96]. Here we confirmed the interaction between AR and Ku70 proteins, which may reveal a mechanistic link between castration and the reduced Ku70 level. Additionally, we demonstrated a correlated and a significant reduction of both nuclear AR and Ku70 proteins in PCa tissue following castration. Since the influential role of Ku70/Ku80 components of D-NHEJ are well-recognized for effective radiation-induced DSB repair [59, 97], severe depletion of Ku70 protein by castration will be expected to impair D-NHEJ in PCa and may explain the increased radiosensitivity following castration. Several studies have been shown that Ku70 mutant cells are the most radiosensitive [63, 98]. Moreover, we also demonstrated that castration reduces the levels of phosphorylated DNA-PKcs in PCa following RT. Undoubtedly, the later bring more comprehensive evidence suggesting that castration suppresses D-NHEJ activity in PCa, hence promoting radiosensitivity. Since D-NHEJ is confirmed to have a crucial role in IR-induced DSBs repair and since Ku70 and DNA-PKcs proteins have an essential role in the D-NHEJ repair pathway [59, 97, 99-102], the up-regulation of these proteins enhances radioresistance, whilst their downregulation promote radiosensitivity [103-106]. *In vitro* models targeting the catalytic motif of DNA-PKcs induce radiosensitive phenotype cells [107-109]. Likewise, repressed expression of Ku70 and DNA-PKcs in a mutant xenograft model has been shown to enhance radiosensitivity [110, 111]. Furthermore, ADT in an LNCaP cell model reduces D-NHEJ-mediated repair [96]. It is evident that DNA-PKcs is a key target in AR-mediated DNA repair and DNA-PKcs activity is promoted after genotoxic insult while it is repressed by ADT [112]. Obviously, the aforementioned provide a plausible explanation of how the AR regulates DDR, supporting our hypothesis that castration improves radiosensitivity by downregulating D-NHEJ.

Since the AR is a major transcription factor involved in growth regulation and progression of PCa and since HR is an indispensable pathway involved in DSBs repair during S/G2 phase of cell cycle, we wanted to further investigate the role of AR in regulating the HR signalling. Both in *in vitro* and *in vivo* xenograft models, we showed that several essential genes

regulating the HR repair pathway were downregulated following the loss of AR activity. It has been evident that targeting HR pathway promotes radiosensitization in *in vivo* studies [113, 114]. In fact, the observed lower levels of RAD51 foci and consequently lower HR activity following AR knockdown shown in paper III, support that the AR regulates the overall HR response. It is well-established that MRE11, a protein comprised in the MRN complex, is activated early as a response to DSBs and consequently activates ATM [115], which in turn activates ATM-mediated HR signalling [116]. Our study demonstrates that the AR regulates MRE11 and ATM activity, which subsequently regulates DNA end-resection, therefore committing cells to undergo DSBs repair via HR. Furthermore, γ-H2AX foci form an early response to DSBs and they co-localize with other components of DDR including MRE11, ATM, RAD51 and 53BP1 [117, 118]. γ-H2AX is an active component of DDR and is involved in ATM signalling. H2AX-depleted mice models have a defected DNA-repair and an increased radiosensitivity [119, 120]. In our in vivo study (n=15), we showed that castration significantly reduces the level of γ-H2AX foci. Moreover, in an *in vitro* study, we showed that IR induces significantly higher levels of γ-H2AX foci in AR-full cells than in AR-depleted cells. Expectedly, we also showed that the inhibition of ATM leads to less increase in γ-H2AX foci in AR-full cells suggesting that AR regulates γ-H2AX via ATM signalling. In summary, these experiments propose a central role of AR signalling in regulating DDR in PCa as it regulates a number of key steps in both D-NHEJ and HR mediated repair.

Generally expected, an impaired DDR leads to slower repair kinetics, thus higher amount of unrepaired DSBs following IR. In fact, in our first cohort study (n=14), we observed a significant correlation between the decrease in nuclear Ku70 levels and the increase in γ-H2AX foci, a marker for DSBs and sensitivity to IR [121, 122]. However, we did not observe any significant difference in γ-H2AX foci levels in biopsies before and after castration. These apparently contradictory results may be explained by the effect of castration on cell proliferation. Cancer cells, due to their high proliferative rate, acquire high levels of endogenous oxygen radicals that consequently leads to more DNA damages. If these damages remain unrepaired during replication, this consequently leads to collapsed replication forks [123] and subsequently to an accumulation of γ-H2AX foci. Since we demonstrate that the proliferation rate, measured by Ki67 levels, and DDR is suppressed after castration, we suggest that castration initiates processes that can lead to either increase or decrease of γ-H2AX foci. Notably, no or minor castration-induced decrease of Ku70 levels leads to a decrease of γ-H2AX foci, meanwhile a large decrease of the Ku70 levels following castration leads to an increase of γ-H2AX foci, implicating a functional linkage of decreased Ku70 levels and impaired DDR.

In the second cohort study (n=48) in vivo, as expected we observed that the induced changes of γ-H2AX foci, after combined castration and RT were significantly higher than after RT only. This indicates a higher accumulation of unrepaired DSBs subsequent to a lower rejoining-rate of the damaged DNA strands, which may further strengthen our finding of impaired D-NHEJ after castration. On the other hand, in an *in vitro* assay, we showed that

AR regulates γ-H2AX via ATM signalling and IR induces less γ-H2AX in AR depleted cells. This finding might seem contradictory. However, a newly published study showed that low dose IR induces a prolonged and ATM-independent expression of γ-H2AX [124]. We believe that several factors may contribute to these differences in dose-response for γ-H2AX foci in our studies. Most importantly, in the biopsies, the IR-induced DNA damages and the overall repair after 5 days treatment are measured. Upon IR *in vivo*, a repair defect will result in an accumulation of lesions, while *in vitro*, we immediately uncover the DDR defect observed. Other potential explanations are in the first place that there are sample dissimilarities, i.e. cell models *in vitro* vs. prostate tumour tissue *in vivo* with subsequently different postulated milieu of microenvironment and background mutation, which will react in different ways. Secondly, there is the deference in the exposed IR dose, i.e. single dose of 10 Gy for *in vitro* experiments vs. fractionated doses of 2 Gy/day for 5 consecutive days for the *in vivo* patient situation. Thirdly, the time measured to calculate the levels of γ-H2AX foci after exposure to IR alone, i.e. 2 hours after a single dose of IR in the *in vitro* experiment and 3 hours after the last IR at the 5th consecutive day of the *in vivo* situation. The aforementioned may be the reasons for the accumulation of the high levels of γ-H2AX foci following IR alone in *in vivo* experiments.

Interestingly, we observed that castration reduces the overall intensity of 53BP1 significantly. This finding emphasizes the critical role of AR in regulating DDR in PCa and may lead to novel therapeutic applications in the future. However, surprisingly castration did not affect the number of 53PB1 foci after RT. These seemingly contradictory results might be explained by the decrease of overall 53BP1 intensity after castration. Hence, a shortage of the protein pool leads to less foci formation despite massive DNA damage following RT. This would be most pronounced in patients with high levels of DNA damage after combined castration and RT. Thus, the lower mean intensity of 53BP1 protein will probably mask the difference between the level of persistent DSBs after combined castration and RT as compared with RT alone.

It has remained unclear which repair system dominates the IR-induced DSBs repair pathway, D-NHEJ or HR. Currently, it is evident that castration reduces the proliferative activity of prostate cells (cells in S and G2 phases), as measured by reduced Ki67 expression. However, there is still contradictory evidence that castration leads to a long-term apoptotic effect in human PCa [43, 125]. A consequence of a genotoxic event such as RT will be a varying amount of DNA damage and activation of DDR. We have shown that both castration and RT reduces cell proliferation dramatically, suggesting that the majority of cells had exited the cell cycle and entered into cell cycle arrest i.e. G0, where D-NHEJ is the most dominant DSB-mediated DNA repair pathway. Since HR repair of IR-induced DSBs predominantly operates during the S/G2 phase of the cell cycle, we may conclude that D-NHEJ, rather than HR, is the most dominant pathway involved in the repair of radiation induced DSBs following castration.

In fact, effective DNA repair reduces the efficacy of RT. As previously discussed, a reduced level of hypoxia following castration would be expected to improve the DNA repair, thereby increasing radioresistance. However, since it is evident by many clinical studies that the sensitivity to RT improves after castration [13] and since it has been shown that castration impairs the DNA repair of DSBs, we suggest that any enhancement in DNA repair caused by decreased hypoxia is of less importance than the castration-induced impairment of DNA repair.

Since we have shown that castration suppresses both D-NHEJ- and HR-mediated repair of IR-induced DSBs, it becomes crucial to investigate the role of androgen depletion on alternative DNA repair so called B-NHEJ mediated by PARP-1. Interestingly, a newly published in vivo study reported that prostate tumour cells carried TMPRSS2-ERG gene fusion, the most common genetic aberration, which is found in approximately 50% of patients with PCa [126, 127]. That means an impaired D-NHEJ repair pathway by inhibiting DNA-PKcs and enhancing the PARP inhibitor-mediated radiosensitization [128]. Furthermore, TMPRSS2-ERG expressing tumour cells have elevated levels Rad51 foci and HR activity after IR, indicating an HR compensatory effect for the defective D-NHEJ and the plausible synthetic lethal interaction that may exert between TMPRSS2-ERG expressing tumour cells and PARP inhibitors [128]. We hypothesised that PARP-mediated B-NHEJ will gain a more predominant roll in IR-induced DSBs repair following castration and combined treatment of ADT and PARP inhibitor leads to synthetically lethal effect in PCa. It is well-established that HR-defective BRCA2 mutant cells rely on PARP-1 for DSBs repair and PARP inhibitors have a synthetic lethal effect on these cells [70, 82, 129]. More interestingly, for irradiated *in vivo* cells, it has been shown a high binding affinity of Ku70 to damaged DNA-ends that hampers the contribution of PARP-1 in DSB repair. On the other hand, depletion of indispensable components of D-NHEJ, especially Ku70, leads to recruitment of PARP-1 for DSBs repair via the B-NHEJ pathway [67]. To our knowledge for the first time, our finding demonstrates that castration significantly increases PARP-1 activity *in vivo*, hence indicating ongoing B-NHEJ-mediated DSBs repair, whereas the activity of essential D-NHEJ and HR repair pathways were repressed following castration in hormone naïve PCa. Although the role of PARP-1 in DNA-damage repair is well-understood, a recent *in vivo* study demonstrates the dual function of PARP-1. In addition to its involvement in DNA repair, it promotes an AR transcriptional function on DNA repair genes in AR-positive PCa cells. Furthermore, PARP-1 inhibitors reduce the expression of AR-target genes [130]. Actually the fundamental issue to address here is obviously the high biochemical recurrence rate despite adequate local treatment of high risk PCa with combined neoadjuvant castration and RT [131]. Indeed this may provide a rationale to exploit the dual inhibition of both AR and PARP functions in early treatment of patients with high risk diseases.

Our *in vitro* work showed that combined ADT and PARP inhibition repress growth kinetics and cell viability in CRPC cell lines and provide a mechanistic insight into the observed synthetic lethality between AR and PARP inhibition. Although germ-line BRCA1/BRCA2

mutations, which are often associated with aggressive malignant characteristics, are present in only a few percent of patients with PCa [132], a lot of sporadic PCa cells will gain a molecular and clinical characteristic similar to those of BRCA-related tumours, with BRCA1-like mutations detected in 13–46% of cases [133] and BRCA2-like and ATM mutations in approximately 30 % (unpublished data). The development of CRPC is associated with reactivation of the AR signalling through either an inadequate suppression of intratumoural androgen, by primary castration, or through a divergent molecular mechanism including gain-of-function mutations in the genes of the androgen biosynthetic pathway [134]), point mutations in the AR gene leading to anti-androgen resistance [135] and constitutively active AR splice variants [136]. On the other hand, despite PARP-1 is overexpressed in multiple cancer types including PCa, not all BRCA-defective cancers seem to respond to PARP inhibitor monotherapy. The limited success of PARP inhibitor therapy may relate to BRCA gene reversion [137] or other factors that functionally compensate for the loss of HR proficiency such as loss of 53BP1 function in BRCA1 depleted mammary tumours [138]. Our data support the hypothesis that prostate tumour cells treated with ADT may rely on B-NHEJ for DSBs repair and combination of ADT and PARP inhibitor could be synthetically lethal. Rather interesting in the current heterogeneity study, is the observed inverse correlation between PARP-1 activity and AR and D-NHEJ. In a previous *in vivo* study, we showed that PARP-1 activity was increased after castration (Asim et al., in preparation). The current study aimed at further investigating the correlation between AR and PARP-1 activity in the heterogeneous landscape of AR in prostate cancer. Interestingly, an individual analysis of the patients (n=5), showed significant inverse correlation between the levels of PAR and nuclear AR and nuclear Ku70 were observed following different treatments. Furthermore, in depth analysis of different tumour areas throughout the whole needle biopsy specimen, showed a tendency to such an inverse correlation between the PAR levels and the levels of AR, Ku70 and P-DNA-PKcs, suggesting that prostate tumour cells, where castration leads to impairment of D-NHEJ, could rely on PARP-mediated DNA repair pathway and vice versa.

Another interesting finding in our AR heterogeneity study is that despite of castration levels in serum testosterone we can see an inadequate suppression of AR in subclones of cells throughout prostate tumour areas with a co-variation between the high expression levels of AR and nuclear Ku70 and phosphorylated DNA-PKcs proteins. This indicates an activation of D-NHEJ despite of castration.

The important question addressed here is the biological nature of castration-resistant prostate cancer cells. Are they evolutionary mutated cells from otherwise primary androgen sensitive cells according to selective pressure of ADT or are they quiescent castration resistant tumour cells that acquire growth-promoting function according to clonal selection. The mechanism behind, and timing for the development of CRPC may lead to a comprehensive understanding of the underlying mechanism behind the emergence of such resistant cells after primary hormone manipulation. In line with this, two models have been proposed: the adaptation model which hypothesized that selective pressure of ADT encourages mutational

events in the androgen signalling pathway, and the clonal selection model which hypothesized the heterogeneous nature of prostate cancer and the pre-existing clone of castration-resistant cells [139, 140].

Several scientific observations support the adaptation models and provide a rationale for the emergence of these resistant subclones observed in our heterogeneity study. Gene expression analyses of hormone naïve PCa, PCa subjected to ADT, and CRPC have revealed that the overall expression patterns of genes for CRPC were more similar to those of the untreated, hormone-naive primary tumours than to tumours undergoing ADT [141]. Several studies have previously reported that ADT decreases intraprostatic androgens such as testosterone and dihydrotestosterone by only 75% to 80% after accomplishing castrate serum testosterone levels with a GnRH analogue [49, 142, 143]. Residual prostatic androgen levels in castrated patients are sufficient to stimulate androgen-responsive genes and activate the AR [144]. An *in vivo* study by *Mostaghel et al* showed that many androgen-regulated genes were not suppressed after 3 - 9 months of neoadjuvant castration [145]. The heterogeneity in AR response in the current study highlights the findings in previous studies that demonstrated continued substantial androgen-dependent gene expression after castration.

Treatment with intense ADT with a GnRH analogue in combination with the novel antiandrogen agent, abiraterone acetate, in patients with primarily localized hormone-naïve PCa show further suppression of intraprostatic androgens [146]. The afore-mentioned support the assumption that continued AR-mediated signalling after primary hormone manipulation is probably driven by the presence of residual tissue androgen. Furthermore, clinical trials for patients with CRPC using second-generation anti-androgens, such as abiraterone acetate and enzalutamid, suggest that AR signalling remains a fundamental promoting mechanism of CRPC [147, 148]. To date, different spliced variants of AR, which lacks the ligand-binding domain and are functionally active despite the absence of androgens, have shown a putative role in developing resistance to anti-androgen therapy in CRPC [149]. This finding suggests that the production of an AR spliced variant could be the consequence of suboptimal intraprostatic androgen ablation, which in turn may lead to adaptation of prostate tumour cells to survive in low-level androgen environment and thereby undergo mutations.

Several scientific observations back up the clonal model and provide a rationale for our current findings. Interestingly, they have shown that AR gene mutations were common and could arise in early hormone-naïve PCa, yet more frequently in advanced disease before ADT [150, 151]. Animal studies on the Dunning R-3327-H rat prostate adenocarcinoma model with a heterogeneous mixture of androgen-dependent and pre-existing androgen-resistant tumour cells subjected to ADT, showed that castration provided selective pressure and enhanced growth prosperity of castration-resistant tumour cells while androgen-dependent cells were eliminated [152].

The cancer stem cell (CSC) hypothesis, which has been frequently discussed during the last years, is another theory that can strengthen the clonal selection model. CSCs are a subgroup

of tumour cells about 0.1% in number [153], characterized by a high level of expression of cluster differentiation 44 (CD44) and CD133 and low expression level of AR, with properties of self-renewal and differentiation [154]. The most important question is whether these castration-resistant tumour cells are CSCs or not. Since CSCs in PCa are usually characterized by high levels of CD44 and CD133 and low levels of AR, our finding of high AR expression in these cells indicates that they are not CSCs.

Unfortunately, the absence of any CSC-marker staining such as cytokeratin (CK) or CD may be regarded as a limitation of our current study.

In the current work the observed tendency of inverse correlation between PARP-1 activity and AR and D-NHEJ is interesting. Previously we demonstrated that PARP-1 activity was induced after castration (Asim et al., in preparation). In fact, PARP-1 plays pivotal roles in the processing and resolution of a variety of repair of DNA damages such as single-strand break, HR and NHEJ [155]. Our study suggests that prostate tumour cells, in which castration leads to impairment of D-NHEJ repair, may rely on PARP-mediated B-NHEJ DNA repair. We believe this to be an important finding calling for further investigations in the future.

7 GENERAL CONCLUSIONS AND FUTURE PROSPECTIVE

Neoadjuvant castration combined with radiotherapy remains the standard of care treatment for patients with intermediate and high risk, localized prostate cancer. In our studies we tried to explore the molecular mechanisms underlying the synergistic effect between those two treatment modalities.

• Generally, we conclude that in *in vivo* material, RT following castration leads to impaired DNA repair and, therefore, increased DNA damage compared with that observed after RT alone.

• Our data show that neo-adjuvant castration lowers intranuclear AR leading to a down-regulation of D-NHEJ activity through both the depletion of the Ku70 protein and reduced activity in the DNA-PKcs protein, thereby promoting the radiosensitivity of prostate cancer (Study II & IV).

• Neoadjuvant castration reduces tumour cell hypoxia, measured by expression of HIF-1α, which may provide a plausible mechanism of enhanced radiosensitivity following castration (Study I).

• AR regulates HR repair, which provides an additional explanation for the improved radiosensitivity following neoadjuvant castration (Study III).

• Moreover, ADT leads to activation of PARP signalling and treatment with combined ADT and PARP inhibitors enhance cell killing *in vitro* (Study III).

• Despite castration levels of serum testosterone and consequently significant suppression of the nuclear AR and Ku70 following castration, there is remarkably suboptimal suppression of these proteins in some subclones of prostate tumour cells. The aforementioned may presumably be one of the plausible mechanisms underlying radioresistance and the subsequent high incidence rate of recurrence among patients with high risk disease (Study V).

Fundamentally, we showed that AR signalling regulates the DDR in PCa. Castration impairs the DNA repair pathways of DSBs and castration reduces hypoxia, hence improving radiosensitivity. Furthermore, our data indicate that following ADT the compromised DSBs repair either by D-NHEJ or HR tends to activate PARP-mediated B-NHEJ. This provides a rationale for synthetic lethality between ADT and PARP inhibitors and the dual targeting of both pathways may improve therapy outcome in advanced or high risk prostate cancer. We believe that castration-induced activation of B-NHEJ needs further investigation in future clinical studies. Stratifying patient cohorts using genetic markers could probably define patient populations responding to targeted therapies. This concept has been best implemented in the field of oncology. The tumour heterogeneity may be an important factor to predict response to individually based targeted therapies. In details investigation of the concept of intratumoural heterogeneity, to the single cell level, would be essential. It is well established

that tumour microenvironment and surrounding non-malignant tissue may influence the growth and progression of tumour cells. The CSCs population may need to be characterized using single cell resolution in tumour tissues. New technology such as spatial transcriptomics (ST), which is a novel approach that combines histology with RNA sequencing, would be a promising tool in future studies.

8 SAMMANFATTNING PÅ SVENSKA

Målet med behandling av icke-spridd prostatacancer är i första hand att helt slå ut tumören, d.v.s. bota patienten, i andra hand att förlänga överlevnaden. Med botande behandling, såsom radikal operation eller full dos strålbehandling med eller utan neoadjuvant kastrationsbehandling, kan man närma sig dessa mål, men resultaten är ibland ovissa och behandlingsmetoderna är förknippade med biverkningar, som tenderar att sänka livskvaliteten. Dessutom får en betydande del av män med högrisk prostatacancer återfall i sin sjukdom trots behandling med kurativ intention.

Kliniska studier har visat att neoadjuvant kastration ger en synergistisk effekt vid strålbehandling av prostatacancer. Mekanismen bakom denna synergism har inte varit klarlagd. Strålbehandlingen åstadkommer skador i cellernas genom (DNA). Om dessa skador inte repareras, dör cellen. DNA-skadorna kan repareras med hjälp av vissa proteiner, som kallas reparationsenzymer.

I detta arbete, ville vi undersöka om kastrationsbehandling medför en lägre nivå av reparationsenzymer i prostatacancerceller, vilket i så fall skulle leda till försämrad DNA-reparation och bättre strålbehandlingseffekt. En djupare förståelse för vad som sker på cellnivå och molekylnivå i prostatacancercellerna, när man först reducerar deras tillgång på manligt könshormon och därefter utsätter dem för joniserande strålning medför, att man bättre kan optimera behandlingen. Förmodligen kan det även ge uppslag till helt nya terapeutiska angreppspunkter.

Delarbete I. Fjorton patienter med prostatacancer rekryterades och prostatabiopsier togs före och efter kastrationsbehandling. Biopsierna analyserades med tanke på samband mellan kastrationsbehandling och nivån av HIF-1α protein som ett mått på hypoxi, brist i mängden syre, som når vävnaderna. Efter kastration observerades en minskning av uttrycket HIF-1α hos fem patienter med initialt starkt HIF-1α uttryck samt hos två av tre patienter med initialt svagt HIF-1α uttryck. Dessa data tyder på att neoadjuvant kastration minskar hypoxi i tumörceller vid prostatacancer (= ökad syrehalt), vilket kan förklara ökad strålkänslighet efter kastration.

Arbetet är publicerat: Castration therapy of prostate cancer results in downregulation of HIF-1α Levels. Al-Ubaidi et al., 2012 Int J Radiat Oncol Biol Phys. 82: 1243-8.

Delarbete II. Prostatabiopsier från samma kohort patienter som i arbete I användes i detta arbete. Biopsierna analyserades med avseende på samband mellan kastrationsbehandling och Ku70-protein, ett nödvändigt protein för reparation av dubbelsträngsbrott (DSB) i DNA-molekylen. Efter kastration observerades minskning av Ku70-nivåerna hos tio av fjorton patienter. Minskningen av Ku70 varierade från 43 % till 97 % ($p < 0{,}001$). Den samtida minskningen av serum-PSA och serum-testosteron efter kastrationen korrelerade direkt med sänkta halter av Ku70-proteinet.

Vår konklusion är att kastration resulterar i minskade nivåer av Ku70-protein som följaktligen medför en försämrad reparationskapacitet av D-NHEJ-systemet och därmed försämrad reparation av dubbelsträngsbrott, vilket i sin tur sannolikt innebär ökad strålkänslighet hos prostatacancerceller efter kastration.

Arbetet är publicerat: Castration Therapy Results in Decreased Ku70 Levels in Prostate Cancer, Al-Ubaidi FL, Schultz N, Loseva O, Egevad L, Granfors T, Helleday T. 2013 Clin Cancer Res. 19(6);1-10.

Delarbete III. Aktiv signalering av androgen receptor (AR) är ett kännetecken för en aggressiv prostatacancer. I detta arbete har vi använt olika prostatacancercellinjer med både kastrationskänsliga och kastrationsresistenta celler. Vi visade att AR-signalering reglerar DNA reparationssystemen och att den främjar homolog rekombination (HR), ett DNA-reparationssystem, som är nödvändigt för reparation av dubbelsträngsbrott. Dessutom visade vi att AR främjar ATM-signalering (ataxi telangiectasia muterat) med MRN (Mre11a, RAD50 och Nbs1) aktivering. Androgen deprivationsbehandling (ADT) minskar reparationskapaciteten hos HR. I ett kliniskt material från samma kohort som i delarbete IV, visade vi att PARP-aktiviteten ökar i prostatacancerceller efter ADT jämfört med PARP-aktivitet före ADT. Vår hypotes är att PARP-proteinet krävs för prostatacancercellernas överlevnad efter ADT. Slutligen visade vi en förbättrad hämning av tumörtillväxten genom att kombinera ADT och PARP-hämmare. Detta ger en logisk grund för användningen av PARP-hämmare i kombination med ADT. Vårt arbete ger avgörande insikter i mekanismen bakom androgensignaleringens betydelse för prostatacancerprogression och en logisk grund för samtidig hämning av AR och PARP vid behandling av prostatacancer.

Manuskriptet ska skickas till en internationell tidskrift för publicering.

Delarbete IV. Patienter med lokaliserad eller lokalt avancerad prostatacancer, som rekommenderades kurativt syftande strålbehandling inkluderades och delades i två grupper.

Patienterna i grupp 1 fick neoadjuvant farmakologisk kastration och 8 veckor senare, d.v.s. när deras serum-testosteronvärde var på kastrationsnivå, fick de strålbehandling i fraktioner om 2 Gy till totalt 78 Gy mot prostatakörteln. Prostatabiopsier togs strax innan strålbehandlingen och sedan omedelbart efter att patienten hade fått inledande 5 x 2 Gy.

Patienterna i grupp 2 fick först strålbehandling 5 x 2 Gy mot prostatakörteln och därefter neoadjuvant farmakologisk kastration i 8 veckor. Sedan fick de strålbehandling 36 x 2 Gy till totalt 82 Gy. Prostatabiopsier togs omedelbart efter den initiala strålbehandlingsstarten och sedan 8 veckor efter insättning av endokrin behandling d.v.s. när deras S-testosteronvärde låg på kastrationsnivå och innan patienterna fick kompletterande strålbehandling med 36 x 2 Gy.

Genom att analysera nivåerna av Ki67, en proliferationsmarkör, observerades att flertalet prostataceller går ur cellcykeln efter både kastration och strålbehandling. Genom att analysera DSB-markörerna γ-H2AX och 53BP1 visade vi att strålbehandling efter neoadjuvant kastration ledde till betydligt mera dubbelsträngsbrott än efter enbart

strålbehandling. Nivåerna av androgenreceptorn (AR) och D-NHEJ-proteinerna Ku70 och aktivt DNA-PKcs analyserades. I grupp 1minskade medelvärdet av AR och Ku70 efter kastration och även efter kombinerad kastration och strålbehandling. I grupp 2 såg vi ingen skillnad i AR-uttrycket efter inledande 5 x 2 Gy strålning. Däremot sågs en betydande ökning av Ku70 efter denna stråldos. För att bedöma aktiviteten hos D-NHEJ-reparationen analyserades aktivt DNA-PKcs. I grupp 1 förblev detta aktivt DNA-PKcs oförändrat efter både kastration och kombinerad kastration och strålbehandling. Men i grupp 2 såg vi en signifikant ökning av aktivt DNA-PKcs efter strålbehandling.

Sammanfattningsvis, har vi påvisat att den förbättrade totala överlevnaden efter kombinerad kastration och strålbehandling kan förklaras av försämrad D-NHEJ-reparation, vilket betyder många kvarstående dubbelsträngsbrott. Detta i sin tur ger en toxisk effekt på prostatacancercellerna. Denna studie visar att kastration försämrar D-NHEJ-reparationskapaciteten hos prostatacancerceller, vilket förklarar den förbättrade strålkänsligheten hos tumören efter kombinerad neoadjuvant kastration och strålbehandling.

Arbetet är accepterat av tidskriften ” Science Translational Medicine” för publicering.

Delarbete V. Trots tidig diagnos och därefter effektiv behandling av mellanrisk och högrisk prostatacancer förblir återfallsfrekvensen tyvärr hög. Det är väl etablerat att primär prostatatumör är en multifokal sjukdom. Vi ville undersöka hur effektivt en genomförd kastration sänker AR-signaleringen, vilket påverkar reparationen av DNA-skador hos primär hormonkänslig prostatacancer. Från samma kohort patienter som i delarbetet IV, valdes fem patienter till denna studie. Fyra patienter ingick i grupp 1, och fick kombinerad neoadjuvant farmakologisk kastration och strålbehandling (RT) medan en patient i grupp 2, det vill säga han fick en låg dos strålning före den kombinerade behandlingen. Mellannålsbiopsier från prostata säkrades vid diagnos, efter kastration och efter strålbehandling. Serum-PSA mättes vid diagnos och efter kastration medan serum-testosteron mättes endast efter kastration. Nivåerna av AR, Ku70, aktivt DNA-PKcs och PAR mättes. En signifikant, korrelerad minskning av medelintensiteten av AR i cellkärnorna observerades hos de fyra patienter, vars serum-PSA reducerades med 90 % eller mera ($\rho = 1$, $p < 0{,}001$). Trots kastrationsnivåer av serum-testosteron hos dessa patienter, var halterna av AR och följaktligen Ku70 och aktivt DNA-PKcs fortsatt höga i kluster av prostatacancerceller. Samtidigt observerades en tendens till en omvänd korrelation mellan AR, Ku70 och aktivt DNA-proteinkinas katalytisk subenhet (P-DNA-PKcs) jämfört med PARP-1-aktivitet. Sammanfattningsvis, är vi de första att påvisa det heterogena landskapet hos AR och dess ofullständiga respons på kastration hos kluster av hormonkänsliga prostatacancerceller. Det heterogena AR-landskapet efter kastration medför även en korrelerad respons på det samvarierade svaret av hur DNA-skador repareras. Än så länge är det fortfarande oklart hur dessa kastrationsresistenta celler uppstår. De kan antingen vara androgenberoende celler, som trots kastrationsnivåer hos serum-testosteron är fortsatt aktiva på grund av de höga halterna av androgen i prostatavävnaden, eller så är de vilande kastrationsresistenta celler, som främjar progressionen av

prostatacancer efter att de androgenberoende cellerna har slagits ut av kastrationsbehandling. Detta behöver förvisso studeras ytterligare i framtiden.

Manuskriptet ska skickas till en internationell tidskrift för publicering.

9 ACKNOWLEDGEMENTS

I would like to express my sincere gratitude and appreciation to all the people who have contributed to my doctoral work.

Professor Thomas Helleday, my supervisor. I am deeply grateful for you, for your strong interest and support from the very beginning. Your commitment to science and research has really affected me. It has been a pleasure and an intellectual adventure to be your student. Your patience with me has finally resulted in this thesis, a victory for all. I'm really happy.

Niklas Schultz, my supervisor. I want to express my sincere gratitude for the guidance and the wonderful help during my entire project. Thanks for all help and support I received during my work in the laboratory, with the microscope and data analysis. Thanks for the insightful comments and suggestions. You are not only a great scientist, but also a wonderful person and teacher.

Torvald Granefors, my mentor, colleague and friend. I really want to thank you for your wonderful support and involvement from the beginning of my journey as a researcher and doctoral student. You always see the possibilities and bring out the positive. Thank you for the time you have spent revising, reading and correcting my projects, manuscripts and thesis book. Thank you especially for your generosity.

Lars Egevad, thank you for your generous support to watch and assess all biopsies in the first project.

Hans Hamberg, thanks for introducing me to the world of pathology. Thank you for your tremendous support with assessing my second project biopsies. You have many times made life easier for me.

Henry Letocha, thanks for all the help and support that I got with revising my project plan and manuscripts.

Anna Tanoglidi, thanks for your help with the assessment of biopsies.

Katalin Karaszi, thank you for helping me with scanning hundreds of slides.

Eivor Gerdin, Tina Siverbo and **Annette Backman,** thanks for the generous help I received from you at the urological clinic with collecting so many biopsies over a relatively short period. Without your support and commitment, I would never have succeeded. Thank you for always creating a pleasant working environment.

Thanks to all the wonderful colleagues and staff at the department of urology, Västerås Central Hospital.

Thanks to the staff at the department of radiation oncology, Västerås Central Hospital, for the coordination of radiation therapy for the patients in the study.

Thanks to all research colleagues and the staff at SciLifelab/Helleday group – Karolinska Institutet in Stockholm for the support and help I received during my PhD work.

Thanks to the staff at the Centre for the Clinical Research CKF, Västerås, Central Hospital, for supporting my PhD work.

Last but not least, I want to thank my family, my mother, my wife, **Luma**, my daughters **Tina** and **Sara** for their support and patience.

10 REFERENCES

1. Ferlay J, Shin HR, Bray F, Forman D, Mathers C, Parkin DM: **Estimates of worldwide burden of cancer in 2008: GLOBOCAN 2008**. *Int J Cancer* 2010, **127**(12):2893-2917.

2. Siegel RL, Miller KD, Jemal A: **Cancer statistics, 2015**. *CA Cancer J Clin* 2015, **65**(1):5-29.

3. Cerovic SJ, Brajuskovic GR, Vukotic Maletic VD, Micic SR: **Neuroendocrine differentiation in prostate cancer**. *Vojnosanit Pregl* 2004, **61**(5):513-518.

4. Epstein JI, Allsbrook WC, Jr., Amin MB, Egevad LL: **Update on the Gleason grading system for prostate cancer: results of an international consensus conference of urologic pathologists**. *Adv Anat Pathol* 2006, **13**(1):57-59.

5. Roach M, 3rd, Bae K, Speight J, Wolkov HB, Rubin P, Lee RJ, Lawton C, Valicenti R, Grignon D, Pilepich MV: **Short-term neoadjuvant androgen deprivation therapy and external-beam radiotherapy for locally advanced prostate cancer: long-term results of RTOG 8610**. *Journal of clinical oncology : official journal of the American Society of Clinical Oncology* 2008, **26**(4):585-591.

6. Mohiuddin JJ, Baker BR, Chen RC: **Radiotherapy for high-risk prostate cancer**. *Nat Rev Urol* 2015, **12**(3):145-154.

7. Epstein JI, Allsbrook WC, Jr., Amin MB, Egevad LL: **The 2005 International Society of Urological Pathology (ISUP) Consensus Conference on Gleason Grading of Prostatic Carcinoma**. *Am J Surg Pathol* 2005, **29**(9):1228-1242.

8. Bostwick DG: **Grading prostate cancer**. *Am J Clin Pathol* 1994, **102**(4 Suppl 1):S38-56.

9. D'Amico AV, Whittington R, Malkowicz SB, Schultz D, Blank K, Broderick GA, Tomaszewski JE, Renshaw AA, Kaplan I, Beard CJ *et al*: **Biochemical outcome after radical prostatectomy, external beam radiation therapy, or interstitial radiation therapy for clinically localized prostate cancer**. *JAMA* 1998, **280**(11):969-974.

10. Zagars GK, von Eschenbach AC: **Prostate-specific antigen. An important marker for prostate cancer treated by external beam radiation therapy**. *Cancer* 1993, **72**(2):538-548.

11. Cleutjens KB, van der Korput HA, van Eekelen CC, van Rooij HC, Faber PW, Trapman J: **An androgen response element in a far upstream enhancer region is essential for high, androgen-regulated activity of the prostate-specific antigen promoter**. *Mol Endocrinol* 1997, **11**(2):148-161.

12. D'Amico AV, Whittington R, Malkowicz SB, Schnall M, Tomaszewski J, Schultz D, Kao G, VanArsdalen K, Wein A: **A multivariable analysis of clinical factors predicting for pathological features associated with local failure after radical prostatectomy for prostate cancer**. *Int J Radiat Oncol Biol Phys* 1994, **30**(2):293-302.

13. Bolla M, Van Tienhoven G, Warde P, Dubois JB, Mirimanoff RO, Storme G, Bernier J, Kuten A, Sternberg C, Billiet I *et al*: **External irradiation with or without long-**

term androgen suppression for prostate cancer with high metastatic risk: 10-year results of an EORTC randomised study. *Lancet Oncol* 2010, **11**(11):1066-1073.

14. Kumar S, Shelley M, Harrison C, Coles B, Wilt TJ, Mason MD: **Neo-adjuvant and adjuvant hormone therapy for localised and locally advanced prostate cancer**. *Cochrane Database Syst Rev* 2006(4):CD006019.

15. Aus G, Abrahamsson PA, Ahlgren G, Hugosson J, Lundberg S, Schain M, Schelin S, Pedersen K: **Hormonal treatment before radical prostatectomy: a 3-year followup**. *The Journal of urology* 1998, **159**(6):2013-2016; discussion 2016-2017.

16. Harmenberg U, Hamdy FC, Widmark A, Lennernas B, Nilsson S: **Curative radiation therapy in prostate cancer**. *Acta Oncol* 2011, **50 Suppl 1**:98-103.

17. Nilsson S, Norlen BJ, Widmark A: **A systematic overview of radiation therapy effects in prostate cancer**. *Acta Oncol* 2004, **43**(4):316-381.

18. Zaorsky NG, Harrison AS, Trabulsi EJ, Gomella LG, Showalter TN, Hurwitz MD, Dicker AP, Den RB: **Evolution of advanced technologies in prostate cancer radiotherapy**. *Nat Rev Urol* 2013, **10**(10):565-579.

19. Hanks GE, Hanlon AL, Pinover WH, Horwitz EM, Price RA, Schultheiss T: **Dose selection for prostate cancer patients based on dose comparison and dose response studies**. *Int J Radiat Oncol Biol Phys* 2000, **46**(4):823-832.

20. Ahel I, Ahel D, Matsusaka T, Clark AJ, Pines J, Boulton SJ, West SC: **Poly(ADP-ribose)-binding zinc finger motifs in DNA repair/checkpoint proteins**. *Nature* 2008, **451**(7174):81-85.

21. Granfors T, Modig H, Damber JE, Tomic R: **Long-term followup of a randomized study of locally advanced prostate cancer treated with combined orchiectomy and external radiotherapy versus radiotherapy alone**. *J Urol* 2006, **176**(2):544-547.

22. Zietman AL, Prince EA, Nakfoor BM, Park JJ: **Androgen deprivation and radiation therapy: sequencing studies using the Shionogi in vivo tumor system**. *Int J Radiat Oncol Biol Phys* 1997, **38**(5):1067-1070.

23. Kaminski JM, Hanlon AL, Joon DL, Meistrich M, Hachem P, Pollack A: **Effect of sequencing of androgen deprivation and radiotherapy on prostate cancer growth**. *Int J Radiat Oncol Biol Phys* 2003, **57**(1):24-28.

24. Pollack A, Salem N, Ashoori F, Hachem P, Sangha M, von Eschenbach AC, Meistrich ML: **Lack of prostate cancer radiosensitization by androgen deprivation**. *Int J Radiat Oncol Biol Phys* 2001, **51**(4):1002-1007.

25. Milecki P, Martenka P, Antczak A, Kwias Z: **Radiotherapy combined with hormonal therapy in prostate cancer: the state of the art**. *Cancer Manag Res* 2010, **2**:243-253.

26. Pisansky TM: **Use of neoadjuvant and adjuvant therapy to prevent or delay recurrence of prostate cancer in patients undergoing radiation treatment for prostate cancer**. *Urology* 2003, **62 Suppl 1**:36-45.

27. Mahler C: **Is disease flare a problem?** *Cancer* 1993, **72**(12 Suppl):3799-3802.

28. Langenhuijsen JF, van Lin EN, Hoffmann AL, Spitters-Post I, Alfred Witjes J, Kaanders JH, Mulders PF: **Neoadjuvant androgen deprivation for prostate volume reduction: the optimal duration in prostate cancer radiotherapy**. *Urol Oncol* 2011, **29**(1):52-57.

29. Alexander A, Crook J, Jones S, Malone S, Bowen J, Truong P, Pai H, Ludgate C: **Is biochemical response more important than duration of neoadjuvant hormone therapy before radiotherapy for clinically localized prostate cancer? An analysis of the 3- versus 8-month randomized trial**. *Int J Radiat Oncol Biol Phys* 2010, **76**(1):23-30.

30. de Crevoisier R, Slimane K, Messai T, Wibault P, Eschwege F, Bossi A, Koscielny S, Bridier A, Massard C, Fizazi K: **Early PSA decrease is an independent predictive factor of clinical failure and specific survival in patients with localized prostate cancer treated by radiotherapy with or without androgen deprivation therapy**. *Ann Oncol* 2010, **21**(4):808-814.

31. Roach M, 3rd, Bae K, Speight J, Wolkov HB, Rubin P, Lee RJ, Lawton C, Valicenti R, Grignon D, Pilepich MV: **Short-term neoadjuvant androgen deprivation therapy and external-beam radiotherapy for locally advanced prostate cancer: long-term results of RTOG 8610**. *J Clin Oncol* 2008, **26**(4):585-591.

32. Laverdiere J, Nabid A, De Bedoya LD, Ebacher A, Fortin A, Wang CS, Harel F: **The efficacy and sequencing of a short course of androgen suppression on freedom from biochemical failure when administered with radiation therapy for T2-T3 prostate cancer**. *J Urol* 2004, **171**(3):1137-1140.

33. Yeh S, Tsai MY, Xu Q, Mu XM, Lardy H, Huang KE, Lin H, Yeh SD, Altuwaijri S, Zhou X *et al*: **Generation and characterization of androgen receptor knockout (ARKO) mice: an in vivo model for the study of androgen functions in selective tissues**. *Proceedings of the National Academy of Sciences of the United States of America* 2002, **99**(21):13498-13503.

34. Heinlein CA, Chang C: **Androgen receptor in prostate cancer**. *Endocr Rev* 2004, **25**(2):276-308.

35. Prins GS, Birch L: **The developmental pattern of androgen receptor expression in rat prostate lobes is altered after neonatal exposure to estrogen**. *Endocrinology* 1995, **136**(3):1303-1314.

36. Lamb DJ, Weigel NL, Marcelli M: **Androgen receptors and their biology**. *Vitam Horm* 2001, **62**:199-230.

37. Chang CS, Kokontis J, Liao ST: **Molecular cloning of human and rat complementary DNA encoding androgen receptors**. *Science* 1988, **240**(4850):324-326.

38. Lubahn DB, Joseph DR, Sullivan PM, Willard HF, French FS, Wilson EM: **Cloning of human androgen receptor complementary DNA and localization to the X chromosome**. *Science* 1988, **240**(4850):327-330.

39. Hsing AW: **Hormones and prostate cancer: what's next?** *Epidemiol Rev* 2001, **23**(1):42-58.

40. English HF, Kyprianou N, Isaacs JT: **Relationship between DNA fragmentation and apoptosis in the programmed cell death in the rat prostate following castration**. *Prostate* 1989, **15**(3):233-250.

41. **Maximum androgen blockade in advanced prostate cancer: an overview of the randomised trials. Prostate Cancer Trialists' Collaborative Group**. *Lancet* 2000, **355**(9214):1491-1498.

42. Seidenfeld J, Samson DJ, Hasselblad V, Aronson N, Albertsen PC, Bennett CL, Wilt TJ: **Single-therapy androgen suppression in men with advanced prostate cancer: a systematic review and meta-analysis**. *Ann Intern Med* 2000, **132**(7):566-577.

43. Westin P, Stattin P, Damber JE, Bergh A: **Castration therapy rapidly induces apoptosis in a minority and decreases cell proliferation in a majority of human prostatic tumors**. *Am J Pathol* 1995, **146**(6):1368-1375.

44. Brandstrom A, Westin P, Bergh A, Cajander S, Damber JE: **Castration induces apoptosis in the ventral prostate but not in an androgen-sensitive prostatic adenocarcinoma in the rat**. *Cancer research* 1994, **54**(13):3594-3601.

45. Granfors T, Damber JE, Bergh A, Landstrom M, Lofroth PO, Widmark A: **Combined castration and fractionated radiotherapy in an experimental prostatic adenocarcinoma**. *Int J Radiat Oncol Biol Phys* 1997, **39**(5):1031-1036.

46. Zimmermann M, de Lange T: **53BP1: pro choice in DNA repair**. *Trends Cell Biol* 2014, **24**(2):108-117.

47. Hermann RM, Schwarten D, Fister S, Grundker C, Rave-Frank M, Nitsche M, Hille A, Thelen P, Schmidberger H, Christiansen H: **No supra-additive effects of goserelin and radiotherapy on clonogenic survival of prostate carcinoma cells in vitro**. *Radiat Oncol* 2007, **2**:31.

48. Salerno R, Moneti G, Forti G, Magini A, Natali A, Saltutti C, Di Cello V, Costantini A, Serio M: **Simultaneous determination of testosterone, dihydrotestosterone and 5 alpha-androstan-3 alpha,-17 beta-diol by isotopic dilution mass spectrometry in plasma and prostatic tissue of patients affected by benign prostatic hyperplasia. Effects of 3-month treatment with a GnRH analog**. *J Androl* 1988, **9**(4):234-240.

49. Mohler JL, Gregory CW, Ford OH, 3rd, Kim D, Weaver CM, Petrusz P, Wilson EM, French FS: **The androgen axis in recurrent prostate cancer**. *Clinical cancer research : an official journal of the American Association for Cancer Research* 2004, **10**(2):440-448.

50. Nishiyama T, Ikarashi T, Hashimoto Y, Wako K, Takahashi K: **The change in the dihydrotestosterone level in the prostate before and after androgen deprivation therapy in connection with prostate cancer aggressiveness using the Gleason score**. *The Journal of urology* 2007, **178**(4 Pt 1):1282-1288; discussion 1288-1289.

51. Yuan X, Cai C, Chen S, Yu Z, Balk SP: **Androgen receptor functions in castration-resistant prostate cancer and mechanisms of resistance to new agents targeting the androgen axis**. *Oncogene* 2014, **33**(22):2815-2825.

52. Ward JF: **DNA damage produced by ionizing radiation in mammalian cells: identities, mechanisms of formation, and reparability**. *Prog Nucleic Acid Res Mol Biol* 1988, **35**:95-125.

53. Bucher N, Britten CD: **G2 checkpoint abrogation and checkpoint kinase-1 targeting in the treatment of cancer**. *Br J Cancer* 2008, **98**(3):523-528.

54. Bartek J, Bartkova J, Lukas J: **DNA damage signalling guards against activated oncogenes and tumour progression**. *Oncogene* 2007, **26**(56):7773-7779.

55. Vadnais C, Davoudi S, Afshin M, Harada R, Dudley R, Clermont PL, Drobetsky E, Nepveu A: **CUX1 transcription factor is required for optimal ATM/ATR-mediated responses to DNA damage**. *Nucleic acids research* 2012, **40**(10):4483-4495.

56. Lee JH, Paull TT: **ATM activation by DNA double-strand breaks through the Mre11-Rad50-Nbs1 complex**. *Science* 2005, **308**(5721):551-554.

57. Smith J, Tho LM, Xu N, Gillespie DA: **The ATM-Chk2 and ATR-Chk1 pathways in DNA damage signaling and cancer**. *Adv Cancer Res* 2010, **108**:73-112.

58. Branzei D, Foiani M: **Regulation of DNA repair throughout the cell cycle**. *Nat Rev Mol Cell Biol* 2008, **9**(4):297-308.

59. Helleday T, Lo J, van Gent DC, Engelward BP: **DNA double-strand break repair: from mechanistic understanding to cancer treatment**. *DNA repair* 2007, **6**(7):923-935.

60. Dvir A, Peterson SR, Knuth MW, Lu H, Dynan WS: **Ku autoantigen is the regulatory component of a template-associated protein kinase that phosphorylates RNA polymerase II**. *Proceedings of the National Academy of Sciences of the United States of America* 1992, **89**(24):11920-11924.

61. Lees-Miller SP, Chen YR, Anderson CW: **Human cells contain a DNA-activated protein kinase that phosphorylates simian virus 40 T antigen, mouse p53, and the human Ku autoantigen**. *Mol Cell Biol* 1990, **10**(12):6472-6481.

62. Mayeur GL, Kung WJ, Martinez A, Izumiya C, Chen DJ, Kung HJ: **Ku is a novel transcriptional recycling coactivator of the androgen receptor in prostate cancer cells**. *J Biol Chem* 2005, **280**(11):10827-10833.

63. Gu Y, Jin S, Gao Y, Weaver DT, Alt FW: **Ku70-deficient embryonic stem cells have increased ionizing radiosensitivity, defective DNA end-binding activity, and inability to support V(D)J recombination**. *Proceedings of the National Academy of Sciences of the United States of America* 1997, **94**(15):8076-8081.

64. Gibson BA, Kraus WL: **New insights into the molecular and cellular functions of poly(ADP-ribose) and PARPs**. *Nat Rev Mol Cell Biol* 2012, **13**(7):411-424.

65. Ame JC, Spenlehauer C, de Murcia G: **The PARP superfamily**. *Bioessays* 2004, **26**(8):882-893.

66. Mangerich A, Burkle A: **How to kill tumor cells with inhibitors of poly(ADP-ribosyl)ation**. *Int J Cancer* 2011, **128**(2):251-265.

67. Wang M, Wu W, Rosidi B, Zhang L, Wang H, Iliakis G: **PARP-1 and Ku compete for repair of DNA double strand breaks by distinct NHEJ pathways**. *Nucleic acids research* 2006, **34**(21):6170-6182.

68. De Vos M, Schreiber V, Dantzer F: **The diverse roles and clinical relevance of PARPs in DNA damage repair: current state of the art**. *Biochem Pharmacol* 2012, **84**(2):137-146.

69. Iyama T, Wilson DM, 3rd: **DNA repair mechanisms in dividing and non-dividing cells**. *DNA repair* 2013, **12**(8):620-636.

70. Lee JM, Ledermann JA, Kohn EC: **PARP Inhibitors for BRCA1/2 mutation-associated and BRCA-like malignancies**. *Ann Oncol* 2014, **25**(1):32-40.

71. Kaelin WG, Jr.: **The concept of synthetic lethality in the context of anticancer therapy**. *Nat Rev Cancer* 2005, **5**(9):689-698.

72. Kaelin WG, Jr.: **ROS: really involved in oxygen sensing**. *Cell Metab* 2005, **1**(6):357-358.

73. Muzandu K, Shaban Z, Ishizuka M, Kazusaka A, Fujita S: **Nitric oxide enhances catechol estrogen-induced oxidative stress in LNCaP cells**. *Free Radic Res* 2005, **39**(4):389-398.

74. Zhong H, Semenza GL, Simons JW, De Marzo AM: **Up-regulation of hypoxia-inducible factor 1alpha is an early event in prostate carcinogenesis**. *Cancer Detect Prev* 2004, **28**(2):88-93.

75. Huss WJ, Hanrahan CF, Barrios RJ, Simons JW, Greenberg NM: **Angiogenesis and prostate cancer: identification of a molecular progression switch**. *Cancer research* 2001, **61**(6):2736-2743.

76. Kimbro KS, Simons JW: **Hypoxia-inducible factor-1 in human breast and prostate cancer**. *Endocr Relat Cancer* 2006, **13**(3):739-749.

77. Boddy JL, Fox SB, Han C, Campo L, Turley H, Kanga S, Malone PR, Harris AL: **The androgen receptor is significantly associated with vascular endothelial growth factor and hypoxia sensing via hypoxia-inducible factors HIF-1a, HIF-2a, and the prolyl hydroxylases in human prostate cancer**. *Clinical cancer research : an official journal of the American Association for Cancer Research* 2005, **11**(21):7658-7663.

78. Bostwick DG: **Grading prostate cancer**. *Am J Clin Pathol* 1994, **102**(4 Suppl 1):S38-56.

79. Schneider CA, Rasband WS, Eliceiri KW: **NIH Image to ImageJ: 25 years of image analysis**. *Nat Methods* 2012, **9**(7):671-675.

80. Ozawa H, Matsuda T, Iwaguchi T: **Whole-body hyperthermia maintains the secondary immune response of specific antitumour immune T cells**. *Int J Hyperthermia* 1991, **7**(1):125-130.

81. Farmer H, McCabe N, Lord CJ, Tutt AN, Johnson DA, Richardson TB, Santarosa M, Dillon KJ, Hickson I, Knights C *et al*: **Targeting the DNA repair defect in BRCA mutant cells as a therapeutic strategy**. *Nature* 2005, **434**(7035):917-921.

82. Bryant HE, Schultz N, Thomas HD, Parker KM, Flower D, Lopez E, Kyle S, Meuth M, Curtin NJ, Helleday T: **Specific killing of BRCA2-deficient tumours with inhibitors of poly(ADP-ribose) polymerase**. *Nature* 2005, **434**(7035):913-917.

83. Al-Ubaidi FL, Schultz N, Loseva O, Egevad L, Granfors T, Helleday T: **Castration therapy results in decreased Ku70 levels in prostate cancer**. *Clin Cancer Res* 2013, **19**(6):1547-1556.

84. Kuban DA, Levy LB, Cheung MR, Lee AK, Choi S, Frank S, Pollack A: **Long-term failure patterns and survival in a randomized dose-escalation trial for prostate cancer. Who dies of disease?** *Int J Radiat Oncol Biol Phys* 2011, **79**(5):1310-1317.

85. Talks KL, Turley H, Gatter KC, Maxwell PH, Pugh CW, Ratcliffe PJ, Harris AL: **The expression and distribution of the hypoxia-inducible factors HIF-1alpha and HIF-2alpha in normal human tissues, cancers, and tumor-associated macrophages**. *Am J Pathol* 2000, **157**(2):411-421.

86. Ponten F, Jirstrom K, Uhlen M: **The Human Protein Atlas--a tool for pathology**. *J Pathol* 2008, **216**(4):387-393.

87. Milosevic M, Warde P, Menard C, Chung P, Toi A, Ishkanian A, McLean M, Pintilie M, Sykes J, Gospodarowicz M *et al*: **Tumor hypoxia predicts biochemical failure following radiotherapy for clinically localized prostate cancer**. *Clinical cancer research : an official journal of the American Association for Cancer Research* 2012, **18**(7):2108-2114.

88. Vergis R, Corbishley CM, Norman AR, Bartlett J, Jhavar S, Borre M, Heeboll S, Horwich A, Huddart R, Khoo V *et al*: **Intrinsic markers of tumour hypoxia and angiogenesis in localised prostate cancer and outcome of radical treatment: a retrospective analysis of two randomised radiotherapy trials and one surgical cohort study**. *The Lancet Oncology* 2008, **9**(4):342-351.

89. Semenza GL: **HIF-1: upstream and downstream of cancer metabolism**. *Curr Opin Genet Dev* 2010, **20**(1):51-56.

90. Dewhirst MW, Cao Y, Moeller B: **Cycling hypoxia and free radicals regulate angiogenesis and radiotherapy response**. *Nat Rev Cancer* 2008, **8**(6):425-437.

91. Mabjeesh NJ, Willard MT, Frederickson CE, Zhong H, Simons JW: **Androgens stimulate hypoxia-inducible factor 1 activation via autocrine loop of tyrosine kinase receptor/phosphatidylinositol 3'-kinase/protein kinase B in prostate cancer cells**. *Clinical cancer research : an official journal of the American Association for Cancer Research* 2003, **9**(7):2416-2425.

92. Bristow RG, Hill RP: **Hypoxia and metabolism. Hypoxia, DNA repair and genetic instability**. *Nat Rev Cancer* 2008, **8**(3):180-192.

93. Moeller BJ, Cao Y, Li CY, Dewhirst MW: **Radiation activates HIF-1 to regulate vascular radiosensitivity in tumors: role of reoxygenation, free radicals, and stress granules**. *Cancer Cell* 2004, **5**(5):429-441.

94. Luoto KR, Kumareswaran R, Bristow RG: **Tumor hypoxia as a driving force in genetic instability**. *Genome Integr* 2013, **4**(1):5.

95. Mayeur GL, Kung WJ, Martinez A, Izumiya C, Chen DJ, Kung HJ: **Ku is a novel transcriptional recycling coactivator of the androgen receptor in prostate cancer cells**. *The Journal of biological chemistry* 2005, **280**(11):10827-10833.

96. Polkinghorn WR, Parker JS, Lee MX, Kass EM, Spratt DE, Iaquinta PJ, Arora VK, Yen WF, Cai L, Zheng D *et al*: **Androgen receptor signaling regulates DNA repair in prostate cancers**. *Cancer Discov* 2013, **3**(11):1245-1253.

97. Valerie K, Povirk LF: **Regulation and mechanisms of mammalian double-strand break repair**. *Oncogene* 2003, **22**(37):5792-5812.

98. Uehara Y, Ikehata H, Komura J, Ito A, Ogata M, Itoh T, Hirayama R, Furusawa Y, Ando K, Paunesku T *et al*: **Absence of Ku70 gene obliterates X-ray-induced lacZ mutagenesis of small deletions in mouse tissues**. *Radiat Res* 2008, **170**(2):216-223.

99. Takata M, Sasaki MS, Sonoda E, Morrison C, Hashimoto M, Utsumi H, Yamaguchi-Iwai Y, Shinohara A, Takeda S: **Homologous recombination and non-homologous end-joining pathways of DNA double-strand break repair have overlapping roles in the maintenance of chromosomal integrity in vertebrate cells**. *Embo J* 1998, **17**(18):5497-5508.

100. Blunt T, Finnie NJ, Taccioli GE, Smith GC, Demengeot J, Gottlieb TM, Mizuta R, Varghese AJ, Alt FW, Jeggo PA *et al*: **Defective DNA-dependent protein kinase activity is linked to V(D)J recombination and DNA repair defects associated with the murine scid mutation**. *Cell* 1995, **80**(5):813-823.

101. Lees-Miller SP, Godbout R, Chan DW, Weinfeld M, Day RS, 3rd, Barron GM, Allalunis-Turner J: **Absence of p350 subunit of DNA-activated protein kinase from a radiosensitive human cell line**. *Science* 1995, **267**(5201):1183-1185.

102. Jeggo PA, Tesmer J, Chen DJ: **Genetic analysis of ionising radiation sensitive mutants of cultured mammalian cell lines**. *Mutat Res* 1991, **254**(2):125-133.

103. Beskow C, Skikuniene J, Holgersson A, Nilsson B, Lewensohn R, Kanter L, Viktorsson K: **Radioresistant cervical cancer shows upregulation of the NHEJ proteins DNA-PKcs, Ku70 and Ku86**. *Br J Cancer* 2009, **101**(5):816-821.

104. Negroni A, Stronati L, Grollino MG, Barattini P, Gumiero D, Danesi DT: **Radioresistance in a tumour cell line correlates with radiation inducible Ku 70/80 end-binding activity**. *Int J Radiat Biol* 2008, **84**(4):265-276.

105. Raju U, Ariga H, Dittmann K, Nakata E, Ang KK, Milas L: **Inhibition of DNA repair as a mechanism of enhanced radioresponse of head and neck carcinoma cells by a selective cyclooxygenase-2 inhibitor, celecoxib**. *Int J Radiat Oncol Biol Phys* 2005, **63**(2):520-528.

106. Shintani S, Mihara M, Li C, Nakahara Y, Hino S, Nakashiro K, Hamakawa H: **Up-regulation of DNA-dependent protein kinase correlates with radiation resistance in oral squamous cell carcinoma**. *Cancer Sci* 2003, **94**(10):894-900.

107. An J, Yang DY, Xu QZ, Zhang SM, Huo YY, Shang ZF, Wang Y, Wu DC, Zhou PK: **DNA-dependent protein kinase catalytic subunit modulates the stability of c-Myc oncoprotein**. *Mol Cancer* 2008, **7**:32.

108. Zhang Y, Zhou J, Cao X, Zhang Q, Lim CU, Ullrich RL, Bailey SM, Liber HL: **Partial deficiency of DNA-PKcs increases ionizing radiation-induced mutagenesis and telomere instability in human cells**. *Cancer letters* 2007, **250**(1):63-73.

109. Kim CH, Park SJ, Lee SH: **A targeted inhibition of DNA-dependent protein kinase sensitizes breast cancer cells following ionizing radiation**. *J Pharmacol Exp Ther* 2002, **303**(2):753-759.

110. Taccioli GE, Amatucci AG, Beamish HJ, Gell D, Xiang XH, Torres Arzayus MI, Priestley A, Jackson SP, Marshak Rothstein A, Jeggo PA *et al*: **Targeted disruption of the catalytic subunit of the DNA-PK gene in mice confers severe combined immunodeficiency and radiosensitivity**. *Immunity* 1998, **9**(3):355-366.

111. Gu Y, Seidl KJ, Rathbun GA, Zhu C, Manis JP, van der Stoep N, Davidson L, Cheng HL, Sekiguchi JM, Frank K *et al*: **Growth retardation and leaky SCID phenotype of Ku70-deficient mice**. *Immunity* 1997, **7**(5):653-665.

112. Goodwin JF, Schiewer MJ, Dean JL, Schrecengost RS, de Leeuw R, Han S, Ma T, Den RB, Dicker AP, Feng FY *et al*: **A hormone-DNA repair circuit governs the response to genotoxic insult**. *Cancer Discov* 2013, **3**(11):1254-1271.

113. Mo N, Lu YK, Xie WM, Liu Y, Zhou WX, Wang HX, Nong L, Jia YX, Tan AH, Chen Y *et al*: **Inhibition of autophagy enhances the radiosensitivity of nasopharyngeal carcinoma by reducing Rad51 expression**. *Oncol Rep* 2014, **32**(5):1905-1912.

114. Lim YC, Roberts TL, Day BW, Stringer BW, Kozlov S, Fazry S, Bruce ZC, Ensbey KS, Walker DG, Boyd AW *et al*: **Increased sensitivity to ionizing radiation by targeting the homologous recombination pathway in glioma initiating cells**. *Mol Oncol* 2014, **8**(8):1603-1615.

115. Uziel T, Lerenthal Y, Moyal L, Andegeko Y, Mittelman L, Shiloh Y: **Requirement of the MRN complex for ATM activation by DNA damage**. *Embo J* 2003, **22**(20):5612-5621.

116. Morrison C, Sonoda E, Takao N, Shinohara A, Yamamoto K, Takeda S: **The controlling role of ATM in homologous recombinational repair of DNA damage**. *Embo J* 2000, **19**(3):463-471.

117. Schultz LB, Chehab NH, Malikzay A, Halazonetis TD: **p53 binding protein 1 (53BP1) is an early participant in the cellular response to DNA double-strand breaks**. *J Cell Biol* 2000, **151**(7):1381-1390.

118. Paull TT, Rogakou EP, Yamazaki V, Kirchgessner CU, Gellert M, Bonner WM: **A critical role for histone H2AX in recruitment of repair factors to nuclear foci after DNA damage**. *Curr Biol* 2000, **10**(15):886-895.

119. Bassing CH, Chua KF, Sekiguchi J, Suh H, Whitlow SR, Fleming JC, Monroe BC, Ciccone DN, Yan C, Vlasakova K *et al*: **Increased ionizing radiation sensitivity and genomic instability in the absence of histone H2AX**. *Proceedings of the National Academy of Sciences of the United States of America* 2002, **99**(12):8173-8178.

120. Celeste A, Petersen S, Romanienko PJ, Fernandez-Capetillo O, Chen HT, Sedelnikova OA, Reina-San-Martin B, Coppola V, Meffre E, Difilippantonio MJ *et al*: **Genomic instability in mice lacking histone H2AX**. *Science* 2002, **296**(5569):922-927.

121. Sak A, Stuschke M: **Use of gammaH2AX and other biomarkers of double-strand breaks during radiotherapy**. *Semin Radiat Oncol* 2010, **20**(4):223-231.

122. Olive PL, Banath JP: **Phosphorylation of histone H2AX as a measure of radiosensitivity**. *Int J Radiat Oncol Biol Phys* 2004, **58**(2):331-335.

123. Arnaudeau C, Lundin C, Helleday T: **DNA double-strand breaks associated with replication forks are predominantly repaired by homologous recombination involving an exchange mechanism in mammalian cells**. *J Mol Biol* 2001, **307**(5):1235-1245.

124. Osipov AN, Pustovalova M, Grekhova A, Eremin P, Vorobyova N, Pulin A, Zhavoronkov A, Roumiantsev S, Klokov DY, Eremin I: **Low doses of X-rays induce prolonged and ATM-independent persistence of gammaH2AX foci in human gingival mesenchymal stem cells**. *Oncotarget* 2015.

125. Laitinen S, Martikainen PM, Tammela TL, Visakorpi T: **Cellular changes in prostate cancer cells induced by intermittent androgen suppression**. *Eur Urol* 2007, **52**(3):725-732.

126. Salagierski M, Schalken JA: **Molecular diagnosis of prostate cancer: PCA3 and TMPRSS2:ERG gene fusion**. *The Journal of urology* 2012, **187**(3):795-801.

127. Perner S, Mosquera JM, Demichelis F, Hofer MD, Paris PL, Simko J, Collins C, Bismar TA, Chinnaiyan AM, De Marzo AM *et al*: **TMPRSS2-ERG fusion prostate cancer: an early molecular event associated with invasion**. *Am J Surg Pathol* 2007, **31**(6):882-888.

128. Chatterjee P, Choudhary GS, Alswillah T, Xiong X, Heston WD, Magi-Galluzzi C, Zhang J, Klein EA, Almasan A: **The TMPRSS2-ERG Gene Fusion Blocks XRCC4-Mediated Nonhomologous End-Joining Repair and Radiosensitizes Prostate Cancer Cells to PARP Inhibition**. *Mol Cancer Ther* 2015, **14**(8):1896-1906.

129. Bryant HE, Petermann E, Schultz N, Jemth AS, Loseva O, Issaeva N, Johansson F, Fernandez S, McGlynn P, Helleday T: **PARP is activated at stalled forks to mediate Mre11-dependent replication restart and recombination**. *Embo J* 2009, **28**(17):2601-2615.

130. Schiewer MJ, Goodwin JF, Han S, Brenner JC, Augello MA, Dean JL, Liu F, Planck JL, Ravindranathan P, Chinnaiyan AM *et al*: **Dual roles of PARP-1 promote cancer growth and progression**. *Cancer Discov* 2012, **2**(12):1134-1149.

131. Roach M, 3rd: **Current trends for the use of androgen deprivation therapy in conjunction with radiotherapy for patients with unfavorable intermediate-risk, high-risk, localized, and locally advanced prostate cancer**. *Cancer* 2014, **120**(11):1620-1629.

132. Bancroft EK, Page EC, Castro E, Lilja H, Vickers A, Sjoberg D, Assel M, Foster CS, Mitchell G, Drew K *et al*: **Targeted prostate cancer screening in BRCA1 and BRCA2 mutation carriers: results from the initial screening round of the IMPACT study**. *Eur Urol* 2014, **66**(3):489-499.

133. Bednarz N, Eltze E, Semjonow A, Rink M, Andreas A, Mulder L, Hannemann J, Fisch M, Pantel K, Weier HU *et al*: **BRCA1 loss preexisting in small subpopulations of prostate cancer is associated with advanced disease and metastatic spread to lymph nodes and peripheral blood**. *Clinical cancer research : an official journal of the American Association for Cancer Research* 2010, **16**(13):3340-3348.

134. Chang KH, Li R, Kuri B, Lotan Y, Roehrborn CG, Liu J, Vessella R, Nelson PS, Kapur P, Guo X *et al*: **A gain-of-function mutation in DHT synthesis in castration-resistant prostate cancer**. *Cell* 2013, **154**(5):1074-1084.

135. Korpal M, Korn JM, Gao X, Rakiec DP, Ruddy DA, Doshi S, Yuan J, Kovats SG, Kim S, Cooke VG *et al*: **An F876L mutation in androgen receptor confers genetic and phenotypic resistance to MDV3100 (enzalutamide)**. *Cancer Discov* 2013, **3**(9):1030-1043.

136. Nyquist MD, Li Y, Hwang TH, Manlove LS, Vessella RL, Silverstein KA, Voytas DF, Dehm SM: **TALEN-engineered AR gene rearrangements reveal endocrine uncoupling of androgen receptor in prostate cancer**. *Proc Natl Acad Sci U S A* 2013, **110**(43):17492-17497.

137. Sakai W, Swisher EM, Karlan BY, Agarwal MK, Higgins J, Friedman C, Villegas E, Jacquemont C, Farrugia DJ, Couch FJ *et al*: **Secondary mutations as a mechanism of cisplatin resistance in BRCA2-mutated cancers**. *Nature* 2008, **451**(7182):1116-1120.

138. Jackson SP, Bartek J: **The DNA-damage response in human biology and disease**. *Nature* 2009, **461**(7267):1071-1078.

139. Zong Y, Goldstein AS: **Adaptation or selection--mechanisms of castration-resistant prostate cancer**. *Nat Rev Urol* 2013, **10**(2):90-98.

140. Ahmed M, Li LC: **Adaptation and clonal selection models of castration-resistant prostate cancer: current perspective**. *Int J Urol* 2013, **20**(4):362-371.

141. Holzbeierlein J, Lal P, LaTulippe E, Smith A, Satagopan J, Zhang L, Ryan C, Smith S, Scher H, Scardino P *et al*: **Gene expression analysis of human prostate carcinoma during hormonal therapy identifies androgen-responsive genes and mechanisms of therapy resistance**. *Am J Pathol* 2004, **164**(1):217-227.

142. Page ST, Lin DW, Mostaghel EA, Hess DL, True LD, Amory JK, Nelson PS, Matsumoto AM, Bremner WJ: **Persistent intraprostatic androgen concentrations after medical castration in healthy men**. *The Journal of clinical endocrinology and metabolism* 2006, **91**(10):3850-3856.

143. Forti G, Salerno R, Moneti G, Zoppi S, Fiorelli G, Marinoni T, Natali A, Costantini A, Serio M, Martini L *et al*: **Three-month treatment with a long-acting gonadotropin-releasing hormone agonist of patients with benign prostatic hyperplasia: effects on tissue androgen concentration, 5 alpha-reductase activity and androgen receptor content**. *The Journal of clinical endocrinology and metabolism* 1989, **68**(2):461-468.

144. Mostaghel EA: **Steroid hormone synthetic pathways in prostate cancer**. *Transl Androl Urol* 2013, **2**(3):212-227.

145. Mostaghel EA, Page ST, Lin DW, Fazli L, Coleman IM, True LD, Knudsen B, Hess DL, Nelson CC, Matsumoto AM *et al*: **Intraprostatic androgens and androgen-regulated gene expression persist after testosterone suppression: therapeutic implications for castration-resistant prostate cancer**. *Cancer Res* 2007, **67**(10):5033-5041.

146. Taplin ME, Montgomery B, Logothetis CJ, Bubley GJ, Richie JP, Dalkin BL, Sanda MG, Davis JW, Loda M, True LD *et al*: **Intense androgen-deprivation therapy**

with abiraterone acetate plus leuprolide acetate in patients with localized high-risk prostate cancer: results of a randomized phase II neoadjuvant study. *Journal of clinical oncology : official journal of the American Society of Clinical Oncology* 2014, **32**(33):3705-3715.

147. Scher HI, Fizazi K, Saad F, Taplin ME, Sternberg CN, Miller K, de Wit R, Mulders P, Chi KN, Shore ND *et al*: **Increased survival with enzalutamide in prostate cancer after chemotherapy**. *The New England journal of medicine* 2012, **367**(13):1187-1197.

148. de Bono JS, Logothetis CJ, Molina A, Fizazi K, North S, Chu L, Chi KN, Jones RJ, Goodman OB, Jr., Saad F *et al*: **Abiraterone and increased survival in metastatic prostate cancer**. *The New England journal of medicine* 2011, **364**(21):1995-2005.

149. Antonarakis ES, Lu C, Wang H, Luber B, Nakazawa M, Roeser JC, Chen Y, Mohammad TA, Fedor HL, Lotan TL *et al*: **AR-V7 and resistance to enzalutamide and abiraterone in prostate cancer**. *The New England journal of medicine* 2014, **371**(11):1028-1038.

150. Tilley WD, Buchanan G, Hickey TE, Bentel JM: **Mutations in the androgen receptor gene are associated with progression of human prostate cancer to androgen independence**. *Clinical cancer research : an official journal of the American Association for Cancer Research* 1996, **2**(2):277-285.

151. Koivisto P, Kononen J, Palmberg C, Tammela T, Hyytinen E, Isola J, Trapman J, Cleutjens K, Noordzij A, Visakorpi T *et al*: **Androgen receptor gene amplification: a possible molecular mechanism for androgen deprivation therapy failure in prostate cancer**. *Cancer research* 1997, **57**(2):314-319.

152. Isaacs JT, Coffey DS: **Adaptation versus selection as the mechanism responsible for the relapse of prostatic cancer to androgen ablation therapy as studied in the Dunning R-3327-H adenocarcinoma**. *Cancer research* 1981, **41**(12 Pt 1):5070-5075.

153. Collins AT, Berry PA, Hyde C, Stower MJ, Maitland NJ: **Prospective identification of tumorigenic prostate cancer stem cells**. *Cancer research* 2005, **65**(23):10946-10951.

154. Maitland NJ, Collins A: **A tumour stem cell hypothesis for the origins of prostate cancer**. *BJU Int* 2005, **96**(9):1219-1223.

155. Wang Z, Wang F, Tang T, Guo C: **The role of PARP1 in the DNA damage response and its application in tumor therapy**. *Front Med* 2012, **6**(2):156-164.

I

Int. J. Radiation Oncology Biol. Phys., Vol. 82, No. 3, pp. 1243–1248, 2012

0360-3016/$ - see front matter

ELSEVIER

doi:10.1016/j.ijrobp.2011.10.038

CLINICAL INVESTIGATION **Genitourinary Cancer**

CASTRATION THERAPY OF PROSTATE CANCER RESULTS IN DOWNREGULATION OF HIF-1α LEVELS

Firas L. T. Al-Ubaidi, M.B., Ch.B.,*† Niklas Schultz, Ph.D.,* Lars Egevad, M.D., Ph.D.,‡ Torvald Granfors, M.D., Ph.D.,† and Thomas Helleday, Ph.D.*§¶

*Department of Genetics, Microbiology and Toxicology, Stockholm University, Stockholm, Sweden; ‡Department of Oncology-Pathology, Karolinska Institutet, Stockholm, Sweden; †Department of Urology, Central Hospital, Västerås, Sweden; ¶Science for Life Laboratory, Stockholm University, Solna, Sweden; and §Gray Institute for Radiation Oncology and Biology, University of Oxford, Oxford, UK

Background and Purpose: Neoadjuvant androgen deprivation in combination with radiotherapy of prostate cancer is used to improve radioresponsiveness and local tumor control. Currently, the underlying mechanism is not well understood. Because hypoxia causes resistance to radiotherapy, we wanted to test whether castration affects the degree of hypoxia in prostate cancer.

Methods and Materials: In 14 patients with locally advanced prostate cancer, six to 12 prostatic needle core biopsy specimens were taken prior to castration therapy. Bilateral orchidectomy was performed in 7 patients, and 7 were treated with a GnRH-agonist (leuprorelin). After castrationm two to four prostatic core biopsy specimens were taken, and the level of hypoxia-inducible factor-1α (HIF-1α) in cancer was determined by immunofluorescence.

Results: Among biopsy specimens taken before castration, strong HIF-1α expression (mean intensity above 30) was shown in 5 patients, weak expression (mean intensity 10–30) in 3 patients, and background levels of HIF-1α (mean intensity 0–10) in 6 patients. Downregulation of HIF-1α expression after castration was observed in all 5 patients with strong HIF-1α precastration expression. HIF-1α expression was also reduced in 2 of 3 patients with weak HIF-1α precastration expression.

Conclusions: Our data suggest that neoadjuvant castration decreases tumor cell hypoxia in prostate cancer, which may explain increased radiosensitivity after castration. © **2012 Elsevier Inc.**

Hypoxia-inducible factor, HIF-1α, Prostate cancer.

INTRODUCTION

Prostate cancer is the most common cancer in the western countries (1). Most patients with localized prostate cancer (*ie*, the tumor is confined to the prostate gland), who have relatively long life expectancy and low comorbidity, may be offered curative treatment with either radical prostatectomy or radiotherapy. In the case of poorly differentiated high-risk tumors, the latter treatment is currently combined with neoadjuvant hormone therapy with the use of a gonadotropin-releasing hormone (GnRH) agonist. Clinical studies have demonstrated synergism between androgen ablation and radiotherapy (2), which improves tumor control and patient survival, although the biologic explanation of the mechanism is not yet fully defined.

Growth of solid tumors such as prostate cancer is characterized by neovascularization and increased glycolysis as a result of the hypoxic microenvironment of the tumor. The hypoxia-inducible factor 1 (HIF-1) complex is an important transcription factor that regulates cellular adaptation to hypoxia and transcription of genes involved in angiogenesis, cell survival, glucose metabolism, and tumor invasion (3).

HIF-1 is a member of the basic helix-loop-helix (bHLH)-PER-ARNT-Sim (PAS) family of transcription factors. HIF-1 is a heterodimer composed of the HIF-1α and HIF-1β subunits (4). The β subunit is ubiquitously expressed in most cells, and the α subunit, which is the critical determinant of HIF-1 activity, is regulated posttranslationally in response to hypoxia. In normoxic conditions, HIF-1α is ubiquitinated by the von Hippel-Lindau tumor suppressor protein (pVHL) and degraded by the proteasome. However, in response to hypoxia, HIF-1α is stabilized and can thus bind to the β subunit. Upon dimerization of the two subunits. the HIF-1 complex translocates to the nucleus, where it

Reprint requests to: Thomas Helleday, Ph.D., Gray Institute for Radiation Oncology and Biology, University of Oxford, Oxford, OX3 7DQ, UK. Tel: (+46) 8-16-2914; Fax: (+46) 8-16-4315; E-mail: helleday@gmt.su.se

Supported by the Västmanland County Cancer Foundation, The Swedish Cancer Society, the Swedish Research Council, the Swedish Children's Cancer Foundation, and the Swedish Pain Relief Foundation.

Conflict of interest: none.

Received May 5, 2011, and in revised form Sept 19, 2011. Accepted for publication Oct 14, 2011.

binds to DNA at hypoxia-responsive elements (HREs), which are common to HIF-1–responsive genes, thus modifying transcription. Resulting gene expression increases metabolic resistance of the cell to hypoxia and apoptosis and stimulates angiogenesis by subsequent production of vascular endothelial growth factor (VEGF) (5). HIF-1α is upregulated in most cancers, including prostate cancer (6).

Immunohistochemical studies show upregulation of HIF-1α in prostate cancer compared with normal prostate and benign prostatic hyperplasia (7). Moreover, upregulation of HIF-1α is likely to be an early event in the development of prostate cancer, given that increased levels were observed in high-grade intraepithelial neoplasia, which is considered the precursor of prostatic adenocarcinoma. Furthermore, prostate tumor tissue adjacent to the intraepithelial neoplasia showed an even more pronounced upregulation of HIF-1α expression (8).

Tumor hypoxia is associated with poor prognosis and increased resistance to radiotherapy. HIF-1α has an important role in regulating tumor radiosensitivity through its impact on apoptosis, metabolism, proliferation, and angiogenesis (9). Tumor cells with upregulated HIF-1α levels are more radioresistant than HIF-1α–deficient counterparts (10). For localized prostate cancer, it has been shown that increased expression of HIF-1α identifies patients at high risk for biochemical failure (11). Studies in prostate cancer cell lines have found that acute hypoxia promotes a more aggressive metastatic phenotype (12). Here, we hypothesize that androgen ablation downregulates hypoxia, as measured by the expression of HIF-1α in human prostate cancer.

METHODS AND MATERIALS

Patients and biopsy specimen collection

After approval from the regional ethics committee at Uppsala University (Dnr 2007/170), 20 patients with newly diagnosed prostate cancer were enrolled. At diagnosis, six to 12 prostatic needle core biopsy specimens were taken from each patient. All patients were treated with castration. After castration (*ie*, approximately 1 month after surgery or 2 months after initiation of pharmacologic castration, respectively), another two to four core biopsy specimens were taken. At diagnosis, the biopsy specimens were taken randomly. After castration, we took fewer samples and focused on palpable nodules to increase the likelihood of finding cancer cells.

Both before and after castration, we chose biopsy specimens rich in cancer cells and used them for HIF-1 staining. Thus, there was a high probability that the same tumor areas were represented at both biopsy occasions. In 6 patients the postcastration biopsy specimens did not include representative cancer areas and hence were excluded from this study. The median age of the 14 patients included in this study was 78 years (range, 59–87 years). Thirteen patients had locally advanced cT3-4 tumors, and only 1 patient had an organ-confined cT2 tumor. The median serum prostate-specific antigen was 98 ng/mL (range, 3–1021 ng/mL). The median serum testosterone level was 11.0 nmol/L (range, 6.6–23.0 nmol/L). The median prostate volume measured with transrectal ultrasound was 52 mL (range, 20–100 mL).

Bilateral orchidectomy was performed in half of the patients, and the other half was treated with a GnRH agonist (leuprorelin) (Table 1). The mean time and standard deviation from orchidectomy to repeated biopsy was 26 $\pm$ 19 days and from administration of GnRH-agonist to repeated biopsy 54 $\pm$ 14 days. At the time of postcastration biopsy, the serum testosterone levels varied from 0.3 to 0.9 nmol/L in surgically castrated patients and 0.3 to 1.7 nmol/L in patients receiving GnRH agonist therapy.

Histologic and immunofluorescence evaluation

Two biopsy specimens before and two after castration were analyzed in each patient. The biopsy speciens were embedded in paraffin and sectioned. One section from each biopsy specimen was stained with hematoxylin and eosin (HE) and graded according to the Gleason system (13). Sections adjacent to the HE-stained sections were used for immunofluorescence studies. These sections were deparaffinized and rehydrated before antigen retrieval in Tris/EDTA pH 9.0 in a pressure cooker. After blocking in 3% BSA, the sections were incubated with the primary antibody HIF-1α (1:500, H-206 St. Cruz) at 4°C overnight. After extensive rinsing, the sections were incubated with the secondary antibody (donkey

Table 1. Characteristics of patients and tumors in the study

Patient number	Patient age (y)	Prostate volume, mL	cT	GS	PSA, ng/mL		Testosterone, nmol/L		Days between biopsies	Castration method
					Before castration	After castration	Before castration	After castration		
6	70	71	4	8	1021	21	12	0.9	53	GnRH agonist
9	83	20	3	7	8	0.3	14	0.8	70	GnRH agonist
10	87	59	3	7	34	1.9	15	0.7	60	GnRH agonist
12	61	26	2	7	17	6.4	ND	1.7	42	GnRH agonist
14	78	90	3	7	326	55	7	0.3	88	GnRH agonist
18	69	50	3	10	380	5.4	11	0.3	105	GnRH agonist
19	77	34	3	7	107	2.6	11	1.0	55	GnRH agonist
2	67	65	3	10	2.9	3.7	23	0.3	16	Orchidectomy
5	86	52	3	9	70	53	7	1.0	8	Orchidectomy
8	63	44	3	8	650	134	13	0.9	83	Orchidectomy
15	59	90	4	9	736	29	8	0.9	46	Orchidectomy
16	82	ND	3	7	16	1.1	16	0.6	49	Orchidectomy
17	84	46	4	8	438	138	9	0.6	29	Orchidectomy
20	83	100	3	9	89	23	10	0.3	40	Orchidectomy

Abbreviations: ND = not done; cT = clinical tumor stage; GG = Gleason grade; GS = Gleason score.

antirabbit-alexa 555, Molecular probe) for 1 hour at room temperature. DNA was counterstained with ToPro (Molecular probe), and slides were mounted with prolong gold (Molecular probe).

A tumor area with a good immunofluorescence signal was selected in each slide. To verify the tumor, the corresponding area in the HE-stained section was identified. In the tumor area, three images 100 × 100 μm, containing approximately 50 to 150 cells, were chosen for analysis. The images were analyzed with ImageJ software (National Institute of Health) with respect to mean intensity of HIF-1α in the nucleus and cytoplasm. The ToPro signal was used as a marker for nuclei (Fig. 1). Biopsy specimens without cancer were excluded. Fluorescence images were obtained with a Zeiss LSM 510 inverted confocal microscope using a planapochromat 20X/NA 0.75 objective. Bright light images were obtained with a Nikon eclipse C600 microscope using a planapochromat 20X/NA 0.75 objective.

RESULTS

Castration therapy of prostate cancer resulted in downregulation of HIF-1α levels

HIF-1α expression was observed in the nucleus and in the cytoplasm (Fig. 1). After castration, the intensity of HIF-1α decreased to approximately half of the original values, both in the nuclei and in the cytoplasm (Wilcoxon matched pairs, $p < 0.001$) (Fig. 2A, B). Because no differences were observed of HIF-1α expression between the nucleus and the cytoplasm, mean intensities of total HIF-1α signal were determined in all the following experiments (Fig. 2C).

Reduction of HIF-1α was most pronounced in tumors with strong HIF-1α expression

Among the biopsy specimens taken from the 14 patients before castration, a strong HIF-1α expression (mean intensity more than 30) was shown in 5 patients, a weak expression (mean intensity 10–30) in 3 patients, and background levels of HIF-1α (mean intensity 0–10) in 6 patients (Fig. 3A). This is in accordance with other studies showing that not all malignant prostate tumors have elevated levels of HIF-1α (14, 15). Downregulation of HIF-1α after castration was pronounced in the patients with high initial HIF-1α levels, whereas levels were unaffected in the group who initially had background levels of HIF-1α (Figure 3A, Table 2).

Inspection of individual patients showed that a large and statistically significant downregulation of HIF-1α after castration was observed in 100% (5/5) of patients belonging to the group showing strong HIF-1α expression before castration, and 67% (2/3) of the group showing a weak HIF-1α expression (Fig. 3B). In the group with background level HIF-1α, only a minor difference in HIF-1α signal was seen after castration, even though 1 patient showed

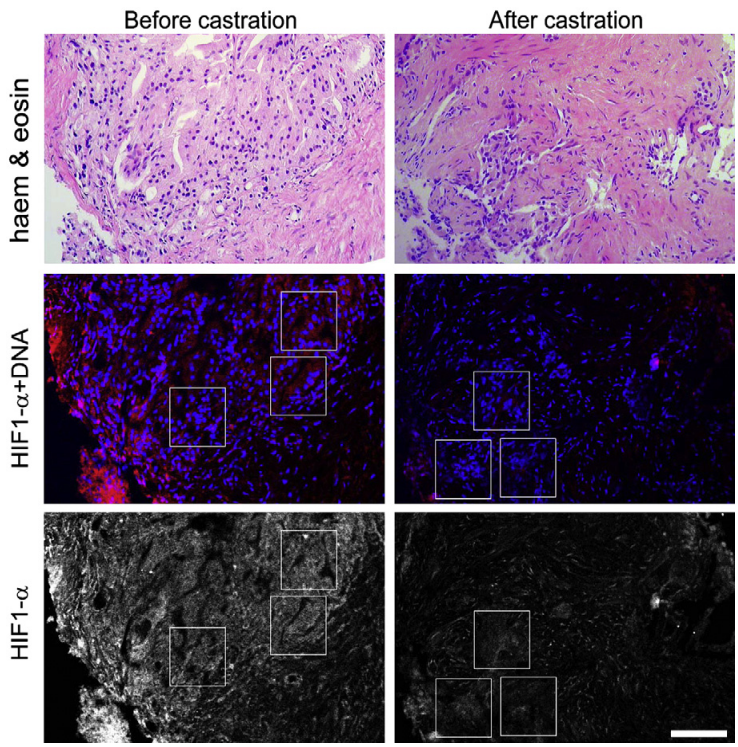

Fig. 1. HIF-1α levels in prostate tumors decrease after castration. Prostate tumor biopsy specimens from prostate cancer patients before castration (left) and after surgical castration (right). Above, common hematoxylin and eosin staining. Below, immunofluorescent staining with antibodies against HIF-1α. Middle, HIF-1α expression (red) superimposed on ToPro-staining (DNA, blue). Bar = 100 μm.

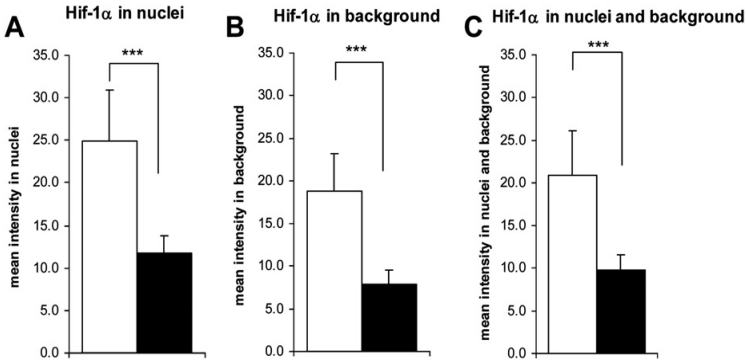

Fig. 2. HIF-1α is expressed at equal levels in the nucleus and cytoplasm. Quantification of HIF-1α immunofluorescent staining intensity in (A) nuclei, (B) cytoplasm, and (C) nuclei and cytoplasm of prostate tumor biopsy specimens taken before (white bars) and after (black bar) castration. The means and standard errors of 14 patients are shown. Values marked with asterisks are statistically significant (*** $p < 0.001$: Wilcoxon matched pairs).

a significant decrease and 1 other patient a significant increase of HIF-1α after castration (Figure 3B).

Factors correlated to HIF-1α downregulation

To further investigate factors that might be related to HIF-1α downregulation, we calculated the coefficient of determination (R^2) to get the explanatory power of the variables (Table 3). The level of HIF-1α before castration correlated well with the decrease of HIF-1α. Approximately 40% of the variation in the HIF-1α decrease could be explained by the initial HIF-1α value. Besides that, we found no significant correlations with other parameters investigated (Table 3).

DISCUSSION

We report that HIF-1α levels are decreased after castration in prostate cancer. We suggest that decreases in HIF-1α levels reflect a decrease in tumor hypoxia after castration. It is well established that tumor hypoxia is correlated with radioresistance (10), likely owing to the need for oxygen to produce tissue toxicity by radiotherapy. The concentration of oxygen dissolved in tissues at the time of irradiation is

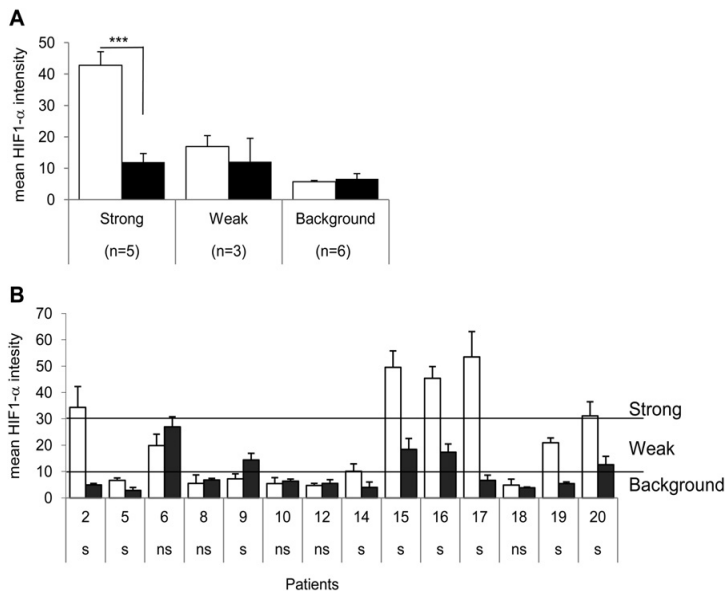

Fig. 3. HIF-1α is upregulated in a fraction of prostate tumors. Quantification of HIF-1α immunofluorescent staining intensity in prostate tumor biopsy specimens before (white bars) and after (black bars) castration. Upregulation of HIF-1α was classified as strong, weak, or at background level. (A) Patients pooled after HIF-1α classification. The means and standard errors of indicated number of patients are shown. Values marked with asterisks are statistically significant (*** $p < 0.001$; t test). (B) Individual patients are depicted. The means and standard errors of six images from two different biopsy specimens are shown (s = significant, $p < 0.05$; ns = not significant, $p > 0.05$; t test).

Table 2. Mean values for parameters used in this study for the three groups sorted after their HIF-1α levels before castration

Parameters	HIF-1α expression before castration			
	Strong (above 30) mean	Weak (10–30) mean	Background (0–10) mean	Background Vsv strong*
HIF-1α before castration	42.8	16.9	5.7	$p < 0.001$
HIF-1α after/HIF-1α before	0.29	0.67	1.13	$p < 0.01$
Age (y)	76	77	76	NS
PSA before castration (ng/mL)	256	485	193	NS
Testosterone before castration (nmol/L)	13	10,1	11,9	NS
PSA after castration (ng/mL)	39.0	26.2	33.5	NS
Testosterone after castration (nmol/L)	0.59	0.78	0.91	NS
Days between biopsies	36	65	61	NS
PSA decrease (%)	85	94	83	NS
Testosterone decrease (%)	95	92	94	NS

Abbreviations: HIF-1α = hypoxia-inducible factor-1α; PSA = prostate-specific antigen; NS = not significant; Vsv = Vis-à-vis.
* *t* test, $p > 0.05$ = NS.

a critical factor in determining the efficiency in radiotherapy. Inasmuch as tumor hypoxia seems to decrease after castration, the increase of oxygen in tumors would be a plausible explanation for the improved response to radiotherapy in patients receiving neoadjuvant castration.

The influence of castration on hypoxia has previously been investigated in mice bearing Shionogi tumors, which is a model for androgen-sensitive prostate cancer (16). The authors reported decreased hypoxia in regressed mouse tumors 7 days after castration, in accordance with our results in human prostate cancer. In the mouse experiment, this is likely explained by increased apoptosis of tumor cells, which may not be the case in the human prostate cancer observed here. In the relapsed androgen-independent tumors, the authors reported increased hypoxia (16). If this is applicable to human prostate cancer, the timing of radiotherapy after castration is crucial, and radiotherapy should be carried out at the right time before the outgrowth of androgen-independent tumor cells. Most patients with localized untreated prostate cancer show a good biochemical response to androgen deprivation therapy, but unfortunately this correlates only weakly with the long-term prognosis of the disease (17). Randomized clinical studies have shown improvement on the long-term effect of androgen deprivation therapy in combination with radiotherapy in high-risk patients (2).

Here, we investigated the levels of HIF-1α as a marker of hypoxia. Previously, it was shown that the androgen receptor (AR) is coexpressed with HIF-1α and VEGF in androgen-sensitive tumors (18). There is a possibility that the AR itself may influence HIF-1α and VEGF expression, stimulating angiogenesis in early prostate cancer development (8, 18). In this scenario, it is possible that the decrease in HIF-1α levels observed after castration is related to AR expression. However, in a previous report of 22 patients, it was observed that androgen withdrawal (through castration) reduced hypoxia in prostate cancer, as measured by the ultrasound-guided transrectal needle electrode technique (19), which suggests that the decreased levels of HIF-1α observed here could be associated with a reduction in hypoxia.

It has previously been shown that tumor hypoxia downregulates DNA repair, which could potentially contribute to genetic instability in prostate cancer and decreased repair

Table 3. Coefficient of determination (R^2) for HIF-1α levels and different parameters used in this study

Parameters	HIF–1α levels before castration			HIF–1α decrease		
	R^2	Sign	*p*	R^2	Sign	*p*
HIF1-1α decrease	0.39	+	*	1.00	+	
Age	0.00	–	NS	0.00	+	NS
PSA before castration (ng/ml)	0.03	+	NS	0.01	–	NS
Testosterone before castration (nmol/L)	0.00	+	NS	0.02	–	NS
Gleason grade	0.04	+	NS	0.13	+	NS
PSA after castration (ng/mL)	0.03	+	NS	0.02	+	NS
Testosterone after castration (nmol/L)	0.08	–	NS	0.14	–	NS
Days between biopsies	0.21	–	NS	0.18	–	NS
PSA decrease (ng/mL)	0.02	+	NS	0.02	–	NS
Testosterone decrease (nmol/L)	0.00	+	NS	0.08	+	NS
PSA decrease (%)	0.01	–	NS	0.15	–	NS
Testosterone decrease (%)	0.00	+	NS	0.01	–	NS

Abbreviations: HIF-1α = hypoxia-inducible factor-1α; PSA = prostate-specific antigen; NS = not significant.
$p > 0.05$ = NS, $p < 0.05$ =*.

capacity in response to DNA-damaging agents (20). Effective DNA repair reduces the efficiency of radiotherapy; thus, a reduced level of hypoxia in castrated prostate cancers would be expected to be associated with an increase in DNA repair, causing radioresistance in tumors. Clearly, sensitivity to radiotherapy is enhanced after castration, which suggests that any change in DNA repair caused by decreased hypoxia is of less importance to the overall effect of radiotherapy. Indeed, the influence of castration on DNA repair should be the focus for future studies.

In conclusion, we demonstrate reduced levels of HIF-1α in prostate cancer after castration, which is likely explained by reduced hypoxia and may explain the increased radiosensitivity of neoadjuvant castration in prostate cancer.

REFERENCES

1. Ferlay J, Parkin DM, Steliarova-Foucher E. Estimates of cancer incidence and mortality in Europe in 2008. *Eur J Cancer* 2010; 46:765–781.
2. Bolla M, Van Tienhoven G, Warde P, *et al*. External irradiation with or without long-term androgen suppression for prostate cancer with high metastatic risk: 10-year results of an EORTC randomised study. *Lancet Oncol* 2010;11:1066–1073.
3. Harris AL. Hypoxia—a key regulatory factor in tumour growth. *Nat Rev Cancer* 2002;2:38–47.
4. Wang GL, Jiang BH, Rue EA, *et al*. Hypoxia-inducible factor 1 is a basic-helix-loop-helix-PAS heterodimer regulated by cellular O2 tension. *Proc Natl Acad Sci U S A* 1995;92: 5510–5514.
5. Kimbro KS, Simons JW. Hypoxia-inducible factor-1 in human breast and prostate cancer. *Endocr Relat Cancer* 2006;13: 739–749.
6. Zhong H, De Marzo AM, Laughner E, *et al*. Overexpression of hypoxia-inducible factor 1alpha in common human cancers and their metastases. *Cancer Res* 1999;59:5830–5835.
7. Du Z, Fujiyama C, Chen Y, *et al*. Expression of hypoxia-inducible factor 1alpha in human normal, benign, and malignant prostate tissue. *Chin Med J (Engl)* 2003;116:1936–1939.
8. Zhong H, Semenza GL, Simons JW, *et al*. Up-regulation of hypoxia-inducible factor 1alpha is an early event in prostate carcinogenesis. *Cancer Detect Prev* 2004;28:88–93.
9. Moeller B, Dewhirst MW. HIF-I and tumour radiosensitivity. *Br J Cancer* 2006;95:1–5.
10. Moeller BJ, Cao YT, Li CY, *et al*. Radiation activates HIF-1 to regulate vascular radiosensitivity in tumors: role of reoxygenation, free radicals, and stress granules. *Cancer Cell* 2004;5: 429–441.
11. Vergis R, Corbishley CM, Norman AR, *et al*. Intrinsic markers of tumour hypoxia and angiogenesis in localised prostate cancer and outcome of radical treatment: a retrospective analysis of two randomised radiotherapy trials and one surgical cohort study. *Lancet Oncol* 2008;9:342–351.
12. Dai Y, Bae K, Siemann DW. Impact of hypoxia on the metastatic potential of human prostate cancer cells. *Int J Radiat Oncol Biol Phys* 2011;81:521–528.
13. Bostwick DG. Grading prostate cancer. *Am J Clin Pathol* 1994; 102(4 Suppl. 1):S38–S56.
14. Talks KL, Turley H, Gatter KC, *et al*. The expression and distribution of the hypoxia-inducible factors HIF-1α and HIF-2α in normal human tissues, cancers, and tumor-associated macrophages. *Am J Pathol* 2000;157:411–421.
15. Ponten F, Jirstrom K, Uhlen M. The Human Protein Atlas: a tool for pathology. *J Pathol* 2008;216:387–393.
16. Yapp DTT, Woo J, Kartono A, *et al*. Non-invasive evaluation of tumour hypoxia in the Shionogi tumour model for prostate cancer with F-18-EF5 and positron emission tomography. *BJU Int* 2007;99:1154–1161.
17. Janoff DM, Peterson C, Mongoue-Tchokote S, *et al*. Clinical outcomes of androgen deprivation as the sole therapy for localized and locally advanced prostate cancer. *BJU Int* 2005;96: 503–507.
18. Boddy JL, Fox SB, Han C, *et al*. The androgen receptor is significantly associated with vascular endothelial growth factor and hypoxia sensing via hypoxia-inducible factors HIF-1a, HIF-2a, and the prolyl hydroxylases in human prostate cancer. *Clin Cancer Res* 2005;11:7658–7663.
19. Milosevic M, Chung P, Parker C, *et al*. Androgen withdrawal in patients reduces prostate cancer hypoxia: implications for disease progression and radiation response. *Cancer Res* 2007; 67:6022–6025.
20. Bristow RG, Hill RP. Hypoxia, DNA repair and genetic instability. *Nat Rev Cancer* 2008;8:180–192.

II

Published OnlineFirst January 24, 2013; DOI: 10.1158/1078-0432.CCR-12-2795

Cancer Therapy: Clinical

Clinical Cancer Research

Castration Therapy Results in Decreased Ku70 Levels in Prostate Cancer

Firas L. T. Al-Ubaidi[1,3], Niklas Schultz[1], Olga Loseva[1], Lars Egevad[2], Torvald Granfors[3], and Thomas Helleday[1]

Abstract

Purpose: Neoadjuvant castration improves response to radiotherapy of prostate cancer. Here, we determine whether castration therapy impairs nonhomologous end-joining (NHEJ) repair of DNA double-strand breaks (DSB) by downregulating Ku70 protein expression.

Experimental Design: Twenty patients with locally advanced prostate cancer were enrolled, and 6 to 12 needle core biopsy specimens were taken from the prostate of each patient before treatment. Bilateral orchidectomy was conducted in eight patients and 12 patients were treated with a GnRH agonist. After castration, two to four similar biopsies were obtained, and the levels of Ku70 and γ-H2AX foci were determined by immunofluorescence in verified cancer tissues.

Results: We observed that the androgen receptor binds directly to Ku70 in prostate tissue. We also found a reduction of the Ku70 protein levels in the cell nuclei in 12 of 14 patients ($P < 0.001$) after castration. The reduction in Ku70 expression correlated significantly with decreased serum prostate-specific antigen (PSA) levels after castration, suggesting that androgen receptor activity regulates Ku70 protein levels in prostate cancer tissue. Furthermore, a significant correlation between the reductions of Ku70 after castration versus changes induced of castration of γ-H2AX foci could be seen implicating a functional linkage of decreased Ku70 levels and impaired DNA repair.

Conclusions: Castration therapy results in decreased levels of the Ku70 protein in prostate cancer cells. Because the Ku70 protein is essential for the NHEJ repair of DSBs and its downregulation impairs DNA repair, this offers a possible explanation for the increased radiosensitivity of prostate cancer cells following castration. *Clin Cancer Res; 19(6); 1547–56. ©2013 AACR.*

Introduction

Approximately one million new cases of prostate cancer are diagnosed in the world each year (1). Nonmetastatic prostate cancer is potentially curable and one treatment modality is radiotherapy, either alone or in combination with neoadjuvant castration therapy using gonadotropin-releasing hormone (GnRH) agonists for a limited period of time. Clinical studies have shown synergistic effects between castration and radiotherapy (2). A more detailed understanding of the cellular and molecular mechanisms behind this synergism would allow us to optimize treatment and may also give rise to novel therapeutic applications. We have previously shown that the hypoxia levels in prostate cancer tissue decrease following castration (3). Because hypoxia is associated with poor response to radiotherapy (4, 5), reduced hypoxia after castration may offer one plausible mechanistic explanation.

The androgen receptor plays an important role in the genesis, growth, and survival of normal prostate cells. Epidemiologic studies have failed to show any relationship between high serum levels of testosterone/dihydrotestosterone or adrenal androgen and prostate cancer risk (6, 7). In a rat model, a reduction in serum dihydrotestosterone after castration resulted in a 70% loss of secretory epithelial prostate cells by means of apoptosis (8). In the cytoplasm, the androgen receptor is found in inactive complexes bound to the HSP70 and HSP90 and as a corepressor. Testosterone and dihydrotestosterone bind to the androgen receptor as ligands. Androgen receptor translocates to the nucleus and binds to androgen response elements (ARE) in the promoter regions of target genes, thus inducing cell proliferation (9).

Castration therapy by orchidectomy or pharmacologic castration adequately reduces the serum testosterone below 1.7 nmol/L. However, intraprostatic tissue testosterone levels reduce only by 75% (10) which in turn leads to reduction rather than abrogation of androgen receptor activities. Castration is not curative as a single treatment

Authors' Affiliations: [1]Science for Life Laboratory, Division of Translational Medicine and Chemical Biology, Department of Medical Biochemistry and Biophysics, Karolinska Institutet; [2]Department of Oncology-Pathology, Karolinska Institutet, Karolinska University Hospital, Stockholm; and [3]Department of Urology, Västmanland Hospital Västerås, Västerås, Sweden

Note: Supplementary data for this article are available at Clinical Cancer Research Online (http://clincancerres.aacrjournals.org/).

Corresponding Author: Thomas Helleday, Science for Life Laboratory, Karolinska Institutet, Box 1031, Stockholm S-171 21, Sweden. Phone: 46-852480000; Fax: 46-852481530; E-mail: thomas.helleday@scilifelab.se

doi: 10.1158/1078-0432.CCR-12-2795

Published OnlineFirst January 24, 2013; DOI: 10.1158/1078-0432.CCR-12-2795

Translational Relevance

Clinical studies have shown improved radiotherapy response and longer overall survival for patients with prostate cancer after neoadjuvant androgen deprivation, but mechanistic insights are missing. In this study, the levels of the Ku70 protein, critical for DNA double-strand break repair, decrease after castration in parallel with corresponding reduction in serum prostate-specific antigen (PSA). This reduced level of the repair protein offers a probable explanation for the increased treatment efficiency, when radiotherapy is combined with castration therapy. Furthermore, according to our data, the castration-induced decrease in PSA may predict a successful response to radiotherapy.

modality but is the most effective palliative treatment in metastasized prostate cancer. There is no difference in long-term survival between the 2 castration methods (11, 12). Castration is achieved almost immediately after bilateral orchidectomy and approximately 4 weeks after initiating treatment with GnRH agonists (13). Randomized clinical trials have shown longer survival of patients with prostate cancer after combined castration and radiotherapy of the primary tumor than after radiotherapy alone (2, 14). This clinically observed increased radiosensitivity of prostate cancer after castration was not seen *in vitro* with cell lines LNCaP and PC-3 (15, 16).

The expression of prostate-specific antigen (PSA) is primarily regulated by androgen receptor via AREs (17) and is considered to be the most effective single biomarker for monitoring the metabolic activity of prostate cancer cells before, during, and after radiotherapy (18).

Nonhomologous end-joining (NHEJ) is the major DNA repair pathway involved in the repair of DNA double-strand breaks (DSB) after ionizing radiation (IR; ref. 19). Unrepaired or misrepaired DSBs lead either to cell death or chromosomal translocations and genomic instability. DNA protein kinase (DNA-PK) is a key component of NHEJ (20), which consists of the Ku70–Ku80 heterodimer and the DNA-PK catalytic subunit (DNA-PKcs) to form the DNA-PK complex. Ku proteins play a central role in NHEJ by detecting DSB ends and tethering them together (21, 22). Cells deficient in Ku70 and Ku80 proteins are extremely sensitive to IR (23, 24). Even though Ku70 is mainly located in the nucleus, a fraction of it is located in the cytoplasm. The cytoplasmic fraction of Ku70 binds the proapoptotic protein Bax, preventing its translocation to mitochondria and thereby suggesting that Ku70 suppresses mitochondrially mediated apoptosis. Depletion of the level of cytosolic Ku70 has been shown to induce apoptosis in colorectal cancer (25). Because the Ku70 protein has been shown, in prostate cell lines, to act as a coactivator of androgen receptor (26), we wanted to test whether the differential AR function after castration influences Ku70 protein levels. If so, it might offer an explanation for increased apoptosis and radiosensitivity after castration.

Using prostate needle core biopsy specimens from patients with prostate cancer, we tested whether castration downregulates the expression of Ku70 proteins in prostate cancer specimens, subsequently leading to defective DNA repair and increased cell death.

Materials and Methods

Patient material and collection

Twenty patients with newly diagnosed prostate cancer were enrolled in the study, after the approval of the regional ethics committee at Uppsala University (Uppsala, Sweden; Dnr 2007/170).

At diagnosis, the first biopsy setting, 6 to 12 prostatic needle core biopsy specimens were taken randomly from each patient. All patients were then treated with castration therapy, either with bilateral orchidectomy or with a GnRH-agonist (leuprorelin; Table 1). After castration, that is, approximately 1 month after orchidectomy and 2 months after the initiation of the GnRH agonist, the second biopsy setting, 2 to 4 prostatic needle core biopsy specimens were taken from each patient. To increase the likelihood of obtaining representative specimens, only presumed tumor areas were chosen for the second biopsy setting. Six patients were excluded from the study because biopsy specimens from their second biopsy setting did not contain representative cancer areas. Fourteen patients were included in the study and their median age was 78 years (range, 59–89 years). The median PSA level was 98 ng/mL (range, 3–1,021 ng/mL). The median serum testosterone level was 11.0 nmol/L (range, 6.6–23.0 nmol/L). The median prostate volume measured by means of transrectal ultrasound was 52 mL (range, 20–160 mL). Thirteen patients had locally advanced *c*T3-4 tumors and only one patient had an organ-confined *c*T2 tumor. Half of the patients received a GnRH agonist, whereas bilateral orchidectomy was conducted in the other half. The mean time and SD from orchidectomy to the second biopsy was 26 $\pm$ 19 days and from initiating GnRH agonist treatment to second biopsy was 54 $\pm$ 14 days. After orchidectomy, the PSA levels varied from 1 to 148 ng/mL and the serum testosterone levels from 0.3 to 0.9 nmol/L. After GnRH agonist treatment, the PSA was 0.3 to 55 ng/mL and serum testosterone 0.3 to 1.7 nmol/L.

Histological and immunofluorescence evaluation

From each patient, 2 biopsy specimens before and two after castration were chosen. The specimens were embedded in paraffin and sectioned. One section from each biopsy specimen was stained with hematoxylin and eosin (HE) and graded according to the Gleason system (27). Sections adjacent to the HE-stained sections were used for immunofluorescence studies.

Deparaffinization and rehydration of the sections from 2 series of slides were conducted before antigen retrieval in Tris/EDTA, pH 9.0, in a pressure cooker. The sections were blocked in 3% bovine serum albumin (BSA). Afterward, sections from the first set were incubated with the primary

Published OnlineFirst January 24, 2013; DOI: 10.1158/1078-0432.CCR-12-2795

Table 1. Patient demography and tumor characteristics of patients included in this study

					PSA, ng/mL		Testosterone, nmol/L			
Patient number	Patient age	Prostate volume, ml	cT	GS	Before castration	After castration	Before castration	After castration	Days between castration and biopsies II	Castration method
6	70	71	4	8	1,021	21	12	0.9	47	GnRH agonist
9	83	20	3	7	8	0.3	14	0.8	62	GnRH agonist
10	87	59	3	7	34	1.9	15	0.7	36	GnRH agonist
12	61	26	2	7	17	6.4	ND	1.7	36	GnRH agonist
14	78	90	3	7	326	55	7	0.3	48	GnRH agonist
18	69	50	3	10	380	5.4	11	0.3	83	GnRH agonist
19	77	34	3	7	107	2.6	11	1.0	48	GnRH agonist
2	67	65	3	10	2.9	3.7	23	0.3	4	Orchidectomy
5	86	52	3	9	70	53	7	1.0	6	Orchidectomy
8	63	44	3	8	650	134	13	0.9	8	Orchidectomy
15	59	90	4	9	736	29	8	0.9	46	Orchidectomy
16	82	ND	3	7	16	1.1	16	0.6	49	Orchidectomy
17	84	46	4	8	438	138	9	0.6	29	Orchidectomy
20	83	100	3	9	89	23	10	0.3	40	Orchidectomy

Abbreviations: cT, clinical tumor stadium; GS, Gleason score; ND, not done.

antibody KU-70 (1:500, 3C3.11 Santa Cruz) at 4°C overnight. While sections from the second set were incubated with the primary antibody γ-H2AX (1:500, 3F2, Abcam) at 4°C overnight. Extensive rinsing was conducted once the sections were incubated with the secondary antibody (donkey anti mouse IgG-Alexa 488, Molecular probe) for 1 hour at room temperature. DNA was counterstained with TO-PRO-3 iodide (Molecular probe) and slides mounted with pro long gold (Molecular probe).

An image from a tumor area with a good degree of immunofluorescence signals from each biopsy was selected. The corresponding area in the HE-stained section was identified for the histologic verification of the tumor area. In Ku70-stained slides, 3 areas containing approximately 50 to 100 cells were chosen for analysis. The 3 areas were analyzed, using NIH ImageJ, with respect to medium intensity in the nucleus (TO-PRO-3 was used as DNA marker), and medium intensity outside the nucleus. In the γ-H2AX–stained slides, a tumor area containing approximately 150 to 300 cells were chosen for analysis with NIH ImageJ. Areas inside the nucleus with a γ-H2AX intensity higher than 75% of max intensity were considered as γ-H2AX foci. The number of foci were counted and expressed as foci/DNA unit.

Fluorescence images were obtained with a Zeiss LSM 510–inverted confocal microscope using a planapochromat 20×/numerical aperture (NA) 0.75 objective. Bright light images were obtained with a Nikon eclipse C600 microscope using a planapochromat 20×/NA 0.75 objective.

Coimmunoprecipitation of androgen receptor with Ku70

Frozen prostate tissue biopsies were disintegrated in a Potter homogenizer, and proteins were extracted with a lysis buffer 10 mmol/L HEPES, pH 7.5, 300 mmol/L NaCl, 0.2 mmol/L EDTA, 10 mmol/L dithiothreitol (DTT), 20% glycerol, and 0.1% Triton X-100 supplemented with a complete protease inhibitor cocktail (Roche Applied Science). After centrifugation at 23,000 × *g* for 20 minutes, the supernatant was incubated with mouse monoclonal anti-Ku70 Ab (sc-12729, Santa Cruz) by rotation at 4°C overnight. Protein A/G-agarose beads (sc-2003, Santa Cruz) were added and the mixture was incubated for 2 hours at 4°C. The beads were collected at 1,000 × *g* and washed twice with a lysis buffer and once with a lysis buffer without glycerol. The coimmunoprecipitated proteins were eluted by boiling in LDS sample buffer with a reducing agent (Invitrogen). Samples were, after electrophoresis, blotted on to nitrocellulose membranes and probed with the monoclonal mouse anti-human androgen receptor Ab (Dako M356201-2), anti-Ku70 Ab (sc-12729), and anti-actin Ab (sc-1616) followed by incubation with a horseradish peroxidase–conjugated secondary antibody (Thermo Scientific), and protein bands were visualized using a SuperSignal West Femto chemiluminescence substrate (Thermo Scientific).

Results

Ku70 interacts with the androgen receptor in prostate cancer tissue

Radiosensitive cells have previously been isolated, and the underlying mechanism explaining the sensitivity has, in most cases, been defects in DNA repair (28). We hypothesized that castration therapy may alter the DNA repair capacity of prostate cancer cells. Androgen receptor activity is altered following castration and it has previously been reported that Ku70 interacts with the androgen receptor in the prostate cell line LNCaP (26). To investigate whether this interaction is also present in *in vivo* material, a coimmunoprecipitation of androgen receptor with Ku70 from

Published OnlineFirst January 24, 2013; DOI: 10.1158/1078-0432.CCR-12-2795

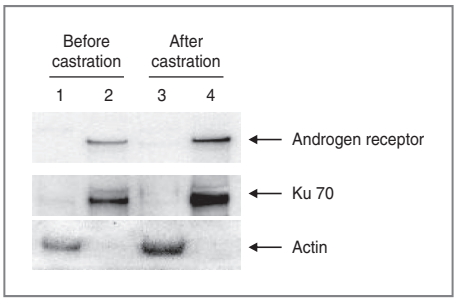

Figure 1. Ku70 interacts with the androgen receptor (AR) in prostate cancer tissue. Coimmunoprecipitation of AR with Ku70 from prostate cancer tissue extract. Lanes 1 and 3, 10% of tissues extract input. Lanes 2 and 4, AR eluted from anti-Ku70 Ab + Protein A/G beads. Western blot analysis of total tissue extract and eluted AR. Antibodies used for immunoblots are identified on the right.

prostate tissue extracts before and after castration indicated an interaction between androgen receptor and Ku70 both before and after castration (Fig. 1), and we also found that the castration itself did not influence the interaction between the two proteins.

Ku70 protein levels decrease following castration

Because the androgen receptor and Ku70 proteins interact, we subsequently wanted to determine whether the Ku70 protein levels are influenced by castration. We quantified the levels of Ku70 protein in cancer areas in paired slides from 14 eligible patients (Table 1) with high-grade prostate cancer before and after castration (Fig. 2). The levels of Ku70 in the nuclei were reduced by approximately half the value observed before castration ($P = 0.001$; Fig. 3A). A decrease of the same magnitude could also be seen in the Ku70 localized outside the nuclei ($P = 0.006$; Fig. 3B). However, the intensity of Ku70 was always higher in the nuclei than outside, both before and after castration (Figs. 2 and 3A and B).

We observed large individual variations in Ku70 protein levels both for the intranuclear fraction, ranging from 20 to 180, and the extranuclear fraction, ranging from 4 to 120 arbitrary intensity units (Fig. 3C and D). After castration, a decrease in the Ku70 level was seen in almost all patients in both fractions of Ku70 (Fig. 3C and D). Patients who did not respond with a Ku70 decrease after castration had very low initial Ku70 values (Fig. 3C and D). In fact, the initial Ku70 value, that is, before castration, correlated well with the decrease in Ku70 after castration in both fractions of Ku70 (intranuclear $R^2 = 0.811$, $P < 0.0001$; Fig. 3E, extranuclear ($R^2 = 0.944$, $P \leq 0.0001$; Fig. 3F). Even though the level of Ku70 varied greatly between patients, the Ku70 value between the 2 fractions, intra- and extranuclear, correlated well for each patient ($R^2 = 0.817$, $P < 0.0001$; Fig. 3G).

Ku70 does not correlate with prostate size, serum PSA, serum testosterone, Gleason score, or patient age

The interindividual variations in initial Ku70 levels are large and can vary by a factor of 10 for both nuclear and cytoplasmic Ku70 (see Fig. 3C and D). We investigated whether there was any correlation between the Ku70 levels and other parameters measured in this study. There was no significant correlation to prostate size ($R^2 = 0.14$, $P = 0.97$), PSA level ($R^2 = 0.004$, $P = 0.97$), testosterone level ($R^2 = 0.0004$, $P = 0.80$), Gleason score ($R^2 = 0.09$, $P = 0.81$), or age ($R^2 = 0.007$, $P = 0.48$) versus the nucleic fraction of Ku70. This observation was also valid for the cytoplasmic fraction of Ku70 [prostate size ($R^2 = 0.20$, $P = 0.66$), PSA level ($R^2 = 0.0001$, $P = 0.94$), testosterone level ($R^2 = 0.02$, $P = 0.49$), Gleason score ($R^2 = 0.07$, $P = 0.82$), and age ($R^2 = 0.004$, $P = 0.60$)].

Ku70 reduction after castration correlates with decreased PSA, but not with decreased testosterone levels

Although there was significant decrease in Ku70 levels in prostate cancer cells after castration, the interindividual variations of the castration-induced changes in Ku70 levels were large, spanning from 2% to 126% in nuclei and 2% to 340% in cytoplasm. There was also a large variation in the testosterone and PSA reductions. The castration-induced reduction in serum PSA varied from 24% to 99% (Table 1). For patient number 2, who had a low PSA and did not respond to hormonal treatment, we noticed a 28% increase of PSA compared with the precastration value. The reduction of serum testosterone varied from 85% to 98%.

We compared pharmacologically castrated with orchidectomized patients. Patient number 8 belonged to the surgical castration group and showed atypical data in comparison with the rest of this subgroup and was, therefore, considered an outlier and was excluded from the calculations of coefficient of determination and probability values. The value of patient 8 is depicted as an unfilled circle in every figure. Between the 2 subgroups, there were no significant differences in measured parameters. Both types of castration show a significant correlation between the decrease in Ku70, both in the nuclear and the cytoplasmic fractions, and the decrease in PSA after castration (chemical nuclear $R^2 = 0.91$, $P = 0.003$, cytoplasmic $R^2 = 0.77$, $P = 0.023$ and surgical nuclear $R^2 = 0.73$, $P = 0.018$, cytoplasmic $R^2 = 0.84$, $P = 0.005$ Fig. 4A–D). No such correlation could be seen between the decrease in Ku70 and the decrease in testosterone after castration (chemical nuclear $R^2 = 0.014$, $P = 0.96$, cytoplasmic $R^2 = 0.002$, $P = 0.70$ and surgical nuclear $R^2 = 0.002$, $P = 0.96$, cytoplasmic $R^2 = 0.11$, $P = 0.62$).

Ku70 and PSA kinetics after castration are related

The kinetics of PSA and testosterone decrease depends on the castration method and this may influence the effect on Ku70 levels differently. Therefore, PSA kinetics could potentially be used to calculate the optimal time for starting radiotherapy.

To obtain an indication of the kinetics of the Ku70 decrease, the correlation between Ku70 decrease and the interval between the first and second biopsies was investigated. Patients treated with bilateral orchidectomy showed a strong significant correlation ($R^2 = 0.77$, $P = 0.02$; Fig.

Published OnlineFirst January 24, 2013; DOI: 10.1158/1078-0432.CCR-12-2795

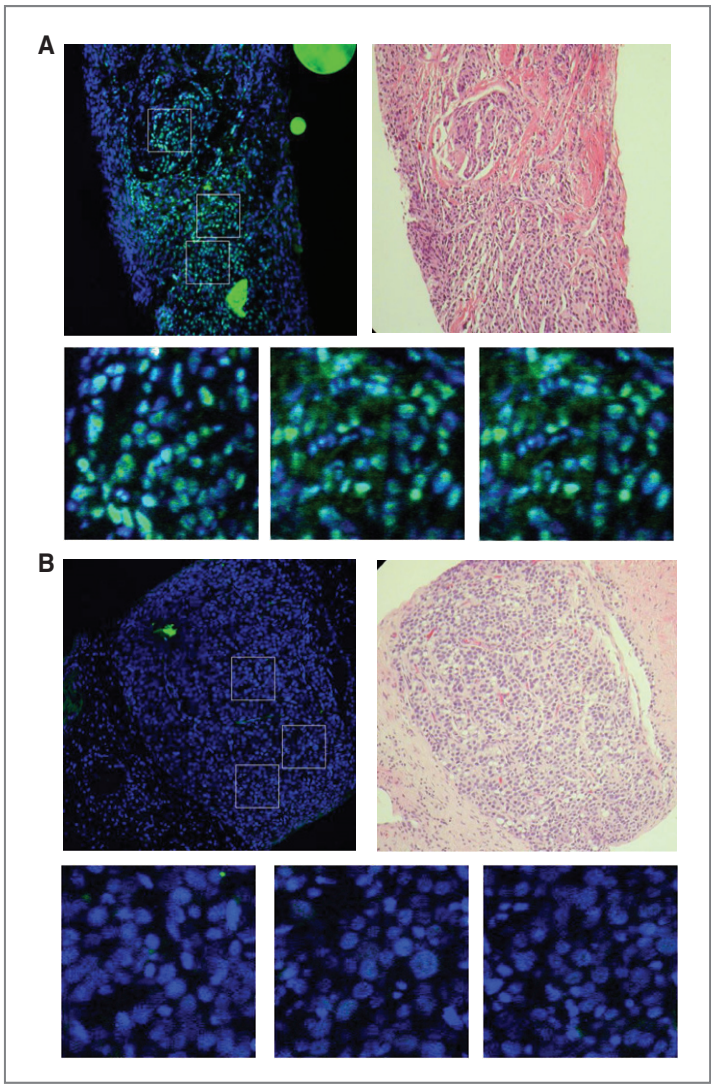

Figure 2. Determination of Ku70 in prostate tumors. A, top left, an immunohistofluorescence-stained section of a prostate biopsy before castration. The 3 squares outlined in the middle of the image mark the area chosen for intensity measurement. Ku70 is stained with a mouse-monoclonal antibody (green) and the DNA is costained with TO-PRO-3 (blue). Top right, a corresponding area from an adjacent section stained with hematoxylin and eosin. The 3 panels below are close-ups of the 3 areas depicted for intensity measurements. B, as in A, but the biopsy is taken after castration, but from the same patient.

5A), whereas patients treated with GnRH agonist had no significant correlation ($R^2 = 0.36$, $P = 0.26$; Fig. 5B). Similar results were achieved for the cytoplasmic fraction of Ku70 (Supplementary Fig. S1). This suggests that the Ku70 level in patients treated with bilateral orchidectomy is still decreasing in the time span used here, whereas the Ku70 levels in patients treated with GnRH agonist have reached a plateau. To see whether the PSA levels had similar kinetics, the correlation between PSA decrease and the number of days between biopsies was analyzed. Indeed, in patients treated with bilateral orchidectomy, a significant correlation was seen between the decrease in the PSA value and the number of days after castration ($R^2 = 0.84$, $P = 0.019$; Fig. 5C). In contrast, patients treated with GnRH agonist did not show a significant correlation ($R^2 = 0.25$, $P = 0.26$; Fig. 5D). Investigating the decrease in testosterone versus the days after castration, we found that patients treated with bilateral orchidectomy had no significant correlation ($R^2 = 0.03$, $P = 0.66$; Fig. 5E), which was expected because all the reduction in testosterone levels normally occurs the first few days after bilateral orchidectomy. A similar picture was seen in the group treated with a GnRH agonist ($R^2 = 0.19$, $P =$

Published OnlineFirst January 24, 2013; DOI: 10.1158/1078-0432.CCR-12-2795

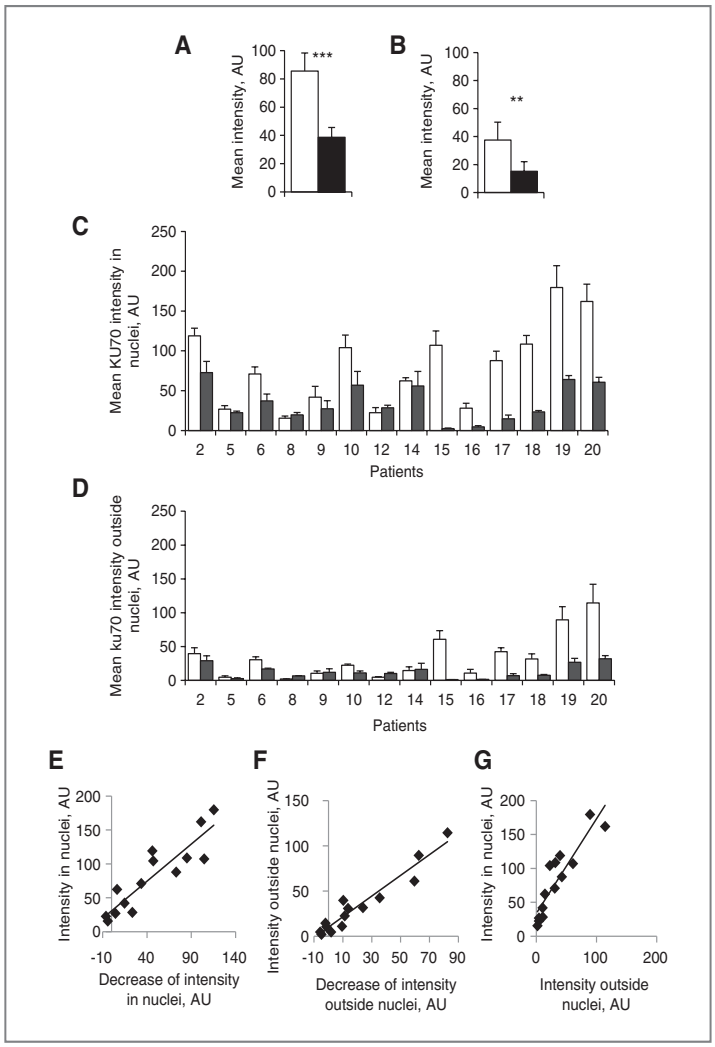

Figure 3. Effect of castration on Ku70 in prostate tumors. A, mean intensity of Ku70 in nuclei before (white bars) and after (black bars) castration. Error bars show SEM. ***, $P < 0.001$, Student t test. B, mean intensity of Ku70 outside the nuclei before (white bars) and after (black bars) castration. Error bars show SEM. **, $P < 0.01$, Student t test. C, Ku70 intensity in nuclei of individual patients before (white bars) and after (black bars) castration. Error bars show SEM. D, Ku70 intensity outside the nuclei of individual patients before (white bars) and after (black bars) castration. Error bars show SEM. E, correlation between the Ku70 intensity in nuclei before castration versus the decrease in intensity in the nuclei after castration. $R^2 = 0.81$; $P < 0.0001$. F, correlation between the Ku70 intensity outside the nuclei before castration versus the decrease in intensity outside the nuclei after castration. $R^2 = 0.94$; $P < 0.0001$. G, correlation between the Ku70 intensity in nuclei before castration versus the intensity outside the nuclei before castration. $R^2 = 0.82$; $P < 0.0001$. Statistics used: Spearman rank correlation coefficient.

0.062; Fig. 5F). These data suggest that the kinetics of PSA decrease is the most relevant parameter to use for predicting when the minimum level of Ku70 has been reached and, thereby, the most optimal time point for radiation treatment.

Ku70 reduction after castration correlates with an increase of γ-H2AX foci

To investigate whether the initial Ku70 values or the decrease of Ku70 after castration would be reflected in the amount of unrepaired endogenous DNA damages, we stained slides from the biopsies with an antibody against γ-H2AX. Images of tumor areas were then analyzed with respect to the number of γ-H2AX foci/DNA unit with a program written in ImageJ (Fig. 6A–C). No significant difference in γ-H2AX foci could be seen in mean values of biopsies before and after castration (Fig. 6D). Neither could any correlation between the initial Ku70 values versus the amount of γ-H2AX foci be seen ($R^2 = 0.009$, $P = 0.3$). However, a significant correlation between the reductions of Ku70 after castration versus changes induced of castration of γ-H2AX foci could be seen (Fig. 6E, $R^2 = 0.37$, $P = 0.022$). These data could point to a reduced repair of DNA damage following a decrease of Ku70 levels.

Published OnlineFirst January 24, 2013; DOI: 10.1158/1078-0432.CCR-12-2795

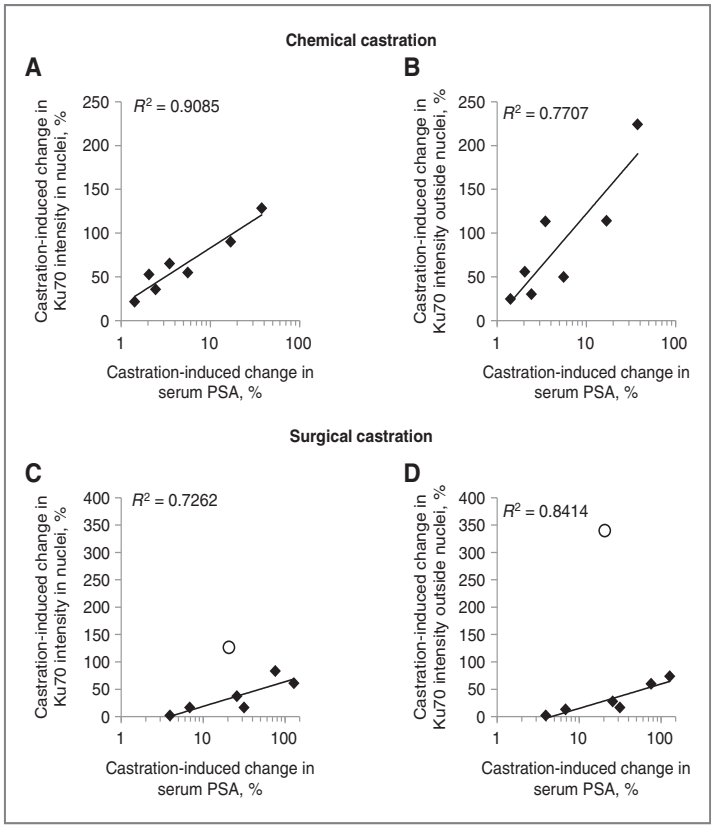

Figure 4. ADT-induced Ku70 decrease correlates with a decrease in PSA in patients with prostate cancer. A, correlation between the changes induced by chemical castration in Ku70 in the nuclei versus changes induced by chemical castration in serum PSA. $R^2 = 0.91$; $P = 0.003$. The values of Ku70 and PSA are given in percentage of value before castration. B, as in A, but for Ku70 outside the nuclei. $R^2 = 0.77$; $P = 0.023$. C, correlation between the changes induced by surgical castration in Ku70 in the nuclei versus changes induced by surgical castration in serum PSA. $R^2 = 0.73$; $P = 0.018$. The values of Ku70 and PSA are given in percentage of value before castration. D, as in C, but for Ku70, outside the nuclei. $R^2 = 0.84$; $P = 0.005$. Statistics used: Spearman rank correlation coefficient. The unfilled circles in C and D represent the value from patient 8, who was considered an outlier and is therefore not included in the calculations of R^2 and P.

Discussion

We show a reduction of the Ku70 protein in prostate cancer tissues after castration. The Ku70 protein is a major determinant of radiosensitivity. In several unbiased mutational screens in mammalian cells, the Ku70 mutant cells, defective in NHEJ (24), were isolated as the most radiosensitive (28). It is well established that the Ku70/Ku80 components of NHEJ are the most critical for effective DSB repair and they work in a DNA-PK–dependent manner after irradiation (19, 29). Hence, the severe depletion of Ku70 protein levels after castration is likely to impair NHEJ in the prostate cancer tissues and explain the increased sensitivity to radiotherapy. Several previous studies have shown that cells depleted with Ku70 are using an alternative backup pathway termed B-NHEJ in repairing irradiation-induced DSBs and PARP-1 is a major component of this alternative repair pathway (30). After castration, effective B-NHEJ mediated by PARP-1 would be expected to improve DSBs repair and reduce the efficacy of radiotherapy. Thus, suppression of B-NHEJ by PARP inhibitors would further improve radiosensitivity. However, the role of PARP-1 in prostate cancer is very complex as it has recently been shown to mediate androgen receptor function (31). Certainly, the role of PARP-1 in the repair of irradiation induced DSBs and androgen receptor transcription with and without castration warrant further studies.

To test whether the reduction of Ku70 seen after castration changed the repair kinetics of endogenous DNA lesions, we stained for the DNA DSB marker γ-H2AX. A significant positive correlation could be seen between Ku70 reductions and increase in γ-H2AX foci (Fig. 6E). However, no significant difference could be seen between biopsies before and after castration (Fig. 6D). This seemingly contradictory result may be explained by the castration effect on cell proliferation. Cells are constantly exposed to endogenous reactive oxygen species (ROS) production and replication failure leading to DNA lesions. This is particularly true for cancer cells that often have an elevated ROS level. A high ROS level leads to DNA single-strand breaks, and if not repaired, collapsed replication forks during replication (32). Collapsed replication forks are one ended DNA DSBs and will be marked with γ-H2AX. Androgen depletion leads to decreased rates of proliferation and thereby fewer collapsed replication forks. On the other hand, as shown

Published OnlineFirst January 24, 2013; DOI: 10.1158/1078-0432.CCR-12-2795

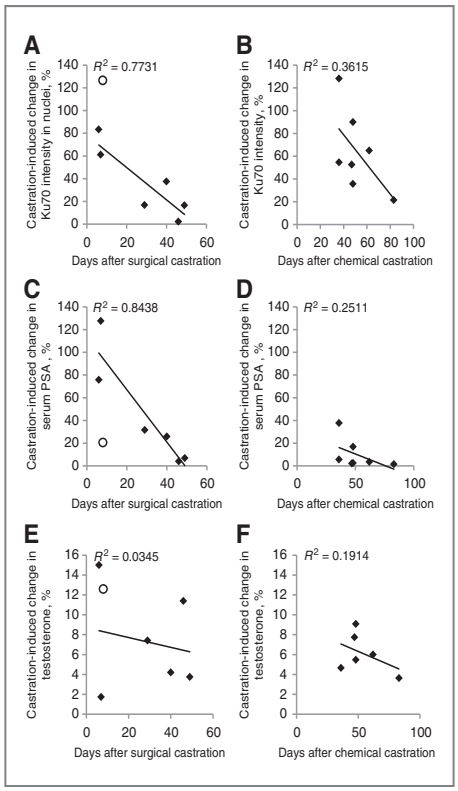

Figure 5. ADT-induced Ku70 decrease correlates with a decrease in PSA in patients with prostate cancer. A, correlation between the changes induced by surgical castration in Ku70 in the nuclei versus days after castration. $R^2 = 0.77$; $P = 0.02$. The values of Ku70 are given as a percentage of the value before castration. B, as in A, but patients who had undergone chemical castration. $R^2 = 0.36$; $P = 0.26$. C, correlation between the changes induced by surgical castration in serum PSA versus days after castration. $R^2 = 0.84$; $P = 0.019$. The values of PSA are given as a percentage of the value before castration. D, as in C, but patients who had undergone chemical castration. $R^2 = 0.25$; $P = 0.26$. E, correlation between the changes induced by surgical castration in testosterone versus days after castration. $R^2 = 0.03$; $P = 0.66$. The values of testosterone are given as a percentage of the value before castration. F, as in E, but patients who had undergone chemical castration. $R^2 = 0.19$; $P = 0.062$. Statistics used: Spearman rank correlation coefficient. The unfilled circles in A, C, and E represent the values from patient 8 who was considered an outlier and these values are therefore not included in the calculation of R^2 and P.

herein, androgen deprivation leads to reduction of Ku70 levels which may slow down the repair kinetics and thereby lead to an increased amount of unrepaired DNA lesions. Thus, androgen deprivation starts processes that can lead to either increase or decrease of γ-H2AX. Indeed, as shown in Fig. 6E, patients with no or minor decrease of Ku70 after androgen depletion shows a decrease of γ-H2AX, meanwhile patients with a large decrease of Ku70 shows an increase of γ-H2AX, implicating a functional linkage of decreased Ku70 levels and impaired DNA repair.

An interaction between the androgen receptor and Ku70 has been reported in the prostate cell line LNCaP (26) and we can confirm the interaction between the androgen receptor and Ku70 proteins in prostate cancer tissue. The interaction between the androgen receptor and Ku70 may unveil a mechanistic link between castration treatment and reduced Ku70 protein levels. It is indeed very difficult to test this potential mechanistic link experimentally in patients. However, the high correlation between decreased levels of PSA and decreased Ku70 levels (Fig. 4) supports the notion that the downregulation of Ku70 is related to a decrease in androgen receptor activity. We speculate that the binding between Ku70 and androgen receptor may influence the long-term stability of the Ku70 protein in prostate cancer cells. Another possibility is that androgen receptor inhibition or downregulation results in a decrease in the expression of NHEJ proteins.

In this study, none of the included patients were offered any curative therapy such as radiotherapy because they all had an advanced prostate cancer with a short life expectancy. However, all patients were treated with castration. Androgen deprivation leads to decreased rates of cell proliferation and induces apoptosis in prostate cancer cells (33). The pool of cytoplasmic Ku70 has been shown to totally disappear in cells entering senescence (34). Furthermore, the cytoplasmic fraction of Ku70 has been shown to sequester the proapoptotic protein Bax and, thereby, functions as an antiapoptotic protein (35). Because the cytoplasmic Ku70 was reduced to approximately half following castration, this may contribute to apoptosis induced by androgen depletion (36).

The optimal duration of neoadjuvant hormonal treatment is unknown. However, to achieve an optimal outcome of combined castration and radiotherapy, it might be of importance to start the radiation therapy when the level of Ku70 has reached its lowest value. Nevertheless, in most clinical studies, neoadjuvant hormonal therapy is recommended to start 2 to 6 months before the initiation of radiotherapy (37–39). To date, many studies have tried to relate the time of neoadjuvant hormonal therapy to their effect on prostate volume (40). However, other studies, have tried to find out a cutoff point for the serum PSA level (41–43)

The results of this study suggest that the PSA decrease after castration reflects the decrease in Ku70 levels in prostate cancer cells and, therefore, could be a good marker for defining the optimal time for radiotherapy.

Future studies should investigate the correlation between Ku70 and PSA decrease over time to validate the findings made in this study and, thereby, open for an improved clinical outcome of combined castration and radiotherapy. Furthermore, it would be of great interest to investigate whether the huge individual variations in Ku70 levels in cancerous prostate tissue also reflect radiation sensitivity.

Abiraterone and enzalutamide (formerly known as MDV3100) are 2 new target therapies with clinical benefits

Published OnlineFirst January 24, 2013; DOI: 10.1158/1078-0432.CCR-12-2795

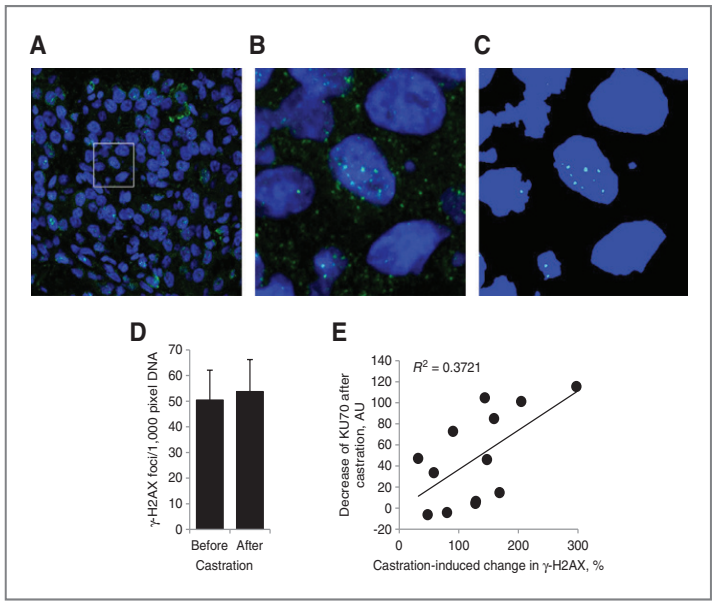

Figure 6. ADT-induced Ku70 decrease correlates with an increase in γ-H2AX foci in cells from patients with prostate cancer. For every patients, 2 biopsies before and 2 after castration were stained for γ-H2AX with a mouse monoclonal antibody (green) and the DNA were costained with TO-PRO-3 (blue). An image from a cancerous area containing approximately 200 cells was taken from all biopsies. A, an example of a γ-H2AX–stained image. B, a close-up of the marked square in A. C, the area in B, after processed in ImageJ. The number of γ-H2AX foci in DNA was calculated and expressed as number of γ-H2AX foci/1,000 pixel DNA. D, mean number of γ-H2AX foci/DNA area before and after castration. Error bars show SEM. E, correlation between the castration-induced decrease of Ku70 in the nuclei versus castration-induced changes of γ-H2AX foci ($R^2 = 0.37$; $P = 0.022$). The decrease of Ku70 is given in arbitrary units of fluorescence and the change in γ-H2AX foci is given in percentage of value before castration.

in treatment of castration-resistant prostate cancer (44, 45). However, any connections between these therapies and Ku70/NHEJ remain unexplored. Because the mechanism of action of these new target therapies will lead to further suppression of active androgen receptor, we presume that used neoadjuvantly they will consequently lead to further suppression of Ku70 and increase the radiosensitivity of prostate cancer cells. Obviously, this issue will be a matter of future studies.

In conclusion, we observed that the Ku70 protein level decreases in prostate cancer cells following castration and this may possibly explain the increased response to radiotherapy observed after neoadjuvant castration.

Disclosure of Potential Conflicts of Interest

No potential conflicts of interest were disclosed.

Authors' Contributions

Conception and design: F. Al-Ubaidi, N. Schultz, T. Granfors, T. Helleday
Development of methodology: F. Al-Ubaidi, N. Schultz, T. Helleday
Acquisition of data (provided animals, acquired and managed patients, provided facilities, etc.): F. Al-Ubaidi, N. Schultz, O. Loseva, L. Egevad
Analysis and interpretation of data (e.g., statistical analysis, biostatistics, computational analysis): F. Al-Ubaidi, N. Schultz, O. Loseva, L. Egevad, T. Helleday
Writing, review, and/or revision of the manuscript: F. Al-Ubaidi, N. Schultz, O. Loseva, L. Egevad, T. Granfors, T. Helleday
Administrative, technical, or material support (i.e., reporting or organizing data, constructing databases): F. Al-Ubaidi, T. Helleday
Study supervision: N. Schultz, T. Helleday

Grant Support

The authors thank the Västmanland Centre for Clinical Research (CKF), the Västmanland County Cancer Foundation, the Percy Falk Foundation, the AFA Foundation, the Swedish Cancer Society, the Swedish Research Council, the Swedish Children's Cancer Foundation, and The Swedish Pain Relief Foundation, Torsten and Ragnar Söderberg Foundations, and the European Research Council for financial support.

The costs of publication of this article were defrayed in part by the payment of page charges. This article must therefore be hereby marked *advertisement* in accordance with 18 U.S.C. Section 1734 solely to indicate this fact.

Received August 28, 2012; revised January 2, 2013; accepted January 15, 2013; published OnlineFirst January 24, 2013.

References

1. Ferlay J, Parkin DM, Steliarova-Foucher E. Estimates of cancer incidence and mortality in Europe in 2008. Eur J Cancer 2010;46:765–81.
2. Bolla M, Van Tienhoven G, Warde P, Dubois JB, Mirimanoff RO, Storme G, et al. External irradiation with or without long-term androgen suppression for prostate cancer with high metastatic risk: 10-year results of an EORTC randomised study. Lancet Oncol 2010;11:1066–73.
3. Al-Ubaidi FL, Schultz N, Egevad L, Granfors T, Helleday T. Castration therapy of prostate cancer results in downregulation

Published OnlineFirst January 24, 2013; DOI: 10.1158/1078-0432.CCR-12-2795

of HIF-1alpha levels. Int J Radiat Oncol Biol Phys 2012;82: 1243–8.
4. Milosevic M, Warde P, Menard C, Chung P, Toi A, Ishkanian A, et al. Tumor hypoxia predicts biochemical failure following radiotherapy for clinically localized prostate cancer. Clin Cancer Res 2012;18:2108–14.
5. Moeller BJ, Cao Y, Li CY, Dewhirst MW. Radiation activates HIF-1 to regulate vascular radiosensitivity in tumors: role of reoxygenation, free radicals, and stress granules. Cancer Cell 2004;5:429–41.
6. Muller RL, Gerber L, Moreira DM, Andriole G, Castro-Santamaria R, Freedland SJ. Serum testosterone and dihydrotestosterone and prostate cancer risk in the placebo arm of the reduction by dutasteride of prostate cancer events trial. Eur Urol 2012;62:757–64.
7. Hsing AW. Hormones and prostate cancer: what's next? Epidemiol Rev 2001;23:42–58.
8. English HF, Kyprianou N, Isaacs JT. Relationship between DNA fragmentation and apoptosis in the programmed cell death in the rat prostate following castration. Prostate 1989;15:233–50.
9. Heinlein CA, Chang C. Androgen receptor in prostate cancer. Endocr Rev 2004;25:276–308.
10. Mostaghel EA, Page ST, Lin DW, Fazli L, Coleman IM, True LD, et al. Intraprostatic androgens and androgen-regulated gene expression persist after testosterone suppression: therapeutic implications for castration-resistant prostate cancer. Cancer Res 2007;67:5033–41.
11. Prostate Cancer Trialists' Collaborative Group. Maximum androgen blockade in advanced prostate cancer: an overview of the randomised trials. Lancet 2000;355:1491–8.
12. Seidenfeld J, Samson DJ, Hasselblad V, Aronson N, Albertsen PC, Bennett CL, et al. Single-therapy androgen suppression in men with advanced prostate cancer: a systematic review and meta-analysis. Ann Intern Med 2000;132:566–77.
13. Mahler C. Is disease flare a problem? Cancer 1993;72(12 Suppl):3799–802.
14. Granfors T, Modig H, Damber JE, Tomic R. Long-term followup of a randomized study of locally advanced prostate cancer treated with combined orchiectomy and external radiotherapy versus radiotherapy alone. J Urol 2006;176:544–7.
15. Pollack A, Salem N, Ashoori F, Hachem P, Sangha M, von Eschenbach AC, et al. Lack of prostate cancer radiosensitization by androgen deprivation. Int J Radiat Oncol Biol Phys 2001;51:1002–7.
16. Hermann RM, Schwarten D, Fister S, Grundker C, Rave-Frank M, Nitsche M, et al. No supra-additive effects of goserelin and radiotherapy on clonogenic survival of prostate carcinoma cells *in vitro*. Radiat Oncol 2007;2:31.
17. Cleutjens KB, van der Korput HA, van Eekelen CC, van Rooij HC, Faber PW, Trapman J. An androgen response element in a far upstream enhancer region is essential for high, androgen-regulated activity of the prostate-specific antigen promoter. Mol Endocrinol 1997;11:148–61.
18. Zagars GK, von Eschenbach AC. Prostate-specific antigen. An important marker for prostate cancer treated by external beam radiation therapy. Cancer 1993;72:538–48.
19. Helleday T, Lo J, van Gent DC, Engelward BP. DNA double-strand break repair: From mechanistic understanding to cancer treatment. DNA Repair (Amst) 2007;6:923–35.
20. Blunt T, Finnie NJ, Taccioli GE, Smith GC, Demengeot J, Gottlieb TM, et al. Defective DNA-dependent protein kinase activity is linked to V(D)J recombination and DNA repair defects associated with the murine scid mutation. Cell 1995;80:813–23.
21. Dvir A, Peterson SR, Knuth MW, Lu H, Dynan WS. Ku autoantigen is the regulatory component of a template-associated protein kinase that phosphorylates RNA polymerase II. Proc Natl Acad Sci U S A 1992;89:11920–4.
22. Lees-Miller SP, Chen YR, Anderson CW. Human cells contain a DNA-activated protein kinase that phosphorylates simian virus 40 T antigen, mouse p53, and the human Ku autoantigen. Mol Cell Biol 1990;10: 6472–81.
23. Barlow AL, Benson FE, West SC, Hulten MA. Distribution of the Rad51 recombinase in human and mouse spermatocytes. EMBO J 1997; 16:5207–15.
24. Finnie NJ, Gottlieb TM, Blunt T, Jeggo PA, Jackson SP. DNA-dependent protein kinase activity is absent in xrs-6 cells: implications for site-specific recombination and DNA double-strand break repair. Proc Natl Acad Sci U S A 1995;92:320–4.
25. Lee JC, Lee CH, Su CL, Huang CW, Liu HS, Lin CN, et al. Justicidin A decreases the level of cytosolic Ku70 leading to apoptosis in human colorectal cancer cells. Carcinogenesis 2005;26:1716–30.
26. Mayeur GL, Kung WJ, Martinez A, Izumiya C, Chen DJ, Kung HJ. Ku is a novel transcriptional recycling coactivator of the androgen receptor in prostate cancer cells. J Biol Chem 2005;280:10827–33.
27. Bostwick DG. Grading prostate cancer. Am J Clin Pathol 1994;102 Suppl 1:S38–56.
28. Thacker J. The RAD51 gene family, genetic instability and cancer. Cancer Lett 2005;219:125–35.
29. Valerie K, Povirk LF. Regulation and mechanisms of mammalian double-strand break repair. Oncogene 2003;22:5792–812.
30. Wang M, Wu W, Rosidi B, Zhang L, Wang H, Iliakis G. PARP-1 and Ku compete for repair of DNA double strand breaks by distinct NHEJ pathways. Nucleic Acids Res 2006;34:6170–82.
31. Schiewer MJ, Goodwin JF, Han S, Brenner JC, Augello MA, Dean JL, et al. Dual Roles of PARP-1 Promote Cancer Growth and Progression. Cancer Discov 2012;2:1134–49.
32. Arnaudeau C, Lundin C, Helleday T. DNA double-strand breaks associated with replication forks are predominantly repaired by homologous recombination involving an exchange mechanism in mammalian cells. J Mol Biol 2001;307:1235–45.
33. Pernicova Z, Slabakova E, Kharaishvili G, Bouchal J, Kral M, Kunicka Z, et al. Androgen depletion induces senescence in prostate cancer cells through down-regulation of Skp2. Neoplasia 2011;13:526–36.
34. Seluanov A, Danek J, Hause N, Gorbunova V. Changes in the level and distribution of Ku proteins during cellular senescence. DNA Repair (Amst) 2007;6:1740–8.
35. Sawada M, Sun W, Hayes P, Leskov K, Boothman DA, Matsuyama S. Ku70 suppresses the apoptotic translocation of Bax to mitochondria. Nat Cell Biol 2003;5:320–9.
36. Tovar C, Higgins B, Kolinsky K, Xia M, Packman K, Heimbrook DC, et al. MDM2 antagonists boost antitumor effect of androgen withdrawal: implications for therapy of prostate cancer. Mol Cancer 2011;10:49.
37. Roach M3rd, Bae K, Speight J, Wolkov HB, Rubin P, Lee RJ, et al. Short-term neoadjuvant androgen deprivation therapy and external-beam radiotherapy for locally advanced prostate cancer: long-term results of RTOG 8610. J Clin Oncol 2008;26:585–91.
38. Laverdiere J, Nabid A, De Bedoya LD, Ebacher A, Fortin A, Wang CS, et al. The efficacy and sequencing of a short course of androgen suppression on freedom from biochemical failure when administered with radiation therapy for T2-T3 prostate cancer. J Urol 2004;171:1137–40.
39. D'Amico AV, Manola J, Loffredo M, Renshaw AA, DellaCroce A, Kantoff PW. 6-month androgen suppression plus radiation therapy vs. radiation therapy alone for patients with clinically localized prostate cancer: a randomized controlled trial. JAMA 2004;292:821–7.
40. Langenhuijsen JF, van Lin EN, Hoffmann AL, Spitters-Post I, Alfred Witjes J, Kaanders JH, et al. Neoadjuvant androgen deprivation for prostate volume reduction: the optimal duration in prostate cancer radiotherapy. Urol Oncol 2011;29:52–7.
41. Alexander A, Crook J, Jones S, Malone S, Bowen J, Truong P, et al. Is biochemical response more important than duration of neoadjuvant hormone therapy before radiotherapy for clinically localized prostate cancer? An analysis of the 3- versus 8-month randomized trial. Int J Radiat Oncol Biol Phys 2010;76:23–30.
42. de Crevoisier R, Slimane K, Messai T, Wibault P, Eschwege F, Bossi A, et al. Early PSA decrease is an independent predictive factor of clinical failure and specific survival in patients with localized prostate cancer treated by radiotherapy with or without androgen deprivation therapy. Ann Oncol 2010;21:808–14.
43. Rene N, Faria S, Cury F, David M, Duclos M, Shenouda G, et al. Hypofractionated radiotherapy for favorable risk prostate cancer. Int J Radiat Oncol Biol Phys 2010;77:805–10.
44. Berruti A, Pia A, Terzolo M. Abiraterone and increased survival in metastatic prostate cancer. N Engl J Med 2011;365:766; author reply 777–8.
45. Scher HI, Fizazi K, Saad F, Taplin ME, Sternberg CN, Miller K, et al. Increased survival with enzalutamide in prostate cancer after chemotherapy. N Engl J Med 2012;367:1187–97.

AACR American Association for Cancer Research

Clinical Cancer Research

Castration Therapy Results in Decreased Ku70 Levels in Prostate Cancer

Firas L. T. Al-Ubaidi, Niklas Schultz, Olga Loseva, et al.

Clin Cancer Res 2013;19:1547-1556. Published OnlineFirst January 24, 2013.

III

Synthetic Lethality between PARP inhibition and Androgen Deprivation Therapy in Prostate Cancer, explained by Androgen Receptor driving Homologous Recombination

Mohammad Asim[1,2*], Heather I. Zecchini[1], Firas Tarish[3,4], Charles E. Massie[1], Ajoeb Baridi[1], Anne Y. Warren[5], Wanfeng Zhao[5], Leigh-Anne McDuffus[1], Patrice Mascalchi[1], Greg Shaw, Harveer Dev[1], Karan Wadhwa[1], Paul Wijnhoven[6], Scott Lyons[1], Roslin Russell[1], Andy G. Lynch[1], Cormac McONeill[1], Vincent R. Zecchini[1], Paul S. Rennie[7], Aria Baniahmad[8], Simon Tavaré[1], Ian G. Mills[9], Niklas Schultz[3], Yaron Galanty[6], Thomas Helleday[3*], and David Neal[1,8]

Affiliations:
[1]Cancer Research UK Cambridge Institute, University of Cambridge, Li Ka Shing Centre, Cambridge CB2 0RE, United Kingdom
[2]Department of Oncology, University of Cambridge, Cambridge CB2 2QQ, United Kingdom
[3]Science for Life Laboratory, Division of Translational Medicine and Chemical Biology, Department of Medical Biochemistry and Biophysics, Karolinska Institutet, S-171 21 Stockholm, Sweden
[4]Department of Urology, Central Hospital, Västerås, Sweden
[5]Department of Pathology, Addenbrooke's Cambridge University Hospital, Cambridge CB2 0QQ, United Kingdom
[6]The Wellcome Trust and Cancer Research UK Gurdon Institute, University of Cambridge, Cambridge CB2 1QN, United Kingdom
[7]The Vancouver Prostate Centre, Department of Urologic Sciences, University of British Columbia, Vancouver BC, Canada
[8]Institute of Human Genetics, Jena University Hospital, 07743 Jena, Germany
[9]Centre for Molecular Medicine Norway, Nordic European Molecular Biology Laboratory Partnership, University of Oslo, Oslo, Norway

*Corresponding author. Mailing address: Cancer Research UK Cambridge Institute, University of Cambridge, Li Ka Shing Centre, Cambridge CB2 0RE, United Kingdom mohammad.asim@cruk.cam.ac.uk or Thomas Helleday, Science for Life Laboratory, Division of Translational Medicine and Chemical Biology, Department of Medical Biochemistry and Biophysics, Karolinska Institutet, S-171 21 Stockholm, Sweden Thomas.helleday@scilifelab.se

One Sentence Summary: Androgen-deprivation therapy and PARP inhibitors synergistically kill androgen receptor (AR) positive cancers, and that is explained by a novel role of AR in regulating homologous recombination repair.

Abstract

Emerging data demonstrate homologous recombination (HR) defects in castration resistant prostate cancers, rendering these sensitive to PARP inhibitor treatments. Here, we demonstrate a direct link between the androgen receptor (AR) being required for maintenance of HR gene expression and activity in prostate cancer cells, as well as in maintenance of DNA damage response signaling. As a consequence, we show PARP-mediated backup repair pathway is upregulated in prostate cancer tissues in patients following androgen-deprivation therapy (ADT). Furthermore, upregulation of PARP activity is essential for prostate cancer survival, and we demonstrate a synthetic lethality between ADT and PARP inhibitors *in vivo*. These data demonstrate that HR may be functionally impaired earlier in prostate cancer etiology as a consequence of ADT; prior to emerging castration resistance and that this potentially can be exploited therapeutically using PARP inhibitors in combination with in ADT upfront in advanced or high risk prostate cancer.

Introduction

The androgen receptor (AR) is a ligand-inducible transcription factor that plays a key role in the initiation, growth and progression of Prostate cancer {Chen, 2004 #69}. Therefore androgen-deprivation therapy (ADT), which targets the androgen-signalling axis, provides an effective first line treatment for advanced prostate cancer {Attard, 2009 #278}. Progression to lethal castration-resistant prostate cancer (CRPC) is accompanied by reactivation or maintenance of AR signalling involved in cell cycle checkpoints {Sharma, 2010 #195}, promotion of metastatic phenotypes {Lucas, 2014 #268} and regulation of DNA repair {Goodwin, 2013 #202;Polkinghorn, 2013 #221;Al-Ubaidi, 2013 #734}. Recent data also demonstrate aberrations of BRCA2, BRCA1, and ATM in about 20% of advanced prostate cancer (Robinsson Cell May 2015). PARP is a backup repair pathway in cells that lost BRCA1, BRCA2 or ATM function (Helleday Mol Oncol 2011 Aug;5(4):387-93). As a result, BRCA2 deficient cells are acutely sensitive to PARP inhibition {Bryant, 2005 #655;Farmer, 2005 #595}, a phenomenon known as synthetic lethality. In line with this, emerging data demonstrate profound clinical responses using PARP inhibitors in CRPC mutated in BRCA2 (VanderWeele DJ1, Paner GP2, Fleming GF1, Szmulewitz RZ1. Front Oncol. 2015 Jul 22;5:169; Mateo J Annals Oncol 2014;Robinsson Cell May 2015).

In Prostate cancer, a number of clinical studies have shown that ADT combined with radiotherapy which induces DNA DSBs, is a more effective treatment option for locally advanced Prostate cancer and is associated with better survival and disease-free outcome compared with radiotherapy alone {D'Amico, 2008 #630;Mason, 2015 #820}. Previously others and we demonstrated that non-homologous end joining repair of DNA double-strand breaks (DSBs) is affected by ADT, which could be one explanation for this increased sensitivity {Al-Ubaidi, 2013 #734;Polkinghorn, 2013 #192;Goodwin, 2013 #202}. Since HR is also important in radiation-induced DSB repair, we here investigated a functional link between AR signalling and HR in prostate cancer, which also could open up a novel therapeutic opportunity using PARP inhibitors.

Results

The Androgen Receptor Promotes Homologous Recombination and DNA damage signalling

We set out to study how AR regulates genes involved in DNA repair. In-depth analysis of the expression pattern of DNA repair genes induced by AR signalling revealed a potential link between AR signaling and HR (Figure 1A). In line with these results we observed that the expression of RAD51, a key player in HR, was significantly upregulated in prostate cancer tumours compared with normal benign tissue (Supplementary Figure 1A, available online). To interrogate the functional link between AR signalling and HR, we tested whether AR signalling can affect ionizing radiation (IR)-induced RAD51 foci formation. To test this we used an isogenic CRPC model cell line C4-2 with “high AR” and “low AR” levels, with low AR levels achieved by the doxycycline-mediated induction of a short-hairpin RNA targeting the AR (Supplementary Figure 1B, available online). In line with AR regulating HR genes, we observed impaired IR-induced RAD51 foci in “low AR” cells (Figure 1B).

To test a direct role of the AR in regulating HR, we performed a direct repeat-green fluorescent protein (DR-GFP) based gene conversion assay in C4-2 cells with a stably integrated DR-GFP reporter. Consistent with its role in promoting RAD51 foci formation, cells with AR knockdown

showed a 40% reduction of HR (Figure 1C and Supplementary Figure 1C, available online), which is a true effect on HR, as no difference in cell cycle stage was observed (Supplementary Figure 1C, available online).

Next, we wanted to determine in detail how AR regulates the DNA damage response and repair and found a strong correlation between ATM and the AR-regulated transcriptome of DNA repair genes in prostate cancer cells (Supplementary Figure 1D, available online). In agreement with this we find patients treated with degarelix, a gonadotropin-releasing hormone antagonist, have overall lower levels of γH2AX foci (Supplementary Figure 1E, available online). To test if AR influences DDR directly we observe an overall defect in IR-induced γH2AX foci formation in "low AR" cells 2 h after 10 Gy irradiation (Figure 1D). We also observed that siRNA depletion of ATM in "AR high" cells bring down the γH2AX intensity to "low AR" levels (Supplementary Figure 1F, available online). Further links between AR and ATM signalling was observed used isogenic inducible AR mutant (T877A) expressed in the PC3 cell line in which doxycycline treatment triggered AR expression. We observed that from 48 hr after exposure to radiation the "full AR" cells grew faster than "AR null" cells, but this differential response was eliminated by ATMi treatment (Supplementary Figure 1G, available online). No differential growth response was observed in PC3-EV cells (Supplementary figure 1H, available online).

The ATM protein affect MRE11 activity to resect DNA ends, which is required or HR. Mining the AR transcriptome (GEO identifier GDS4113), we observed a down-regulation of the MRE11 transcript by AR knockdown, which was also directly suppressed at the protein level by AR knock down (Supplementary Figure 1I and 1J, available online). As ATM regulates MRE11 activity we tested formation of hydroxyurea-induced MRE11 foci which were higher in "high AR" cells (Figure 1E). That the MRE11 foci represent active MRE11 resection was demonstrated by addition of MRE11 inhibitor Mirin, which when added reduced the number of MRE11 foci.

Taken together these data suggest that AR, in prostate cancer is required for effective ATM signalling in response DNA damage, influencing MRE11 mediated resection required for proficient HR.

Anti-Androgen Therapy Activates PARP in Prostate cancer

Previously, we demonstrated that PARP1 is activated in HR defective cells and that sensitivity to PARP inhibitors is related to PARP activation {Gottipati, 2010 #800}. Since AR promotes HR, we hypothesized that ADT may then impair HR leading to an increase in backup PARP activity. To test this hypothesis, we set up a prospective study with prostate cancer patients (n=48). The Prostate cancer was diagnosed at biopsy and then received pharmacological castration with neo-adjuvant leuprolide, a gonadotropin-releasing hormone analogue. A second biopsy was taken eight weeks post leuprolide treatment. Half the cohort had leuprolide before radiation treatment, the other half started radiotherapy before leuprolide. Immunofluorescence signalling levels of PARP1 and its substrate PAR were quantified in cancer areas in corresponding paired slides (Figure 2A and Supplementary Figure 2A, available online). To measure the activity of the PARP1 enzyme, we calculated the ratio of PAR and PARP1 intensity in the nuclei. In castrated patients, we found a significant increase in PARP1 activity as reflected in increased PARylation ($p=0.003$) (Figure 2A and 2B) suggesting that PARP1 is activated as a result of androgen repression further strengthening our findings that AR regulates HR in Prostate cancer.

Synthetic lethality between the AR and inhibition of Poly (ADP-ribose) polymerase

Previously, we demonstrated that HR defective cells show an increased reliance on PARP activity and demonstrated a synthetic lethality between PARP and BRCA mutated cancers {Bryant, 2005 #597}{Farmer, 2005 #727}. Here, we observed an ADT-induced HR defect, suggesting that it may be possible to generate a context dependent synthetic lethality with PARP inhibitors, induced by ADT. Because we observed high PARP activity after ADT in patients (Figure 2A and 3B) and also high PARP activity in Prostate cancer cells (Supplementary Figure 2B, available online), we reasoned that a combined inhibition of both pathways might selectively induce a synthetic lethality in Prostate cancer.

To test this hypothesis, we used the anti-androgens bicalutamide or enzalutamide in combination with olaparib, which decreased cell viability of AR positive cell line C4-2 but not in AR negative PC3 cells (Figure 3A and 3B), which was also confirmed by using other prostate cancer cell lines (Supplementary Figure 3A-C, available online). The proliferation of C4-2 cells was also reduced by co-treatment with olaparib and either bicalutamide or enzalutamide, (Figure 3C) and the effects of AR shRNA-mediated knockdown in decreasing proliferation was enhanced by olaparib (Figure 3D). Consistent with that the synthetic lethality is AR-dependent, knockdown of the ectopically expressed T877A AR mutant in PC3-T877A and C4-2 cell lines (which endogenously express this mutant) had only marginal effects on the cell viability. However, AR knockdown coupled with increasing doses of Olaparib decreased the viability of both cell lines, demonstrating a functional synthetic lethality (Supplementary Figure 3D and 3E, available online). The clonogenic potential of control shNT expressing C4-2 cells was unchanged by dox treatment, while Olaparib treated cells formed fewer colonies independent of doxycycline treatment (Figure 3E). In contrast, clonogenic potential of shAR expressing "low AR" C4-2 cells was severely compromised by Olaparib (Figure 3F) indicating synthetic lethality. Two primary modes by which PARP inhibitors act are (1) catalytic inhibition of the PARP enzyme blocking PARylation of proteins and (2) trapping PARP on ssDNA intermediates generated by the DNA damage {Strom, 2011 #733}. If they are left unrepaired, these PARP trapped-ssDNA intermediates may be converted into DSBs in S-phase and may lead to cell death. In our study, we observed a complete loss of the growth inhibitory effect of Olaparib in C4-2 cells in which PARP1 was knocked down with RNAi, indicating that the growth inhibitory effect of Olaparib could be partially manifested via the trapping of PARP1 (Supplementary Figure 3F, available online). These experiments suggest that AR and PARP may act through functionally distinct pathways that converge to promote cell growth under genotoxic stress, further strengthening the model of contextual synthetic lethality.

Next, we wanted to evaluate the synthetic lethality between ADT and PARP inhibitors *in vivo* and generated tumour xenografts of C4-2 cells. In the vehicle, bicalutamide and Olaparib-treated groups a progressive increase in tumour volume was observed. However, combined treatment with bicalutamide and Olaparib significantly suppressed the growth of the xenografts (Figure 4A), decreased tumour weight and size (Figure 4B and Supplementary Figure 4A, available online) and without causing any obvious toxicity to mice (Supplementary Figure 4B, available online). To reproduce in another model, we generated xenografts of PC3-ctrl or PC3-AR expressing cells (Supplementary Figure 4C, available online) and administered vehicle or Olaparib to the mice, demonstrating decreased tumour volume with olaparib only in the AR defective context (Figure 4C) and without any adverse effect on mice weight (Supplementary

Figure 4D, available online). To test this in clinically relevant material, we used an *ex vivo* human tumour culture assay, were treatment of prostate cancer tissue explants with bicalutamide or Enzalutamide had no effect of proliferation index (measured by Ki67), but proliferation was strongly repressed by the combination of Olaparib with bicalutamide or Enzalutamide (Figure 4D and 4E). Treatment by Olaparib alone and by combined Bicalutamide and Olaparib increased levels of cleaved caspase-3 (CC3) (a marker of apoptosis) compared to controls or single treatments (Supplementary Figure 4E, available online). However, the combination of Enzalutamide and Olaparib did not result in increased CC3 (Supplementary Figure 4F, available online).

Discussion

ADT is used palliative in advanced prostate cancer or neo-adjuvant or adjuvant to radiotherapy. Relapse is common and previous reports of altered gene expression of DNA repair genes in CRPC {Rosen, 2005 #602}, has now been extended with identification of somatic mutations in DNA repair genes in about 20% of CRPC (Robinsson Cell May 2015), particularly in BRCA2 and ATM. The reason BRCA2 and ATM is mutated or lost in CRPC is likely because they act as tumour suppressors in the CRPC setting. Here, we report that that loss of AR signalling by siRNA treatment of AR or ADT result in reduced HR and ATM signaling. It is tempting to speculate that HR or ATM signaling would have a tumour suppressor function after ADT and that downregulation is a way for the tumour to increase fitness and survival. More studies into the reason HR or ATM signaling is lost in CRPC and also after ADT, reported here is warranted.

Mechanistically, we demonstrate that MRE11 foci formation is impaired following loss of AR, which a likely consequence of lost ATM signaling upon DNA damage. MRE11 activity is required for resection at DSBs to generate a substrate to which RAD51 can be loaded. So we demonstrate impairment of HR following AR loss through lost ATM signaling, lost MRE11 and RAD51 foci as well as impaired HR repair between GFP genes. Altogether, these data are overwhelming to demonstrate HR loss in the AR negative setting. It is well established that PARP is a backup repair system required for survival in absence of HR {Bryant, 2005 #597;Farmer, 2005 #595}. Here, we demonstrate, in a prospective study, that PARP activity is increased in prostate cancer tissue following ADT, in line with the hypothesis that HR is downregulated after ADT *in vitro*.

Reports demonstrate remarkable responses to PARP inhibitors in CRPC (VanderWeele DJ1, Paner GP2, Fleming GF1, Szmulewitz RZ1. Front Oncol. 2015 Jul 22;5:169; Mateo J Annals Oncol 2014 http://annonc.oxfordjournals.org/content/25/suppl_4/mdu438.20.abstract?sid=56a9081d-2292-48d6-8f58-a53c76d79b63%20). Here, we demonstrate pre-clinical evidence that PARP inhibitors potentiate ADT *in vivo*, also providing a mechanistic insight into the observed synthetic lethality between AR and PARP inhibition. This provides a rationale for the treatment of prostate cancer patients with therapies based on the dual inhibition of both AR and PARP function. CRPC patients with high levels of AR may be effectively treated with a combination of AR and PARP inhibitors, while patients with loss of AR expression, or expressing an AR truncation, such as V7 {Nyquist, 2013 #297} may benefit from PARP inhibitor based monotherapy. Based on this phenomenon of synthetic lethality between the AR and PARP, clinical trials are in development

with PARP inhibitors in Prostate cancer patients likely to benefit from the combined inhibition of androgen and PARP pathways (identifier NCT02324998, clinicaltrials.gov).

Materials and Methods

A detailed description of all methods and any associated references is provided in the Extended Experimental Procedures, which can be found in the supplemental data section.

Acknowledgments:

We thank the prostate cancer patients enrolled in this study for their informed consent and participation. Study sponsors had no role in the design of this study; the collection, analysis and interpretation of the data; the writing of the manuscript; and the decision to submit the manuscript for publication. We acknowledge members of the David Neal and Steve Jackson laboratories for helpful discussions. We thank Atsushi Shibata, Richard Grenfall, Jane Gray, Ian Halls, Ludmila Sabolcikova, Jeleana Dutton, Wendy Partridge, Matt Clayton, Mike Mitchell, and Will Howat for technical support. We acknowledge the Cambridge Institute core facilities for technical assistance, and the support of the NIHR Cambridge Biomedical Research Centre and the Medical Research Council (ProMPT grant). We acknowledge Dr Shutsung Liao for PC3 and PC3-AR cells, Dr Olga Volpert for inducible PC3-T877A cells and Dr Curtis Pettaway for the gift of LNCaP-LN3 cells. We are thankful to Dr Ashok Venkitaraman for the gift of PARP inhibitor KU0058948. We also thank Drs. Axel Behrens, Steve Jackson and Wayne Tilley for advice and support on this project. We thank Dr Davina Honess for critically reading the manuscript and suggestions. The authors would like to thank those men with prostate cancer and the subjects who have donated their time and their samples to the Cambridge Bio-repository, which were used in this research. We also would like to acknowledge the support of the research staff in S4 who so carefully curated the samples and the follow-up data (Jo Burge, Marie Corcoran, Anne George, and Sara Stern).

Funding:

This study was supported by the National Cancer Research Institute (National Institute of Health Research (NIHR) Collaborative Study: "Prostate Cancer: Mechanisms of Progression and Treatment (PROMPT)" (grant G0500966/75466). We thank the National Institute for Health Research, Hutchison Whampoa Limited, the Human Research Tissue Bank (Addenbrooke's Hospital), and Cancer Research UK. This work was funded by a Cancer Research UK program grant (D.N.), the Swedish Research Council (T.H.), AFA insurance (T.H.), Swedish Cancer Society (T.H.), the Swedish Pain Relief Foundation (T.H.), the Torsten and Ragnar Söderberg Foundation (T.H.), Centre for Clinical Research (CKF) (F.T.), the Västmanland Research Foundation for Cancer in Vasteras (F.T.), the Henning and Ida Persson Research Foundation (F.T.).

Author Contributions:

M.A. devised the concept and designed the study. NN supervised the project. NN performed and analysed clinical experiments. NN. carried out pathological evaluations. M.A. and T.H. wrote the paper. All authors discussed results and approved the manuscript.

Competing interests:

T.H. is named inventor on a patent using PARP inhibitors in treatment of HR defective cancers and receives royalty on sales of PARP inhibitors.

Supplementary Materials

References:

Al-Ubaidi, F. L., Schultz, N., Loseva, O., Egevad, L., Granfors, T., and Helleday, T. (2013). Castration therapy results in decreased Ku70 levels in prostate cancer. Clin Cancer Res *19*, 1547-1556.

Antonarakis, E. S., Lu, C., Wang, H., Luber, B., Nakazawa, M., Roeser, J. C., Chen, Y., Mohammad, T. A., Fedor, H. L., Lotan, T. L.*, et al.* (2014). AR-V7 and resistance to enzalutamide and abiraterone in prostate cancer. N Engl J Med *371*, 1028-1038.

Attard, G., Reid, A. H., A'Hern, R., Parker, C., Oommen, N. B., Folkerd, E., Messiou, C., Molife, L. R., Maier, G., Thompson, E.*, et al.* (2009). Selective inhibition of CYP17 with abiraterone acetate is highly active in the treatment of castration-resistant prostate cancer. J Clin Oncol *27*, 3742-3748.

Balk, S. P., and Knudsen, K. E. (2008). AR, the cell cycle, and prostate cancer. Nucl Recept Signal *6*, e001.

Brenner, J. C., Ateeq, B., Li, Y., Yocum, A. K., Cao, Q., Asangani, I. A., Patel, S., Wang, X., Liang, H., Yu, J.*, et al.* (2011). Mechanistic rationale for inhibition of poly(ADP-ribose) polymerase in ETS gene fusion-positive prostate cancer. Cancer Cell *19*, 664-678.

Bryant, H. E., Petermann, E., Schultz, N., Jemth, A. S., Loseva, O., Issaeva, N., Johansson, F., Fernandez, S., McGlynn, P., and Helleday, T. (2009). PARP is activated at stalled forks to mediate Mre11-dependent replication restart and recombination. EMBO J *28*, 2601-2615.

Bryant, H. E., Schultz, N., Thomas, H. D., Parker, K. M., Flower, D., Lopez, E., Kyle, S., Meuth, M., Curtin, N. J., and Helleday, T. (2005a). Specific killing of BRCA2-deficient tumours with inhibitors of poly(ADP-ribose) polymerase. Nature *434*, 913-917.

Bryant, H. E., Schultz, N., Thomas, H. D., Parker, K. M., Flower, D., Lopez, E., Kyle, S., Meuth, M., Curtin, N. J., and Helleday, T. (2005b). Specific killing of BRCA2-deficient tumours with inhibitors of poly(ADP-ribose) polymerase. Nature *434*, 913-917.

Castro, E., Goh, C., Olmos, D., Saunders, E., Leongamornlert, D., Tymrakiewicz, M., Mahmud, N., Dadaev, T., Govindasami, K., Guy, M.*, et al.* (2013). Germline BRCA mutations are associated with higher risk of nodal involvement, distant metastasis, and poor survival outcomes in prostate cancer. J Clin Oncol *31*, 1748-1757.

Chang, K. H., Li, R., Kuri, B., Lotan, Y., Roehrborn, C. G., Liu, J., Vessella, R., Nelson, P. S., Kapur, P., Guo, X.*, et al.* (2013). A gain-of-function mutation in DHT synthesis in castration-resistant prostate cancer. Cell *154*, 1074-1084.

Chen, C. D., Welsbie, D. S., Tran, C., Baek, S. H., Chen, R., Vessella, R., Rosenfeld, M. G., and Sawyers, C. L. (2004). Molecular determinants of resistance to antiandrogen therapy. Nat Med *10*, 33-39.

Cheng, H., Snoek, R., Ghaidi, F., Cox, M. E., and Rennie, P. S. (2006). Short hairpin RNA knockdown of the androgen receptor attenuates ligand-independent activation and delays tumor progression. Cancer Res *66*, 10613-10620.

D'Amico, A. V., Chen, M. H., Renshaw, A. A., Loffredo, M., and Kantoff, P. W. (2008). Androgen suppression and radiation vs radiation alone for prostate cancer: a randomized trial. Jama *299*, 289-295.

D'Amico, A. V., Manola, J., Loffredo, M., Renshaw, A. A., DellaCroce, A., and Kantoff, P. W. (2004). 6-month androgen suppression plus radiation therapy vs radiation therapy alone for patients with clinically localized prostate cancer: a randomized controlled trial. Jama *292*, 821-827.

Denham, J. W., Steigler, A., Lamb, D. S., Joseph, D., Turner, S., Matthews, J., Atkinson, C., North, J., Christie, D., Spry, N. A.*, et al.* (2011). Short-term neoadjuvant androgen deprivation and radiotherapy for locally advanced prostate cancer: 10-year data from the TROG 96.01 randomised trial. Lancet Oncol *12*, 451-459.

Downs, J. A., Nussenzweig, M. C., and Nussenzweig, A. (2007). Chromatin dynamics and the preservation of genetic information. Nature *447*, 951-958.
El-Khamisy, S. F., Masutani, M., Suzuki, H., and Caldecott, K. W. (2003). A requirement for PARP-1 for the assembly or stability of XRCC1 nuclear foci at sites of oxidative DNA damage. Nucleic Acids Res *31*, 5526-5533.
Farmer, H., McCabe, N., Lord, C. J., Tutt, A. N., Johnson, D. A., Richardson, T. B., Santarosa, M., Dillon, K. J., Hickson, I., Knights, C.*, et al.* (2005). Targeting the DNA repair defect in BRCA mutant cells as a therapeutic strategy. Nature *434*, 917-921.
Glinsky, G. V., Berezovska, O., and Glinskii, A. B. (2005). Microarray analysis identifies a death-from-cancer signature predicting therapy failure in patients with multiple types of cancer. J Clin Invest *115*, 1503-1521.
Goggins, M., Schutte, M., Lu, J., Moskaluk, C. A., Weinstein, C. L., Petersen, G. M., Yeo, C. J., Jackson, C. E., Lynch, H. T., Hruban, R. H., and Kern, S. E. (1996). Germline BRCA2 gene mutations in patients with apparently sporadic pancreatic carcinomas. Cancer Res *56*, 5360-5364.
Goodwin, J. F., Schiewer, M. J., Dean, J. L., Schrecengost, R. S., de Leeuw, R., Han, S., Ma, T., Den, R. B., Dicker, A. P., Feng, F. Y., and Knudsen, K. E. (2013). A hormone-DNA repair circuit governs the response to genotoxic insult. Cancer Discov *3*, 1254-1271.
Gottipati, P., Vischioni, B., Schultz, N., Solomons, J., Bryant, H. E., Djureinovic, T., Issaeva, N., Sleeth, K., Sharma, R. A., and Helleday, T. (2010). Poly(ADP-ribose) polymerase is hyperactivated in homologous recombination-defective cells. Cancer Res *70*, 5389-5398.
Granfors, T., Modig, H., Damber, J. E., and Tomic, R. (2006). Long-term followup of a randomized study of locally advanced prostate cancer treated with combined orchiectomy and external radiotherapy versus radiotherapy alone. J Urol *176*, 544-547.
Hartlerode, A. J., and Scully, R. (2009). Mechanisms of double-strand break repair in somatic mammalian cells. Biochem J *423*, 157-168.
Jackson, S. P., and Bartek, J. (2009). The DNA-damage response in human biology and disease. Nature *461*, 1071-1078.
Jensen, R. B., Carreira, A., and Kowalczykowski, S. C. (2010). Purified human BRCA2 stimulates RAD51-mediated recombination. Nature *467*, 678-683.
Korpal, M., Korn, J. M., Gao, X., Rakiec, D. P., Ruddy, D. A., Doshi, S., Yuan, J., Kovats, S. G., Kim, S., Cooke, V. G.*, et al.* (2013). An F876L mutation in androgen receptor confers genetic and phenotypic resistance to MDV3100 (enzalutamide). Cancer Discov *3*, 1030-1043.
Lin, B., Wang, J., Hong, X., Yan, X., Hwang, D., Cho, J. H., Yi, D., Utleg, A. G., Fang, X., Schones, D. E.*, et al.* (2009). Integrated expression profiling and ChIP-seq analyses of the growth inhibition response program of the androgen receptor. PLoS One *4*, e6589.
Liu, J., Doty, T., Gibson, B., and Heyer, W. D. (2010). Human BRCA2 protein promotes RAD51 filament formation on RPA-covered single-stranded DNA. Nat Struct Mol Biol *17*, 1260-1262.
Loveday, C., Turnbull, C., Ruark, E., Xicola, R. M., Ramsay, E., Hughes, D., Warren-Perry, M., Snape, K., Eccles, D., Evans, D. G.*, et al.* (2012). Germline RAD51C mutations confer susceptibility to ovarian cancer. Nat Genet *44*, 475-476; author reply 476.
Lucas, J. M., Heinlein, C., Kim, T., Hernandez, S. A., Malik, M. S., True, L. D., Morrissey, C., Corey, E., Montgomery, B., Mostaghel, E.*, et al.* (2014). The Androgen-Regulated Protease TMPRSS2 Activates a Proteolytic Cascade Involving Components of the Tumor Microenvironment and Promotes Prostate Cancer Metastasis. Cancer Discov.
Mason, M. D., Parulekar, W. R., Sydes, M. R., Brundage, M., Kirkbride, P., Gospodarowicz, M., Cowan, R., Kostashuk, E. C., Anderson, J., Swanson, G.*, et al.* (2015). Final Report of the Intergroup Randomized Study of Combined Androgen-Deprivation Therapy Plus Radiotherapy Versus Androgen-Deprivation Therapy Alone in Locally Advanced Prostate Cancer. J Clin Oncol.
Massie, C. E., Lynch, A., Ramos-Montoya, A., Boren, J., Stark, R., Fazli, L., Warren, A., Scott, H., Madhu, B., Sharma, N.*, et al.* (2011). The androgen receptor fuels prostate cancer by regulating central metabolism and biosynthesis. Embo J *30*, 2719-2733.
Matsuoka, S., Ballif, B. A., Smogorzewska, A., McDonald, E. R., 3rd, Hurov, K. E., Luo, J., Bakalarski, C. E., Zhao, Z., Solimini, N., Lerenthal, Y.*, et al.* (2007). ATM and ATR substrate analysis reveals extensive protein networks responsive to DNA damage. Science *316*, 1160-1166.
Moynahan, M. E., Pierce, A. J., and Jasin, M. (2001). BRCA2 is required for homology-directed repair of chromosomal breaks. Mol Cell *7*, 263-272.

Nyquist, M. D., Li, Y., Hwang, T. H., Manlove, L. S., Vessella, R. L., Silverstein, K. A., Voytas, D. F., and Dehm, S. M. (2013). TALEN-engineered AR gene rearrangements reveal endocrine uncoupling of androgen receptor in prostate cancer. Proc Natl Acad Sci U S A *110*, 17492-17497.
Peasland, A., Wang, L. Z., Rowling, E., Kyle, S., Chen, T., Hopkins, A., Cliby, W. A., Sarkaria, J., Beale, G., Edmondson, R. J., and Curtin, N. J. (2011). Identification and evaluation of a potent novel ATR inhibitor, NU6027, in breast and ovarian cancer cell lines. Br J Cancer *105*, 372-381.
Pierce, A. J., and Jasin, M. (2005). Measuring recombination proficiency in mouse embryonic stem cells. Methods Mol Biol *291*, 373-384.
Polkinghorn, W. R., Parker, J. S., Lee, M. X., Kass, E. M., Spratt, D. E., Iaquinta, P. J., Arora, V. K., Yen, W. F., Cai, L., Zheng, D*., et al.* (2013). Androgen receptor signaling regulates DNA repair in prostate cancers. Cancer Discov *3*, 1245-1253.
Polo, S. E., and Jackson, S. P. (2011). Dynamics of DNA damage response proteins at DNA breaks: a focus on protein modifications. Genes Dev *25*, 409-433.
Rosen, E. M., Fan, S., and Isaacs, C. (2005). BRCA1 in hormonal carcinogenesis: basic and clinical research. Endocr Relat Cancer *12*, 533-548.
Schmidt-Hansen, M., Hoskin, P., Kirkbride, P., Hasler, E., and Bromham, N. (2014). Hormone and radiotherapy versus hormone or radiotherapy alone for non-metastatic prostate cancer: a systematic review with meta-analyses. Clin Oncol (R Coll Radiol) *26*, e21-46.
Sharma, A., Yeow, W. S., Ertel, A., Coleman, I., Clegg, N., Thangavel, C., Morrissey, C., Zhang, X., Comstock, C. E., Witkiewicz, A. K*., et al.* (2010). The retinoblastoma tumor suppressor controls androgen signaling and human prostate cancer progression. J Clin Invest *120*, 4478-4492.
Shiloh, Y., and Ziv, Y. (2013). The ATM protein kinase: regulating the cellular response to genotoxic stress, and more. Nat Rev Mol Cell Biol *14*, 197-210.
Siegel, R. L., Miller, K. D., and Jemal, A. (2015). Cancer statistics, 2015. CA Cancer J Clin *65*, 5-29.
Strom, C. E., Johansson, F., Uhlen, M., Szigyarto, C. A., Erixon, K., and Helleday, T. (2011). Poly (ADP-ribose) polymerase (PARP) is not involved in base excision repair but PARP inhibition traps a single-strand intermediate. Nucleic Acids Res *39*, 3166-3175.
Uziel, T., Lerenthal, Y., Moyal, L., Andegeko, Y., Mittelman, L., and Shiloh, Y. (2003). Requirement of the MRN complex for ATM activation by DNA damage. Embo J *22*, 5612-5621.
Wang, M., Wu, W., Rosidi, B., Zhang, L., Wang, H., and Iliakis, G. (2006). PARP-1 and Ku compete for repair of DNA double strand breaks by distinct NHEJ pathways. Nucleic Acids Res *34*, 6170-6182.
Weston, V. J., Oldreive, C. E., Skowronska, A., Oscier, D. G., Pratt, G., Dyer, M. J., Smith, G., Powell, J. E., Rudzki, Z., Kearns, P*., et al.* (2010). The PARP inhibitor olaparib induces significant killing of ATM-deficient lymphoid tumor cells in vitro and in vivo. Blood *116*, 4578-4587.
Williamson, C. T., Kubota, E., Hamill, J. D., Klimowicz, A., Ye, R. Q., Muzik, H., Dean, M., Tu, L. R., Gilley, D., Magliocco, A. M*., et al.* (2012). Enhanced cytotoxicity of PARP inhibition in mantle cell lymphoma harbouring mutations in both ATM and p53. Embo Mol Med *4*, 515-527.
Wo, J. Y., and Zietman, A. L. (2008). Why does androgen deprivation enhance the results of radiation therapy? Urol Oncol *26*, 522-529.
Wooster, R., and Weber, B. L. (2003). Breast and ovarian cancer. N Engl J Med *348*, 2339-2347.
Yuan, S. S. F., Lee, S. Y., Chen, G., Song, M. H., Tomlinson, G. E., and Lee, E. Y. H. P. (1999). BRCA2 is required for ionizing radiation-induced assembly of rad51 complex in vivo. Cancer Res *59*, 3547-3551.

Figures and figure Legends

Fig 1

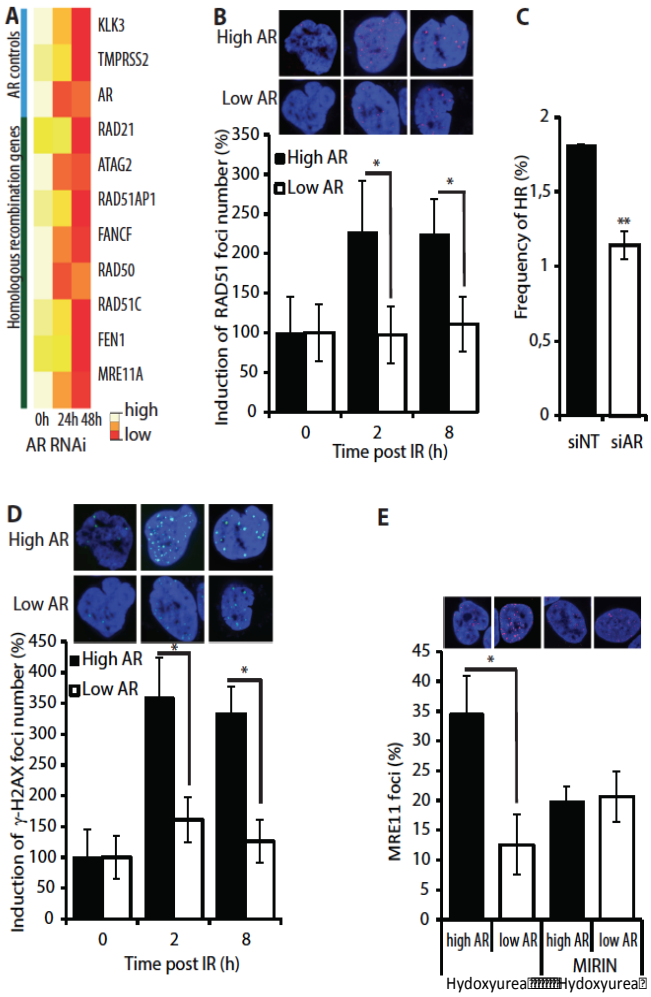

Figure 1. AR signalling regulates homologous recombination (HR) and its inhibition triggers PARP activation in PCa.

(A) Heatmap showing expression of homologous recombination regulators following AR RNAi knock-down, AR transcript and known AR targets controls are shown from microarray data (Cheng et al., 2006). **(B)** Upper panel showing confocal microscopy images showing Rad51 foci in the nuclei of "high AR" and "low AR" C4-2 cells exposed to IR. Lower panel showing bar graphs with mean error of Rad51 foci formation time course showing high content cytometry based quantification of Rad51 nuclear foci intensity in "high AR" (black bars) and "low AR"

(white bars) C4-2 cells in response to IR (10Gy) on per nuclear basis. Statistical significance determined using the Holm-Sidak method, with alpha=5.000%. **(C)** Quantification of gene conversion assay from analysis of GFP positive C4-2-DRGFP cells transfected with siScr or siAR along with ISce1 endonuclease for 72 hrs followed by detection of GFP positive cells by flow cytometry. Significance determined by unpaired students's t-test. **(D)** Upper panel showing confocal microscopy images of γH2AX foci in the nuclei of "high AR" and "low AR" C4-2 cells exposed to IR. Lower panel showing bar graphs with mean of error of γH2AX foci analysis time course showing high content cytometry based quantification of γH2AX foci number in "high AR" (black bars) and "low AR" (white bars) C4-2 cells in response to IR (10Gy). Statistical significance determined using the Holm-Sidak method, with alpha=5.000%. **(E)** High content cytometry analysis of MRN foci in "high AR" and "low AR" C4-2 cells treated with hydroxyl Urea (HU). Upper panel shows "high AR" and "low AR" cells with MRN foci, Lower panel showing bar graph with mean of error analysis of MRN foci in "high AR" (black bar) and "low AR" (white bar) C4-2 cells treated with hydroxyl Urea (HU).

Fig 2

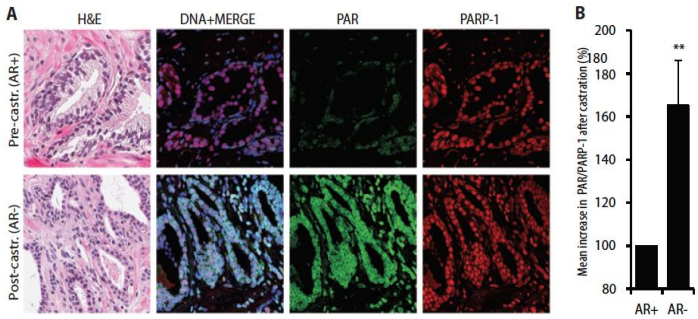

Figure 2. AR inhibition triggers PARP activation in human prostate cancer.
Left panel showing Immunofluorescence microscopy images showing levels of PAR and PARP-1 in men with prostate cancer 8 weeks pre- (pre-castration or AR+) and post-Leuprolide (post-castration or AR-) treatment. Right panel showing bar graphs show PARP activity in prostate cancer patients pre- and post-Leuprolide treatment. One sample T test, 2- tailed, test value 100.

Fig 3

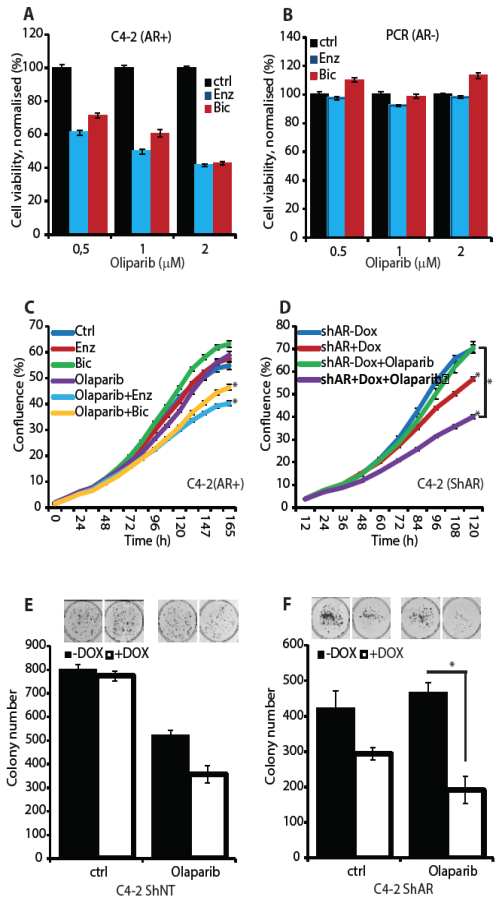

Figure 3. Synthetic lethality between AR and PARP pathways in prostate cancer.
Bar graphs with mean of error showing viable fraction of **(A)** C4-2 and **(B)** PC3 cells treated with indicated doses of Olaparib and/or Enzalutamide (blue colour) or Bicalutamide (red colour) (both at 10μM) for 7 days or 95% confluence. Graph indicates results of a MTS cell viability assay. **(C)** Live cell imaging based confluence analysis of C4-2 cells treated with Olaparib (1μM), Enzalutamide (10μM) or Bicalutamide (10μM) for 7 days. **(D)** Live cell imaging based confluence analysis of a "high AR" and "low AR" C4-2 treated with doxycycline and Olaparib (1μM) as indicated for 5 days, significance calculated using two-way ANOVA. Clonogenic survival assay with inducible **(E)** shNT or **(F)** shAR expressing C4-2 cells. Cells were treated with Olaparib (2μM).

Fig 4

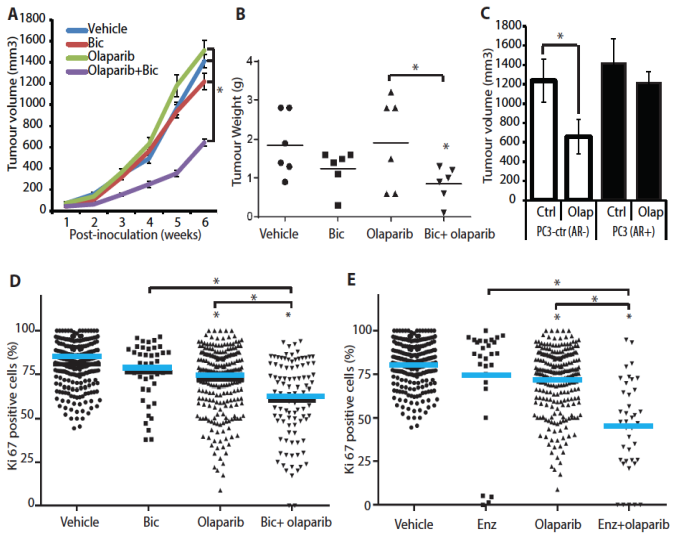

Figure 4. Dual inhibition of AR and PARP1/2 function represses PCa growth.
(A) Tumour xenograft of C4-2 cells, mice administered with DMSO (vehicle) or Bicalutamide and/or Olaparib as indicated. **(B)** Scatter plot showing weight C4-2 xenograft in NSG mice treated with indicated drugs. **(C)** Tumour xenografts of PC3-controll (AR-) (white bars) or PC3-AR (AR+) (black bars) cells, NSG mice were administered with DMSO (vehicle) or Olaparib as indicated. **(D)** Quantification of ki67 expression in *ex vivo* culture of human PCa treated with Bicalutamide (10µM) and/or Olaparib (2µM) for 72 hrs. **(E)** Quantification of ki67 expression in *ex vivo* culture of human PCa treated with Enzalutamide (10µM) and/or Olaparib (2µM) for 72 hrs.

Asim et al.

Inventory of supplementary Information:

Supplementary experimental methods

Supplementary figure legends for

Supplementary Figure 1

Supplementary Figure 2

Supplementary Figure 3

Supplementary Figure 4

Supplementary references

SUPPLEMENTARY EXPERIMENTAL METHODS

Reagents/Antibodies/Consumables

Methyltrienolone (R1881) and Enzalutamide were obtained from Perkin Elmer and Axon Medchem respectively. Camptothecin, dihydro testosterone (DHT), DMSO, doxycycline, bicalutamide, hydroxyl urea and Mirin were obtained from Sigma. Olaparib was purchased from LC laboratories and ATM inhibitor KU0055399 from Calbiochem. Cell culture media, FBS and other cell culture reagents including antibiotics were obtained from Life Technologies. Antibodies were obtained from commercial suppliers as below:

1. Phospho-Histone H2A.X (Ser139) (JBW301; cat # 05-636) from Millipore-used in foci analysis.
2. Rad51 (cat no. H-92; sc8349) from Santa cruz- used in high content cytometry.
3. Mre11 (cat no. 4895S) from Cell signalling- used in high content cytometry.
4. Total ATM (2C1; cat no. sc-23921) Santa cruz used in Western blot analysis.
5. PhosphoS1981-ATM (EP1890Y from Abcam cat. ab81292)-used in Western blot analysis.
6. Phospho KAP-1 (S824; cat no. A300-767A, Bethyl laboratories) used in Western blot analysis.
7. Total Kap1 (A300-274A from Bethyl laboratories) used in Western blot analysis.
8. Total p53 (1C12; cat no. 2524) and phospho-p53 (Ser15; cat # 9284) from cell signalling-used in Western blot analysis.
9. PAR antibody (cat no. GTX75054 from Source bioscience) for Western blot.
10. Phsopho-histone H2A.X (ser139; cat # 2577) used in flow cytometry.
11. γH2A.X (phosphoS139; cat # ab2893) from Abcam used for immuno histochemistry.
12. AR (AR441; cat # M356201-2 from Dako) used in Western blot analysis.
13. beta-actin antibody (Rabbit actin: Cell signaling (cat #4970), 1:1000
Mouse actin: Abcam (cat #ab6276), 1:5000)

Cell culture

LNCaP, PC3, PNT1a, DUCaP cells were obtained from commercial suppliers and grown in RPMI cell culture media containing 10% foetal bovine serum (FBS) and 1% penicillin/Streptomycin in a humidified incubator at 37 ºC. C4-2 was grown as described previously (1). We generated and cultured C4-2-NT control (expressing non-targeting RNA; siNT) and C4-2-shAR cells as described earlier (2). LNCaP-LN3 cells have been described previously (3).

Analysis of γH2AX and Rad51 foci in cells

C4-2 “high AR” and “low AR” shRNA cells were grown in 10% hormone-depleted serum containing RPMI media treated with R1881 (1 nM) or doxycycline (1 µg/mg) for 72 hr to induce shRNA expression. Cells were exposed to ionising radiation (10 Gy) using a CS^{137} source. For imaging, cells were grown in Ibidi ibiTreat 8 well µ-slides (Ibidi GmbH, Germany), precleared with PBST containing (0.2% triton-X-100) for 1 min then fixed in 3% PFA-2% sucrose solution in PBS for 10 min, washed with PBS 3X and blocked in Odyssey buffer for 30 min at room temperature. Cells were incubated with the combination of antibodies against γH2AX (1:2500) and Rad51 (1:500) overnight in Odyssey blocking solution and washes thrice with PBST (0.1%). Cells were incubated with secondary antibodies Alexa Fluor® 488 and Alexa Fluor® 647 antibodies (both 1:1000; Life technologies) for 1 hr at room temperature. Cells were again washed with PBST (0.1%) and DNA counterstained with DAPI for 10 min followed by mounting with vectashield (Ibidi). Images were acquired on a Leica SP5 confocal microscope (Leica Microsystems Ltd). Three channels were used for DAPI (blue), γH2AX_AlexaFluor488 (green) and Rad51_AlexaFluor647 (far red). For analysis, the Leica image file was imported directly into Columbus software (PerkinElmer, UK). Images were analysed using a custom analysis protocol set up on the three channels. The DAPI channel was used to segment individual nuclei using standard algorithms within the software. γH2AX and Rad51 signal per nucleus was calculated by the quantification of the green and far red signals within the DAPI nuclear mask. The “find spots” function was added into the protocol to detect γH2AX foci (green channel) and Rad51 foci (far red channel) within the nucleus, using appropriate settings to correctly detect each individual focus. Functions were then added in to calculate morphology allowing foci number to be extracted.

DR-GFP assay

Stable clones of C4-2 cells harboring DR-GFP were generated by transfecting the cells with Lipofectamine 2000 and stable clones (called C4-2DRGFP cells) were selected on puromycin (2 µg/ml) and maintained in RPMI with 10%FBS. These cells were seeded in six-well culture dishes and transfected using Lipofectamine 200 reagent with ISce1 (0.75 µg/well) and siRNA (50 nM). After 72 hr cells were harvested and percentage of GFP positive cells was determined with flow cytometry using BD FacsCaliber. Data analysis was carried out using Flowjo software.

Immunohistochemistry, Image processing, nuclei segmentation and spot quantification for γH2AX

Immunohistochemistry was performed on formalin-fixed, paraffin-embedded sections (4 µm) using an automated immunostainer with cover tile technology (Bond-III system, Leica Biosystems). Commercial antibody to γH2AX (Cell Signalling; 1:400 dilution) was used as the primary antibody. The Antigen retrieval was carried out using the combination of heat and Bond Epitope Retrieval Solution 1 (Leica Biosystems). The Bond™ Polymer Refine Detection kit (Leica Biosystems) was used for visualising the antigens. Negative control experiments, in which primary antibodies were omitted, resulted in a complete absence of staining.

All the images were processed with FIJI software (or ImageJ, National Institute of Health, Bethesda, MD) using a set of semi- and fully-automated homemade macros. Briefly, artefacts within the image, i.e. bubbles, dust or out-of-focus regions were detected and removed upon user validation. Haematoxylin and DAB staining were then automatically separated as individual channels using a macro calling the “colour deconvolution” plugin (4) set with the “H&E DAB” vectors (see Figure S1E).

A final macro helped discarding any secretion feature that could be further detected as a positive signal within the DAB channel. Processed DAB images were then analyzed with Columbus software (PerkinElmer, Waltham, MA). Nuclei segmentation was performed and small, large or elongated objects were removed. However, as it resulted in a mixed population of cancer and sparse stromal cells, an original method was designed to automatically select cells clustered in a cancer area. Briefly, regions were defined as an extension by 50 pixels (12.5 μm) around each nucleus. By default, as no overlap is allowed by Columbus, measured areas for clustered cells were smaller than isolated stromal cells (see Figure S1E). Spot detection was finally achieved only for individual sorted cancer cells. Low-amplitude (maximum over local background intensity) spots were discarded to limit the contribution of false positives.

Plasmids, siRNA and Transient transfections

In order to achieve potent reduction in target mRNA expression, siRNA smart pool were used for gene knockdown (Dharmacon/Life technologies). Transient transfections with siRNA were performed using Lipofectamine RNAiMAX transfection reagent (Life technologies) as per manufacturer's recommendations. We performed reverse transfections and used 25 nM siRNA in all knockdown experiments; MMTV-Luc and Renilla-Luc reporter plasmids were transfected using Lipofectamine 2000 as per manufacturers' instructions.

Reporter assay

In all luciferase assays, Renilla luciferase plasmid (Promega) was used as an internal control. All cells treated with androgens, R1881 (1nM) were grown in hormone-depleted (charcoal-stripped) FBS. Cells were harvested 48 hr post-transfection using passive lysis buffer provided with dual luciferase assay reagents (Promega) to measure both luciferase activity and Renilla luciferase activity using luminometer (Pherastar).

Cell viability assay

Cells were trypsinised and counted using a Vicell instrument. Cell growth assay was carried out in 96 well plates (1500-2000 cells per well). Cells were then plated and simultaneously treated with indicated chemicals/drugs until control vehicle treated cells reached 95% confluence level (5-7 days for different cell lines). Cell viability was determined by incubating the culture with MTS reagent based (3-(4,5-dimethylthiazol-2-yl)-5-(3-carboxymethoxyphenyl)-2-(4-sulfophenyl)-2H-tetrazolium) colorimetric assay as per manufacturers protocol (Promega).

Clonogenic assay

Cells were seeded in a 6-well culture dish (Corning); (1000 cells per well were seeded) and 48 hr later cells were treated with antagonists (10 μM) /inhibitor (1 μM). Fresh media and drugs were replenished bi-weekly. Two weeks later, cells were fixed in acetone:methanol (1:1) for 5 min and stained with Giemsa stain (from Raymond A Lamb ltd. chemicals; diluted and filtered 1:10 in water) for 10-15 min. Plates were washed with running tap water, air dried and the colonies were counted using colony analyser (Oxford Optronics). All colonies were counted, experiments were conducted in triplicates.

Live cell imaging/confluence analyses

Confluence analyses were performed using the Incucyte instrument (Essen Bioscience). Cells were plated and simultaneously treated with drugs in TPP 96-well culture dishes and placed in a humidified chamber incucyte instruments. Experiments were conducted in 8 replicates

and live cell images were recorded every 3 hr. However, for ease of understanding only 12 hr time interval data are shown.

Western blot analysis

Samples subjected to SDS-PAGE were transferred to a PVDF membrane (Amersham) and transfer efficiency was checked with Ponceau red. Membrane was blocked with Licor blocking buffer for 1 hr at room temperature. Membrane was washed with TBS-T (TBS, 0.05% Tween-20) and incubated with indicated antibody dilutions as per manufacturer's instruction overnight at 4 ºC. Upon washing with TBS-T, membrane was incubated with HRP antibody for 1 hr at room temperature and chemiluminiscence detected by Licor Odyssey instrument.

***Ex vivo* prostate explant culture**

Fresh human PCa tissue was collected after informed consent (70-80 years hormone naïve patient cT3 disease with a PSA value of 82) and according to the institutional policy. Tissue was excised into 1-2 mm^3 size explants and grown on collagen cushions kept on steel grids for one week. The tissue was treated as indicated by drugs in RPMI with 10%FBS, 1%penicilln, streptomycin and gentamycin. To make collagen cushions, 250 µl of collagen mix (rat tail collagen, plain RPMI media, FBS and 10% RPMI in the ratio of 7:1:1:1) was solidified on a nylon membrane. At the end of experiment, tissue was fixed in formalin for 20 hr and then transferred to ethanol followed by immunohistochemistry.

Immuno histo-chemistry for ki67 and cleaved caspase-3 (CC3) of ex vivo culture

Immuno-histochemical staining of paraffin embedded slides was performed to detect ki67 and CC3. Slides were stained on a BondMax Autostainer (Leica, Milton Keynes, UK). Antigen retrieval was performed using standard trisEDTA method at 100 ºC for 20 min followed by a 15 min incubation with primary antibodies for ki67 (Rabbit polyclonal from Santa cruz, sc-816 at 1:750 dilution) and CC3 (cleaved caspase-3; 9664, Cell signalling Technology) at room temperature, 8 min incubation with a secondary antibody (biotinylated donkey anti-rabbit; cat. No 711-065-152 from Jackson immunoresearch) using a polymer secondary system (Leica) followed by developing with Diaminobenzidine using enhancer (SP-2001; vector labs). Haematoxylin counterstaining was performed automatically on the Bond system, and finally, the slides were dehydrated, cleared and mounted using a Leica ST5020 attached coverslipper CV5030 (Leica). Slides were scanned onto Aperio/SpectrumTM v10.2.2.2317 and were analysed using ImageScope (Aperio software v12.0.0.5039). The intensity and number of nuclear AR and CC3 was quantified using an algorithm that identifies nuclear staining, and the number of positive nuclei was counted between the different treatments. In order to identify epithelial structures for quantification, images H&E and cytokeratin staining were used to pinpoint the exact location on serially sectioned slides that have weak AR staining. For each condition at least 400 cells were counted and percentage was calculated based on total number of cells in the tissue explants (n=>3).

Generation of tumour xenografts

All animal experiments were performed in compliance with the Home office directive of Animal (scientific procedures) act, under a project and personal license. In all experiemnts Non-obese non-diabetic NSG mice bearing xenografts were generated by subcutaneous injection of cells as follows:

PC3/PC3-AR xenografts: 1 million cells in 50 µl PBS were mixed with 50 µl high concentrations Matrigel and were injected in the flank region of each mouse. Mice were given vehicle (cyclodextrin) or Olaparib (1 mg/mouse daily) via intra-peritoneal route (n=12 per group). Tumour size was measured weekly using callipers.
C4-2 xenografts: 2 million cells in 50 µl PBS were mixed with 50 µl high concentrations Matrigel and were injected in the flank region of each mouse. Mice were given vehicle (DMSO) or Olaparib (50 mg/kg twice weekly) and/or bicalutamide (20 mg/kg twice weekly) via intra-peritoneal route. Tumour size was measured with callipers weekly, and calculated using the formula volume = (π/6)/abc or (π/6)/abb (if only 2 diameters are available) and a,b,c are the orthogonal axis of the tumour. Mice were culled at completion of experiment or when tumours reached 10% of body weight.

Patients and Leuprorelin study design
After ethical approval from the regional ethics committee of Uppsala University (EPN Dnr 2011:066), patients with localized, i.e. non-metastatic prostate cancer, eligible for curative RT, were enrolled in the study. After the completion of a written informed consent, the patients were allocated to one of the two study arms.
In Arm 1, the patients received neo-adjuvant pharmacological castration with leuprorelin, a GnRH analogue, followed by external beam RT in daily 2 Gy fractions to a total dose of 78 Gy. In Arm 2, the patients first received RT, in 2 Gy daily fractions for 5 consecutive days, followed by neo-adjuvant leuprolide and then an equivalent, higher RT dose to a total of 82 Gy, due to the greater lapse of time. Before treatment, prostate needle-core biopsy specimens were obtained from all patients. In Arm 1, a second biopsy was taken eight weeks after the leuprolide injection, i.e. before RT was started and a third biopsy about three hours after the fifth RT fraction. In Arm 2, a second biopsy was taken about three hours after the fifth RT fraction, i.e. before hormone treatment was initiated and a third biopsy eight weeks after the administration of leuprolide (see flow chart).

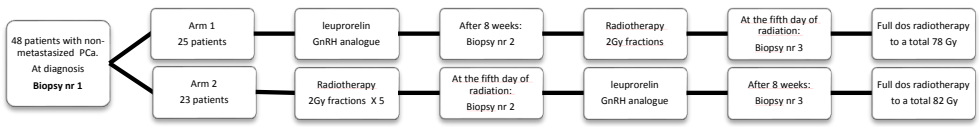

Histological and immunofluorescence evaluation of PAR and PARP-1

All prostatic needle biopsy specimens were embedded in paraffin, sectioned and stained with haematoxylin and eosin (H&E). In all specimens, the cancer area was assessed according to the Gleason system (5) and marked by a uro-pathologist. Two cancer-rich specimens from each batch of biopsies were further sectioned for immunofluorescence analysis. These sections were deparaffinised and rehydrated before antigen retrieval with Tris/EDTA (Citrus buffer, pH 9) in a pressure cooker. After blocking with 2% BSA, the sections were incubated with different primary antibodies at 4 ^{o}C overnight. Extensive rinsing was performed once;

the sections were incubated with the secondary antibodies (donkey anti mouse IgG-alexa 488 (1:500), Molecular probe and donkey anti rabbit IgG-alexa 555 (1:500), Molecular probe) for one hour at room temperature. DNA was counterstained with TO-PRO-3 iodide (Molecular probe) and slides mounted with pro long gold (Molecular probe). Dual staining was performed on the same slide PARP1 (1:200, H-250, sc-7150, Santa Cruz) together with PAR (1:200, pADPr (10H): sc-56198, Santa Cruz). Images from a tumour area with a good degree of immunofluorescence signals were selected from each biopsy. The corresponding areas in the HE-stained section were identified for histological verification of the tumour area. Selected areas from each slide containing 300-600 cells were chosen for analyses. TO-PRO-3 was used as a DNA marker. All images were analysed, with respect to medium intensity inside the nuclei and in the cytoplasm. The nuclear area was defined by the TO-PRO-3 signal (Figure S1D). PARP1 is a protein with both nuclear and cytoplasmic localisation and intensity values are presented without background subtraction. All measurements were performed using an in house-written programme for NIH-imageJ. Fluorescence images were obtained with either a Zeiss LSM 510-inverted confocal microscope or a Zeiss LSM 780-inverted confocal microscope, using a planapochromat 40X/NA 1.2 objectives. Through-focus maximum projection images were acquired from optical sections 0.5µm apart and with a section thickness of 1.0µm. HE-stained images were obtained with a Leica scan system.

Degarelix study design

Full ethical approval was obtained (11/H0311/2) for clinical studies NCT01852864 and NCT00967889. 15 patients with high risk organ confined prostate cancer were treated with 240mg of degarelix s.c. 7 days before surgery. Fresh prostate cancer samples were obtained at the time of radical prostatectomy and snap frozen. Confirmation of castrate levels of serum testosterone in degarelix treated patients was achieved by mass spectrometry. These samples were compared with matched controlled samples from 19 untreated patients. Tissues were spotted on microscopic slides to generate tissue microarray.

Statistical analysis

Unless otherwise indicated in the figure legends, tailed Student's t-test was used in all statistical analyses. Data in the bar graphs are shown as the mean ± SEM., and statistical significance is expressed as follows: *P < 0.05, **P < 0.005, ***P < 0.0005. We have seen consistent differences and significant P values in functional studies however it is possible that some p values may be driven by low variance.

SUPPLEMENTARY REFERENCES

1. Thalmann GN, Anezinis PE, Chang SM, Zhau HE, Kim EE, Hopwood VL, et al. Androgen-independent cancer progression and bone metastasis in the LNCaP model of human prostate cancer. Cancer Res. 1994;54(10):2577-81.
2. Cheng H, Snoek R, Ghaidi F, Cox ME, Rennie PS. Short hairpin RNA knockdown of the androgen receptor attenuates ligand-independent activation and delays tumor progression. Cancer Res. 2006;66(21):10613-20.
3. Pettaway CA, Pathak S, Greene G, Ramirez E, Wilson MR, Killion JJ, et al. Selection of highly metastatic variants of different human prostatic carcinomas using orthotopic implantation in nude mice. Clin Cancer Res. 1996;2(9):1627-36.
4. Ruifrok AC, Johnston DA. Quantification of histochemical staining by color deconvolution. Anal Quant Cytol Histol. 2001;23(4):291-9.
5. Bostwick DG. Grading prostate cancer. Am J Clin Pathol. 1994;102(4 Suppl 1):S38-56.
6. Massie CE, Lynch A, Ramos-Montoya A, Boren J, Stark R, Fazli L, et al. The androgen receptor fuels prostate cancer by regulating central metabolism and biosynthesis. Embo J. 2011;30(13):2719-33.

Supplementary figure 1

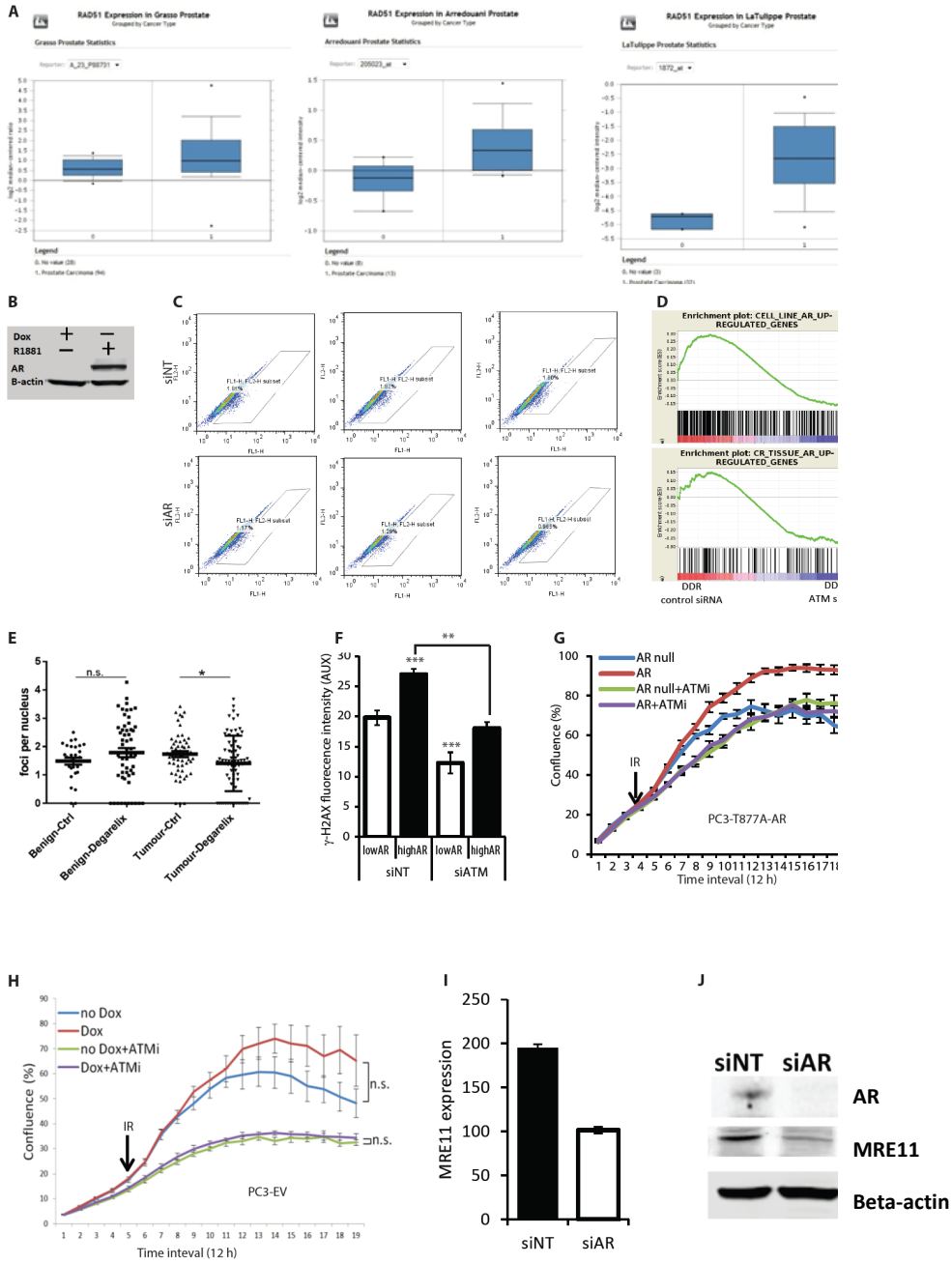

Supplementary figure 2

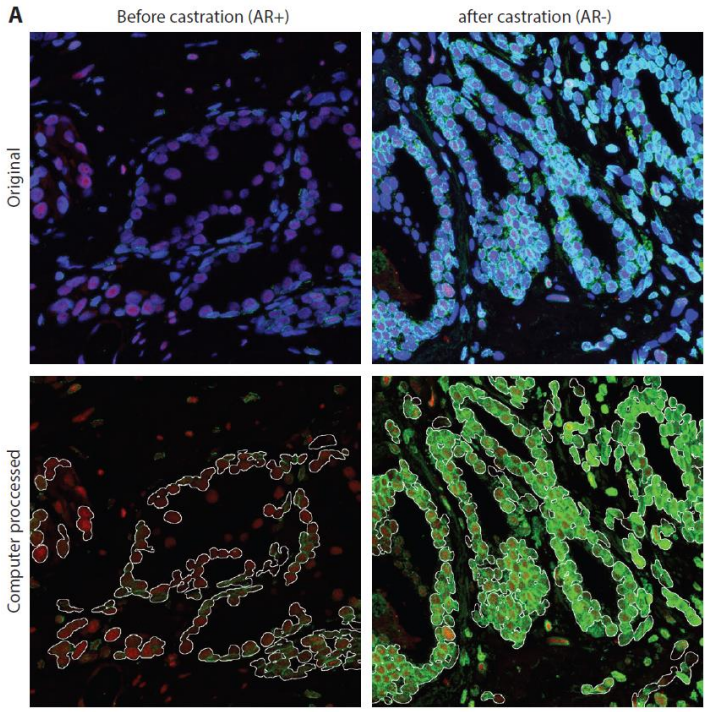

Red= PARP-1, Green=PAR, Blue=DNA,
White lines encircles the area used for intesity measurements.

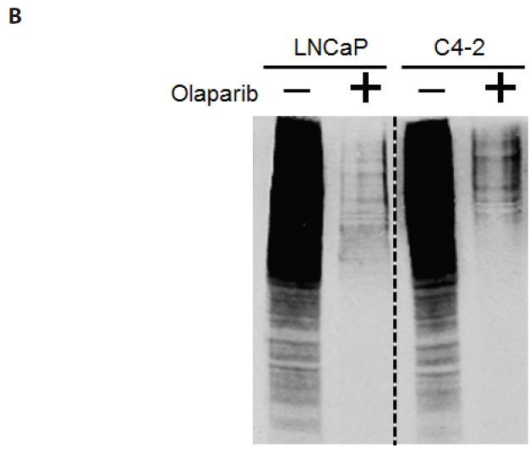

Supplementary figure 3

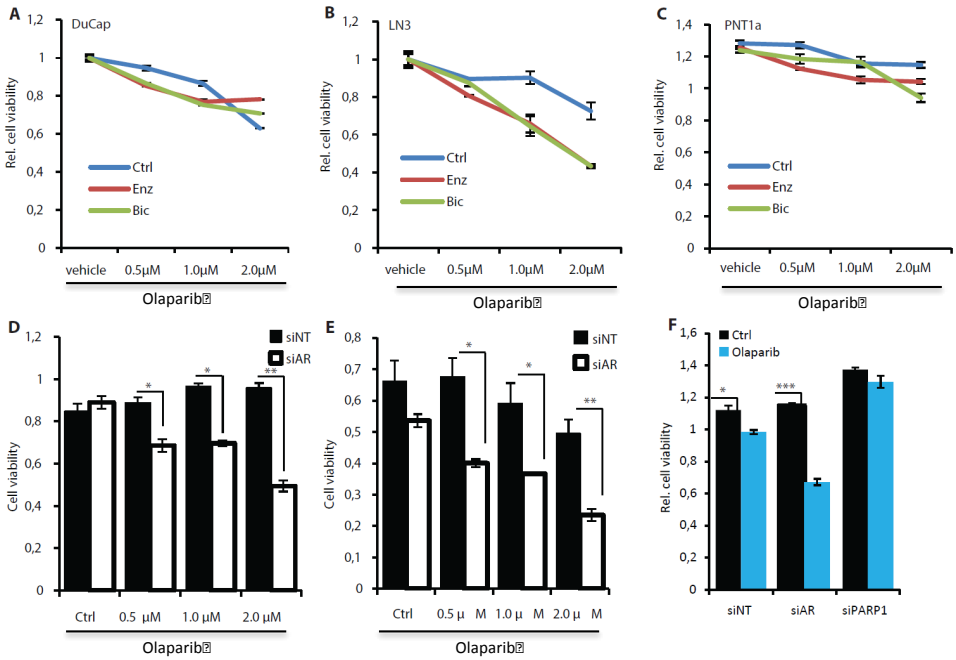

Supplementary figure 4

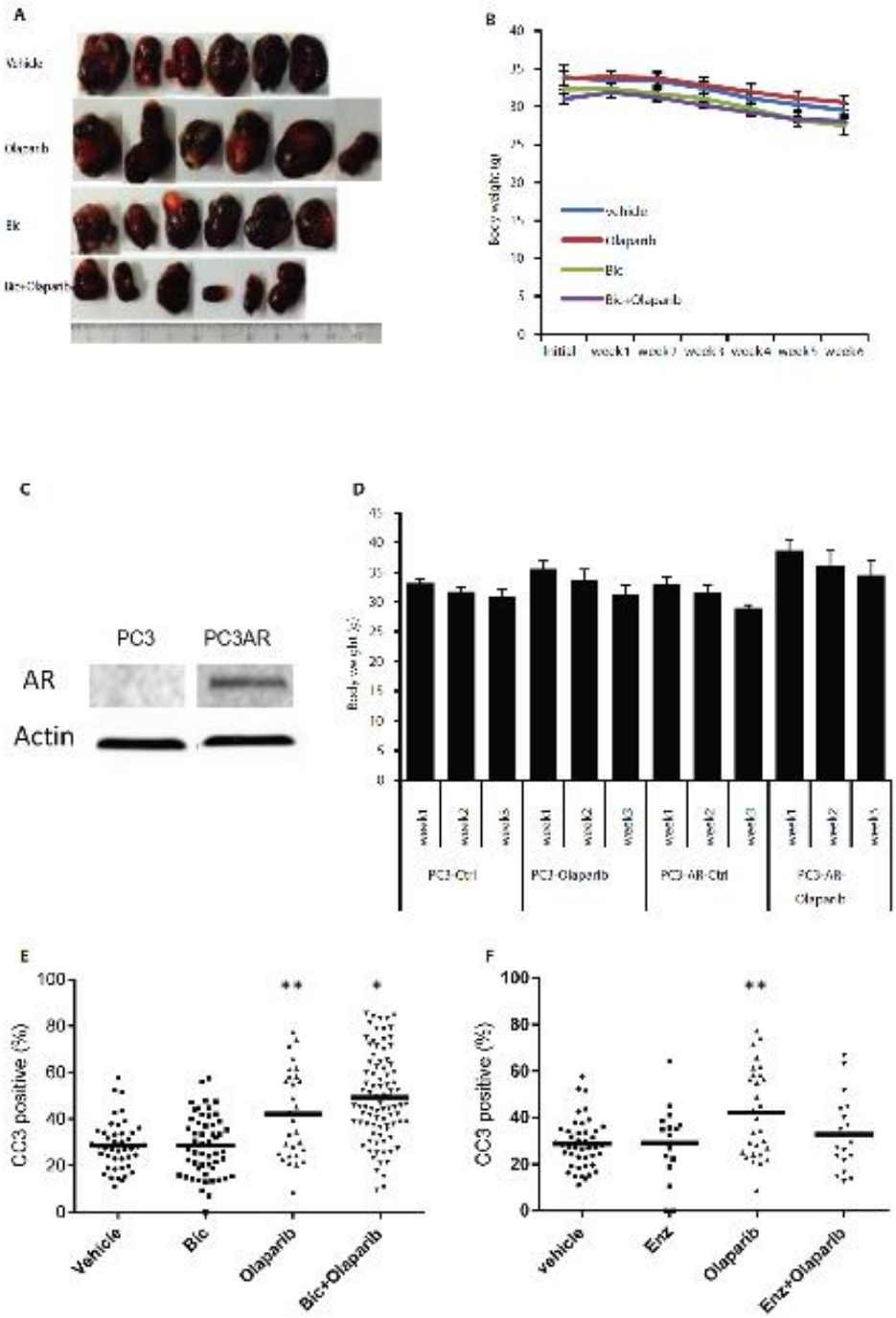

SUPPLEMENTARY FIGURE LEGENDS

Figure S1. AR signalling regulates homologous recombination.

(A) Distribution plot showing log2 expression value of RAD51 transcripts in three different cohorts from PCa clinical samples. **(B)** Western blot showing level of AR in "low AR" and "high AR" C4-2 cells treated with doxycycline (1µg/ml) and androgen R1881 (1nM) for 72 hrs. **(C)** Graphs showing flow cytometry images of C4-2-DRGFP cells, box encircled cells represent percentage of GFP cell population. **(D)** Gene set enrichment plots for AR up-regulated genes versus ATM-regulated DNA damage response gene signature from LNCaP cell line (GDS1852) and AR occupied and downregulated following castration in xenografts (GSE21817). **(E)** Scatter plot showing average number of γH2AX foci per nucleus from benign glands and PCa tissue from patients treated with Degarelix (n=15) or tumour grade matched control (n=19). Each dot represents average number of foci per nucleus in individual glands. Statistical significance was calculated by unpaired two-tailed Students't-test. **(F)** Bar graph show average γH2AX levels per nucleus in "low AR" and "high AR" C4-2 cells using high-content cytometry analysis "low AR" and "high AR" C4-2 cells transfected with siScr or siATM in response to IR (10Gy) for 2 hrs, results showing level of γH2AX with significance calculated by unpaired students' t-test. **(G)** Live cell imaging based confluence analysis of dox-inducible mutant AR (T877A) expressing PC3 cell line treated with ATMi (10µM) and exposed to radiation as indicated by arrow (IR; 10Gy) for indicated times, standard error of mean is presented. **(H)** Live cell imaging based confluence analysis of expressing PC3 cell line treated doxycycline (1µg/ml) with ATMi (10µM) and exposed to radiation as indicated by arrow (10 Gy) for 7 days. **(I)** Bar graph showing MRE11 expression in LNCaP cells transfected with control siRNA or siAR **(J)** Western blot of C4-2 cells transfected with control siRNA (siScr) or siAR, picture shows MRE11 protein expression in indicated conditions, B-actin is used as internal control.

Figure S2.

(A) Immunofluorescence images showing original and computer processed images of the PCa tissue stained with PARP-1 (red), PAR (green) and DNA (blue). While lines encircle the area used for intensity measurement**. (B)** Western blot showing PARylated proteins from LNCaP and C4-2 cells treated with PARP-1/2 inhibitor Olaparib (1µM) for 24 hrs.

Figure S3. Synthetic lethality between AR and PARP signalling pathways in PCa.
Viable fraction of **(A)** DuCaP, **(B)** LN3 and **(C)** PNT1a cells treated with indicated doses of Olaparib and/or Enzalutamide or Bicalutamide (10 µM) for 7 days or 95% confluence. Graph indicates results of a MTS cell viability assay. Viable fraction of **(D)** PC3-AR and **(E)** LN3 cells transfected with control and siAR and treated with indicated doses of Olaparib for 5 days. Graph indicates results of a MTS cell viability assay. **(F)** Viable fraction of C4-2 cell transfected with control, AR or PARP-1 siRNA and treated with Olaparib (1µM) for 5 days. Graph shows results of a MTS cell viability assay.

Figure S4. Dual inhibition of PARP and AR represses tumour growth.
(A) Tumour images of C4-2 xenograft in NSG mice treated with indicated drugs. **(B)** Graph showing body weight of mice bearing C4-2 xenografts administered with indicated drugs. **(C)** Western blot of PC3 and PC3-AR cells shows AR protein expression in indicated cell lines, β-actin is used as internal control. Statistical significance calculated by Mann-Whitney's test. **(D)** Graphs showing body weight of mice bearing PC3 or PC3-AR xenografts administered

with indicated drugs**. (E)** Quantification of cleaved caspase-3 expression in ex vivo culture of human PCa treated with Bicalutamide (10µM) and/or Olaparib (2µM) for 72 hrs, significance calculated by Mann-Whitney test. **(F)** Quantification of cleaved caspase-3 expression in ex vivo culture of human PCa treated with Enzalutamide (10µM) and/or Olaparib (2µM) for 72 hrs, significance calculated by Mann-Whitney test.

IV

Science Translational Medicine
AAAS

Accepted manuscript 2015

Castration radiosensitizes prostate cancer by impairing DNA-PK-mediated DNA double-strand break repair

Firas L. Tarish[1, 2], Niklas Schultz[1], Anna Tanoglidi[3], Hans Hamberg[4], Henry Letocha[5], Katalin Karaszi[6], Freddie C. Hamdy[6], Torvald Granfors[2,§], Thomas Helleday[1,*]

Affiliations:
[1]Science for Life Laboratory, Division of Translational Medicine and Chemical Biology, Department of Medical Biochemistry and Biophysics, Karolinska Institutet, Sweden
[2]Department of Urology, Central Hospital, Västerås, Sweden
[3]Department of Clinical Pathology, Uppsala University Hospital, Uppsala. Sweden
[4]Department of Pathology, Central Hospital, Västerås, Sweden
[5]Department of Oncology, Central Hospital, Västerås, Sweden
[6]Oxford Institute for Radiation Oncology, Department of Oncology, University of Oxford, UK

*Corresponding author. Mailing address: Science for Life Laboratory, Karolinska Institutet, Box 1031, SE-171 21 Stockholm, Sweden

[§]current address: Department of Urology, St. Göran Hospital, Stockholm, Sweden

E-mail: thomas.helleday@scilifelab.se, Tel. +46 8 524 800 00

One Sentence Summary: Chemical castration decreases Ku70 expression impairing non-homologous end joining DNA repair and improving the radiotherapy response of prostate cancer patients.

Abstract

Chemical castration improves responses to radiotherapy in prostate cancer but the mechanism is unknown. We hypothesized that this radiosensitization is caused by castration-mediated down-regulation of non-homologous end joining (NHEJ) repair of DNA double-strand breaks (DSBs). To test this, we enrolled forty-eight patients with localized prostate cancer in two arms of the study: either radiotherapy first or radiotherapy after receiving neo-adjuvant castration treatment. We biopsied patients at diagnosis, and before and after castration and radiotherapy treatments to monitor androgen receptor, NHEJ and DSB repair in verified cancer tissue. We show that patients receiving neo-adjuvant castration treatment prior to radiotherapy had reduced amounts of the NHEJ protein Ku70, impaired radiotherapy-induced NHEJ activity and higher amounts of unrepaired DSBs, measured by γ-H2AX foci in cancer tissues. This study demonstrates that chemical castration impairs NHEJ activity in prostate cancer tissue, explaining the improved response of patients with prostate cancer to radiotherapy after chemical castration. .

Introduction

Despite the technical improvements achieved in radiotherapy, the final outcome of this single treatment modality is still uncertain, with a high risk of recurrence among patients with unfavorable prognostic risk factors (*1-5*). However, several randomized clinical trials have revealed that the addition of neoadjuvant castration improves long-term local control and survival (*6-10*).

Thus, the combination of neo-adjuvant castration with radiotherapy has currently become, in many treatment centres, the standard of care for patients with intermediate and high risk prostate cancer. However, timing and duration of this castration in combination with RT needs to be better defined (*11*). A better understanding of the biological mechanism of action is essential for the optimization of treatment and the development of new therapeutic methods.

Radiotherapy induces various forms of DNA damage, the most important and toxic lesion being DNA double-strand breaks (DSBs). Non-homologous end joining (NHEJ), catalysed by DNA-dependent protein kinase (DNA-PK), is the most effective DNA repair mechanism for DSBs and works during all phases of the cell cycle (*12, 13*). In NHEJ, the DSB ends are bound by the abundant Ku70/80 heterodimer, which in turn attracts the catalytic subunit DNA-PKcs, that orchestrates the end-joining process and phosphorylates itself (on serine 2056) and other proteins, such as ligase IV and XRCC4 for final re-joining and ligation (*14, 15*). Using biopsies from patients with prostate cancer, we previously demonstrated that castration with a neo-adjuvant setting (i.e., therapy given before definitive local treatment with curative intent) decreases the expression of Ku70 (*16*), which, could potentially influence NHEJ and explain improved survival following radiotherapy. These findings have been confirmed by two other studies demonstrating both *in vitro* and *in vivo* with mouse xenografts that androgen receptor regulates the transcription of DNA repair genes (*17, 18*). Here, we test the hypothesis that neo-adjuvant castration reduces the DNA repair capacity of the NHEJ repair pathway in prostate cancer cells after radiotherapy.

Results

Upregulation of Ku70 by radiotherapy is prevented by neo-adjuvant castration

In a previous study, we showed that the Ku70 protein interacts with androgen receptor and the levels of Ku70 protein were reduced following castration in prostate cancer cells (*16*). Since Ku70 is a vital component of NHEJ, we suggested that impaired DSB repair could potentially be the mechanistic explanation for the increased radiosensitivity subsequent to castration. However, androgen receptor regulates numerous genes and the decreased levels of Ku70 or other repair proteins may not influence NHEJ activity and DSB repair in cells. To test this hypothesis directly, we recruited 48 patients with prostate cancer into a two arm prospective study (Fig. 1A), and used a computational approach to measure responses within individual cells in the tissue (Fig. 1B). In the first arm, we performed neo-adjuvant castration prior to 5 days radiotherapy, whereas in the second arm we prescribed radiotherapy 5 days prior to castration. We obtained tumor biopsies along the treatments to analyze the DSB repair. .

In both arms, castration treatment either before or after radiotherapy resulted in a similar decrease in serum Prostate-specific antigen (PSA) ($p<0.001$; Table S1) and median testosterone levels in serum were 0.7 nmol/L in both arms. Serum testosterone <1.7 nmol/L was not achieved in two patients in arm 1 and 4 patients in arm 2 after 8 weeks of chemical castration, although serum PSA decreased markedly.. These patients were still included in our study and statistical analysis.

We determined cytosolic and intra-nuclear Ku70 protein using immunofluorescence and observed no difference between patient arms at diagnosis. In both arms, castration decreased Ku70 levels to the same extent regardless of prior radiotherapy treatment ($p<0.01$) (Fig. 2A, B). There was a statistically significant increase in the mean intensity of intra-nuclear Ku70 after 5 x 2 Gy radiotherapy fractions ($p=0.014$). We interpret this as upregulation of Ku70, and likely other NHEJ proteins, after 5 days of radiotherapy treatment to mediate DSB repair. Interestingly, no such upregulation of Ku70 was found in prostate cancer patients receiving chemical castration alone (Fig. 2B).

Intra-nuclear levels of androgen receptor were determined in prostate tumor material from all patient biopsies. As expected no difference was observed between the arms prior to

castration. It has previously been reported that androgen receptor activity is increased after radiotherapy. Figure 2A shows more distinct staining for androgen receptor after radiotherapy but no statistically significant increase in intra-nuclear androgen receptor (Fig. 2B). No difference was observed in the pre-treatment mean intensity of intra-nuclear androgen receptor between arm 1 and arm 2 ($p=0.3$) (Figure 2B). As expected, intra-nuclear androgen receptor staining intensity decreased following castration (Figure 2B). Using Spearmans´s rho rank correlation test (ρ), we observed in both arms a significant correlation between pre-treatment mean staining intensity of intra-nuclear Ku70 and androgen receptor ($\rho=0.62$, $p<0.001$), and in arm 1 following castration ($\rho=0.65$, $p<0.001$) (Fig. 2C, D). To investigate whether the decrease in nuclear androgen receptor after castration correlated with a decrease in nuclear Ku70, the correlation between the induced decreases in those proteins was measured. The post-castration decrease in nuclear androgen receptor was accompanied by a corresponding decrease in intra-nuclear Ku70. In arm 1, there was a significant correlation after castration ($\rho=0.52$, $p<0.001$), and, after combined castration and radiotherapy ($\rho=0.33$, $p=0.001$). In arm 2, there was a significant correlation after radiotherapy ($\rho=0.64$, $p<0.001$) and after subsequent castration ($\rho=0.53$, $p<0.001$).

Increased residual radiation-induced DNA double-strand breaks after castration

Next, we wanted to assess if neo-adjuvant castration affected DSB repair. To assess the extent of DNA damage after castration alone, or castration plus radiotherapy, biopsies were taken 3 hours after completion of radiotherapy to be stained with antibodies against p53-binding protein 1 (53BP1) and phosphorylated H2AX histone, noted as γ-H2AX. Both 53BP1 and γ-H2AX are involved in early DNA damage signaling and are commonly used as markers of DSBs (*19*). Immunofluorescence staining with antibodies against 53BP1 and γ-H2AX was quantified in prostate cancer tissue in corresponding paired slides (Fig. 3A). Radiotherapy in both arms induced a statistically significant increase in both γ-H2AX and 53BP1 foci ($p<0.001$), and there was co-localization between the γ-H2AX and 53BP1 foci (Fig 3B and Fig. S1). Although castration alone did not increase the amount of DSBs (Fig. 3C), we observed that castration alone induced a significant reduction in the mean staining intensity of intra-nuclear 53BP1 foci in both arms ($p<0.05$, Fig. 3D), indicating that the androgen receptor itself may be involved in mediating the response to DNA damage.

Importantly, we observed a clear increase in radiotherapy-induced γ-H2AX in arm 1 with neo-adjuvant castration treatment ($p<0.05$), demonstrating that the number of toxic DSBs was increased in patients receiving neo-adjuvant castration (Fig.3C). Hence, we predicted that the remaining DSBs would be more lethal to the prostate cancer cells in arm 1, translating to a better overall outcome among prostate cancer patients following radiotherapy. We did not observe a statistically significant difference in staining for 53BP1 foci between the two arms, which is likely owing to the fact that 53BP1 appears to be downregulated by castration itself, leading to reduced foci intensity (Fig. 3C).

Neo-adjuvant castration impairs non-homologous end joining activity

Here, we report that a decrease in Ku70 after castration is correlated with an increase in residual DSBs in prostate cancer tissue, suggesting that lost NHEJ activity may explain decreased DSB repair and improved prostate cancer patient survival after radiotherapy. Next, we wanted to determine if this hypothesis is correct so we measured NHEJ activity in prostate cancer tissue. The Ku70/80 heterodimer recruits DNA-PK to DNA ends, activating its kinase activity which results in DNA-PK autophosphorylation on Serine residue 2056, which is required to complete NHEJ (*20*). Here, we used a phosphorylated DNA-PKcs specific antibody recognizing phosphorylated S2056 on DNA-PK, as a method of measuring ongoing NHEJ repair (Fig. 4A).

DNA-PK phosphorylation was low before treatment and after castration (Fig. 4C). Following radiotherapy, we observed a robust increase in the mean staining intensity of nuclear phosphorylated DNA-PKcs ($p=0.01$) (Fig. 4B, C), demonstrating strong activation of DNA-PK-mediated NHEJ repair of DSBs. In contrast, neo-adjuvant castration treatment before radiotherapy completely abolished radiotherapy-induced phosphorylated DNA-PKcs in arm 1. Interestingly, since the biopsies after radiotherapy and castration in arm 2 were taken 8 weeks after the last fraction of radiation, the subsequent phosphorylation of DNA-PKcs dropped below background levels (35%, $p<0.001$) (Fig.4C).

NHEJ and homologous recombination are two major DNA repair pathways that mediate DSB repair. NHEJ is the most efficient DSB repair pathway and works in all cell cycle phases (*21, 22*), whereas homologous recombination is a slow multistep process that requires several proteins and operates exclusively during the S and G_2 phases of the cell cycle (*23*). Next, we

tested the possibility that homologous recombination could play a major role in repair of DSBs induced during radiotherapy.

Using the Ki67 protein as a marker of proliferative activity (cells in S and G_2 phases), we assessed how castration and/or radiotherapy affected prostate cancer cells during the cell cycle. The number of proliferating cells according to Ki67 staining was 7% in both arms prior to castration and radiotherapy (Fig. S2). Castration treatment resulted in a decrease to about 1.5% Ki67-positive cells in both arms, and 5 days of radiotherapy treatment resulted in a dramatic reduction in Ki67-positive cells in both arms to about 0.5% ($p<0.001$ for both) (Fig. S2). These results suggest that the prostate cancer cells entered into cell cycle arrest (G_0) following both castration and radiotherapy treatment and therefore relied solely on NHEJ for repair of radiotherapy-induced DSBs.

Discussion

Prostate cancer is the most common type of cancer in many countries and the incidence is increasing worldwide. It is well established that the combination of chemical castration and radiotherapy improves survival of patients with localized intermediate and high-risk prostate cancer (*9*). Understanding the underlying molecular mechanism explaining how neo-adjuvant castration improves overall responses to radiotherapy is critical in order to rationally improve clinical protocols to increase overall patient survival. Previously, we reported a reduction in the Ku70 protein in prostate cancer tissue following castration (*16*), suggesting that NHEJ may be affected by castration. Pre-clinical results obtained using the LNCaP prostate cancer cell line showed that androgen deprivation therapy decreased NHEJ (*17*) and that androgen receptor expression induced and promoted DNA-PKcs expression and activity (*18*). However, these results were complicated by the fact that DNA-PKcs also serves as a co-factor in androgen receptor-mediated transcription (*18*, *24*). Hence, the role of DNA-PK and androgen receptor is complex and the situation in prostate cancer patients may differ from the behavior of prostate cancer cell lines grown *in vitro* in the absence of a functional tumor microenvironment. Here, we demonstrate in prostate tumor tissue from patients that the decrease in Ku70 after chemical castration correlated with an increase in residual radiotherapy-induced DSBs, indicating a failure in NHEJ repair. Impaired activation of NHEJ was also supported by the decrease in DNA-PK (pS2056) in prostate tumor tissue after radiotherapy but before castration. As the specificity of

the DNA-PK (pS2056) antibody has not been validated in human formalin fixed, paraffin embedded samples, we cannot exclude that castration impairs other radiotherapy-induced phosphorylation cascades, such as the ATM signaling pathway. Previous *in vitro* studies only showed marginal reduction in NHEJ repair (*17*). However, in the current study the decrease in Ku70 after castration was more robust about 30% compared to its initial value before castration Altogether, these data suggest that androgen receptor regulation of NHEJ is more rigorous in prostate cancer tissue from patients than observed *in vitro* in cell lines. Also, this suggests that NHEJ proteins other than Ku70 may be regulated by androgen receptor to maintain proficient NHEJ. Homologous recombination repair of radiotherapy-induced DSBs appears not to be operating in prostate cancer tissue as there are too few (<1%) cells in the S or G_2 phases of the cell cycle during radiotherapy, when homologous recombination is active.

An interesting observation is that the overall staining intensity for 53BP1 was reduced following castration. These data suggest that the DNA damage response is affected by castration in prostate cancer patients, which potentially could be exploited therapeutically in the future by combining DNA repair inhibitors.

Chemical castration affects only the androgen-synthesizing testicular Leydig cells, which are under the control of the pituitary-gonadal axis. Following castration, serum androgen decreases by 90-95% leaving the 5-10% of androgen produced by the adrenal glands (*8*). Emerging evidence suggests that residual androgen production by the adrenal glands and *de novo* steroid synthesis from cholesterol or progesterone precursors eventually lead to continued prostate cancer growth. Abiraterone and Enzalutamide prevent intratumoral androgen production by targeting androgen biosynthesis (through CYP17A) (*25*) or inhibiting androgen receptor nuclear translocation (*26*), respectively. Enzalutamide and ARN-509 (another anti-androgen drug) downregulate NHEJ and improve radiosensitivity in pre-clinical cancer models (*17, 18*). Clinical trials have shown that the use of second-generation drugs such as Abiraterone and Enzalutamide improves overall survival of patients with castration-resistant prostate cancer (*25, 26*). Since castration alone does not suppress androgen-regulated genes sufficiently, the second-generation drugs may be efficacious because they suppress these genes, potentially leading to further impairment of NHEJ in a neo-adjuvant setting and improving radiosensitivity (*27*). A remaining open question is whether prostate cancer relapse after castration plus radiotherapy is due to insufficient androgen depletion after castration.

A limitation of our study is that we cannot describe in detail how the androgen receptor mediates NHEJ repair, for example, if it is solely through transcriptional regulation of proteins involved in NHEJ or if there is a more direct role for androgen receptor in NHEJ. Such questions are more difficult to resolve with patient material and are better addressed in vitro. Our current study is focused on NHEJ repair but it is possible that androgen receptor also mediates other repair or signaling pathways that are important for sensitizing prostate cancer cells to radiotherapy.

We have shown that the improved survival of prostate cancer patients achieved by combined castration and radiotherapy may be explained by impaired NHEJ repair of DSBs. This results in an increase in radiotherapy-induced DSBs leading to apoptosis of prostate cancer cells. Importantly, given that radiosensitization of prostate cancer tissue is optimally achieved after a combination of radiotherapy and castration we predict even better radiosensitization of prostate tumor tissue that expresses more androgen-sensitive androgen receptor .

Materials and Methods

Study design

Patients with localized, i.e. non-metastatic prostate cancer, eligible for curative radiotherapy, were enrolled in the study. Before inclusion, patients underwent examinations with bone scans and complementary imaging with computerized tomography or magnetic resonance imaging to exclude distant metastases. After completion of written informed consent, the patients were allocated to one of the two study arms. After signing the informed consent, three patients in arm 1 and one patient in arm 2 refused further biopsies, so there remained 25 participants in arm 1 and 23 in arm 2 who were eligible for this study. Patient characteristics are summarized in Table 1. The regional ethics committee of Uppsala University granted ethical approval, EPN Dnr 2011:066.

In arm 1, the patients received neo-adjuvant chemical castration with leuprorelin, a gonadotropin-releasing hormone analogue, followed by external beam radiotherapy in daily 2 Gy fractions to a total dose of 78 Gy. In arm 2, the patients first received radiotherapy in 2Gy daily fractions for 5 consecutive days followed by neo-adjuvant leuprorelin and then an equivalent higher radiotherapy dose to a total of 82 Gy (see Figure 1A). Before treatment, prostate needle-core biopsy specimens were obtained from all patients. In arm 1, a second biopsy was taken eight

weeks after the leuprorelin injection, i.e. before radiotherapy was started, and a third biopsy was taken about three hours after the fifth radiotherapy fraction. In arm 2, a second biopsy was taken about three hours after the fifth radiotherapy fraction, i.e. before hormone treatment was initiated, and a third biopsy was taken eight weeks after the administration of leuprorelin (Fig. 1A).

Histology and Immunofluorescence

All prostate tissue needle biopsy specimens were embedded in paraffin, sectioned and stained with haematoxylin and eosin. In all specimens, the cancer areas were assessed according to the Gleason system (*28*) and marked by a uro-pathologist. Two cancer-rich specimens from each batch of biopsies were further sectioned for immunofluorescence analysis. These sections were deparaffinised and rehydrated before antigen retrieval with R-buffer A (Electron Microscopy Sience) in a pressure cooker. After blocking with 2% BSA, the sections were incubated with different primary antibodies at 4^{o}C overnight. Extensive rinsing was performed once; the sections were incubated with the secondary antibodies (donkey anti mouse IgG-alexa 488 (1:500; Molecular probe) and donkey anti rabbit IgG-alexa 555 (1:500; Molecular probe) for one hour at room temperature. DNA was counterstained with TO-PRO-3 iodide (Molecular probe) and slides mounted with prolong gold (Molecular probe). Slides were stained with antibodies against (1) androgen receptor (1:500, N-20, sc-816 Santa Cruz) and Ku-70 (1:500, E-5, sc-17789 Santa Cruz) or (2) 53BP1 (1:1000, Bethyl laboratories) and γ-H2AX (1:1000, 3F2, Abcam) or (3) phosphorylated DNA-PKcs alone (1:750, S2056, Abcam) or (4) Ki67 alone (1:200, MIB-1, Dako).

Images from a tumor area with a good immunefluorescence signal were selected from each biopsy. The corresponding areas in the haematoxylin and eosin-stained section were identified for histological verification of the tumor area. In slides stained for Ku70, androgen receptor, Ki67 or phosphorylated DNA-PKcs two areas from each slide containing 300-600 cells were chosen for analyses. TO-PRO-3 was used as a DNA marker.

All images were analysed, with respect to medium staining intensity inside the nuclei and in the cytoplasm. The nuclear area was defined by the TO-PRO-3 signal and the cytoplasmic area as a 5 μm extension outside the nuclear area (Fig. 2A). For those proteins with exclusively nuclear localisation (53BP1 and phosphorylated DNA-PKcs), the intensity in the cytoplasm was

considered as background. For other proteins, with both nuclear and cytoplasmic localisation (Ku70 and androgen receptor), staining intensity values are presented without background subtraction (Fig. 1B). The measurement of the number of Ki67-positive cells was performed using a threshold for Ki67 intensity in the nucleus in order to distinguish positive from negative cells (Fig. 1C). For those markers that form foci, the number and area of foci per DNA unit was measured (Fig. 1D). All measurements were performed using an in house-written program for NIH-imageJ.

(*29*). Fluorescence images were obtained with either a Zeiss LSM 510-inverted confocal microscope or a Zeiss LSM 780-inverted confocal microscope, using a planapochromat 40X/NA 1.2 objective. Through-focus maximum projection images were acquired from optical sections 0.5 μm apart and with a section thickness of 1.0 μm. Haematoxylin and eosin-stained images were obtained with a Leica scan system.

Statistical analysis

Non-parametric test methods were applied. Related outcomes after different treatments within each arm were compared using the Wilcoxon Signed Ranks Test. Unrelated outcomes between the study's two arms were compared using the Mann-Whitney U Test. Correlation analysis was conducted using Spearman´s rho rank correlation test (ρ). All statistical tests were two-tailed with significance established at $p < 0.05$. Statistical analysis was performed using the Statistical Package for the Social Sciences (SPSS), version 21.0.

Supplementary Materials

Figure S1. **Effects of castration and/or radiotherapy on the nuclear staining of 53BP1 and γ-H2AX.** Bar graph showing the number of 53BP1 foci (blue bars), γH2AX foci (red bars) and the number of co-localised foci (green bars) in nuclei before treatment (base) and after different modalities of treatment in Arm 1 and Arm 2. Error bars show standard error of mean.

Figure S2. Effects of castration and/or radiotherapy on the cell proliferation rate. Determination of proliferation rate using Ki67 in nuclei of prostate cancer tissue before and after different treatments.

Table S1. Characteristics of patients at the time of diagnosis and after different treatments in arm 1 and arm 2.

Table S2. Correlation tests between different antibodies and the clinical parameters at the time of diagnosis for patients in the study.

References

1. A. V. D'Amico *et al.*, *JAMA : the journal of the American Medical Association* **280**, 969 (Sep 16, 1998).
2. A. V. D'Amico *et al.*, *Cancer* **95**, 281 (Jul 15, 2002).
3. J. A. Del Regato, A. H. Tralins, D. D. Pittman, *Bull Acad Natl Med* **177**, 1083 (Oct, 1993).
4. G. K. Zagars, A. C. von Eschenbach, A. G. Ayala, *Cancer* **72**, 1709 (Sep 1, 1993).
5. E. Lalonde *et al.*, *Lancet Oncol* **15**, 1521 (Dec, 2014).
6. M. J. Zelefsky *et al.*, *Eur Urol* **60**, 1133 (Dec, 2011).
7. G. Housman *et al.*, *Cancers (Basel)* **6**, 1769 (2014).
8. K. Oishi, O. Yoshida, *Gan To Kagaku Ryoho* **20**, 2300 (Dec, 1993).
9. M. Bolla *et al.*, *Lancet Oncol* **11**, 1066 (Nov, 2010).
10. M. J. Schiewer *et al.*, *Cancer Discov* **2**, 1134 (Dec, 2012).
11. A. Dal Pra, F. L. Cury, L. Souhami, *Curr Oncol* **17**, 28 (Oct, 2010).
12. T. Helleday, J. Lo, D. C. van Gent, B. P. Engelward, *DNA Repair (Amst)* **6**, 923 (Jul 1, 2007).
13. A. A. Goodarzi, P. A. Jeggo, *Adv Genet* **82**, 1 (2013).
14. P. Ahnesorg, P. Smith, S. P. Jackson, *Cell* **124**, 301 (Jan 27, 2006).
15. P. A. Jeggo, *Radiat Res* **150**, S80 (Nov, 1998).
16. F. L. Al-Ubaidi *et al.*, *Clinical cancer research : an official journal of the American Association for Cancer Research* **19**, 1547 (Mar 15, 2013).

17. W. R. Polkinghorn *et al.*, *Cancer Discov* **3**, 1245 (Nov, 2013).

18. J. F. Goodwin *et al.*, *Cancer Discov* **3**, 1254 (Nov, 2013).

19. A. Sak, M. Stuschke, *Semin Radiat Oncol* **20**, 223 (Oct, 2010).

20. K. Meek, P. Douglas, X. Cui, Q. Ding, S. P. Lees-Miller, *Mol Cell Biol* **27**, 3881 (May, 2007).

21. M. Takata *et al.*, *Embo J* **17**, 5497 (Sep 15, 1998).

22. K. Valerie, L. F. Povirk, *Oncogene* **22**, 5792 (Sep 1, 2003).

23. A. Kakarougkas, P. A. Jeggo, *Br J Radiol* **87**, 20130685 (Mar, 2014).

24. G. L. Mayeur *et al.*, *J Biol Chem* **280**, 10827 (Mar 18, 2005).

25. K. Fizazi *et al.*, *The Lancet. Oncology* **13**, 983 (Oct, 2012).

26. H. I. Scher *et al.*, *N Engl J Med* **367**, 1187 (Sep 27, 2012).

27. E. A. Mostaghel *et al.*, *Cancer Res* **67**, 5033 (May 15, 2007).

28. D. G. Bostwick, *Am J Clin Pathol* **102**, S38 (Oct, 1994).

29. C. A. Schneider, W. S. Rasband, K. W. Eliceiri, *Nat Methods* **9**, 671 (Jul, 2012).

Acknowledgments:

We thank the prostate cancer patients enrolled in this study for their informed consent and participation and members of the Central Hospital, Västerås for assistance.

Funding: This study was financed by the Prostate Cancer UK (T.H., F.C.H.), the Swedish Research Council (T.H.), the European Research Council (T.H.), AFA insurance (T.H.), Swedish Cancer Society (T.H.), the Swedish Pain Relief Foundation (T.H.), the Torsten and Ragnar Söderberg Foundation (T.H.), the Centre for Clinical Research (CKF) (F.L.T.), Västmanland Research Foundation for Cancer in Vasteras (F.L.T.), Henning and Ida Persson Research Foundation (F.L.T.), and by a grant from Astra-Zeneca (T.H.). The study sponsors had no role in study design, in the writing of the report and in the decision to submit the paper for publication.

Author Contributions: F.L.T., N.S., T.H. devised the concept and designed the study. T.H. and F.C.M. supervised the project. F.L.T., N.S., H.L., T.G., K.K. and T.H. performed and analysed clinical experiments. A.T. and H.H. carried out pathological evaluations. F.L.T., N.S., T.H. wrote the paper. All authors discussed results and approved the manuscript.

Competing interests: The authors declare that they have no competing interests.

Figures:

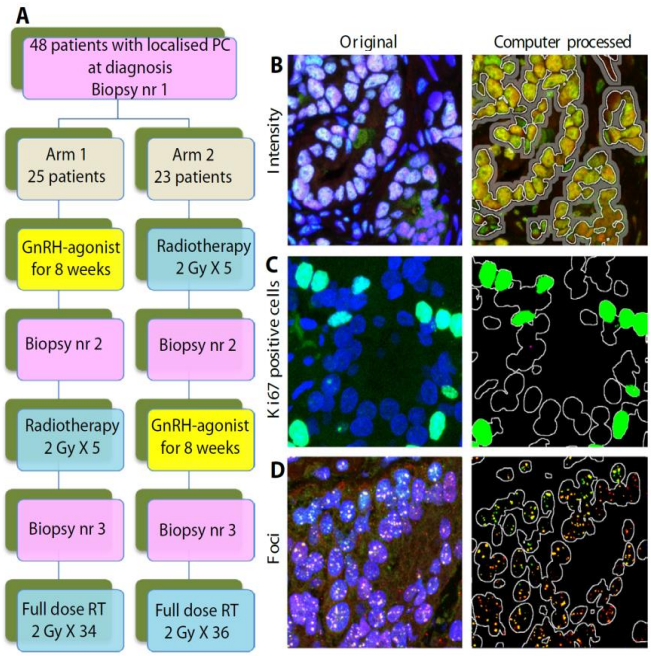

Figure 1. Flow chart and images shows different technical methods applied for the measurement of immunofluorescence staining signals of different antibodies.

(A) Flow chart of patients enrolled in the study. Patients received castration treatment with an gonadotropin-releasing hormone analogue for 8 weeks. 2 Gy x5 radiotherapy treatments were given on consecutive days and biopsies were taken 3 hours after the fifth dose of radiotherapy. **(B)** Upper left panel shows an original image used for intensity measurements. Upper right panel shows the same images after computer processing. Areas encircled with white lines were used for measurements of staining intensity inside the nuclei and were extracted by using the DNA signal as a mask. The DNA mask was processed with an algorithm to exclude stromal cells. Background measurements were performed in the 5 µm wide area outside the nuclei depicted as grey in the figure. Between the nucleus and the grey area there was a 1µm wide strip that was not measured to avoid background signals. **(C)** Original images were used for classification of Ki67-positive cells. Extraction of nuclei was done as described above. A threshold was applied to the Ki67 staining intensity signal. The areas with a signal above the threshold were used to calculate the fraction of Ki67-positive cells. **(D)** Original images were used for DSB foci (53BP1 and γ-H2AX**)** measurements. Lower right panel shows the same images after computer processing. Extraction of nuclei was done as described above. To extract the foci an algorithm that considers the local changes in staining intensity was used.

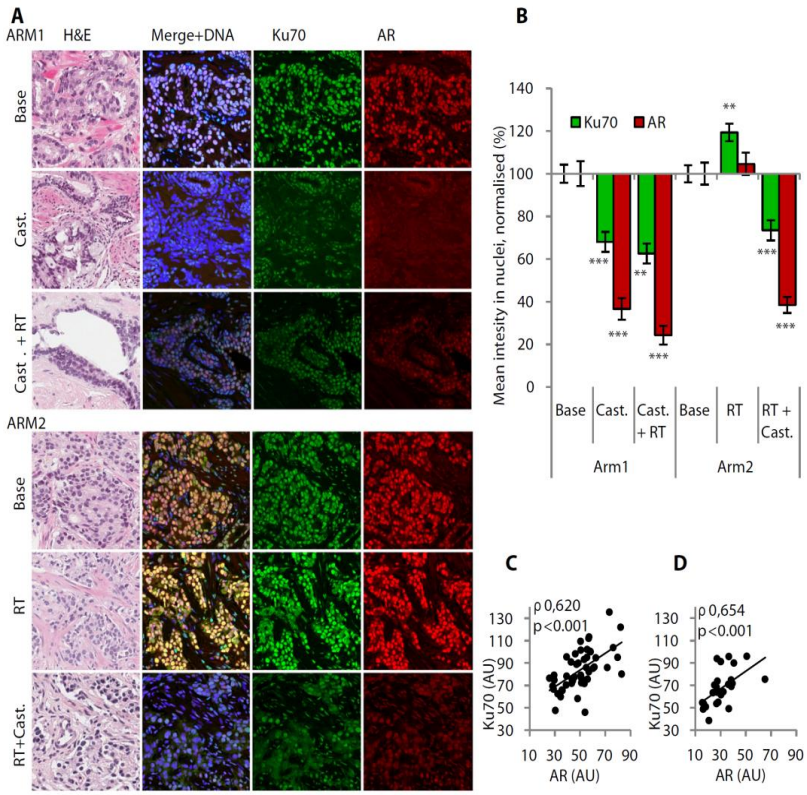

Figure 2. Effects of castration and/or radiotherapy on the nuclear staining of androgen receptor (AR) and Ku70. Determination of nuclear AR and Ku70 in prostate cancer tissue before treatment (Baseline) and after different treatment modalities in arm 1 and arm 2. (**A)** Different sections of prostate cancer biopsies are shown and each biopsy is sectioned and stained. The first section was stained with hematoxylin and eosin (H&E) to identify tumor areas. A further corresponding adjacent section obtained from the same biopsy was stained for Ku70 with an anti-Ku70 mouse-monoclonal antibody (green color) and an anti-androgen receptor rabbit-polyclonal antibody (red color). The DNA was co-stained with TO-PRO-3 (blue color). Upper sections were from a patient in arm 1; the upper panel was before treatment (baseline), middle panel was after castration and lower panel was after castration and radiotherapy (RT).. Lower sections were from a patient in arm 2; the upper panel was before treatment (baseline), middle panel was after RT and lower panel was after RT and castration. (**B)** Percentage of normalized mean staining intensity for androgen receptor (AR) (red bars) and Ku70 (green bars) in nuclei before treatment (baseline) and after different treatment modalities in arm 1 and arm 2 for all patients. Error bars show standard error of the mean. (**C)** Spearman´s rho rank correlation test (ρ) between mean intensity of androgen receptor (AR) and Ku70 in nuclei in biopsies from all patients before treatment (baseline) in arm 1 and arm 2. (**D)** Spearman´s rho rank correlation test (ρ) between mean intensity of androgen receptor (AR) and Ku70 in nuclei in biopsies from all patients in arm 1 after chemical castration treatment.

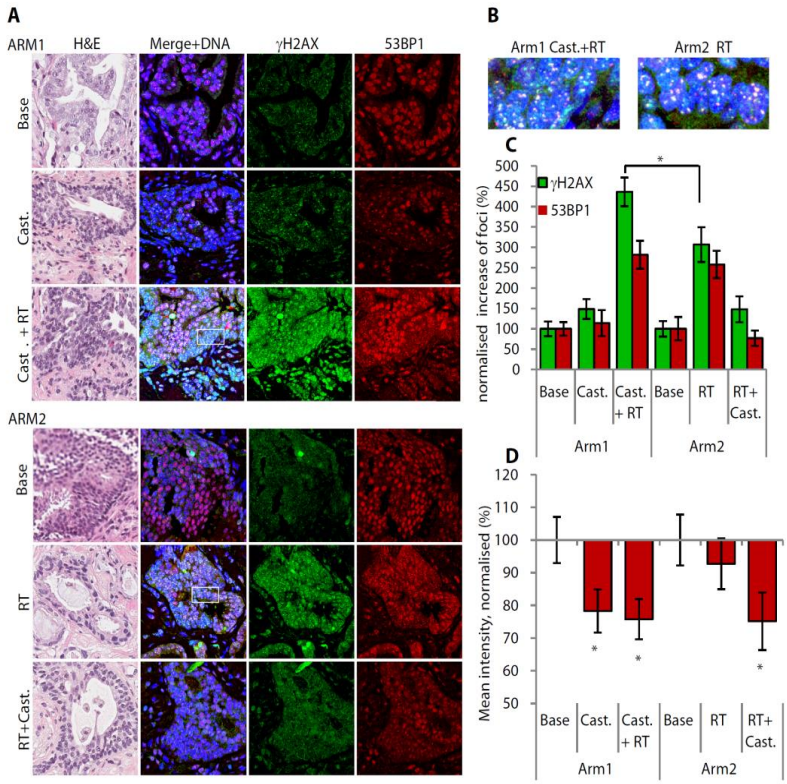

Figure 3. Effects of castration and/or radiotherapy on the nuclear staining of 53BP1 and γ-H2AX. Determination of nuclear 53BP1 and γ-H2AX in prostate cancer tissue before treatment (Baseline) and after different treatment modalities in arm 1 and arm 2. (**A)** Different sections of prostate cancer biopsies are shown and each biopsy is sectioned and stained. The first section was stained with haematoxylin and eosin (H&E) to identify cancer areas. A corresponding adjacent section obtained from the same biopsy was stained with anti- γ-H2AX mouse-monoclonal antibody (green color) and anti-53BP1 rabbit-polyclonal antibody (red color). The DNA was co-stained with TO-PRO-3 (blue color). Upper sections were from a patient in arm 1; the upper panel was before treatment (baseline), middle panel was after castration and lower panel was after castration and radiotherapy (RT). Lower sections were from a patient in arm 2; the upper panel was before treatment (baseline), middle panel was after RT and lower panel was after RT and castration. (**B)** A selected section from previous patient images in Arm 1 after castration and RT and Arm 2 after RT (merged staining for 53BP1, γ-H2AX and DNA). (**C)** Normalized percentage of γ-H2AX foci (green bars) and 53BP1 foci (red bars) in nuclei in prostate cancer biopsy material before treatment (baseline) and after different treatment modalities in arm 1 and arm 2 for all patients. Error bars show standard error of the mean. (**D)** Normalised mean staining intensity for 53BP1 in nuclei of prostate cancer biopsies before treatment (baseline) and after different treatment modalities in arm 1 and arm 2 for all patients. Error bars show standard error of the mean.

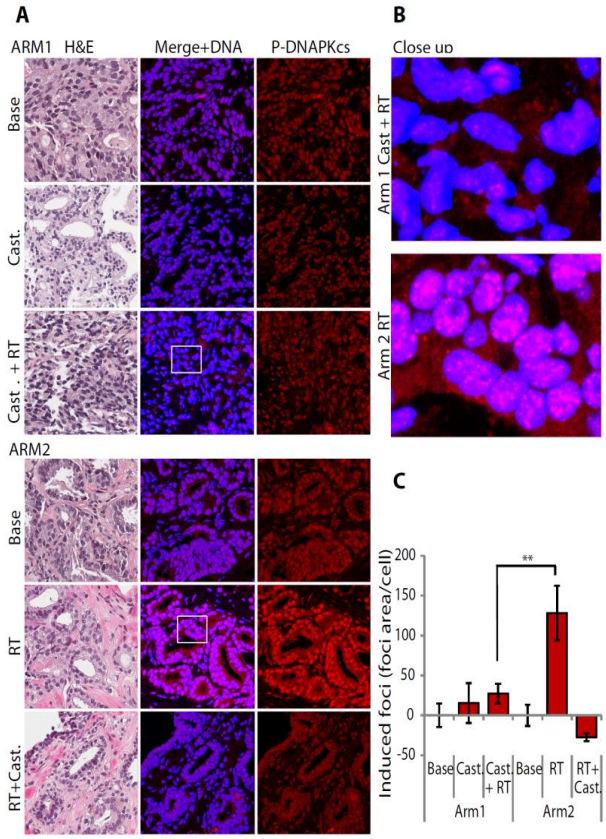

Figure 4. Effects of castration and/or radiotherapy on the nuclear staining of phosphorylated DNA-PKcs (pS2056). Determination of nuclear phosphorylated DNA-PKcs (P-DNA-PKcs) in prostate cancer tissue before treatment (Baseline) and after different treatment modalities in arm 1 and arm 2. (**A)** Different sections of prostate cancer biopsies are shown and each biopsy is sectioned and stained. The first section was stained with hematoxylin and eosin (H&E) to identify cancer areas. A corresponding adjacent section obtained from the same biopsy was stained with P-DNA-PKcs rabbit-polyclonal antibody (red color). The DNA was co-stained with TO-PRO-3 (blue color).). Upper sections were from a patient in arm 1; the upper panel was before treatment (baseline), middle panel was after castration and lower panel was after castration and radiotherapy (RT). Lower sections were from a patient in arm 2; the upper panel was before treatment (baseline), middle panel was after radiotherapy (RT) and lower panel was after RT and castration. (**B)** A selected section from previous images in Figure 4A of patients both in arm 1 after castration and RT and in arm 2 after RT (merge P-DNA-PKcs with DNA). (**C)** Changes in P-DNA-PKcs foci/cell (normalized value) in nuclei in prostate cancer biopsies before treatment (baseline) and after different treatment modalities in arm 1 and arm 2 for all patients. Error bars show standard error of the mean.

SUPPLEMENTARY MATERIAL

Castration radiosensitizes prostate cancer by impairing DNA-PK-mediated DNA double-strand break repair

Firas L. Tarish[1, 2], Niklas Schultz[1], Anna Tanoglidi [3], Hans Hamberg[4], Henry Letocha[5], Katalin Karaszi[6],Freddie C. Hamdy[6], Torvald Granfors[2], Thomas Helleday[1]

Supplementary Figures:

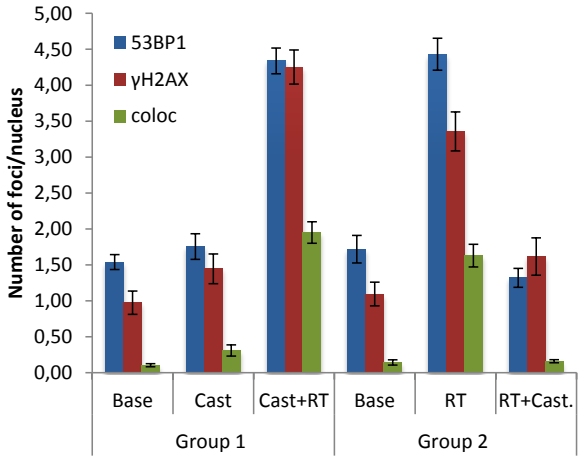

Figure S1: Effects of castration and/or radiotherapy on the nuclear staining of 53BP1 and γ-H2AX and their co-localization. Bar graph showing the number of 53BP1 foci (blue bars), γH2AX foci (red bars) and the number of co-localised foci (green bars) in nuclei before treatment (base) and after different modalities of treatment in Arm 1 and Arm 2 for all patients. Error bars show standard error of mean.

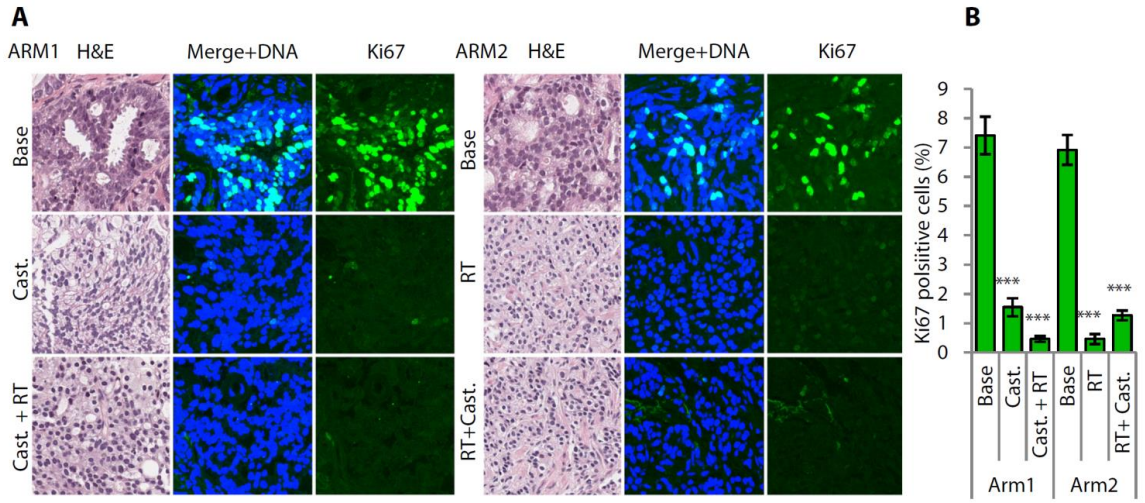

Figure S2: Effects of castration and/or radiotherapy on the cell proliferation rate. Determination of proliferation rate using Ki67 levels in nuclei of prostate cancer tissue before and after different modalities of treatment. **A)** Different sections of prostate biopsies are shown and each biopsy is sectioned and stained. The first section was stained with Haematoxylin and Eosin staining for identifying cancer areas. A further corresponding adjacent section obtained from the same biopsy was stained with immunofluorescence staining with Ki67 mouse-monoclonal antibody (green). The DNA was co-stained with TO-PRO-3 (blue). Sections in left panel were from a patient in arm 1; the upper left was before treatment (base), middle left was after castration and lower left after castration and RT. Sections in right panel were from patient in arm 2; the upper right was before treatment (base), middle right was after RT and lower right after RT and castration. **B)** Percentage of Ki67 positive cells before treatment (base) and after different modalities of treatment in arm 1 and arm 2 for all patients. Error bars show standard error of mean.

Table S1: Characteristics of patients at the time of diagnosis and after different treatments in arm 1 and arm 2.

	Arm 1	**Arm 2**	**p value**
Number of patients	**25**	**23**	
Median age years (Min – Max)	70 (56-78)	69 (55-78)	0.6
Median Gleason Score (%)	6 (4%) 7 (60%) 8 (12%) 9 (24%)	6 (8%) 7 (65%) 8 (8%) 9 (17%)	ns ns ns ns
Median time to prostate needle biopsy specimen in days (Quartiles)	55 (54-59)	58 (55-57)	ns
Median serum PSA ng/ml (Quartiles) At diagnoses After castration After castration and RT After RT After RT and castration	 11 (7.6-19.5) 0.8 (0.36-1.6) 1.2 (0.34-2.2)	 8.3 (3.9-15) 9.5 (4.7-19.25) 0.69 (0.26-1.5)	 0.16
Median serum Testosterone nmol/L (Quartiles) At diagnosis After castration After castration and RT After RT After RT and castration	 ND 0,7 (0-0.95) 0.5 (0-0.93)	 ND 9,4 (7.8-12.5) 0,7 (0-1.0)	
Median volume prostate cm^3 (Quartiles) At diagnosis After castration After castration and RT After RT After RT and castration	 41 (30-49) 24 (19-36) 24 (19-33)	 35 (26-49) 37 (30-47) 26 (19-34)	 0.4

- ND: not done
- ns: not significant

Table S2: Correlation tests between different antibodies and the clinical parameters at the time of diagnosis for patients in the study.
Spearmans´s rho rank correlation (ρ) test between initial values, obtained at the time of diagnosis, of serum PSA, prostate size, age, Gleason score, clinical stage and levels of Ku70, phosphorylated DNA-PKcs, AR, for all valid patients enrolled in the study.

	Serum PSA ng/ml	**Prostate size Cm^3**	**Age Years**	**Gleason score**	**Clinical stage**
Ku70	ρ=0.007 P=0.96	ρ =0.217 P=0.14	ρ =0.193 P=0.18	ρ =0.21 P=0.13	ρ =0.13 P=0.36
phosphorylated DNA-PKcs	ρ =0.15 P=0.29	ρ =0.20 P=0.16	ρ =0.43* P=0.002	ρ =0.04 P=0.76	ρ =0.15 P=0.28
AR	ρ =0.24 P=0.93	ρ =0.15 P=0.32	ρ =0.09 P=0.54	ρ =0.19 P=0.18	ρ =0.01 P=0.94

** Correlation is significant at the 0.05 level (2-tailed), ** Correlation is significant at the 0.01 level (2-tailed)*

V

Manuscripts

Androgen receptor heterogeneity in hormone-naïve prostate cancer

Firas L. Tarish[1,2], Niklas Schultz[2], Karolina Wallenborg[2], Anna Tanoglidi [3], Hans Hamberg[4], Henry Letocha[5], Katalin Karaszi[6],Freddie Hamdy[6],Torvald Granfors[7], Thomas Helleday[2]

Affiliations:

[1]Department of Urology, Central Hospital, Västerås, Sweden

[2]Science for Life Laboratory, Division of Translational Medicine and Chemical Biology, Department of Medical Biochemistry and Biophysics, Karolinska Institute, Sweden

[3]Department of Clinical Pathology, Uppsala University Hospital, Uppsala. Sweden

[4]Department of Pathology, Central Hospital, Västerås, Sweden

[5]Department of Oncology, Central Hospital, Västerås, Sweden

[6]Oxford Institute for Radiation Oncology, Department of Oncology, University of Oxford, UK

[7]Department of Urology, St. Göran's Hospital, Stockholm, Sweden

*Corresponding author. Mailing address: Department of Urology, Central Hospital, 72189 Västerås, Sweden firas.tarish@ltv.se or Thomas Helleday, Science for Life Laboratory, Division of Translational Medicine and Chemical Biology, Department of Medical Biochemistry and Biophysics, Karolinska Institutet, S-171 21 Stockholm, Sweden Thomas.helleday@scilifelab.se

Abstract

Despite the early diagnosis and subsequently effective treatment of intermediate and high-risk prostate cancer, the recurrence rate remains regrettably high. It is well-established that primary prostate tumour is a multifocal disease. Here, we wanted to investigate how effectively castration suppresses androgen receptor (AR) signalling, thereby affecting DNA damage repair in primary hormone-naïve prostate cancer. In a prospective study, five patients with localized prostate cancer, eligible for curative treatment were enrolled. Four patients received combined neo-adjuvant pharmacological castration and radiotherapy (RT) whilst one patient received in addition, low-dose radiation before the combined treatment was initiated. Prostatic needle core biopsies were secured at diagnosis, after castration and after RT. Serum PSA was measured at diagnosis and after castration while serum testosterone was only measured after castration. The levels of AR, Ku70, phosphorylated DNA-PKcs and PAR were measured. We observed a significant and correlated reduction in the mean intensity of nuclear AR in four patients whose serum PSA was reduced to the greatest extent, about 90% ($\rho=1$, $p<0.001$). Although complete castration was obtained using serum testosterone levels in these patients, the levels of AR, and consequently of Ku70 and phosphorylated DNA-PKcs remained high and positively co-varied in clusters of cells throughout prostate tumour areas. Meanwhile, a tendency towards an inverse correlation was observed between AR, Ku70 and phosphorylated DNA-PKcs and PARP-1 activity. In conclusion, we are first to demonstrate the heterogeneous landscape of AR and the consequent divergent although co-varied response of DNA damage repair. To date, it remains unclear whether the emergence of these castration-resistant cells in hormone-naïve

prostate cancer, is due to the high levels of intra-tumoral residual androgen following castration and consequently suboptimal androgen suppression of otherwise androgen-dependent cells or caused by quiescent castration-resistant cells that promote progression according to clonal selection pressure. The current finding certainly warrants further investigation in the future.

Introduction

The extensive availability of PSA testing revolutionized the diagnosis and treatment of localized prostate cancer. However, the recurrence rate following primary curative treatment remains high, in approximately 30-50 % of the patients with intermediate and high risk tumours[1-3]. Prostate cancer recurrence occurs either locally or systemically and cancer fatalities are attributable to metastatic, castration-resistant disease that has progressed despite androgen deprivation therapy (ADT).

Primary prostate cancer is generally multifocal and heterogeneous, co-existing in a single prostate gland and often consisting of a dominant tumour and one or multiple separate smaller tumours with histologically different Gleason grades[4,5]. Multifocal primary cancerous foci are biologically and genetically independent with distinct genetic features that are often characterized by different DNA sequence alterations, which are strongly dominated by copy-number alterations, small insertions or deletions, chromosomal re-arrangements, point mutations[6-8] and aberrant DNA methylations[9]. Divergent clonal populations can be identified in a single biopsy[10]. In contrast to the genomic heterogeneity of primary prostate cancer, metastatic disease often has a monoclonal origin with common genetic signatures[11,12].

Three main cell types can be characterized in normal prostate gland epithelium: basal, luminal and neuro-endocrine. A progenitor basal epithelium made up of undifferentiated stem cells is characterized by the expression of basal cell markers, such as p63 (16). They have low or undetectable levels of androgen receptors (AR)[13]and are independent of androgens for their survival[14]. Their progeny, luminal or so-called glandular cells, are differentiated and express luminal cell-specific markers, viz prostate specific antigen (PSA), prostatic acid phosphatase (PAP) and AR, on which they are dependent for their survival[14,15]. However, they lack expression of basal cell markers, such as p63[16]. The neuro-endocrine cells are sporadically scattered between these two cell layers and are differentiated, androgen-insensitive cells [17]. Human prostate cancer has a luminal phenotype. However,it is currently unclear which cells within the prostate epithelium are the origin of prostate cancer, stem/progenitor cells or their differentiated luminal cells/progeny which acquire tumour-promoting mutations that initiate the formation of cancer stem cells(CSCs)[18,19].

In addition to AR´s critical role in prostate gland development, growth and physiological function, the AR signalling axis is thought to facilitate prostate carcinogenesis, although the mechanisms of cancer initiation and progression are still being elucidated. AR, like several other genes that participate in the development and differentiation of prostate epithelium, are de-regulated in prostate cancer[20]. While AR is not mutated in the primary hormone-naïve tumour, AR is often mutated or amplified in castration-resistant disease [21]. Standard androgen deprivation does not consistently suppress androgen-dependent gene expression[22]. Currently, the point of time at which the development of castration-resistant disease occurs during prostate tumorigenesis, is unclear. The key question is whether castration-resistant cells arise through genetic/epigenetic transformation of previously androgen-dependent cells following ADT, or originate from previously quiescent castration-resistant cell populations

within an otherwise androgen-dependent tumour. The aim of the study is to investigate the heterogeneous landscape of AR in primary hormone-naïve prostate cancer and the impact of castration on certain DNA repair pathways at the single cell level.

Results

Heterogeneous response of prostate tumour cells to castration

In previous prospective clinical studies, we demonstrated that castration impairs the DNA repair capacity of D-NHEJ by reducing the expression of its essential proteins such as Ku70 and impairing phosphorylation of DNA-PKcs. However, a wide range of individual variations in the levels of these proteins was observed ([25]and Tarish et al., accepted in Science Translational Medicine with minor revisions). In this pilot study, we investigated any potential heterogeneity in the expression of AR and DNA repair proteins following castration. Despite the fact that examined patients had a primary untreated hormone-naïve prostate tumour, a remarkable heterogeneous response of AR signalling to castration was observed in different prostate tumour cells. Following castration, a significant decrease in the mean intensity of nuclear AR expression by almost 50% in patients 1-3 and in patient number 5 was observed. However, AR expression remained unaffected at a high level in clusters of tumour cells that gathered as subclones throughout prostate tumour areas with a variety in the number of cells (Figure 4 and Figure S1).

Correlated differences between AR and Ku70 at the single cell level

The levels of expression of nuclear AR and Ku70 at a single cell level in tumour areas were investigated. In a previous cohort study, a positive correlation between nuclear AR and Ku70 levels before and after castration and/or RT (Tarish et al., accepted with minor revisions) was reported. Equally here, using Spearman´s rho rank correlation test (ρ), a significant correlation between the mean intensity of nuclear AR and Ku70 levels in each examined patient before and after different treatments was observed (Table 2, Figure 5 and Figure S2A-C). Interestingly, despite tumour heterogeneity in response to castration**,** almost comparable co-variations between AR and Ku70, at a single cell level, were observed in nearly all patients before and after treatment i.e. cells that retained high levels of AR expression after castration preserved almost comparable, high expression levels of Ku70 (Figure S3).

Correlated differences between AR and phosphorylated DNA-PKcs in tumour areas

In the present study, investigated the correlation between AR and P-DNA-PKcs. We used tumour areas in two adjacent sections that were merged to study the correlations between AR and P-DNA-PKcs (Figure 3). As expected, the mean intensity of nuclear AR and P-DNA-PKcs foci was significantly correlated in nearly all patients before and after treatment (except at the time of diagnosis in patients 2 and 5) (Table 2, Figure 5, and Figure S2A-C). Furthermore, the study revealed that the expressions of P-DNA-PKcs foci in clusters of cells co-varied with the expression pattern of both AR and Ku70 (Figure 5).

Neo-adjuvant castration may trigger alternative DNA repair machinery mediated via PARP-1

We hypothesized that an impairment of D-NHEJ following castration in prostate tumours is critical in affecting genomic integrity and consequently will lead to an enhanced activity of back-up DNA repair machinery, the so-called B-NHEJ mediated by PARP-1. A former study showed that PARP-1 activities increased following castration, suggesting that prostate cancer relies on B-NHEJ, for the repair of its DSBs (Asim et al., in preparation). The current study aimed at further investigating the correlation between AR and PARP-1 activity in the heterogeneous landscape of AR in prostate cancer. Interestingly, a significant inverse correlation between the levels of PAR and nuclear AR (Table 2, Figure 5 and Figure S2 B-C) and nuclear Ku70 were observed following different treatments (Table 3A and Figure S4). However, in the case of P-DNA-PKcs, the inverse correlation with PAR levels was mainly observed after combined castration and RT (Table 3B and Figure S4). Likewise, a tendency of inverse correlation between the PAR levels and the levels of AR, Ku70 and P-DNA-PKcs were observed in different tumour areas (Figure 5).

Divergent responses in AR, Ku70 or PSA despite castration serum testosterone levels

Previously, a significant correlation was demonstrated between the decrease in serum PSA and nuclear Ku70 levels in patients with metastatic PCa following castration, suggesting that the PSA nadir may reflect simultaneously the nadir value of DNA repair activity[25]. A significant reduction in the mean intensities of nuclear AR and Ku70 levels were observed following castration in patients 1-3 and 5, whose serum PSA reduced most, by 89-99%, after castration. However, in patient number 4, whose serum PSA was only reduced by 70% despite castrate levels of serum testosterone, no reduction was observed in the mean intensity of nuclear AR or Ku70 after castration (Table 1).

Nuclear AR and serum PSA levels correlate

A significant correlation between the levels of AR in nuclei and serum PSA levels after castration was observed in all five patients ($\rho=1$, $p < 0.001$). Indeed, the finding was expected, since AR controls PSA expression (Figure S5).

Discussion

The current study demonstrates that, despite castration levels of serum testosterone, achieved by standard pharmacological castration, there is an inadequate suppression of androgen-responsive genes in subclones of cells throughout prostate tumour areas with persistent high levels of activity of AR and AR-related DNA repair genes. In these sub-clones of cells, high levels of AR were observed that co-varied with Ku70 and phosphorylated DNA-PKcs, two central proteins connected to the D -NHEJ repair pathway, thus indicating its inactivation despite castration levels of serum testosterone.

The mechanism behind, and timing for the development of castration-resistant prostate cancer (CRPC) may lead to a comprehensive understanding of the underlying mechanism behind the emergence of such resistant cells after primary hormone manipulation. In line with this, two models have been proposed: the adaptation model which hypothesized that selective pressure of ADT encourages mutational events in the androgen signaling pathway, and the clonal selection model which hypothesized the heterogeneous nature of prostate cancer and the pre-existing clone of castration-resistant cells [26,27]. In fact, about 70% of patients with CRPC remain androgen-dependent and continue responding to further hormonal manipulation such as second-generation anti-androgens[28].

Several scientific observations support the adaptation models and provide a rationale for the emergence of these resistant subclones in current study. To date, it is well-established that ADT leads to a decrease in intraprostatic androgens such as testosterone and dihydrotestosterone by only 75% to 80%, after accomplishing castrate serum testosterone levels with a GnRH -analogue[29-31]. Residual prostatic androgen levels in castrated patients are sufficient to stimulate androgen-responsive genes and activate AR[32]. An in vivo study by *Mostaghel et al* showed that many androgen-regulated genes are not suppressed after 3-9 months of neo-adjuvant castration[22].

Moreover, intense ADT with GnRH analogues in combination with the novel anti-androgen agent, abiraterone acetate, in patients with primarily localized hormone-naïve prostate cancer, showed a further suppression of intraprostatic androgens[33]. The afore-mentioned supports the assumption that the continued AR-mediated signalling after primary hormone manipulation is probably driven by the presence of residual tissue androgen. Furthermore, clinical trials on patients with CRPC using second-generation anti-androgens, such as abiraterone acetate and enzalutamide, suggest that AR signalling remains a fundamental promoting mechanism of CRPC[34,35]. The heterogeneity in AR response in the current study highlights findings in previous studies, which demonstrated continued substantial androgen-dependent gene expression following castration.

To date, different spliced variants of AR, which lack the ligand-binding domain and are functionally active despite the absence of androgens, have shown a putative role in developing resistance to anti-androgen therapy in CRPC[36]. This finding suggests that the production of the AR spliced variant could be a consequence of therapy-mediated selection pressure mediated by suboptimal intraprostatic androgen ablation, which, in turn, may lead to an adaptation by prostate tumour cells to survival in a low-level androgen environment, thereby undergoing mutation.

Several scientific observations back up the clonal model and provide a rationale for our current findings. Interestingly, they have shown that AR gene mutations were common and could arise in early hormone-naïve prostate cancer, yet more frequently in advanced disease before ADT[37,38]. Animal studies on the Dunning R-3327-H rat prostate adenocarcinoma model with a heterogeneous mixture of androgen-dependent and pre-existing androgen-resistant tumour cells subjected to ADT, showed that castration provided selective pressure and enhanced growth prosperity of castration-resistant tumour cells while androgen-dependent cells were eliminated [39].

Interestingly, the CSC hypothesis, which has been frequently discussed during recent years, is another theory that can support the clonal selection model. CSCs are a subgroup of tumour cells, about 0.1% [40] in number, characterized by a high level of expression of CD44 and CD133 and a low expression level of AR, with properties of self-renewal and differentiation[41]. The most important question is whether these castration-resistant tumour cells are CSCs or not. In fact, since CSCs in prostate cancer are usually characterized by high expression levels of CD44 and CD133 and low expression levels of AR, this suggests fairly convincingly that, because of the high expression of AR observed in these sub-populations of cells in the current study, these cells are not CSCs. Unfortunately, the lack of any CSC-marker staining such as CK or CD, may be regarded as a limitation in the current study.

In this study, it was rather expected that the correlation between AR and D-NHEJ proteins be in line with our previous reports and, undoubtedly, support the critical role of AR signalling in regulating DNA damage response. The most exciting findings are the co-variation between, on the one hand, AR and, on the other hand, Ku70 and DNA-PKcs, which were demonstrated at a cellular level or at a level of sub-clones of cells. However, despite the great improvements achieved in radiation technologies during the last decades combined with the more aggressive approach in the treatment of intermediate and high risk PCa, frequently using combined neo-adjuvant ADT and high dose RT, the 5-year recurrence rate remains high [1-3]. Furthermore, clinical trials have failed to identify whether ADT benefits all patients modestly or a sub-group to a greater degree. Our current finding may shed some light on at least some of the possible causes that may explain the high disease recurrence despite adequate oncological treatment. However, the underlining mechanisms behind these recurrences still have to be elucidated.

Interesting in the current work is the observed inverse correlation between PARP-1 activity and AR. Indeed, we previously demonstrated that PARP-1 activity was induced after castration (Asim et al., in preparation). In fact, PARP-1 plays pivotal roles in the processing and resolution of a variety of DNA damaged repair such as single-strand break repair (SSBR), homologous recombination (HR) or NHEJ[42]. However, our study suggests that prostate tumour cells, in which castration leads to impairment of D-NHEJ, may rely on PARP-mediated backup-NHEJ (B-NHEJ) DNA repair. We believe that this is an important finding that certainly warrants further investigation in the future.

Conclusion and future perspectives

Neo-adjuvant castration combined with radiotherapy remains the standard of care treatment for patients with high-risk, localized prostate cancer. In our previous studies [25] (Tarish et al., accepted with minor revisions), we showed that combined castration and RT impair DNA repair due to a down-regulation of D-NHEJ and its essential proteins, Ku70 and p-DNA-PKcs, hence improving radiosensitivity.

However, our current findings revealed that, despite the significant suppression of the mean expression of AR and Ku70 following castration, there is remarkably suboptimal suppression of these proteins at the single cell level, which may in turn raise the question whether the poorer radiosensitization of prostate tumour cells after subsequent RT may be

one of the plausible explanations behind the high incidence rate of recurrence in patients with high-risk disease, who receive curative RT in combination with neo-adjuvant castration [1-3].

It is probable that tumour heterogeneity may be an important factor in predicting response to individually based targeted therapies and a detailed investigation of the concept of intra-tumoral heterogeneity, at the single cell level, would be essential. It is well-established that the tumour microenvironment and surrounding non-malignant tissue may influence the growth and progression of tumour cells. Furthermore, the CSC population may need to be characterized using single cell resolution in tumour tissues. New technology such as spatial transcriptomics (ST), which is a novel approach that combines histology with RNA sequencing, could prove a promising tool in future studies.

Materials and Methods

Five patients with newly diagnosed, localized prostate cancer, eligible for curative radiotherapy were enrolled in the study. Ethical approval from the regional ethics committee at Uppsala University was acquired (EPN, Dnr 20011/066). Before treatment, prostatic needle core biopsy specimens were obtained from all patients. Four patients underwent neo-adjuvant pharmacological castration with leuprorelin, a gonadotropin releasing hormone (GnRH) analogue, followed by external beam radiotherapy to 78 Gy. A second biopsy was taking eight weeks after the leuprorelin injection, when their serum testosterone levels had decreased to castration levels, < 1.7 nmol/L in all patients. At the same time, serum PSA levels decreased between 89-99% in the first three patients and by 70% in the fourth patient (Table 1).

Patient number five first received RT, 2 Gy/fraction for 5 consecutive days followed by neo-adjuvant pharmacological castration with leuprorelin and afterwards an effect-equivalent higher dose of RT to a total of 82 Gy. After castration, serum testosterone decreased to castration levels and serum PSA decreased by 97% (Table 1). A second biopsy was taken three hours after the fifth dose of RT, i.e. before hormone treatment was started, and a third biopsy was taken eight weeks after the administration of leuprorelin.

Histological and immunofluorescence evaluation

All prostatic needle biopsy specimens were embedded in paraffin, sectioned and stained with hematoxylin and eosin (HE). In all specimens, the cancer areas were graded according to the Gleason system [23] and marked by a pathologist. Two cancer-rich specimens from each batch of biopsies were further sectioned for immunofluorescence analysis. These sections were deparaffinized and rehydrated before antigen retrieval with R-buffer A (Electron Microscopy Science) in a pressure cooker. After blocking with 2% BSA, the sections were incubated with different primary antibodies at 4^{o}C overnight. Extensive rinsing was performed once; the sections were incubated with the secondary antibodies (donkey anti mouse IgG-alexa 488 (1:500), Molecular probe and donkey anti rabbit IgG-alexa 555 (1:500), for one hour at room temperature. DNA was counterstained with TO-PRO-3 iodide (Molecular probe) and slides mounted with pro long gold (Molecular probe). To determine the effect of castration on the expression of AR and D-NHEJ activity, the nuclear levels of AR, Ku70 and phosphorylated DNA-PKcs were measured. Moreover, the expression of poly(ADP-ribose) (PAR), which

assesses PARP-1 activity, was measured. Two antibodies were stained on the same slide, AR (1:500, N-20, sc-816 Santa Cruz) together with Ku-70 (1:500, E-5, sc-17789 Santa Cruz) and phosphorylated DNA-PKcs (1:750, S2056, Abcam) together with PAR (1:200, pADPr (10H): sc-56198, Santa Cruz).

Immunofluorescence signals from the whole biopsy specimen were examined. However, the outer edges of all biopsy specimens were excluded from analysis since high expression levels of PAR were observed, which are believed to be caused by direct mechanical damage to the cells during the process of biopsy collecting, rather than a normal biological event in tumour cells owing to castration or RT (Figure 1).

All images were analyzed with respect to the medium intensity inside nuclei for AR, Ku70 and PAR. For P-DNA-PKcs, the area of repair foci in the nucleus was used as a descriptor for ongoing repair. Nuclear areas were defined by the TO-PRO-3, a DNA marker (Figure 2). All measurements were done using an in-house written programme for NIH-image J [24].

The immunofluorescence stainings of these proteins were carried out in two adjacent sections with a thickness of about 5 uM. However, different factors can determine the co-existence and positions of corresponding cells in adjacent sections. Since the stainings of AR and Ku70 were carried out simultaneously, we could match the levels of these two proteins at a single cell level. However, since stainings of AR/Ku70 and phosphorylated DNA-PKcs were carried out in two adjacent sections, the differences in expression between these proteins could only be matched at the level of corresponding cell clusters. A special programme was developed to fit the sections together and merge different proteins´ signals from corresponding clusters of cells (Figure 3).

Tiled fluorescence images of the whole biopsies were obtained with a Zeiss LSM 780-inverted confocal microscope using planapochromat 20X/NA 1.2 objectives. HE-stained images were obtained with a Leica scan system.

Statistical analysis

Correlation analysis was conducted using Spearman´s rho rank correlation test (ρ). All statistical tests were two-tailed with significance established at $p < 0.05$. Statistical analysis was performed using the Statistical Package for the Social Sciences (SPSS), version 21.0.

Acknowledgments:

We would like to thank all patients who participated in this study and all members at the departments of urology, oncology and pathology at the Central Hospital, Västerås who assisted in the study.

Funding:

This study was financed by the Prostate Cancer UK (T.H., F.C.H.), the Swedish Research Council (T.H.), the European Research Council (T.H.), AFA insurance (T.H.), Swedish Cancer Society (T.H.), the Swedish Pain Relief Foundation (T.H.), the Torsten and Ragnar Söderberg Foundation (T.H.) Centre for Clinical Research (CKF) (F.L.T.), Västmanland Research Foundation for Cancer in Vasteras (F.L.T.), Henning and Ida Persson Research

Foundation (F.L.T.), and by a grant from Astra-Zeneca (T.H.). The study sponsors had no role in the study design, in the writing of the report and in the decision to submit the paper for publication.

Author Contributions:

F.L.T., N.S., T.H. devised the concept, designed the study. T.H. and F.C.M. supervised the project. F.L.T., N.S., K.W., H.L., T.G., K.K. and T.H. performed and analyzed clinical experiments. A.T. and H.H. carried out pathological evaluations. F.L.T., N.S., T.H. wrote the paper. All authors discussed results and approved the manuscript.

Competing interests: The authors declare that they have no conflicting financial interests.

References:

1. Rosenbaum E, Partin A, Eisenberger MA: Biochemical relapse after primary treatment for prostate cancer: studies on natural history and therapeutic considerations. Journal of the National Comprehensive Cancer Network : JNCCN 2:249-56, 2004
2. Simmons MN, Stephenson AJ, Klein EA: Natural history of biochemical recurrence after radical prostatectomy: risk assessment for secondary therapy. European urology 51:1175-84, 2007
3. Zumsteg ZS, Spratt DE, Romesser PB, et al: The Natural History and Predictors of Outcome Following Biochemical Relapse in the Dose Escalation Era for Prostate Cancer Patients Undergoing Definitive External Beam Radiotherapy. European urology, 2014
4. Aihara M, Wheeler TM, Ohori M, et al: Heterogeneity of prostate cancer in radical prostatectomy specimens. Urology 43:60-6; discussion 66-7, 1994
5. Arora R, Koch MO, Eble JN, et al: Heterogeneity of Gleason grade in multifocal adenocarcinoma of the prostate. Cancer 100:2362-6, 2004
6. Baca SC, Garraway LA: The genomic landscape of prostate cancer. Frontiers in endocrinology 3:69, 2012
7. Mehra R, Han B, Tomlins SA, et al: Heterogeneity of TMPRSS2 gene rearrangements in multifocal prostate adenocarcinoma: molecular evidence for an independent group of diseases. Cancer research 67:7991-5, 2007
8. Baca SC, Prandi D, Lawrence MS, et al: Punctuated evolution of prostate cancer genomes. Cell 153:666-77, 2013
9. Brocks D, Assenov Y, Minner S, et al: Intratumor DNA methylation heterogeneity reflects clonal evolution in aggressive prostate cancer. Cell reports 8:798-806, 2014
10. Ruiz C, Lenkiewicz E, Evers L, et al: Advancing a clinically relevant perspective of the clonal nature of cancer. Proceedings of the National Academy of Sciences of the United States of America 108:12054-9, 2011
11. Mehra R, Tomlins SA, Yu J, et al: Characterization of TMPRSS2-ETS gene aberrations in androgen-independent metastatic prostate cancer. Cancer research 68:3584-90, 2008
12. Liu W, Laitinen S, Khan S, et al: Copy number analysis indicates monoclonal origin of lethal metastatic prostate cancer. Nature medicine 15:559-65, 2009
13. Bonkhoff H, Remberger K: Widespread distribution of nuclear androgen receptors in the basal cell layer of the normal and hyperplastic human prostate. Virchows Archiv. A, Pathological anatomy and histopathology 422:35-8, 1993
14. Kyprianou N, Isaacs JT: Activation of programmed cell death in the rat ventral prostate after castration. Endocrinology 122:552-62, 1988
15. Sar M, Lubahn DB, French FS, et al: Immunohistochemical localization of the androgen receptor in rat and human tissues. Endocrinology 127:3180-6, 1990

16. Signoretti S, Waltregny D, Dilks J, et al: p63 is a prostate basal cell marker and is required for prostate development. The American journal of pathology 157:1769-75, 2000
17. Bonkhoff H, Stein U, Remberger K: Endocrine-paracrine cell types in the prostate and prostatic adenocarcinoma are postmitotic cells. Human pathology 26:167-70, 1995
18. Visvader JE: Cells of origin in cancer. Nature 469:314-22, 2011
19. Rybak AP, Bristow RG, Kapoor A: Prostate cancer stem cells: deciphering the origins and pathways involved in prostate tumorigenesis and aggression. Oncotarget 6:1900-19, 2015
20. Prins GS, Putz O: Molecular signaling pathways that regulate prostate gland development. Differentiation; research in biological diversity 76:641-59, 2008
21. Visakorpi T, Kallioniemi AH, Syvanen AC, et al: Genetic changes in primary and recurrent prostate cancer by comparative genomic hybridization. Cancer research 55:342-7, 1995
22. Mostaghel EA, Page ST, Lin DW, et al: Intraprostatic androgens and androgen-regulated gene expression persist after testosterone suppression: therapeutic implications for castration-resistant prostate cancer. Cancer research 67:5033-41, 2007
23. Bostwick DG: Grading prostate cancer. Am J Clin Pathol 102:S38-56, 1994
24. Schneider CA, Rasband WS, Eliceiri KW: NIH Image to ImageJ: 25 years of image analysis. Nature methods 9:671-5, 2012
25. Al-Ubaidi FL, Schultz N, Loseva O, et al: Castration therapy results in decreased Ku70 levels in prostate cancer. Clinical cancer research : an official journal of the American Association for Cancer Research 19:1547-56, 2013
26. Zong Y, Goldstein AS: Adaptation or selection--mechanisms of castration-resistant prostate cancer. Nature reviews. Urology 10:90-8, 2013
27. Ahmed M, Li LC: Adaptation and clonal selection models of castration-resistant prostate cancer: current perspective. International journal of urology : official journal of the Japanese Urological Association 20:362-71, 2013
28. Yuan X, Cai C, Chen S, et al: Androgen receptor functions in castration-resistant prostate cancer and mechanisms of resistance to new agents targeting the androgen axis. Oncogene 33:2815-25, 2014
29. Page ST, Lin DW, Mostaghel EA, et al: Persistent intraprostatic androgen concentrations after medical castration in healthy men. The Journal of clinical endocrinology and metabolism 91:3850-6, 2006
30. Forti G, Salerno R, Moneti G, et al: Three-month treatment with a long-acting gonadotropin-releasing hormone agonist of patients with benign prostatic hyperplasia: effects on tissue androgen concentration, 5 alpha-reductase activity and androgen receptor content. The Journal of clinical endocrinology and metabolism 68:461-8, 1989
31. Mohler JL, Gregory CW, Ford OH, 3rd, et al: The androgen axis in recurrent prostate cancer. Clinical cancer research : an official journal of the American Association for Cancer Research 10:440-8, 2004
32. Mostaghel EA: Steroid hormone synthetic pathways in prostate cancer. Translational andrology and urology 2:212-227, 2013
33. Taplin ME, Montgomery B, Logothetis CJ, et al: Intense androgen-deprivation therapy with abiraterone acetate plus leuprolide acetate in patients with localized high-risk prostate cancer: results of a randomized phase II neoadjuvant study. Journal of clinical oncology : official journal of the American Society of Clinical Oncology 32:3705-15, 2014
34. Scher HI, Fizazi K, Saad F, et al: Increased survival with enzalutamide in prostate cancer after chemotherapy. The New England journal of medicine 367:1187-97, 2012
35. de Bono JS, Logothetis CJ, Molina A, et al: Abiraterone and increased survival in metastatic prostate cancer. The New England journal of medicine 364:1995-2005, 2011

36. Antonarakis ES, Lu C, Wang H, et al: AR-V7 and resistance to enzalutamide and abiraterone in prostate cancer. The New England journal of medicine 371:1028-38, 2014

37. Tilley WD, Buchanan G, Hickey TE, et al: Mutations in the androgen receptor gene are associated with progression of human prostate cancer to androgen independence. Clinical cancer research : an official journal of the American Association for Cancer Research 2:277-85, 1996

38. Koivisto P, Kononen J, Palmberg C, et al: Androgen receptor gene amplification: a possible molecular mechanism for androgen deprivation therapy failure in prostate cancer. Cancer research 57:314-9, 1997

39. Isaacs JT, Coffey DS: Adaptation versus selection as the mechanism responsible for the relapse of prostatic cancer to androgen ablation therapy as studied in the Dunning R-3327-H adenocarcinoma. Cancer research 41:5070-5, 1981

40. Collins AT, Berry PA, Hyde C, et al: Prospective identification of tumorigenic prostate cancer stem cells. Cancer research 65:10946-51, 2005

41. Maitland NJ, Collins A: A tumour stem cell hypothesis for the origins of prostate cancer. BJU international 96:1219-23, 2005

42. Wang Z, Wang F, Tang T, et al: The role of PARP1 in the DNA damage response and its application in tumor therapy. Frontiers of medicine 6:156-64, 2012

Figures and Tables

Figure 1

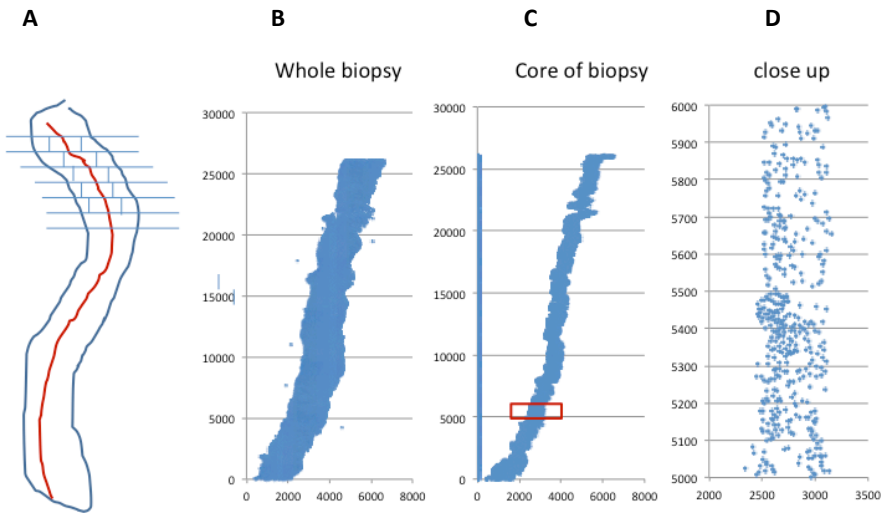

Figure 1. The methodology in selecting the target areas for the measurement of protein signals in the whole needle core biopsy specimens. **A)** Cartoon image shows a graphic line (red colour), always identifying the midpoint of every part in the needle biopsy. The red line prolonged throughout the length of the whole biopsy specimen with perpendicular small lines (blue colour) that run at a certain fixed distance on both sides of the central red line. The tissue areas located in the central part of the biopsy specimen i.e. along the red line and in between the small blue lines were selected for analysis, while tissue areas outside these blue lines were discarded from analysis. **B)** A computerized image of nuclear location from a whole biopsy specimen before preparation. **C)** A computerized image of protein signals from the same biopsy specimen in (fig1B) after preparation, selected for analysis. **D)** A close-up image of an area implemented for analysis. The main intensity of specific protein signals from different cluster of cells in the whole biopsy specimen, were collected and analyzed.

Figure 2

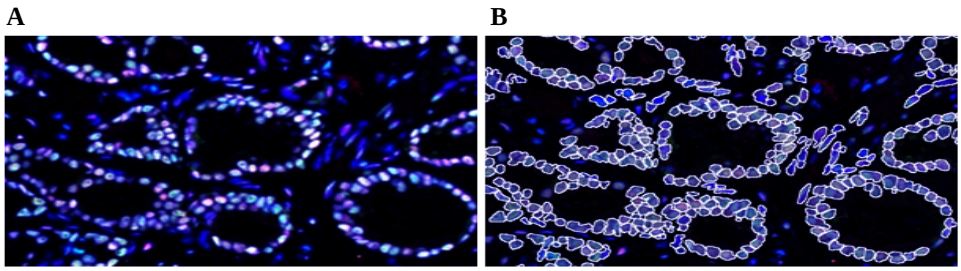

Figure 2.A) an original image used for intensity measurements of different proteins. **B)** The same image after computer processing. Areas encircled with white lines were used for intensity measurement inside the nuclei and had been extracted using the DNA signal as a mask. The DNA mask had been processed with an algorithm to exclude most of the stromal cells.

Figure 3

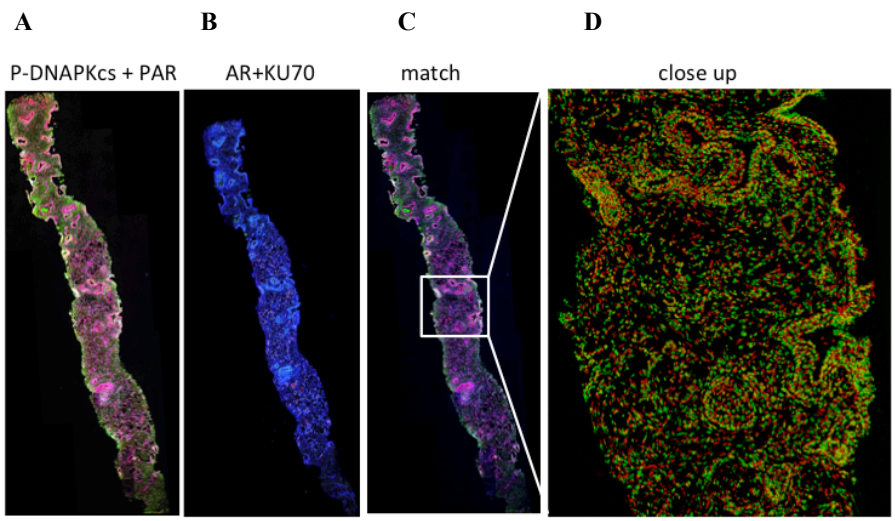

Figure 3. Tiled fluorescence images of a whole biopsy specimen, had been taken from two adjacent sections stained simultaneously with **A)** P-DNA-PKcs and PAR antibodies and **B)** AR and Ku70 antibodies. **C)** The matched two adjacent images, i.e. in fig 3A and fig 3B, were merged using a special computer programme and the above-mentioned protein signals from corresponding clusters of cells in different areas of the core biopsy were merged and analyzed. **D)** A close-up image depicted for the intensity measurements of the afore-mentioned proteins.

Figure 4

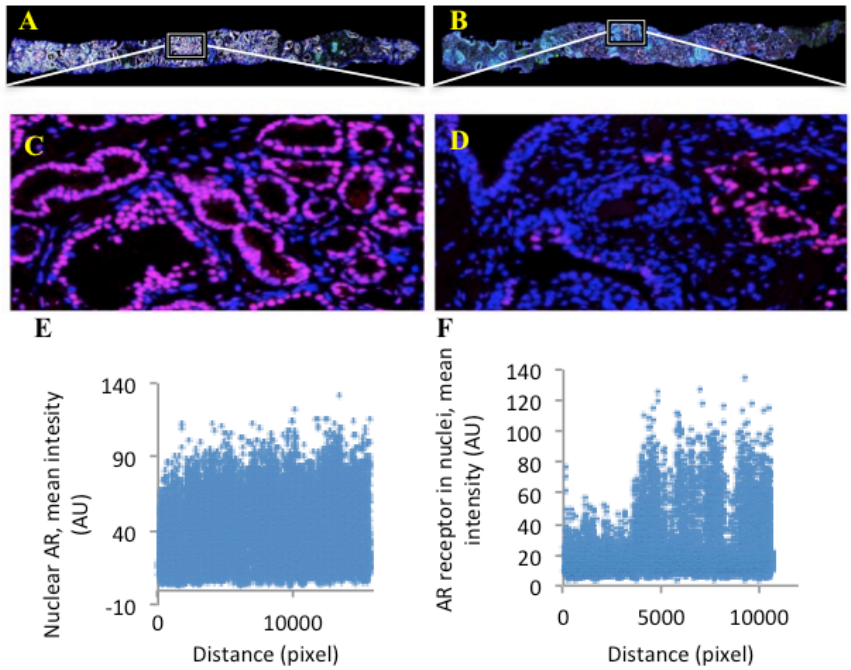

Figure 4. Data from tiled fluorescence images of whole prostate needle biopsies stained for androgen receptor (AR). **A)** Tiled images of prostate needle biopsy stained for AR before castration and **B)** after castration. **C)** Close-up tiled fluorescence images of prostate epithelial cells stained for AR showed the homogeneous staining of AR before castration and **D)** after castration, where we can see an incomplete suppression of AR in clusters of epithelial cells in different areas throughout the prostate needle biopsy. **E)** Signals of nuclear AR from epithelial cells of the same prostate needle biopsy in 4A, plotted against the distance along the length axis of the whole needle biopsies were measured in approximately 16,000 cells before castration. **B)** Signals of nuclear AR from epithelial cells of the same prostate needle biopsy in 4B, plotted against the distance along the length axis of the whole needle biopsies were measured in approximately 12,000 cells after castration.

Figure 5

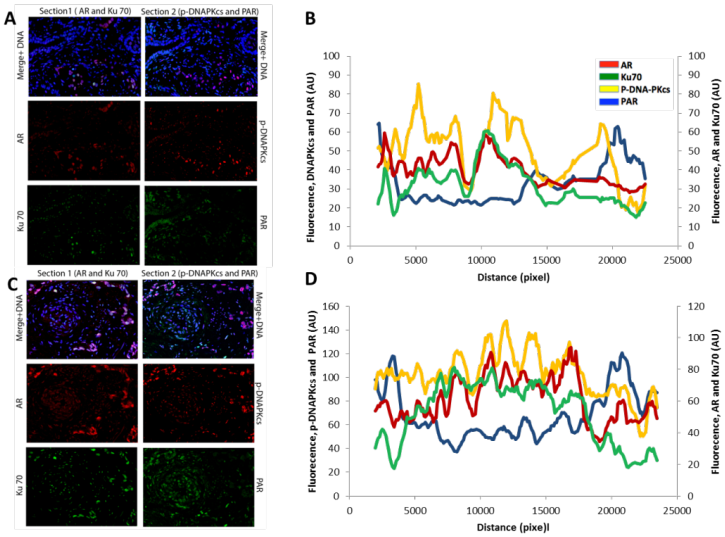

Figure 5. Determination of nuclear AR, Ku70, P-DNA-PKcs and PAR levels from prostate epithelial cells in prostate needle biopsies. **A)** Tiled fluorescence images of two matched adjacent sections in one needle biopsy before castration, where AR and Ku70 signals in section 1 were merged with P-DNA-PKcs and PAR signals from a corresponding area in the adjacent section 2. **B)** Graphs showing signals of AR (red), Ku70 (green), P-DNA-PKcs (yellow) and PAR (blue) plotted against the distance along the length axis of two matched adjacent sections of one whole needle biopsy before castration. The graph shows the positive co-variation between AR (red), Ku70 (green) and P-DNA-PKcs (yellow) and how these three proteins negatively co-variate with PAR (blue). **C)** The same as in fig. 5A, although after castration. **D)** The same as in fig 5B, although after castration.

Table1. Patients and tumour characteristics

Patient nu	Patient Age (y)	cT	GG	GS	PSA, ng/ml		Testosterone nmol/L	Nuclear AR mean intensity, AU		Nuclear Ku70 mean intensity, AU	
					Before castration	After castration (decrease %)	After castration	Before castration	After castration (decrease %)	Before castration	After castration (decrease %)
1	60	3	4+3	7	274	2.4 (99)	<0.4	72	23 (67)	44	21 (51)
2	65	3	4+5	9	95	11 (89)	0.78	57	26 (55)	42	25 (40)
3	62	3	3+4	7	19	1.3 (93)	<0.4	42	23 (46)	45	34 (24)
4	71	3	4+5	9	59	18 (70)	0.43	64	66 (-4)	47	45 (4)
5	62	3	3+3	6	4	0.12 (97)	0.87	41	21 (58)	64	46 (27)

Abbreviations: cT= clinical tumour stage; GG= Gleason grade; GS= Gleason score; AR= androgen receptor; AU = arbitrary unit

Table2. Spearman´s rho correlation co-efficient between AR and Ku70, AR and P-DNA-PKcs, AR and PAR

Spearman´s rho Correlation Coefficient Before castration	Patient nu	Mean intensity nuclear Ku70 (AU)		Mean intensity foci/area P-DNA-PKcs (AU)		Mean intensity nuclear PAR (AU)	
		Rho	p value	Rho	p value	Rho	p value
Mean intensity of nuclear AR (AU)	1	0.533**	<0.001	0.249**	<0.001	-0.023	NS
	2	0.312**	<0.001	-0.181*	0.013	-0.185*	0.011
	3	0.750**	<0.001	0.221**	0.003	-0.062	NS
	4	0.789**	<0.001	0.407**	<0.001	-0.495**	<0.001
	5	0.650**	<0.001	0.019	NS	-0.055	NS

Spearman´s rho Correlation Coefficient After castration	Patient nu	Mean intensity of nuclear Ku70 (AU)		Mean intensity foci/area P-DNA-PKcs (AU)		Mean intensity of nuclear PAR (AU)	
		Rho	p value	Rho	p value	Rho	p value
Mean intensity of nuclear AR (AU)	1	0.364**	<0.001	0.296**	<0.001	-0.173**	0.008
	2	0.712**	<0.001	0.296**	0.001	-0.08	NS
	3	0.338**	<0.001	0.548**	<0.001	-0.343**	<0.001
	4	0.645**	<0.001	0.191**	0.003	-0.139*	0.03
	5	0.896**	<0.001	0.411**	<0.001	-0.359**	<0.001

Spearman´s rho Correlation Coefficient After castration and RT	Patient nu	Mean intensity of nuclear Ku70 (AU)		Mean intensity foci/area P-DNA-PKcs (AU)		Mean intensity of nuclear PAR (AU)	
		Rho	p value	Rho	p value	Rho	p value
Mean intensity of nuclear AR (AU)	1	0.714**	<0.001	0.557**	0.001	-0.482**	<0.001
	2	ND		ND		ND	
	3	ND		ND		ND	
	4	0.659**	<0.001	0.621**	<0.001	-0.474**	<0.001
	5	ND		ND		ND	

*Abbreviations: AR; Androgen receptor, P-DNA-PKcs; phosphorylated DNA-protein kinase catalytic subunit, PAR; poly(ADP-ribose), AU; arbitrary unit; ND 0 not done; NS; non-significant, ** Correlation is significant at the 0.01 level (2-tailed).*

Table 3. Spearman´s rho correlation co-efficient

A. Between nuclear Ku70 and PAR

Spearman´s rho Correlation Coefficient		Mean intensity of PAR (AU)					
		Before treatment		After castration		After combined Cast. &RT	
	Patient nu	Rho	p value	Rho	p value	Rho	p value
Mean intensity of nuclear Ku70 (AU)	1	- 0.513**	<0.001	-0.267**	<0.001	- 0.539**	<0.001
	2	0.428**	<0.001	-0.049*	NS	ND	ND
	3	0.292	<0.001	-0.113	NS	ND	ND
	4	- 0.325**	<0.001	-0.372**	<0.001	- 0.801**	<0.001
	5	- 0.267**	0.001	-0.315**	<0.001	ND	ND

B. Between phosphorylated DNA-PKcs and PAR

Spearman´s rho Correlation Coefficient		Mean intensity of PAR (AU)					
		Before treatment		After castration		After combined Cast. &RT	
	Patient nu	Rho	p value	Rho	p value	Rho	p value
Mean intensity of foci/area P-DNA-PKcs (AU)	1	0.283**	<0.001	0.073	NS	- 0.238**	<0.001
	2	0.356**	<0.001	0.427**	<0.001	ND	ND
	3	- 0.015	NS	0.15	NS	ND	ND
	4	- 0.383**	<0.001	- 0.128*	0.05	- 0.407**	<0.001
	5	0.122	NS	0.173*	0.04	ND	ND

*Abbreviations: P-DNA-PKcs; phosphorylated DNA-protein kinase catalytic subunit, PAR; poly(ADP-ribose), AU; arbitrary unit; ND 0 not done; NS; non-significant, ** Correlation is significant at the 0.01 level (2-tailed)*

Supplementary Figure S1

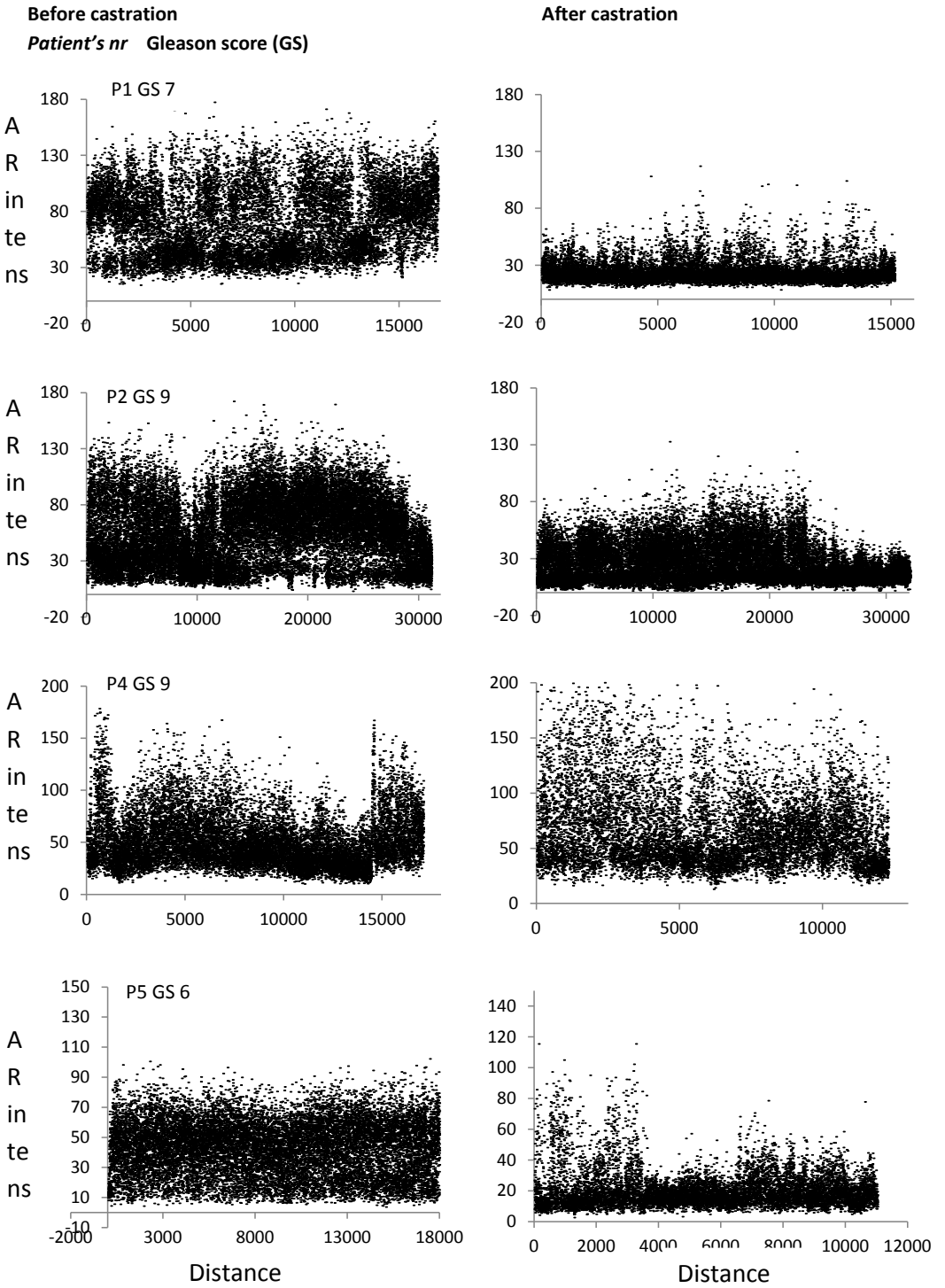

Supplementary Figure S1

The intensity of AR in nuclei of the epithelial prostate cells measured from the whole needle biopsies before and after castration. *Abbreviations P; patient, GS; Gleason score*

Supplementary Figure S2 A

Before treatment

Patients nr **Ku70** **DNA-PKcs** **PAR**

1

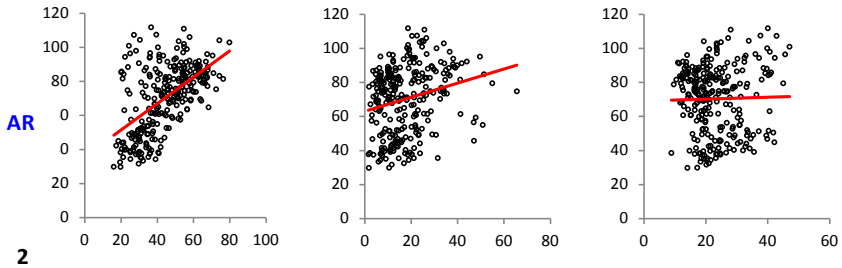

2

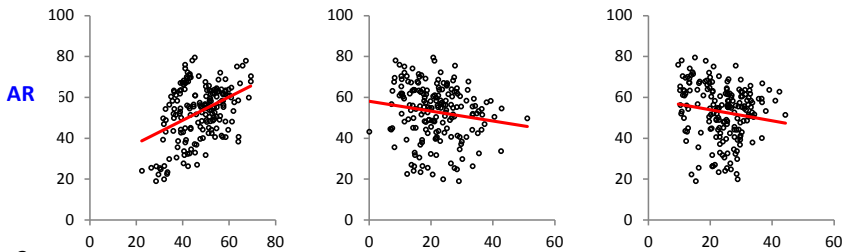

3

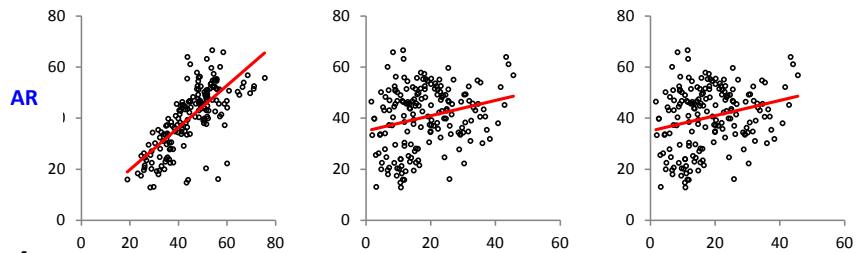

4

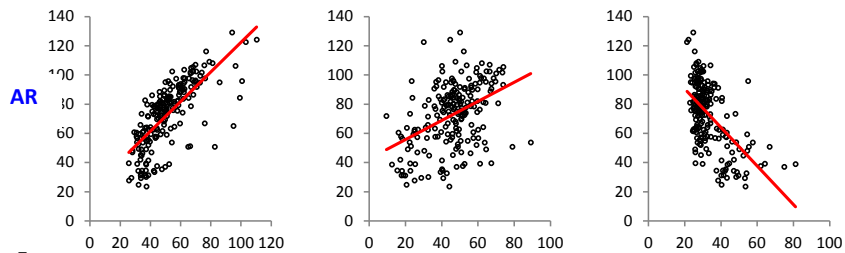

5

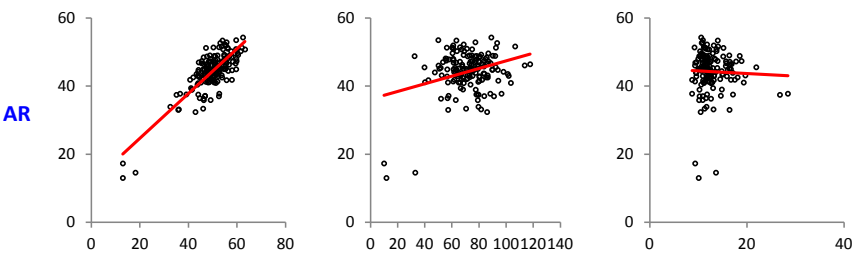

Supplementary Figure S2 B

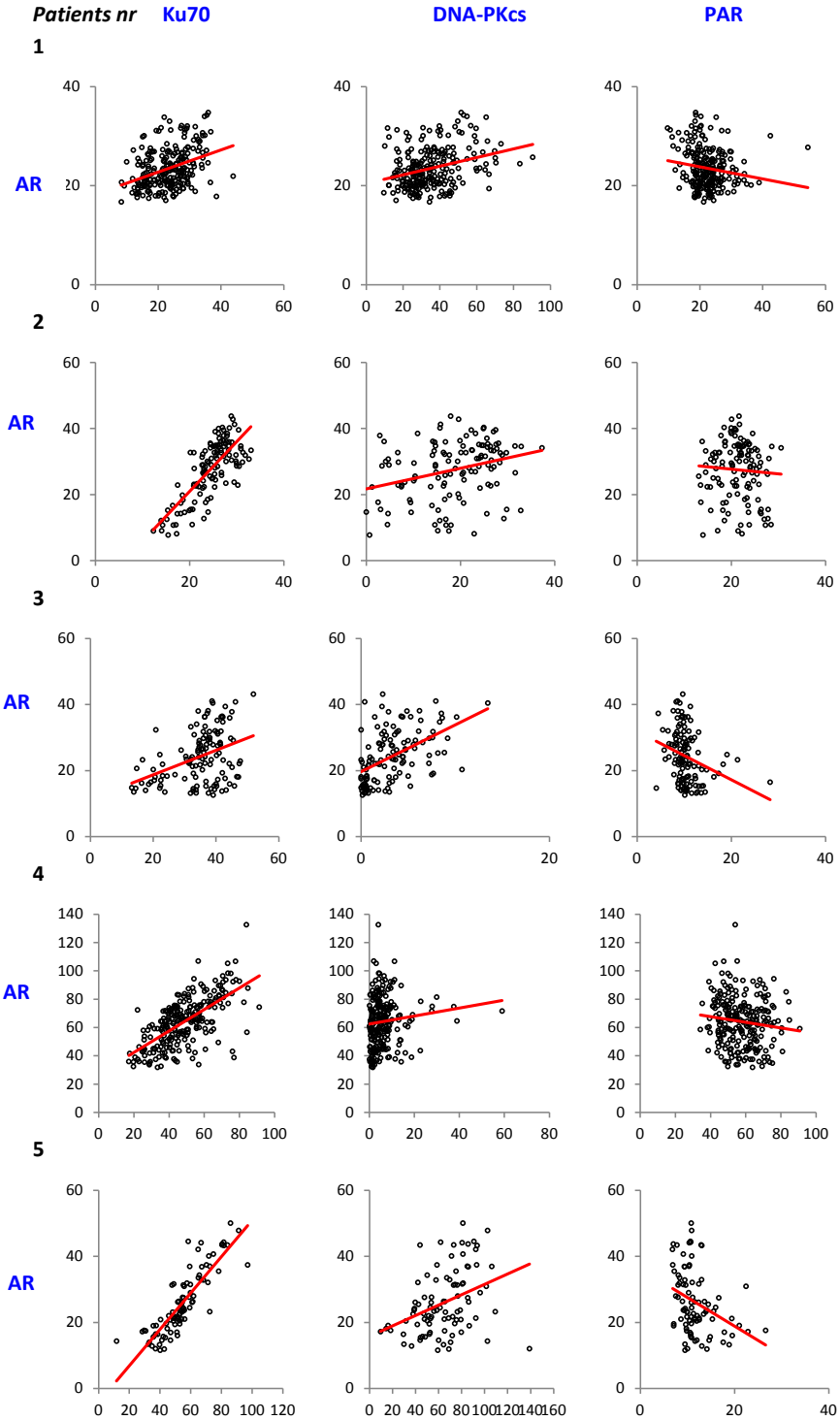

Supplementary Figure S2 C

After castration and radiation

Patients nr **Ku70** **DNA-PKcs** **PAR**

1

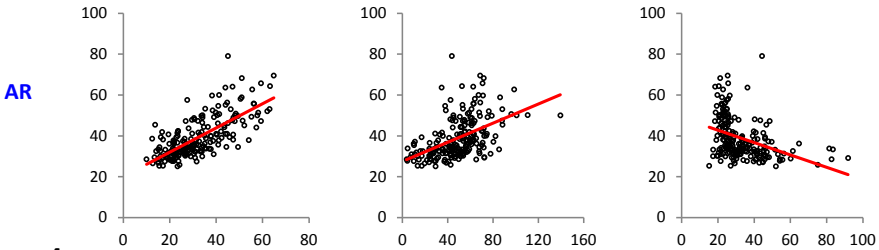

4

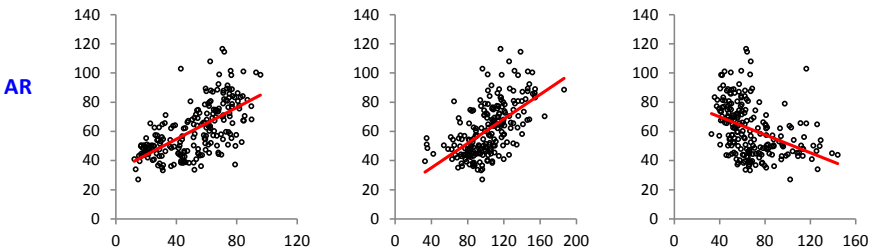

Supplementary Figure S2

Correlation between the intensity of AR versus Ku70, P-DNA-PKcs and PAR in the nuclei of the epithelial prostate cells measured from the whole needle biopsies before treatment in patients 1-5 (S1 A), after castration in patients 1-5 (S1 B) and after combined castration and RT in patients 1 and 4 (S1 C). Statistics used: Spearman´s rho correlation coefficient. For rho and *p value*, se Table 2.

Supplementary Figure S3

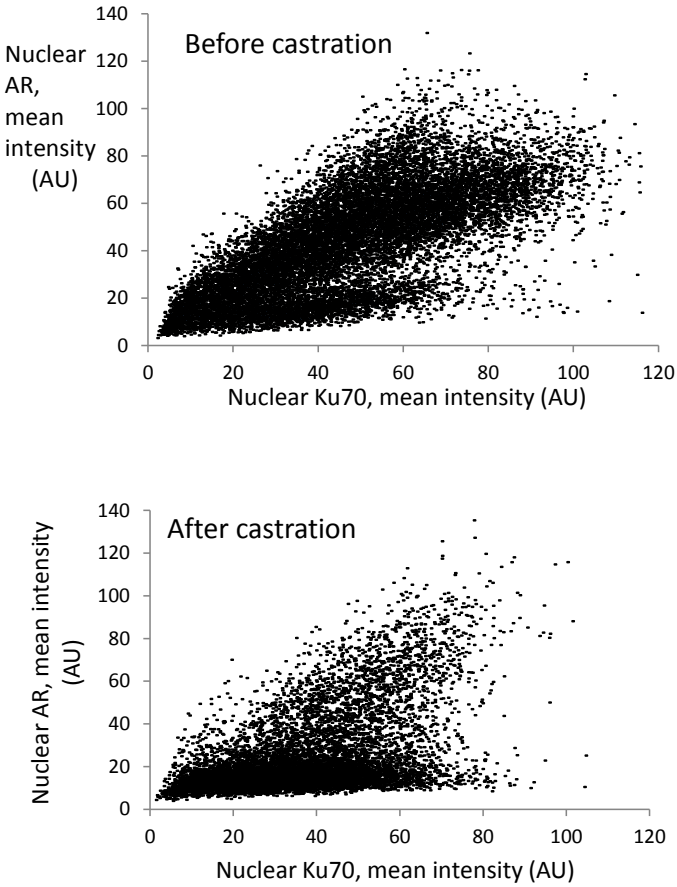

Supplementary Figure S3

Correlation between the intensity of nuclear AR versus Ku70 in the epithelial prostate cells from one whole needle biopsy.

Before castration **(upper figure)**, a wide range of AR expression in different epithelial cell populations was observed. The AR intensity is significantly correlated with KU70 expression.

After castration **(lower figure)**, despite the observed general and significant decrease in AR and Ku70 intensity in the majority of the epithelial cells, the intensity of these proteins remained highly correlated in the sub-population of other epithelial cells in the same biopsy.

Supplementary Figure S4

After castration and radiation

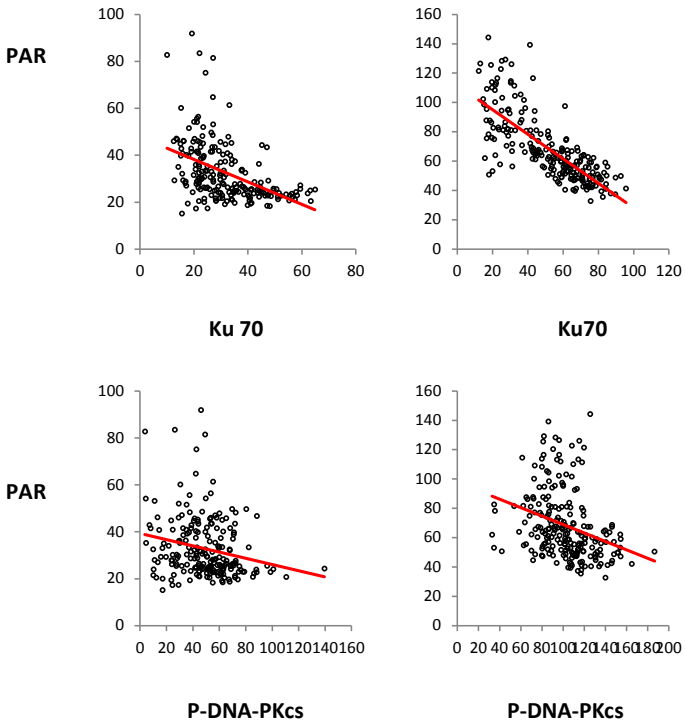

Supplementary Figure S4

Correlation between the intensity of PAR versus Ku70 and P-DNA-PKcs in the nuclei of the epithelial prostate cells measured from the whole needle biopsies after combined castration and RT in patients 1 and 4. Statistics used: Spearman´s rho correlation coefficient. For rho and *p value*, se Table 3A-B

Supplementary Figure S5

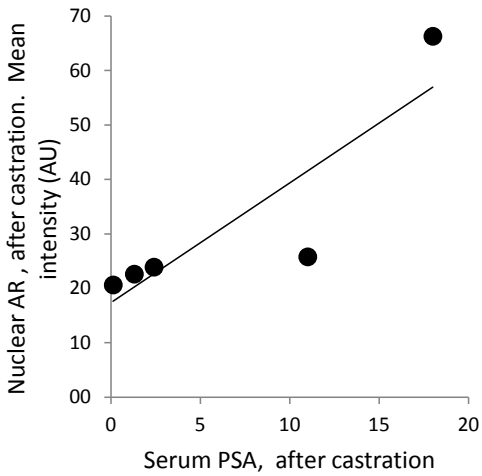

Supplementary Figure S5

Correlation between the main intensity of nuclear AR and serum PSA levels in 5 patients after castration. Spearman´s rho correlation test $\rho=1$, $p<0.001$.

Karolinska
Institutet